Inhibition of SNF1-related protein kinase1 by trehalose 6-phosphate and other metabolites and the interrelation with plant growth

Cátia Maria de Jesus Nunes

Dissertation presented to obtain the Ph.D degree in Biology

Instituto de Tecnologia Química e Biológica António Xavier | Universidade Nova de Lisboa

Oeiras, December, 2014

INSTITUTO
DE TECNOLOGIA
QUÍMICA E BIOLÓGICA
/UNL

Knowledge Creation

PhD supervisors

Pedro Fevereiro, PhD

Matthew Paul, PhD

Anabela Bernardes da Silva , PhD

The work presented in this thesis was performed at:

Rothamsted Research
(from October 2008 until December 2010)
Under the supervision of **Matthew Paul, PhD**

Rothamsted Research receives grant-aided support from the Biotechnological and Biological Sciences Research Council (BBSRC) of the United Kingdom.

Instituto de Tecnologia Química e Biológica (ITQB)
(from January 2011 until October 2012)
Under the supervision of **Pedro Fevereiro, PhD**

ITQB is supported by
Fundação para a Ciência e a Tecnologia through grant PEst-OE/EQB/LA0004/2011.

The student, Cátia Maria de Jesus Nunes received financial support from Fundação para a Ciência e Tecnologia and Fundo Social Europeu in the scope of Quadro Comunitário de Apoio through the PhD fellowship **SFRH/BD/44918/2008**.

“Somewhere, something incredible is waiting to be known.”

Carl Sagan

Even somewhere inside an eppendorf tube…

Acknowledgments/Agradecimentos

I have had the time of my life during my Ph.D. program. Many people encouraged me through the ups and downs that paved my way to this finish line. To all of them I wish to leave here my deepest and most honest “Thank you!”:

- My supervisor *Matthew Paul* for receiving me in his lab and for his valuable scientific guidance and support both when I was nearby at Rothamsted Research and also from the distance when I was already at ITQB. Our path together taught me how personal respect and friendship make the harshness of science so much more bearable and successes so much more meaningful!
- My experience at Rothamsted Research extends naturally to my friend *Lucia Primavesi* for her untiring tutoring, support and teachings in the lab, constant encouragement and meaningful advice before and after the lab and for everything else in between that only a hug could express. Professionally this thesis could never be the same without her and personally I will always carry in me a bit of her kindness.
- Ao meu supervisor *Pedro Fevereiro* pela constante e honesta disponibilidade numa agenda preenchida, sei que estou sempre acompanhada. O nosso trabalho conjunto precede este Doutoramento e a minha admiração e respeito só aumenta.
- À minha supervisora *Anabela Bernardes da Silva* por estar sempre por perto a relembrar-me as datas importantes! Mas principalmente pelo apoio e amizade que repetidamente ao longo de tantos anos me dedicou.
- *Eleazar Martinez-Barajas*, a protein purification expert and smiley new friend unexpectedly arrived from Mexico.
- *Henriette Schluepmann* for welcoming me in her lab at Utrecht University and very importantly for the exchange of ideas that prove that the deepest knowledge of our field produces the best science. Also thankful to her collaborator Thierry Delatte for his constant smile during the valuable T6P measurements.

- *Astrid Wingler* also for the exchange of ideas and helpful comments during our joint lab meetings.
- *Liam O'Hara* for our good time during the SEB Meeting (2012) and most importantly for his contribution to our "Seedlings paper".
- *Alfred Keys* for his expert advice during the enzyme kinetics analysis but especially for his honest friendship. I feel so lucky to have had the honour of meeting and be cared for by him.
- *John Andralojc* for keeping the lab "the safest place on earth" and for countless little helps during lab crises.
- *Till Pellny* for helping me with the wheat grain, the sugar measurements and the qRT-PCR… and for being the best "neighbour" of contiguous desks!
- All other *Rothamsted colleagues* that with friendly eyes made my days away from friends and family so much easier.
- *Elizabete Carmo-Silva* por me incitar a ultrapassar a vergonha e contactar pela primeira vez o meu supervisor… foi o início de tudo!
- *Ana Varela Coelho* e a *sua equipa* sempre disponível, especialmente a *Renata Soares*, pela ajuda na identificação das minhas proteínas mistério.
- A todos os meus *colegas do Plant Cell Biotechnology Laboratory* (somos muitos e bons!) que me receberam e ajudaram na (re)adaptação ao laboratório.

At a more personal note:

- My roommates, who became so much more than that *Sam, Nick and Emma* for always making me feel at home even during bad weather (both literal and figurative!).
- My new friends *Barbora, Adinda, Kevin and Steve* for endless conversations and exchange of experiences.
- E os meus velhos amigos, *Jorge, Luís e companhia* que tornam a minha vida tão mais leve e divertida.

À minha família… Ao meu *marido e amigo Pedro* que se manteve o meu norte durante todo este trajecto e à minha *mãe Celeste* que o sempre foi… Dedico a ambos este pedacinho de mim.

Resumo

Todos os organismos têm necessidade de monitorizar a disponibilidade de carbono e energia para sobreviver, uma afirmação especialmente verdadeira para as plantas devido à necessidade de integrar as inevitáveis condições ambientais com o metabolismo para manter a homeostasia celular. Os açúcares, centrais ao metabolismo, são hoje considerados moléculas sinalizadoras cruciais que traduzem essas condições ambientais. Um desses sinais é a trealose 6-fosfato (T6P), um dímero de moléculas de glucose fosforilado cuja concentração se correlaciona com a de sacarose. Um integrador central que regula condições de stress e energia é a proteína conservada *Snf1-related kinase1* (SnRK1) que responde aos baixos níveis de energia celular regulando positivamente processos conservativos de energia e o catabolismo e diminuindo os processos conducentes a gasto energético. Em 2009 mostrou-se que a T6P inibe a SnRK1. A inibição da actividade da SnRK1 *in vitro* foi confirmada *in vivo* através da observação de que os genes normalmente induzidos pela SnRK1 eram reprimidos pela T6P e vice-versa, promovendo o crescimento. Estas observações ofereceram um modelo de regulação do crescimento pelos açúcares.

A presente tese começa por aprofundar a caracterização da regulação da SnRK1 por metabolitos. Anteriormente foi mostrado que a glucose 6-fosfato (G6P) também inibe a SnRK1 *in vitro* e nós aspirámos investigar se outros metabolitos poderiam também inibir este regulador central. A glucose 1-fosfato (G1P) foi o único outro metabolito central que consistentemente inibiu a SnRK1. Os modelos cinéticos construídos mostram que a T6P, G6P e G1P regulam de forma independente a SnRK1. Por outro lado a G6P em combinação com a T6P têm um efeito cumulativo na inibição da SnRK1 e inesperadamente a G1P em combinação com a T6P inibiram a SnRK1 de forma sinergística. Em adição, a T6P inibe a SnRK1 a concentrações micromolares fora do sítio catalítico através de um factor intermediário ainda desconhecido. Esta inibição é mais forte em tecidos mais jovem e em crescimento e

ausente em folhas maturas que parecem não possuir o factor intermediário. A identificação deste factor intermediário (Factor I) é chave para compreender a regulação da SnRK1. Nós confirmámos a natureza transiente e fraca dessa interacção e identificámos várias proteínas que poderão interagir com a SnRK1. Contudo, experiências adicionais são necessárias para aferir acerca do seu envolvimento na inibição causada pela T6P.

O nosso trabalho continuou com a avaliação da regulação da SnRK1 durante o desenvolvimento da semente de trigo. Sabe-se que tanto a SnRK1 como a T6P afectam o crescimento e desenvolvimento das sementes. Recentemente foi mostrado que a ribose 5-fosfato (R5P) também inibe *in vitro* a SnRK1 das sementes de trigo, o que parecia estar de acordo com o envolvimento da SnRK1 na repressão anabólica. Para aprofundar o envolvimento da T6P e a R5P no desenvolvimento da semente de trigo, a actividade da SnRK1 e o seu grau de inibição foram testados nos diferentes tecidos separados em diferentes estádios de desenvolvimento. Mostrámos que a inibição da SnRK1 pela R5P em preparações de sementes de trigo é na verdade um artefacto experimental que ocorre apenas na presença do tecido verde do pericarpo. Pelo contrário, a acumulação observada de T6P poderá estar na base da alteração da expressão genética observada aos 10 dias após antese e que antecede o período de enchimento dos grãos.

Finalmente, era ainda pouco clara a forma como o modelo, que afirma que na presença de sacarose ocorre acumulação de T6P que por sua vez inibe a SnRK1 para promover o crescimento, opera em condições em que os tecidos consumidores de açúcares não têm capacidade de os usar, isto é, quando a disponibilidade de açúcares está desarticulada com o capacidade de crescimento. Para esclarecer esta questão, a T6P, a actividade da SnRK1, a concentração de açúcares, a expressão de genes e o crescimento foram medidos em plântulas de Arabidopsis após transferência para condições de frio ou sem azoto e comparadas com plântulas mantidas em condições favoráveis ao crescimento. A expressão de genes marcadores (induzidos e reprimidos) da SnRK1 correlacionam-se fortemente com a concentração de T6P acima e abaixo de um valor limiar de 0.3 to 0.5 nmol T6P g^{-1}

peso fresco, próximo da constante de dissociação (4 mM) que encontrámos para o complexo T6P/SnRK1. Esta correlação manteve-se independentemente do nível de crescimento em resposta à disponibilidade de sacarose. Comparativamente com o tipo selvagem, plântulas geneticamente modificadas com menor conteúdo em T6P ou sobre-expressão de SnRK1 após transferência do frio para 22 °C apresentaram uma menor capacidade de restabelecer o crescimento. Estes resultados mostram que a sinalização através da via T6P/SnRK1 responde à acumulação de sacarose causada por restrições de uso dos açúcares ao nível dos tecidos consumidores (por exemplo a baixas temperaturas) permitindo a recuperação do crescimento depois de restabelecidas condições favoráveis ao crescimento.

O trabalho aqui apresentado fornece novos dados sobre a regulação da SnRK1 por metabolitos expondo interessantes interacções entre a T6P, G1P e G6P na inibição da SnRK1 e permitiu aprofundar o conhecimento sobre o papel da via sinalizadora T6P/SnRK1 nas interacções entre tecidos produtores e consumidores de açúcares em plantas.

Abstract

All life forms need to monitor carbon and energy availability to survive and this is especially true for plants which must integrate unavoidable environmental conditions with metabolism for cellular homeostasis maintenance. Sugars, in the heart of metabolism, are now recognized as crucial signaling molecules that translate those conditions. One such signal is trehalose 6- phosphate (T6P), a phosphorylated dimer of glucose molecules which levels correlate well with those of sucrose (Suc). Central integrators of stress and energy regulation include the conserved plant Snf1-related kinase1 (SnRK1) which respond to low cellular energy levels by up-regulating energy conserving and catabolic metabolism and down-regulating energy consuming processes. In 2009 T6P was shown to inhibit SnRK1. The *in vitro* inhibition of SnRK1 by T6P was confirmed *in vivo* through the observation that genes normally induced by SnRK1 were repressed by T6P and *vice-versa*, promoting growth processes. These observations provided a model for the regulation of growth by sugar.

The present thesis starts out by further characterizing the metabolic regulation of SnRK1. Glucose 6-phosphate (G6P) has also been previously shown to inhibit SnRK1 *in vitro* and we have therefore sought to investigate if other metabolites could also inhibit this central regulator. Glucose 1-phosphate (G1P) was the only other central metabolite that consistently inhibited SnRK1. Kinetic models show that T6P, G1P and G6P each provide distinct regulation of SnRK1. Strikingly, G6P in combination with T6P produces cumulative inhibition of SnRK1 and most interestingly G1P in combination with T6P inhibited SnRK1 synergistically. Moreover, T6P inhibits SnRK1 at low micromolar concentrations via a still elusive intermediate factor at a site distinct from the catalytic site. The inhibition was strongest in young growing tissues and absent from mature leaves that lacked the intermediate factor. The identification of this factor is key for the understanding of SnRK1 regulation. We were able to confirm the transient and weak nature of their interaction and found several

proteins that interact with SnRK1. Further work is needed, however, to clarify the involvement of these proteins in T6P inhibition of SnRK1.

The work continued with the evaluation of SnRK1 regulation during wheat seed development. Both SnRK1 and T6P are known to affect seed growth and development and it was recently reported that ribose 5-phosphate (R5P) also inhibits wheat grain SnRK1 *in vitro* fitting very well with the known involvement of SnRK1 in anabolism repression. To investigate T6P and R5P roles in wheat grain development, SnRK1 activity and inhibition was tested in maternal and filial tissues dissected at different developmental stages. The inhibition of SnRK1 by R5P in wheat grain preparations was shown to be an experimental artefact that occurs only in the presence of green pericarp tissue. On the contrary, T6P accumulation could underlie the shift in gene expression in maternal and filial tissues observed at about 10 days after anthesis that proceed the grain filling period.

Lastly, it was still unclear how the model that states that in the presence of available Suc T6P accumulates and inhibits SnRK1 to promote growth, operates under sink-limited conditions, i.e. when tissue sugar content is uncoupled from growth. To clarify this question, T6P, SnRK1 activities, sugars, gene expression, and growth were measured in Arabidopsis seedlings after transfer to cold or zero nitrogen compared with sugar feeding under optimal conditions. SnRK1-induced and -repressed marker gene expression strongly related to T6P above and below a threshold of 0.3 to 0.5 nmol T6P g^{-1} fresh weight close to the dissociation constant (4 mM) of the T6P/ SnRK1 complex. This occurred irrespective of the growth response to Suc. Compared with the wild type, plants with genetically decreased T6P content and SnRK1 overexpression transferred from cold to warm, had impaired immediate growth recovery. These data showed that the T6P/SnRK1 signaling pathway responds to Suc induced by sink restriction enabling growth recovery following relief of limitations such as low temperature.

The work here presented provides further insight into the complex regulation of SnRK1 by metabolites exposing interactions between T6P, G6P and G1P in

SnRK1 inhibition and additional understanding of the role of the T6P/SnRK1 signaling pathway in source/ sink interactions in plants.

List of most used abbreviations

ABA	abscisic acid
ADP	adenosine diphosphate
ADPG	adenosine diphosphate glucose
AGPase	ADP-glucose pyrophosphorylase
AMP	adenosine monophosphate
AMPK	AMP-activated kinase
ATP	adenosine triphosphate
bZIP	basic region-leucine zipper transcription factor
bZIP11	basic region-leucine zipper transcription factor 11
CBS	cystathionine-beta-synthase sequences = Bateman domain
DAA	days after anthesis
DW	dry weight
F1,6BP	fructose 1,6-bisphosphate
F2,6BP	fructose 2,6-bisphosphate
F6P	fructose 6-phosphate
FBPase	fructose 1,6-bisphosphatase
Fru	fructose
FW	fresh weight
G1P	glucose 1-phosphate
G6P	glucose 6-phosphate
GBD	glycogen-binding domain
Gluc	glucose
GRIK	geminivirus rep-interacting kinase
HMG-CoA	3-hydroxy-3-methylglutaryl-coenzime A
HXK	hexokinase
INV	invertases

KIS	kinase interaction sequence
NADH	nicotinamide adenine dinucleotide
NR	nitrate reductase
Pi	orthophosphate
PK	protein kinase
PP	protein phosphatase
PRI	phosphoribo-isomerase
PRK	phosphoribulo-kinase
PRL1	pleiotropic regulatory locus 1
R5P	ribose 5-phosphate
ROS	reactive oxygen species
Ru5P	ribulose 5-phosphate
Ru5P	ribulose 5-phosphate
RuBP	ribulose bis-phosphate
S6P	sucrose 6-phosphate
SnAK	SnRK1-activating kinase
SNF1	sucrose non-fermenting kinase 1
SnRK1	SNF1-related kinase1
SPS	sucrose phosphate synthase
Suc	sucrose
SUS	sucrose synthases
T6P	trehalose 6 –phosphate
TCA	tricarboxylic acid cycle
TFs	transcription factors
TOR	target of rapamycin
TPP	trehalose phosphate phosphatase
TPS	trehalose phosphate synthase
triose-P	triose-phosphates
UDPG	uridine diphosphate glucose

Table of Contents

CHAPTER I

General Introduction

1.1. Sugar sensing and signaling in plants

For sessile organisms integration of environmental conditions with metabolism is vital for cellular homeostasis maintenance. An incredibly complex example of this is plants, which need to constantly monitor their energy and carbon status for proper growth and development and ultimately survival. Through photosynthesis plants capture the energy from the sun, transport and use it in the form of sucrose (Suc) and store it as starch. The existence of both sugar exporting (source) and sugar importing (sink) tissues with very different energy requirements unveil the need for a multitude of molecular signals and cross-talk between regulatory networks. Available sugars are no longer viewed exclusively as energy sources but are now recognized as crucial signaling molecules in this sophisticated regulatory network (Rolland *et al.*, 2006; Mayer *et al.*, 2007). They act as global regulators of gene expression to reflect carbohydrate availability (Koch *et al.*, 1996; Rolland *et al.*, 2002; Koch, 2004) allowing the plant to modulate growth and coordinate developmental stages with other cues such as phytohormones (Gazzarrini and McCourt, 2001; Rolland *et al.*, 2002; Leon and Sheen, 2003; Gibson, 2004), nitrogen cycle (Coruzzi and Bush, 2001; Coruzzi and Zhou, 2001), light conditions (Ellis *et al.*, 2002; Paul and Pellny 2003) and stresses (Baena-González and Sheen, 2008).

The understanding of these signals, regulatory networks and their effects are of extreme societal importance. In a world of increasing population, expanding urbanization, climate change, water shortage and depleted fossil fuels; food security and energy security rely inevitably on science for answers (Beddington, 2010). The ability to modulate plant metabolism and shape biomass accumulation, yield and product quality would be a powerful means of improving crop breeding programs (Pellny *et al.*, 2004; McKibbin *et al.*, 2006).

Both growth-promoting and growth-inhibiting regulatory systems are connected to sugar signals. The first and better described include the hexokinase (HXK) glucose sensor, the Target of Rapamycin (TOR) kinase system and more recently the trehalose 6-phosphate (T6P) signal. The growth inhibiting regulatory systems are the Snf1 (sucrose non-fermenting-1)-related protein kinase (SnRK1) and

S1 bZIP transcription factor network. They may function in a cell-autonomous way with accumulating evidence suggesting their crosstalk (Hanson and Smeekens, 2009; Smeekens *et al.*, 2010). The phosphorylation of glucose (Gluc) by HXK produces glucose 6-phosphate (G6P), which can be converted into T6P by trehalose phosphate synthase (TPS). Both G6P and T6P inhibit SnRK1 (Toroser *et al.*, 2000; Zhang *et al.*, 2009), and SnRK1, can in turn, be involved in stimulating the activity of S1 bZIP group of transcription factors (TFs) (Ma *et al.*, 2011). In mammals, orthologs of the SnRK1 complex are known to inhibit TOR activity (Inoki *et al*., 2003).

SnRK1 and TOR systems are evolutionary conserved but much better described in animals and fungi than in plants, where much work is still needed. New challenges include the understanding of the molecular mechanisms underlying gene regulation by sugars to add to the few cis-regulatory elements and trans-acting factors already known (Yu, 1999; Rolland *et al.*, 2002) and also clarification of all interactions at the biochemical level. **This thesis focuses on the T6P/ SnRK1 signaling pathway presenting new biochemical, molecular and physiological results. Therefore, this theoretical introduction focuses primarily on the description of these two players (SnRK1 and T6P), with this first sub-chapter making an overview of the other sugar signaling components and a brief description of how and where they impact plant growth and development, metabolism and stress responses.**

1.1.1. Sugar signals and responses

1.1.1.1 Sucrose metabolism

Suc is synthesised in the cytosol during photosynthesis and it is the predominant translocated sugar in plants. Many sugar signaling effects are triggered by its hydrolytic hexose products like Gluc and fructose (Fru), their phosphorylated forms or downstream metabolic intermediates. An interesting example is T6P which will be later discussed in detail. The following paragraphs and Fig. 1.1 give an

overview of both Suc and starch synthesis and breakdown and respiration illustrating how intricate these sugar signals can be.

During photosynthesis, triose-phosphates (triose-P) formed in the Calvin cycle by carbon dioxide (CO_2) fixation may be exported from the chloroplast to the cytosol. The combination of two of these triose-P molecules produces fructose 1,6-biphosphate (F1,6BP) which is converted to Suc to be used locally or exported to growing (sink) tissues. Suc synthesis is highly regulated by steps upstream of the pathway (for review, see Huber, 1998). Fructose 1,6-bisphosphatase (FBPase) coordinates available carbon supply from the Calvin cycle with the rate of Suc synthesis through interconversion of F1,6BP to fructose 6-phosphate (F6P). This reaction is inhibited by adenosine monophosphate (AMP) and fructose 2,6-bisphosphate (F2,6BP) (Stitt, 1990). AMP and F2,6BP indicate the amount of energy and carbon available respectively. As photosynthesis increases, F2,6BP decreases and together with rising of F1,6BP, FBPase is stimulated. Increase of hexose phosphates then stimulate sucrose phosphate synthase (SPS), the key enzyme of the Suc synthesis pathway that converts uridine diphosphate glucose (UDPG) and F6P to sucrose 6-phosphate (S6P). Increasing G6P activates SPS allosterically and because it inactivates an SPS-kinase, it also leads to activation of SPS by dephosphorylation (Huber and Huber, 1996) (Fig. 1.1). Naturally, F2,6BP concentration also needs to be controlled. This is achieved through the cytosolic ratio of triose-P to Pi. A low ratio leads to the formation of F2,6BP, which in turn inhibits the hydrolysis of cytosolic F1,6BP and reduces Suc synthesis (and vice versa) (Nielsen *et al.*, 2004).

For a detailed description of starch metabolism refer to the reviews by Kotting *et al.* (2010); Zeeman *et al.* (2010) and Geigenberger (2011). Concisely, besides synthesis from glucose 1-phosphate (G1P) in the amyloplasts, starch is also synthesised in the chloroplast from F6P, a Calvin cycle product. ADP-glucose pyrophosphorylase (AGPase) (key enzyme in starch synthesis) undergoes posttranslational redox regulation both by light and sugars. At night, starch break down, subjected to a fine regulation, provides the carbon necessary to prevent

starvation in the absence of photosynthesis. Regulation is such that the amount of accumulated starch during the day is determined by the amount of starch needed for the following night. Secondly, the starch degradation rate during the night is linear in a way that the “perceived” stored amount is fully used up by the beginning of the following day. In fact, recent work by Scialdone *et al.* (2013) suggests that plants actually perform an arithmetic division to achieve this linear degradation rate during the night and present two chemical kinetic models capable of implementing this operation. The exact signals that allow this calculation are yet to be determined, however, T6P accumulation in ethanol-induced overexpressors of TPS lead to a transient increase in starch content during the day (AGPase activation) and a significant inhibition of starch degradation during the night (Martins *et al.*, 2013). The authors suggest that T6P is part of the feedback regulation pathway of starch breakdown. Also, a work by Sulpice *et al.* (2009) showed a close inverse relationship between starch content and growth, suggesting that plants that grow slowly hold back carbon rather than using it for growth. This is another fact that shows how regulation through metabolic signals may be as or more important than the actual availability of carbon.

To be used as a source of carbon and energy, Suc needs to be broken-down. This is catalyzed either by invertases (INV) that irreversibly hydrolyse Suc to Gluc and Fru or sucrose synthases (SUS), present in the cytosol, which produce UDPG, Fru and Pi (Fig. 1.1). INV have multiple locations in the plant cell (cytosol, chloroplast, mitochondria, nuclei) and were recently considered good candidates for the coordination of metabolic processes that take place in the different cell compartments (Vargas and Salerno, 2010). Important new work shows that INV, unlike SUS, are essential for normal growth in Arabidopsis (Barratt *et al.*, 2009). Several SUS knockout mutants, including a quadruple mutant for 4 of the 6 SUS isoforms had normal growth and reproduction while the loss of two of the nine cytosolic isoforms of INV resulted in severe growth inhibition. The authors concluded that carbon supply to non-photosynthetic cells in Arabidopsis may occur primarily through INV.

During respiration maltose, Gluc and G1P from starch degradation together with Gluc, Fru and UDPG from Suc breakdown are further metabolized and feed into the cytosolic pool of interconvertible hexose-phosphates. In the subsequent glycolytic steps F6P is partially oxidised to two pyruvate molecules, adenosine triphosphate (ATP) and reducing power in the form of nicotinamide adenine dinucleotide (NADH). Alternatively, G6P can be converted to ribulose 5-phosphate (Ru5P) in the oxidative pentose phosphate pathway. Pyruvate is then transported into the mitochondria where it is oxidised completely to CO_2 in the tricarboxylic acid cycle (TCA) with production of 10 NADH equivalents per Gluc molecule. In the electron transport chain all these pyridine nucleotides transfer electrons to oxygen releasing free energy mostly used for the production of ATP. Control points exist at all stages of respiration. Glycolysis is regulated from the "bottom-up" by its own products, the plant demand for ATP regulates the electron transport chain (as well as the other stages), the oxidative pentose phosphate pathway is regulated by ferredoxin/thioredoxin system in close coordination with light and all respiratory stages are in close interaction holding and releasing numerous reversible reactions (Fernie *et al.*, 2004). Moreover, the respiratory stages also influence photosynthetic metabolism not only as ATP providers but also at the molecular level. An example of this was the finding that cellular concentrations of citrate and malate have high impact on the expression of genes related to photosynthesis as well as biotic stress, cell wall and protein synthesis (Finkemeier *et al.*, 2013).

Obviously, not all carbon ends up as CO_2 during respiration. Metabolic intermediates of the glycolytic pathway and TCA cycle are the starting point for many other cellular pathways. Besides initiating glycolysis, F6P is the starting point for other catabolic and anabolic processes yielding amino acids and oils for example. It can also be transformed to G1P for starch synthesis and storage or G1P can be transformed into UDPG and adenosine diphosphate glucose (ADPG) which are substrates for the synthesis of the carbohydrates that comprise cell walls such as cellulose. (Bar-Peled and O'Neill, 2011). UDPG can also be combined with G6P to form T6P, which is dephosphorylated to trehalose. T6P concentrations in plants are

extremely low, agreeing with its signaling role (Paul *et al.*, 2008). This pathway will be described in detail later in this chapter.

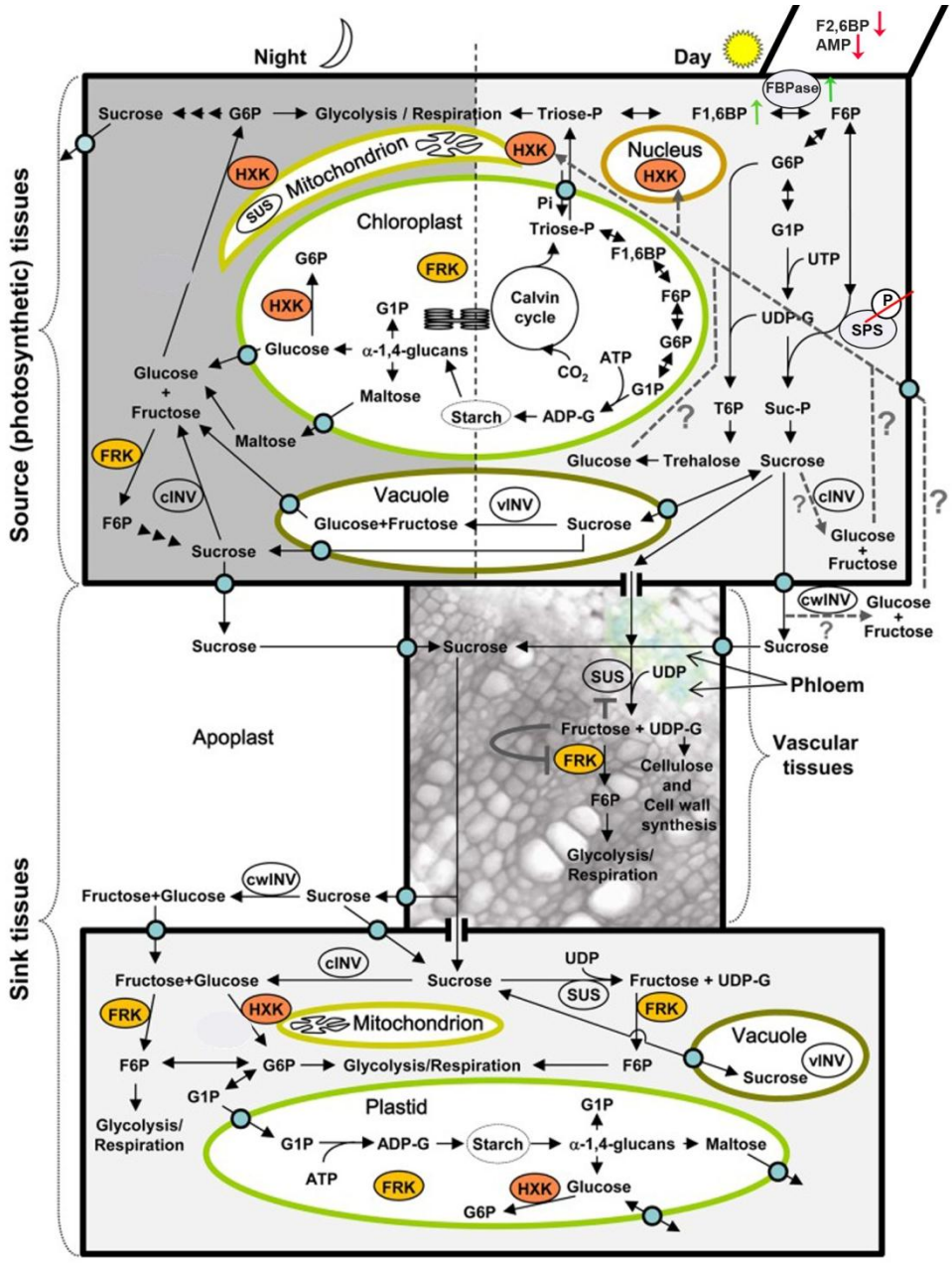

Figure adapted from Granot *et al.*, 2013

Figure 1.1. Schematic representation of sugar metabolism in source and sink tissues during the day and night. During photosynthesis triose-P is exported to the cytoplasm. Consecutive cytoplasmic

enzymatic steps lead to the formation of G6P. Further metabolism of G6P yields Suc. G6P metabolism may also feed the trehalose biosynthetic pathway. During the day in the chloroplast, triose-P is used for the formation of starch. During the dark period, starch is degraded to maltose, Gluc, and G1P. Vacuolar and cytosolic Suc might be cleaved by cytosolic (cINV) and vacuolar (vINV) invertases to produce Gluc and Fru. Within the vascular tissues, Suc can be cleaved by sucrose synthase (SUS) to support vascular development or transported to other sink tissues. Alternatively, Suc might be cleaved by apoplastic (cell wall) invertase (cwINV) to produce Gluc and Fru that would enter sink cells via specific hexose transporters. HXK can also sense Gluc and regulate gene expression. The origin of the Gluc in photosynthetic tissues that is sensed by HXK is not known (possibilities are indicated by dashed lines). The presumed role of Fru and fructokinase (FRK) in vascular tissues is indicated by the grey lines. Blue circles represent transporters. Red and green arrows illustrate an upstream regulation point in Suc synthesis (see text for more detail).

1.1.1.2 Growth and development

Sugars affect plant growth and development directly by providing energy and indirectly through signaling pathways that modulate all aspects of plant morphology, from developmental timings (flowering and senescence onset for example) to organ number and shape (leaf thickness, tuber number, etc). A few examples demonstrate the complexity and broadness of those signaling pathways throughout a plant life cycle.

Starting at the seed germination level, Gluc and Suc have almost opposite effects. During legume seed germination, Suc is linked to cell expansion and starch accumulation whereas Gluc promotes cell division (Borisjuk *et al.*, 2003). However, seed germination can also be inhibited by Gluc through an HXK independent pathway (Dekkers *et al.*, 2004). Interestingly, this sensitivity changes during development (Price *et al.*, 2003); and the same low Gluc levels that are inhibitory for seed germination, are stimulatory for seedling growth and development (Yuan and Wysocka-Diller, 2006). The effects of vacuolar sugar transport activity are still obscure but recent work has shown that Arabidopsis mutants overexpressing the tonoplast monosaccharide transporter TMT1 have modified subcellular sugar distribution, altered assimilate allocation, increased seed biomass and accelerated early plant development (Wingenter *et al.*, 2010). The FUSCA3 transcription factor is

a regulator of seed maturation and was shown to be phosphorylated by AKIN10 (Tsai and Gazzarrini, 2012a). The same authors showed that both FUS3 and AKIN10 act as positive regulators of seed responses to abscisic acid (ABA) but whether phosphorylation of FUS3 by AKIN10 is required for this effect is still not known (Tsai and Gazzarrini, 2012b). Fru was also shown to modulate plant autotrophic transition and early seedling establishment (Cho and Yoo, 2011). This regulation is not linked to the HXK1 Gluc sensor and seems to operate through an FBPase independently of its catalytic activity. Carbon allocation and sugar signals also control transition to flowering. Mutants with no TPS1 expression (enzyme responsible for T6P synthesis in Arabidopsis) have incredibly delayed flowering transition (van Dijken *et al.*, 2004). Sugar metabolic rates also affect leaf longevity and plant senescing onset (Zhang and Zhou, 2012) particularly under low nitrogen availability (Wingler *et al.,* 2006).

Every day new evidences appear showing how plant development is highly dependent on sugar signaling and this holds true for the T6P specific signaling branch which is only starting to be unveiled.

1.1.1.3 Stress

The ability of plants to cope with abiotic and biotic stresses highly impact crop yield and productivity. Abiotic stresses such as heat, cold and drought all cause osmotic stress which is conducive to accumulation of compatible solutes for osmoprotection and osmotic adjustment. Many of these solutes are sugars such as Suc, Gluc, sorbitol or trehalose. However, the signaling role of these carbohydrates and their metabolic intermediates now seem much more relevant in homeostasis maintenance than their osmotic role (Hare *et al.*, 1998). Studies have shown the numerous interactions between metabolic and stress signaling through stress-related hormones such as ABA (Finkelstein and Gibson, 2002) and ethylene (Zhou *et al.*, 1998), through calcium (Guo *et al.*, 2002) and reactive oxygen species (ROS) networks (Bolouri-Moghaddam *et al.*, 2010; Mittler *et al.*, 2011) and through SnRK sub-families SnRK2 and SnRK3 (Hey *et al.*, 2010; Coello *et al.*, 2011). Conditions like

pathogen attack, herbivory, pollutants, shading or drought may cause another very common stressful effect, energy deprivation. The lack of available energy leads to growth arrest, search for alternative nutrient sources through catabolism stimulation and a decrease in biosynthetic pathways (Yu, 1999; Contento *et al.*, 2004; Baena-Gonzalez *et al.,* 2007). SnRK1 is in the centre this energy control and therefore is inevitably linked to stress responses both by controlling the expression of over 1000 homeostasis-linked genes (Baena-González *et al.*, 2007) and by regulating key metabolic enzymes (Sugden *et al.*, 1999b; Harthill *et al.*, 2006). Early sugar-starvation responsive genes include several TPS-like proteins (Osuna *et al.*, 2007) and the observation that T6P inhibits SnRK1 (Zhang *et al.*, 2009) clearly explains previously observed effects of the trehalose pathway manipulation on stress responses (Miranda *et al.*, 2007; Suárez *et al.*, 2009).

Up until now the exact sensors that perceive different stress signals are largely unknown, however, the mechanisms lying behind sugar sensing are beginning to be unveiled.

1.1.2. Sugar Sensing

In plants, different sugar sensing pathways have been identified: the HXK1-dependent and -independent pathways, the glycolysis-dependent pathway (Xiao *et al.*, 2000) and the HXK1-independent, Suc specific pathway (Vaughn *et al.*, 2002). So far the best characterized mechanism is that of Gluc sensing through HXK1.

1.1.2.1 Hexose sensing (HXK-dependent and -independent)

The plant metabolic enzyme hexokinase1 (HXK1), that catalyzes Gluc phosphorylation in the first step of glycolysis, was the first enzyme to also be described as a plant sugar sensor (Jang and Sheen, 1994; Moore *et al.*, 2003). This sensing mechanism seems to be extensively intertwined with plant hormone signaling but the nature of those networks are still not fully understood (Rolland *et al.*, 2006).

The studies that first contributed evidence for this dual-function of HXK followed the expression levels of sugar sensing marker-genes in the presence of different sugars and sugar analogues. Substrate sugars for HXK repressed those marker genes as well as analogues phosphorylated by HXK even if not further metabolizable, whereas non-substrate analogues did not (Jang and Sheen, 1994). Furthermore, overexpression of Arabidopsis AtHXK1 and AtHXK2 produces sugar-hypersensitive transgenic plants whereas plants overexpressing yeast YHXK2 have increased catalytic activity but not Gluc sensing function (Jang *et al.*, 1997). Moore *et al.* (2003) finally confirmed this sensing function of HXK by showing that catalytically inactive HXK1 restored Gluc sensing in the AtHXK1 loss-of-function *glucose insensitive 2* mutant (*gin2*).

HXKs are classified in two groups that differ in their N-terminal sequences that determine their subcellular localization. AtHXK1 (mitochondria-associated) was observed to be transported from the mitochondria to the nucleus (Cho *et al.*, 2006) where it complexes with transcriptional machinery and can bind the promoters of specific genes. This constitutes the first molecular explanation by which HXK1-mediated Gluc sensing may occur (Cho *et al.*, 2006). Besides HXK1, other HXKs were shown to also have regulatory functions (Cho *et al.*, 2009).

HXKs have a plethora of effects from actin-filament reorganization, seed development regulation, control of pollen germination and diverse stress responses but which of these effects are regulated through actual sugar-sensing mechanisms or simply through its metabolic catalytic activity are still not known (Granot *et al.*, 2013).

The hexokinase-independent pathway was established by Xiao *et al.* in 2000 by showing that the expression levels of Gluc-regulated marker genes (like ADP-glucose pyrophosphorylase (AGP), chalcone synthase (CHS), phenylalanine ammonia-lyase (PAL) and asparagine synthetase (ASN)) were the same in wild type and transgenic Arabidopsis either overexpressing or underexpressing HXK1. Also, inhibition of seed germination by Gluc is independent of HXK1 signaling cascade (Dekkers *et al.*, 2004). However, the HXK-dependent and HXK-independent pathways can complement each other in Gluc regulation. A curious example happens

in grape, where VvHT1 (a monosaccharide transporter) is repressed by Gluc through HXK signaling but its post-transcriptional Gluc regulation is HXK-independent (Conde *et al.*, 2006).

The hexose Fru was also suspected to be a sugar signal when an analogue was shown to induce root growth inhibition in lettuce (Kato-Noguchi *et al.*, 2005). A recent work by Cho and Yoo (2011) using a cell-based functional screen identified FINS1 (Fructose Insensitive1), a putative FBPase acting downstream of ABA synthesis as part of that Fru sensing response. Further work is needed to clarify all the interactions among Gluc, Fru and hormone signaling pathways and their effects on plant development.

1.1.2.2 Sucrose sensing

Even though Suc effects can be also caused by its hexose products, there is increasing evidence for Suc-specific regulation of gene expression and plant development processes. Despite several theories (Barker *et al.*, 2000; Li *et al.*, 2012), the actual initial receptor of the Suc sensing pathway is still not known, however, the components of the transduction pathway are better characterized and range from calcium, as a second messenger, (Martínez-Noël *et al.*, 2006), protein kinases (PKs) (Raíces *et al.*, 2003) and protein phosphatases (PPs) (Takeda *et al.*, 1994). A well characterized Suc-regulated process is fructan synthesis where Suc has a double role, both as substrate and initial signal for the transduction pathway. Past a Suc concentration threshold fructans accumulate and the pathway is regulated in a negative feedback manner (Martínez-Noël *et al.*, 2009).

Suc also interacts with SnRK1 (a central integrator of stress and energy signaling) but contrasting results show that in potato Suc activates SnRK1 leading to starch synthesis (Purcell *et al.*, 1998) whereas in maize protoplasts Suc inhibits SnRK1 (Baena-González *et al.*, 2007). This discrepancy may be real and related to differences in metabolic regulation of autotrophic and heterotrophic tissues or experimental inaccuracies due to different growth conditions and sugar treatments

(Baena-González and Sheen, 2008). In fact, feeding high sugar concentrations can itself induce unintended stress responses. Among others, Suc regulates gene expression through TFs such as the basic region-leucine zipper family, bZIP. Particularly, Suc represses translation of the *AtbZIP11* transcription factor (Rook *et al.*, 1998) which regulates numerous sugar-regulated genes in Arabidopsis (Hanson *et al.*, 2008). This regulation happens through a highly conserved upstream open reading frame (Wiese *et al.*, 2004) and requires the full-length of a Suc control peptide of 28 amino acids (Rahmani *et al.*, 2009). Interestingly, KIN10, the catalytic subunit of SnRK1, activates the transcriptional activity of bZIP11 (Baena-Gonzalez *et al.*, 2007), also, bZIP11 increases the expression of the SnRK1 catalytic subunit KIN11 (Hanson *et al.*, 2008) and bZIP11 regulates trehalose metabolism (Ma *et al.*, 2011) that regulates SnRK1. These observations expose a regulatory circuit involving SnRK1, T6P and bZIP11 that links Suc status to growth. The answers to a number of questions, especially concerning the cellular and sub-cellular localization of these players, are still missing pieces of the proposed regulatory loop model (Schluepmann *et al.*, 2011).

1.1.2.3 Cell surface receptors

In yeast and mammals, G-protein-coupled-receptors linked to heterotrimeric guanine nucleotide-binding proteins (G-proteins) sense extracellular Suc and Gluc. Upon sugar binding, the β and γ subunits detach and interact with a variety of downstream effectors launching the desired pathway (reviewed in Bockaert and Pin, 1999). In Arabidopsis one canonical G-protein α-subunit (GPA1) was identified and associated with a wide variety of developmental, light, phospholipid, and hormone responses (Perfus-Barbeoch *et al.*, 2004). GPA1 interacts with two putative receptors: a G-protein coupled receptor1 (GCR1), and a negative regulator of G-protein signaling1 (RGS1) (Chen *et al.*, 2003). Arabidopsis RGS1 overexpressors are hypersensitive to Gluc whereas *rgs1* mutants exhibit insensitivity to 6% Gluc (Chen and Jones, 2004). Accordingly, *gpa1* mutants are hypersensitive to ABA and sugar inhibition of germination confirming their potential role in sugar signaling (Ullah *et al.*,

2002). Furthermore, using different sugars and analogues it was shown that the AtRGS1 functions as a Gluc sensor, independently of HXK (Chen and Jones, 2004).

Again by comparison with yeasts, the Arabidopsis Suc transporter homolog SUT2, was proposed as a putative plant Suc sensor (Barker *et al.*, 2000). However, concrete evidence for such a sensing function was lacking causing a debate (Barth *et al.*, 2003) that still lasts. Further work on this interesting family of Suc transporters is continuing. Recently, using Arabidopsis mutants, the Suc transporter SUT4 was shown to mediate signaling in the Suc/Gluc-induced inhibition of seed germination (Li *et al.*, 2012) further reinforcing the idea that Suc transporters can potentially function as Suc sensors.

1.1.3. Sugar signal transduction

Sugar perception and signal transduction is highly compartmentalized resulting in the establishment of sugar gradients across different subcellular compartments, cells, and organs (Tiessen *et al.*, 2013). Sugars signals are then detected by cellular sensors that pass on information through signal transduction and amplifying cascades to induce a vast array of concerted responses. These final responses will be caused by changes at the gene and protein levels and may involve PKs, PPs, hormones and other signal transduction mediators such as Ca^{2+} (Fig. 1.2).

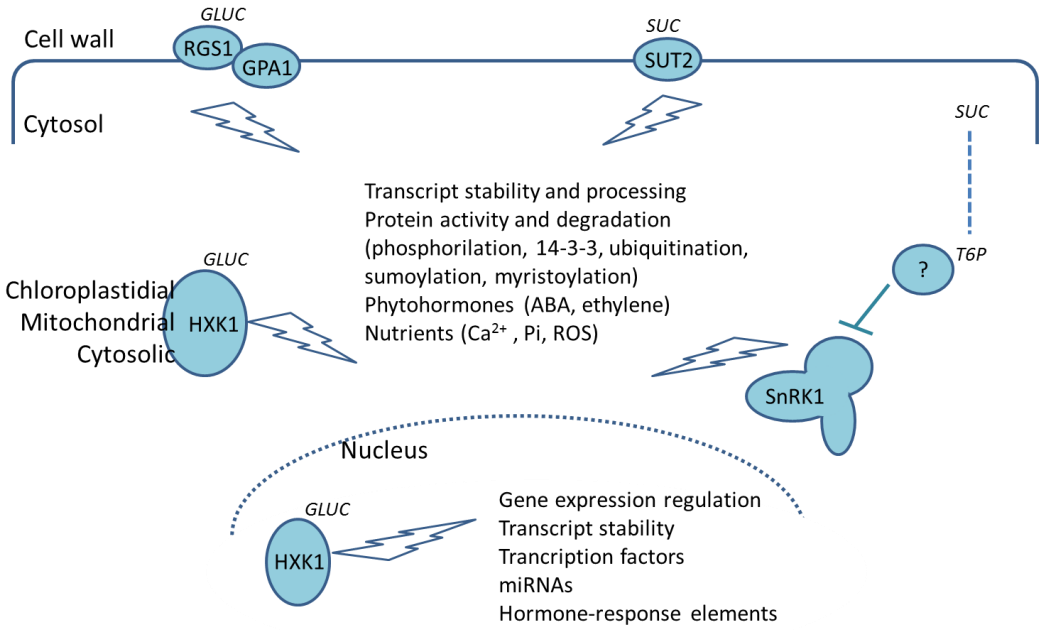

Figure 1.2. Proposed sugar sensors in plants and signal transduction possibilities. Sugar sensors such as regulator of G-protein signaling1 (RGS1), sucrose transporters (Sut2), HXK1 at different locations and T6P interacting protein that inhibits SnRK1 activity sense sugar availability both inside and outside the cell and the signal is transduced/amplified both in the cytosol and nucleus to control cellular metabolism.

1.1.3.1 Gene expression and protein activity regulation

One way in which plants respond to sugar signals is by rapidly adjusting gene expression. Different genetic approaches are used to dissect the complexity of these adjustments. The use of mutants has proven very useful despite the fact that the information on signaling networks became quite limited to early (Arabidopsis) developmental stages due to screens mainly performed in seedlings (Ramon *et al.*, 2008). Two strategies have been used to isolate sugar signaling mutants. A simpler one where the effects of altered external sugar levels on growth and development is observed, with increasing care for osmolarity effects and other vulnerable conditions like high nitrate (Moore *et al.*, 2003). And a more complex one where repression or activation of gene expression in transgenic reporter lines induces altered sugar

responses. A variety of methods allowed the identification of genes specifically regulated by sugars (Sheen, 1990; Rook *et al.*, 1998). And now, microarray techniques allow for a genome-wide identification of sets of sugar-regulated genes (Osuna *et al.*, 2007; Usadel *et al.*, 2008) and the identification of conserved DNA elements in the promoters of co-regulated genes.

During the day/night cycle sugar levels fluctuate and with them transcription levels (Bläsing *et al.*, 2005). Using the starchless *pgm* mutant it was shown that it is the sugar fluctuation that causes the transcriptional responses (Bläsing *et al.*, 2005) and that sugars can even override the expected circadian behaviour (Usadel *et al.* 2008). Decisively, many genes encoding TFs and signaling components are also highly regulated by sugars (Baena-González *et al.*, 2007; Osuna *et al.*, 2007). A good example was the identification of ABA regulated TFs that are required for Gluc signaling (Dekkers *et al.*, 2008). Examples like this provide the molecular link between sugar signaling and multiple regulatory pathways like hormone signaling, unveiling the transcriptional cascades involved in the control of plant growth and development. There is also evidence for regulation at the transcript stability and processing level (Chan and Yu, 1998; Ho *et al.*, 2001). The translation of mRNA can be selective, for instance, through micro-open reading frame control. One example is the transcription of some genes induced by light and sugars which translation is then repressed by high Suc levels (Wiese *et al.*, 2004). All these mechanisms will define the abundance of potential available enzymatic activity to perform a number of tasks, however, proteins themselves are subjected to an array of sugar-regulatory processes that further shape plant responses to sugars.

The most studied post-translational mechanism is perhaps the regulation of protein activity by phosphorylation. Plants express different PKs and PPs. A specific group is the large superfamily of calcium-dependent PKs which are induced by Suc. The SnRK1 proteins, which belong to the calcium-independent kinases group, are also involved in this process and will be later discussed. The binding of 14-3-3 proteins constitutes a further level of regulation. These proteins bind to phosphorylated substrates and can control activity, subcellular localization and

protein-protein interaction (Finnie *et al.*, 1999). The regulated protein degradation by 14-3-3 binding is an important link between nitrate and carbon metabolism during sugar starvation (Cotelle *et al.*, 2000). Sugars can also promote protein degradation via ubiquitin and 26S proteosome binding (Farrás *et al.*, 2001).

1.1.3.2 Phytohormones

Sugar signaling pathways cross-talk with various hormone networks to modulate plant responses.

A link between sugar signaling and hormone biosynthesis was found when the expression of the ABA biosynthetic genes, ABA1–ABA3 was shown to increase with exogenous Gluc causing endogenous ABA to accumulate (Cheng *et al.*, 2002). Also, several sugar-response mutants (like the TF ABI4) are defective in ABA signaling (Niu *et al.*, 2002). Genome-wide analysis will identify additional players in the sugar–ABA signaling network. Recent work showed that in early seedling growth the splicing factor, SR45, negatively regulates sugar signaling by repressing gluc-induced ABA accumulation, and down-regulating ABA signaling genes (Carvalho *et al.*, 2010). An effect that seems to be independent of the sugar sensor HXK1 and instead, related with SnRK1 levels (Carvalho RF, *et al.* unpublished results, in Duque, 2011).

Ethylene signaling pathways also interact with those of sugar and ABA (Gazzarrini and McCourt, 2001; León and Sheen, 2003). The first evidence came from the observation that an ethylene precursor prevented Gluc-induced responses in wild type seedlings (Zhou *et al.*, 1998). Also, ethylene insensitive mutants are Gluc hypersensitive while mutants with ethylene overproduction are Gluc insensitive (Zhou *et al.*, 1998; Yanagisawa *et al.*, 2003). Moreover, auxin also seems involved in these regulatory networks. Work on *hxk/gin2* mutants revealed resistance to exogenous auxin, and auxin-resistant mutants were shown to be insensitive to high Gluc (Moore *et al.*, 2003). More recently genome-wide expression profiling in Arabidopsis

seedlings showed an incredible overlap of Gluc and auxin responses pathways governing root growth and development (Mishra *et al.*, 2009).

Considering the complexity of all this cross-talk, upcoming genome-wide and molecular analyses are likely to bring new clues on the spatio-temporal network and on the nodes that link sugar and hormone signaling.

1.1.3.3 Nutrients and other components

The coordination of carbon and nitrogen metabolism is imperative to maintain proper plant growth and development. It was therefore expected to find intertwined signaling pathways between these two nutrients. There is indeed evidence for this crosstalk that proposes the existence of a single carbon/nitrogen-responsive regulatory cis-element for a subset of genes (Palenchar *et al.*, 2004). In an Arabidopsis genome-wide study the effects of a combination of both Gluc and nitrogen confirmed that most nitrogen responses require the presence of a carbon source (Price *et al.*, 2004). Apparently nitrogen transport is also regulated by sugars. Nitrate and ammonium transporter genes are induced by sugars in Arabidopsis (Lejay *et al.*, 2008). The same happens for the GLB1 gene that encodes an important protein in the regulation of nitrogen assimilation in response to nitrogen, carbon and energy availability (Hsieh *et al.*, 1998). While bZIP11 was suggested as a positive interaction node between Suc-mediated signaling and amino acid metabolism in Arabidopsis (Hanson *et al.*, 2008), a negative correlation between free amino acid biosynthesis and Suc content exists in potato tubers indicating regulatory differences between source and sink tissues (Roessner-Tunali *et al.*, 2003).

Also, Pi has an important role in energy balance and carbon assimilation. Soils are often low in Pi and plants have developed mechanisms to sense and adjust to Pi starvation. Microarray experiments show that about 150 genes are synergistically or antagonistically regulated by Pi and/or Suc revealing crosstalk between the two signaling networks (Müller *et al.*, 2007).

Calcium is another component that interacts with sugar signaling. Calcium channel blockers have revealed that sugar-induced expression of certain genes is actually mediated by calcium signaling (Ohto and Nakamura, 1995).

Stresses cause the production of ROS. Usually seen as damaging agents, ROS can also act as signaling molecules. ROS production and scavenging processes are closely linked and are important for defence signaling, protection against cellular damage and cell-death responses. A new hypothesis is emerging where mitochondria-associated hexokinase is proposed to regulate ROS levels. The synergistic interaction of sugars and phenolic compounds would create an integrated redox system that quenches ROS leading to stress tolerance (Bolouri-Moghaddam *et al.*, 2010).

It seems clear, therefore, that plant sugar signaling is involved in all plant life-cycle stages and in all responses to environmental conditions that lead to alteration of the carbon availability through regulation of cellular activity at multiple levels.

1.2. Trehalose significance and biosynthesis in plants

1.2.1. The trehalose molecule

Trehalose is a dimer of Gluc molecules linked at the reducing ends by a 1-1 alpha bond (Fig. 1.3A), which confers chemical stability. Suc is formed by one molecule of Gluc and one of Fru and together they are the major non-reducing disaccharides in the biosphere. Trehalose is the carbon source in bacteria, fungi, yeast and arthropods while Suc is only found in photosynthetic organisms. The incredibly low levels of trehalose found in plants (to the exception of resurrection species) made it be regarded, until recently, as a vestigial sugar that had been substituted by Suc during plant evolution (Paul *et al.*, 2008).

Contrary to its reactive Gluc moieties, trehalose has a stabilizing nature. It maintains the structure of membranes and macromolecules like enzymes and it is

used as a food additive, cosmetics and vaccine preservative, without loss of structure and bioactivity (Colaço *et al.*, 1992; Paiva and Panek, 1996). In nature it appears at higher concentrations in cells adapted to dehydration, salinity, freezing and heat stress like fungal spores, certain seeds and algae and resurrection plants (Nwaka and Holzer, 1998; Iturriaga *et al.*, 2009). However, it was shown that in yeast, its accumulation was neither necessary nor sufficient for survival under these conditions (Ratnakumar and Tunnacliffe, 2006). This observation and the fact that trehalose pathway genes proliferate in plants (Avonce *et al.*, 2006) despite an accumulation of trehalose metabolites at such low concentrations that are at current instrument detection limits, supported the hypothesis of a signaling role for the trehalose pathway.

1.2.2. Trehalose biosynthetic pathway in plants

About 50 years ago, a first trehalose biosynthetic pathway was discovered (Cabib and Leloir, 1958). In that pathway G6P and UDPG are converted to T6P by trehalose-6-phosphate synthase (TPS) and T6P is then cleaved to trehalose and Pi by trehalose-6-phosphate phosphatase (TPP). It was named TPS/TPP pathway in plants (Fig. 1.3B) or OtsA/OtsB in yeast and was later recognized as the most widespread trehalose biosynthetic pathway in living organisms. There is however four other known pathways found in archea, bacteria and fungi. Plants only possess the TPS/TPP pathway, which is the only one to involve the intermediate T6P. Plants also contain genes that encode trehalase (Muller *et al.*, 2001), the enzyme that cleaves the trehalose 1,1-alpha bond separating the two Gluc moieties in a unique step.

In the mid-1990s, the engineering of *E. coli* trehalose pathway genes into plants, produced phenotypes consistent with altered regulation of growth and development (Goddijn *et al.*, 1997; Vogel *et al.*, 1998). The fact that some of these transformed plants did not accumulate significant amounts of trehalose, made the authors suggest different causes for the observed phenotypes: (1) disturbance of normal plant metabolism; (2) even small amounts of trehalose or T6P could be toxic

to plants; (3) trehalose metabolism might be part of a signaling pathway. Later on, the full sequence of *A. thaliana* genome led to the finding of an unexpected large number of genes coding for TPS and TPP-like proteins (Leyman *et al.*, 2001). Since then, a broad array of effects was found as a consequence of engineering trehalose metabolism confirming a signaling role and supporting the idea that T6P is in fact the mediator of the observed effects (Paul *et al.*, 2008).

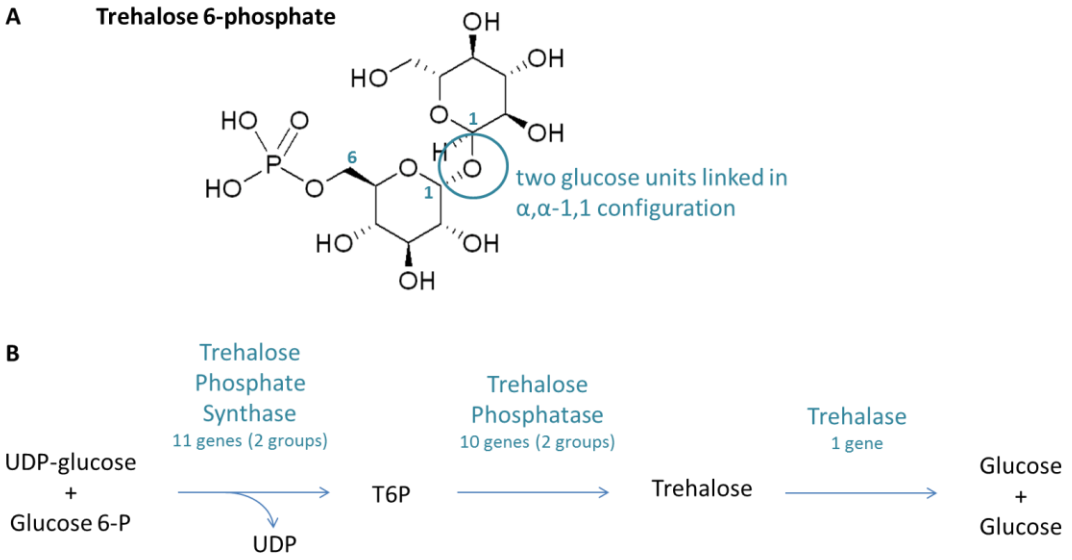

Figure 1.3. The trehalose pathway found in plants. (A) Structure of the naturally occurring isomer of trehalose 6-phosphate presented as Natta projection. **(B)** Enzymatic reactions involved in the biosynthesis and the degradation of trehalose in plants (the TPS/TPP pathway) and indication of the number of Arabidopsis genes that encode for the enzymes of each step. UDP, uridine diphosphate; Glucose 6-P, glucose 6-phosphate; T6P, trehalose 6-phosphate.

1.2.3. The TPS and the TPP genes and enzymes

Interestingly, there are 21 putative genes involved in trehalose synthesis in *A. thaliana,* and only one gene for its breakdown. On the other hand, for Suc metabolism, there are only 8 genes encoding enzymes for its synthesis and as much

as 23 for its breakdown. This suggests the different functions of both disaccharides in plants and unveils the relevant signaling role of T6P in metabolism (Paul, 2007).

Plants contain two classes of *TPS* genes, two classes of *TPP* genes and one class of trehalase genes, all of very ancient origins (Leyman *et al.*, 2001). *TPS* genes seem to have a eukaryotic origin, whereas *TPP* genes are most closely related to those from bacteria and may have derived from the endosymbiotic bacterial ancestor of mitochondria (Avonce *et al.*, 2006). All of the Arabidopsis TPS homologs contain at their C-terminal end a TPP-like domain, but in class I (AtTPS1 to AtTPS4) the TPP-like domain is only weakly conserved whilst class II (AtTPS5 to AtTPS11) contains conserved TPP motifs. An auto-inhibitory N-terminal extension at the AtTPS1 protein that restricts its activity *in vivo* makes it unique among TPSs (van Dijck *et al.*, 2002). In Arabidopsis only TPS1 has demonstrable TPS activity (Blázquez *et al.*, 1998). All the other TPSs lack both TPS and TPP activities (Harthill *et al.*, 2006; Ramon *et al.*, 2009, Vandesteen *et al.*, 2010). *AtTPS1* expresses throughout the plant like flower buds, siliques, small rosette leaves, and embryos (van Dijken *et al.*, 2004; Gómez *et al.*, 2010) and the same is true for class II TPSs (Paul *et al.*, 2008; Ramon *et al.,* 2009). *AtTPS2-4*, in contrast, seems to be restricted to siliques and seeds (Paul *et al.*, 2008).

The 10 Arabidopsis TPP homologs (AtTPPA–J) are single domain proteins. Until very recently out of the 10 *TPPs*, only *AtTPPA* and *AtTPPB* proteins were believed to have catalytic activity (Vogel *et al.*, 1998). However, Vandesteene *et al.* (2012) have just shown by heterologous expression in yeast that all TPP genes encode active TPP enzymes.

Only one trehalase gene exists in Arabidopsis, *AtTRE1* (Muller *et al.*, 2001). Therefore genetic radiation seems to have happened at the level of T6P rather than trehalose (Avonce *et al.*, 2006; Lunn, 2007). In fact, analysing the sequences of TPSs and TPPs homologs it becomes evident that the genetic drift is not random and that evolutionary selection retained the specificity of each of these genes keeping synonymous codons (Avonce *et al.*, 2006) which advocates specific functions for all genes.

In Arabidopsis, trehalase appears to be bound to the plasma membrane with the catalytic domain on the apoplastic side of the cell (Frison *et al.*, 2007). AtTPS1 seems to be cytosolic (Geelen *et al.*, 2007) whereas AtTPPA, AtTPPG and AtTPPI were predicted to localize in the chloroplast (Emanuelsson *et al.*, 2007). These data seems to indicate that T6P is likely synthesised in the cytosol and possibly transported to the chloroplasts where it then could be cleaved to trehalose. Trehalose would be broken down only after export to the apoplast. This proposed subcellular distribution together with the fact that T6P controls redox-regulation of chloroplastidial AGPase (Kolbe *et al.*, 2005) points towards central functions in organelle feedback regulation, for example, carrying information on carbon status from the cytosol to the chloroplast regulating starch synthesis (Schluepmann and Paul, 2009). These considerations are in agreement with a recent work where nonaqueous fractionation of Arabidopsis leaves together with estimation of subcellular volumes predicted that in mesophyll cells T6P is predominantly located in the cytosol (about 70%) with concentrations ranging from 4 and 7 µM, but also present in chloroplasts (around 20%), from 0.2 and 0.5 µM and vacuole (approximately 10%) 0.05 µM (Martins *et al.*, 2013).

1.2.4. Tight control of the trehalose metabolism

Small changes in T6P levels have a big impact on plant metabolism and development (Schluepmann *et al.*, 2003) and both too much or too little can have lethal effects. From this point of view, T6P metabolism must be tightly controlled. In fact, recent evidence shows how all TPS and TPP homologs are differentially regulated, some by hormones (Leonhardt *et al.*, 2004, Brenner *et al.*, 2005), others by stresses such as induced darkness (Piippo *et al.*, 2006), hypoxia (Liu *et al.*, 2005) or nitrogen fluctuation (Wang *et al.*, 2003). The observation that both starvation and high sugar can induce T6P synthesis, for example, brings to mind the importance of differential regulation in different tissues with opposing energy requirements and functions like source versus sink (Paul, 2007). The case of maize *ramosa3* mutants, lacking expression of a TPP in base cells of young axillary meristems that present

radical inflorescence branching defects illustrates well how restricted and directed can be the expression of these genes (Satoh-Nagasawa *et al.*, 2006). To complicate further, post-translational modifications such as phosphorylation of TPSs both by SnRK1 or Ca^{2+}-dependent kinases and interaction with partners like 14-3-3 proteins (Harthill *et al.*, 2006) also contribute to the regulation of trehalose metabolism. Only further work on the regulation of TPS and TPP genes expression, on the subcellular localization of their enzymes and identification of trehalose/T6P transport molecules can clarify the reasons for such a plethora of trehalose metabolic genes.

1.2.5. T6P in plant development

The importance of T6P for normal plant development was first noticed in transformed tobacco plants over-expressing the TPS genes from yeast (Romero *et al.*, 1997) or *E. coli* (Goddijn *et al.*, 1997). Further effects were observed by Pellny *et al.* (2004) in tobacco plants overexpressing either TPS or TPP. Lower T6P produced plants with increased leaf area and decreased photosynthesis while the contrary was observed for plants with higher T6P. However, the larger leaf area of TPP-expressing plants still resulted in increased plant growth. Moreover, Arabidopsis *tps1* mutant, lacking TPS1, stops the germination process at the torpedo stage when cell expansion and storage reserve accumulation should occur (Eastmond *et al.*, 2002; Schluepmann *et al.*, 2003). This phenotype is not rescued by trehalose feeding but it is by expressing the (quite structurally different) *E. coli* TPS (Schluepmann *et al.*, 2003) indicating that T6P is the real cause for the observed effects. Rescuing attempts of *tps1* embryos both with dexamethasone-inducible system (van Dijken *et al.*, 2004) and use of seed-specific promoter (Gómez *et al.*, 2010) produced plants with phenotypic abnormalities throughout development that accumulated soluble sugars and starch. More recently TILLING mutants with weak *TPS1* alleles showed similar phenotypic defects and also ABA hypersensitivity (Gómez *et al.*, 2010). These results showed that T6P has a role in cell cycle activity and cell wall biosynthesis (Gómez *et al.*, 2006) and that it may act through ABA signaling and sugar metabolism to coordinate embryo maturation and vegetative growth.

Flowering time and inflorescence architecture are also affected by T6P. Both rescued *tps1* mutants (van Dijken *et al.*, 2004) and TILLING populations with weak *TPS1* alleles (Gómez *et al.*, 2010) failed or had retarded flowering. In fact, T6P was recently shown to exert its effects on flowering both in the leaves and shoot meristems, adding TPS1 to the genetic background of flowering-time control (Wahl *et al.*, 2013). Flowering is known to be interconnected to starch mobilization and momentary increase in leaf carbohydrate content followed by export to the meristem (Corbesier *et al.*, 1998, 2002). Suc feeding was also shown to induce flowering in mutants and under conditions expected to cause flowering delay (Roldán *et al.*, 1999). The mechanisms involved in this sugar-controlled flowering transition are still not known but seems evident that they pass through T6P as a signal of Suc status. The discovery that *ramosa3* maize mutants, which present aberrant cob morphology due to inflorescence increased branching, was in fact a mutation in a functional TPP gene (Satoh-Nagasawa *et al.*, 2006) further established that trehalose metabolism can influence specific developmental pathways. Bearing in mind that TPS6 seems not to possess catalytic activity (Ramon *et al.*, 2009) it was interesting to learn that Arabidopsis TPS6 mutants have altered inflorescence branching (Chary *et al.*, 2008). This is further indication that TPS and TPP proteins may have signaling functions, possibly by sensing T6P contents.

T6P also seems to have a role in senescence. Arabidopsis with high T6P levels had increased anthocyanin concentrations, whereas plants with reduced T6P accumulated less anthocyanin and have delayed senescence both during normal growth and Gluc treatment to induce senescence (Wingler *et al.*, 2012). Unexpectedly, this T6P-induced senescence was signalled during early development.

During a plant's life cycle, from seed germination to senescence, the trehalose pathway seems to be involved in every step of the way (Fig 1.4).

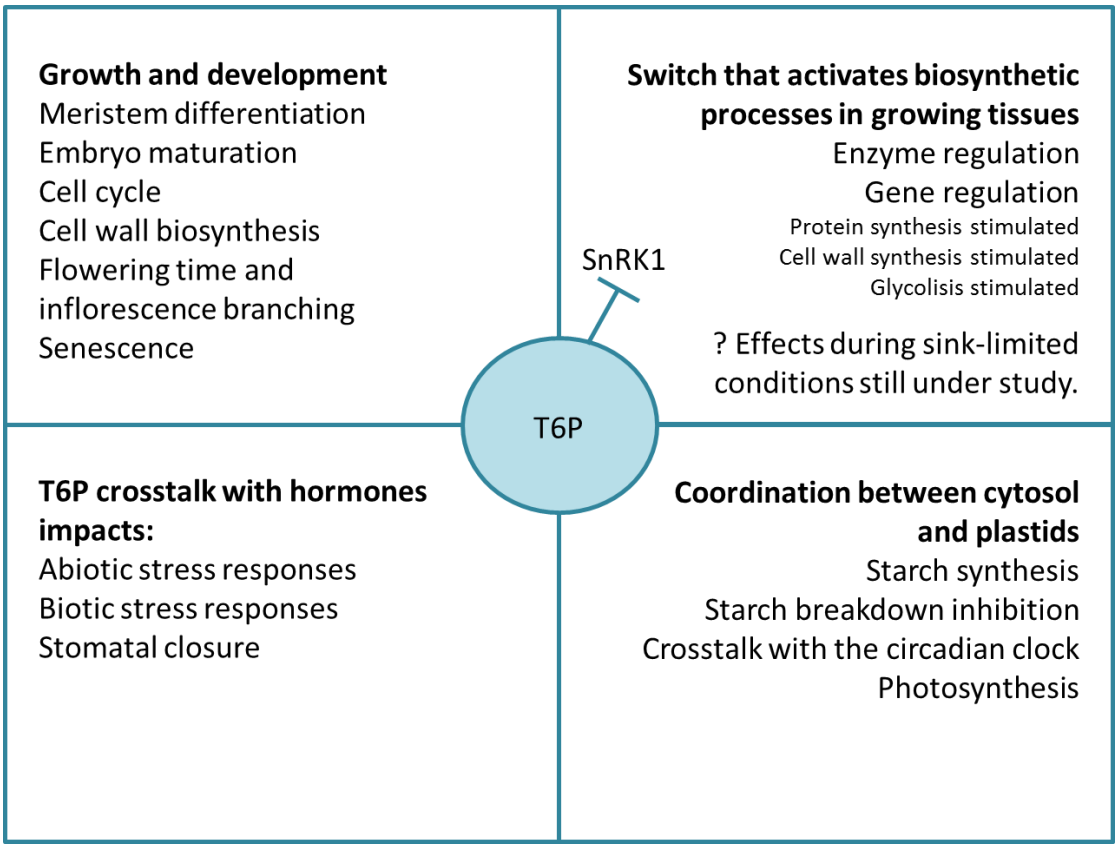

Figure 1.4. Overview of T6P impacts on plant development and environmental responses. Most effects are not fully described and some may be mediated by SnRK1.

1.2.6. T6P signaling role in plant carbohydrate metabolism

T6P levels correlate well with those of Suc either after Suc feeding and re-illumination at the end of the night (Lunn *et al.*, 2006). The same correlation was found during wheat grain development (Martínez-Barajas *et al.*, 2011). These observations indicate that T6P may signal carbon availability in the form of Suc. In accordance, mutants with low levels of T6P stop growing and accumulate respiratory intermediates in sugar-supplied media whereas the same sugar-rich media improves growth in mutants with elevated levels of T6P (Schluepmann *et al.*, 2003). T6P was therefore proposed to be necessary for carbon utilization.

In 2009 T6P was shown to inhibit SnRK1 (Zhang *et al.*, 2009), a global metabolic regulator. The inhibition was achieved at low micromolar T6P concentrations via a still elusive intermediate factor at a site distinct from the catalytic site. The inhibition was strongest in seedlings and young growing tissues and absent from mature leaves that lacked the intermediate factor. The *in vitro* inhibition of SnRK1 by T6P was confirmed *in vivo* by comparing effects on gene expression of Arabidopsis with altered T6P (Zhang *et al.*, 2009) with Arabidopsis with altered AKIN10 expression (Baena-Gonzalez *et al.*, 2007). It was found that genes normally induced by SnRK1 were repressed by T6P and those normally repressed by SnRK1 were induced. Overall there was a strong upregulation of biosynthetic pathways by T6P. These data finally explained how growth of seedlings on Suc was promoted by T6P (Schluepmann *et al.* 2003). More recently, inhibition of SnRK1 by T6P has also been established in a transgenic sugarcane suspension cell line (Wu and Birch, 2010), in wheat grain extracts (Martínez-Barajas *et al.*, 2011), and in potato tubers (Debast *et al.*, 2011).

SnRK1 signals energy deficiency during stress/starvation conditions (Baena-González *et al.*, 2007; Cho *et al.*, 2012). Starvation can for example be induced by extended nights, which cause total depletion of starch reserves, followed by soluble sugars decline (Gibon *et al.*, 2004; Stitt *et al.*, 2007). Growth is not immediately restored by re-illumination but sugars start to accumulate and with them, so does T6P (Lunn *et al.*, 2006), which in turn stimulates the redox activation of AGPase (Kolbe *et al.*, 2005) and inhibits SnRK1 to induce growth (Zhang *et al.*, 2009). T6P is acting here as a central signaling molecule that allows appropriate responses to starvation conditions. However, not all stress conditions lead to starvation, in fact the contrary is sometimes true. Carbohydrates can for example increase under moderate drought stress and cold stress. In grapevine, T6P content was shown to increase and correlate with Suc content in response to chilling (Fernandez *et al.*, 2012) and the same was observed in Arabidopsis seedlings at 10ºC with stationary growth rates (see Chapter 5 and Table 1.1). Under such sink-limited conditions, when tissue sugar

content is uncoupled from growth, it is not clear how the T6P/SnRK1 signaling pathway operates (Table 1.1 and Chapter 5).

The bZIP11 is a transcription factor involved in gene expression regulation in response to sugar starvation (Hanson *et al.*, 2008). Synergisms in gene expression regulated by SnRK1 and bZIP11 (Baena-González *et al.*, 2007) led the authors Baena-González and Sheen (2008) to propose a connection between SnRK1 and bZIP11 transcription factor. Curiously, while Suc induces transcription of the *bZIP11* gene it also inhibits its translation (Rook *et al.*, 1998; Wiese *et al.*, 2004) resulting in reduced T6P levels (Ma *et al.*, 2011). More recently, it was observed that bZIP11 over-expressing plants were resistant to exogenously applied trehalose growth-inhibition and accumulated high levels of T6P with concomitant reduction of SnRK1 activity (Delatte *et al.*, 2011) (Table 1.1). These observations seem to indicate that bZIP11 is overriding the growth inhibitory effect of high T6P. Moreover, *KIN10 o*verexpression also induced resistance to trehalose (Table 1.1) and a subset of genes induced by *bZIP11* were also up-regulated by *KIN10* (Delatte *et al.*, 2011). Because a significant number of these genes respond to trehalose feeding as if both factors were less active, this seems to indicate bZIP11 as a likely target of SnRK1. The behaviour of these transgenic plants (Table 1.1) plus the fact that overexpression of either KIN10 or bZIPP11 do not alter the expression levels of one another and that bZIP11 did not affect SnRK1 activity, indicate that bZIP11 and KIN10 interactions are apparently post-transcriptional with AKIN10 affecting either bZIP11 activity or subcellular localization (Fig. 1.5).

Putting all the pieces together, one can consider the existence of a regulatory loop controlling growth in response to sugars as put forward by Delatte *et al.* (2011): Suc availability increases T6P which inhibits SnRK1 which in turn inhibits bZIP11-dependent gene expression. This explains why both too much and too little T6P can cause growth arrest. Up-regulation of biosynthetic pathways due to elevated T6P during trehalose feeding causes “an attempt to over-expend” inexistent resources and mutants incapable of synthesising or accumulating T6P even with

available sugars do not grow simply because the biosynthetic pathways are shut down by active SnRK1 and bZIP11 (Table 1.1 and Fig. 1.5).

Table 1.1. Impact of available metabolizable sugars and trehalose on growth aptitude, T6P accumulation and SnRK1 and bZIP11-dependent gene expression for growth in Arabidopsis WT, otsB (overexpressor of the yeast TPP gene), bZIP11 (overexpressor of the transcription factor bZIP11) and AKIN10 (overexpressor of SnRK1 catalitic subunit).

The symbols + and – denote plant aptitude or inability for growth respectively, and increased or decreased T6P accumulation/gene expression respectively. When T6P accumulates (+) inhibits SnRK1 promoting anabolism (+) at least in part through the activity of bZIP11 (+). The most recent references that allowed the establishment of a regulatory loop involving T6P-SnRK1-bZIP11 mediating metabolite control over growth are also indicated.

	Plant growth	T6P	SnRK1-dependent gene expression for growth	bZIP11-dependent gene expression for growth	References
	Available metabolizable sugars				
WT	+	+	+	+	Zhang *et al.*, 2009
otsB (TPP)	-	-	-	-	Schluepmann *et al.*, 2003
bZIP11	-	+	+	-	Ma *et al.*, 2011 Delatte *et al.*, 2011
KIN10	-	+	-	-	Baena-González *et al.*, 2007 Delatte *et al.*, 2011
	Trehalose feeding				
WT	-	+	+	+	
WT (high metabolizable sugars)	+	+	+	+	Schluepmann *et al.*, 2004 Delatte *et al.*, 2011
bZIP11	+	+	+	+	Delatte *et al.*, 2011
KIN10	+	+	+	+	Delatte *et al.*, 2011
	Relief of sink-limited conditions				
WT	+	+	+	?	Chapter 5
otsB (TPP)	-	-	-	?	
KIN10	-	+	-	?	

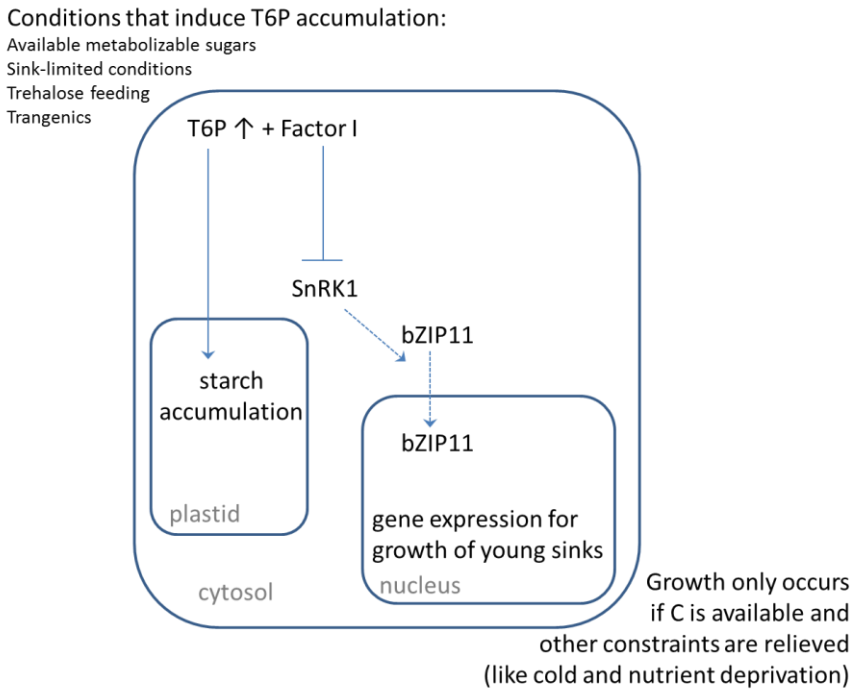

Figure 1.5. Model of the T6P-SnRK1-bZIP11 regulatory loop that mediates metabolite control over growth. Under conditions that induce T6P accumulation SnRK1 is inhibited through a separable factor. With inactivated SnRK1, bZIP11 is not "triggered" (activated and/or transported to the nucleus – dashed lines) and so gene expression for growth can occur. That is why overexpression of bZIP11 may act as a surrogate for inactive SnRK1. However, actual growth can only take place if carbon is available and if simultaneously other growth constraints are relieved (like cold or nutrient deprivation). T6P also induces starch accumulation (possibly involving AGPase redox activation) which can be an important factor influencing the final growth response.

1.3. The SNF1 family of protein kinases

All life forms need to monitor carbon and energy availability to survive. Conserved mechanisms have evolved in eukaryote groups to sense and respond to fluctuating cellular energy levels. One such mechanism is a family of serine/threonine kinases that act as central integrators of stress and energy regulation (reviewed by Halford *et al.*, 2004; Ghillebert *et al.*, 2011). Activated by starvation and low energy conditions, the sucrose non-fermenting1 (SNF1) in yeasts, AMP-activated kinase

(AMPK) in animals and Snf1-related kinase1 (SnRK1) in plants enable energy homeostasis and survival through up-regulation of energy conserving and catabolic metabolism and down-regulation of energy consuming processes (Carling *et al.*, 1994).

SNF1 protein kinase was identified in *Saccharomyces cerevisiae* in 1981 in a screening for mutants unable to utilize Suc as energy source (Carlson *et al.*, 1981). This budding yeast uses Gluc as preferred carbon source and the derepression of genes involved in metabolism for use of alternative carbon sources is crucial to respond to environmental Gluc starvation (Gancedo, 1998; Carlson, 1999). The absence of growth on Suc medium of the isolated *snf1* mutant was caused by defects in expression of the *SUC2* (invertase) gene (Carlson and Botstein, 1982). The *snf1* mutant will also starve on medium containing other sugars, including galactose, maltose or nonfermentable carbon sources such as glycerol or ethanol. SNF1 is also required in various developmental processes like meiosis, and sporulation (Honigberg and Lee, 1998), filamentous growth and biofilm formation (Kuchin *et al.*, 2002) and even in the control of ageing and longevity (Lorenz *et al.*, 2009). Furthermore it is involved in adjusting the biosynthesis of reserve carbohydrates and the recycling of macromolecules and organelles by means of autophagy (Wang *et al.*, 2001). The list continues as SNF1 was also found to be responsive to an array of stresses, such as sodium ion stress, oxidative stress and alkaline pH (Hong and Carlson, 2007).

Only in 1994 was the AMPK catalytic subunit cDNA cloned and identified as the mammalian ortholog of Snf1 (Woods *et al.*, 1994) and realised the functional similarity of both enzymes. AMPK is activated under conditions that increase the AMP/ATP ratio (usually stresses) like Gluc deprivation, hypoxia, ischemia, or oxidative stress. To restore homeostasis AMPK up-regulates energy producing catabolic metabolism, such as glycolysis and fatty acid oxidation and down-regulates energy-consuming anabolism like protein, sterols and fatty acids synthesis (Hardie, 2007). An expressive example of these mechanisms is seen in *Caenorhabditis elegans* larvae during dormancy stage. During this period they stop feeding but

remain active extremely long-lived, non-ageing and stress-resistant. Metabolically, they have reduced insulin-like signaling and accumulate nutrients. However, mutants lacking the AMPK signaling enter this dormancy phase normally, but rapidly consume their stored energy and die prematurely (Narbonne and Roy, 2009). This is consistent with the view that AMPK also acts as a metabolic regulator at the whole body level. In mammals it integrates nutritional and hormonal signals in the hypothalamus to control food intake and body weight (Minokoshi *et al.*, 2008) or by inhibiting insulin production in response to low blood Gluc levels (da Silva Xavier *et al.*, 2003). In humans, this has tremendous impact on growth, development and survival causing a variety of disorders ranging from metabolic syndrome, insulin resistance, obesity, cardiovascular diseases, and age-related pathologies like cancer, dementia and stroke (Steinberg and Kemp, 2009) with possible impact on longevity (Mair *et al.*, 2011).

SnRK1 was first identified when its cDNA was isolated from rye endosperm and shown to complement the snf1 mutation in yeast (Alderson *et al.*, 1991). Other SnRK1 genes have since been characterized in various plant species (reviewed by Halford and Hardie, 1998). It is worth mentioning that in cereals the SnRK1 gene family subdivides into two groups, SnRK1A, expressed throughout the plant and more similar to SnRK1 from dicotyledonous plants and SnRK1B, mainly expressed in the seed and exclusive to monocotyledonous species (Halford and Hardie, 1998). The SnRK family has proliferated further into large SnRK2 and SnRK3 plant sub-families that diverged more from AMPK and SNF1 than have SnRK1s (Halford and Hey, 2009). These sub-families have particularly relevant roles in abiotic stress responses (Coello *et al.*, 2010) and will not be considered further in this thesis. **In this sub-chapter the structure and regulation of the plant SnRK1 will be overviewed and compared when pertinent with SNF1 and AMPK. SnRK1 function in plant metabolism and stress signaling will also be dissected.**

1.2.1. Structure and subunits

SNF1, AMPK and SnRK1 proteins have the same heterotrimeric structure with about 47% identical amino acid sequence; the catalytic subunit is the most conserved with about 60% cross-species similarity (Halford *et al.*, 2000/2003). The complexes require an α catalytic subunit and two regulatory subunits, β and γ that contribute to protein stability, substrate specificity and subcellular localization. Due to the variable number of isoforms for each subunit, the number of possible heterotrimeric combinations varies significantly between organisms. However, the exact number of possibilities is still uncertain due to differential expression, alternative splicing and alternative transcription initiation. In plants, the catalytic α subunit is 58 kDa (Alderson *et al.*, 1991) has two confirmed isoforms AKIN10 and AKIN11 and possibly a pseudogene *KIN12*. The kinase domain is located in the N-terminal half of the protein (Carling *et al.*, 1994; reviewed in Ghillebert *et al.*, 2011). The enzyme is active when a conserved threonine residue located in the activation loop of the kinase domain is phosphorylated by upstream kinases (reviewed in Polge and Thomas, 2007; Ghillebert *et al.*, 2011). The C-terminal half of the subunit contains, from the kinase domain, an auto-inhibitory regulatory sequence (AIS), a β-subunit interaction domain (β-SID), and a leptomycin-sensitive nuclear export sequence (NES) (Kazgan *et al.*, 2010) (Fig. 1.6A). The β-subunits contain a kinase interaction sequence (KIS) domain (Jiang and Carlson, 1997), overlapped by a glycogen-binding domain (GBD) with still questionable regulatory activity (Steinberg and Kemp, 2009). At the C-terminal end of this subunit there is a domain called association with SNF1 complex (ASC) that mediates the interaction with the γ-subunit (Jiang and Carlson, 1997) (Fig. 1.6A). In the plants KIN β3-type subunit the GBD/KIS domain is lacking and is the association-with-SNF1-complex domain that guarantees the interaction of both α- and γ-subunits (Fig. 1.6B). This protein still complements a yeast mutant lacking all β-subunits (Gissot *et al.*, 2004). Moreover, the β-subunits also harbor a variable domain that controls subcellular localization of the kinase complexes (Hedbacker and Carlson, 2006) or N-myristoylation involved in membrane targeting and binding (Steinberg and Kemp, 2009). The γ-subunits have a divergent

N-terminal domain followed by two pairs of cystathionine-beta-synthase (CBS) sequences, called Bateman domains, that bind adenosine derivatives (Steinberg and Kemp, 2009) (Fig. 1.6A). The KINβγ-type is specific to plants and seems to result from γ-subunit fusing with a GBD domain (Fig. 1.6B) that can still complement the yeast snf4D mutant (Lumbreras *et al.*, 2001; Gissot *et al.*, 2006).

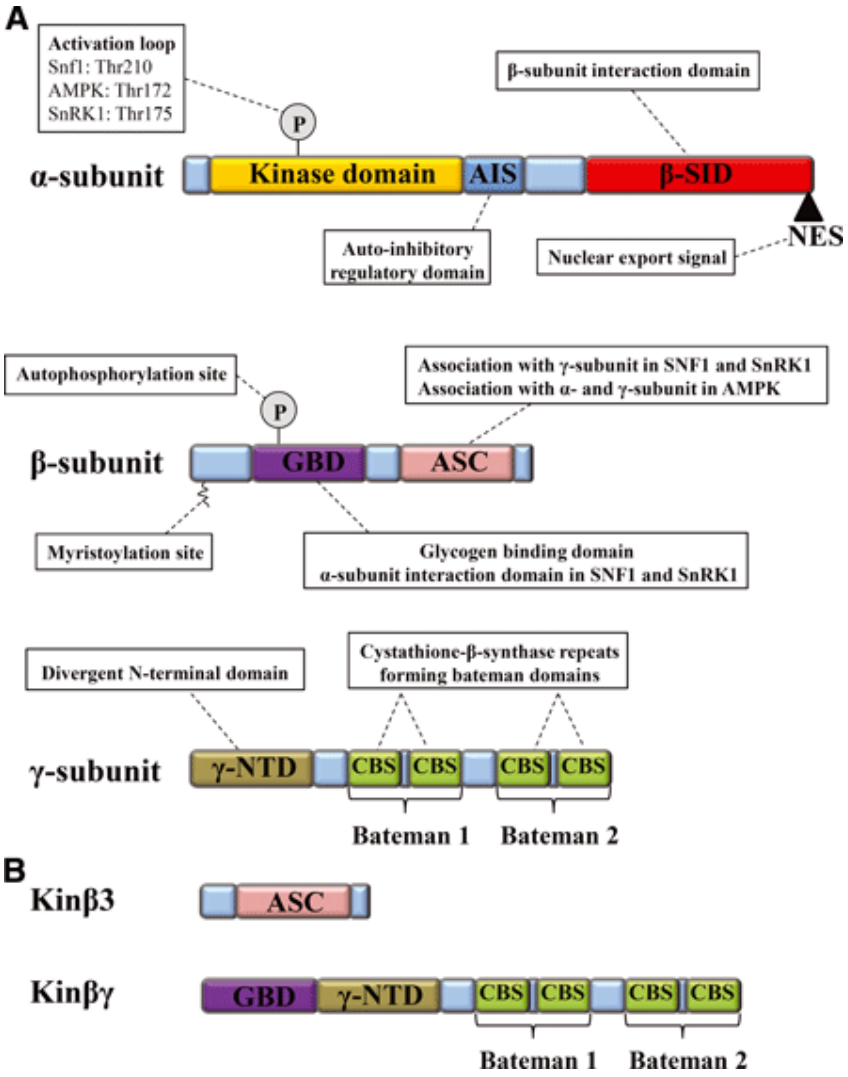

Figure from Ghillebert *et al.*, 2011

Figure 1.6. Structural and functional features of (A) α-, β- and γ-subunits of the SNF1 / SnRK1 / AMPK protein kinase complexes and **(B)** plant specific Kinβ3 and Kinβγ subunits (see text for details).

1.2.2. Activity regulation

The better characterized activation system of SnRK1 kinases is through phosphorylation of a conserved threonine residue located in the activation loop of the kinase domain (Sugden *et al.*, 1999a) by upstream kinases. Two of these kinases were recently identified and named SnRK1-activating kinase-1 and -2 (SnAK1 and SnAK2) (Hey *et al.*, 2007) but are also known as geminivirus rep-interacting kinases (GRIK1 and GRIK2) (Shen *et al.*, 2009). Downstream phosphatases that inactivate SnRK1 *in vivo* through dephosphorylation were recently identified, two clade A type 2C protein phosphatases (Rodrigues *et al.*, 2013) known repressors of the ABA pathway confirmed a point of cross-talk between SnRK1 regulation and ABA responses (Coello *et al.*, 2012). Very recently the PK AvrPto-dependent Pto-interacting protein3 (Adi3), a known suppressor of cell death still without known downstream interactors was shown to phosphorylate a β-subunit on a serine residue inactivating the heterotrimer. The authors suggest that this may be the way by which Adi3 exerts its cell death suppression activity (Avila *et al.*, 2012).

In mammals, regulation processes relate to AMP/ATP ratios where AMP is both able to protect against dephosphorylation, promote phosphorylation and allosterically activate the catalytic subunit (Davies *et al.*, 1995). The nucleotide binding sites are located in two Bateman domains in the γ-subunit. The two Bateman domains form 4 cavities where ligands can bind, however, in mammalian γ1 only three of the cavities bind nucleotides, conventionally numbered 1, 3 and 4. AMP binding in site 4 has no known function and appears to be so tight that it does not exchange with ATP or ADP. There are therefore, only 2 remaining sites where AMP binds reversibly in competition with ADP or ATP (high affinity site 1 and low affinity site 3). Quite differently, in yeast, site 4 binds both AMP or ADP and site 2 can also bind either nucleotide (Townley and Shapiro, 2007). The fact that in mammals the allosteric regulation of AMPK by AMP is antagonized by NADH, which only binds site 1, whereas dephosphorylation is not affected, indicate that this outcome is caused by AMP binding at site 1. It was recently described that ADP also prevents AMPK

dephosphorylation (Xiao *et al.*, 2011), an effect caused by ADP or AMP binding at site 3. Because site 3 binds AMP and ADP with similar affinity, and because ADP concentration in cells is usually much higher than that of AMP, Hardie *et al.*, (2011) argue that ADP and not AMP is the main signal that promotes AMPK phosphorylation, especially under moderate stress. Under severe stress the rise in AMP would amplify AMPK activity through allosteric activation. Yeast SNF1 and plant SnRK1 are not allosterically regulated by AMP/ATP and in fact, little is known about this matter, especially regulation of SnRK1. However, mutations in yeast that contribute to AMP binding, relieve Gluc inhibition of Snf1 (Momcilovic *et al.*, 2008); and SnRK1 dephosphorylation was shown to be inhibited by physiological concentrations of AMP (Sugden *et al.*, 1999a). The authors speculate that AMP may be an important intracellular messenger not only in animals but also in plants.

Other regulatory processes have been recently uncovered, especially for AMPK, and are under scrutiny for SnRK1. One such case is ubiquitination. The binding of small ubiquitin peptides to receptor proteins controls proteasomal degradation, membrane trafficking, protein translation and DNA repair (Miranda and Sorkin, 2007). In 2008 Qi *et al.* showed that AMPKβ subunit could undergo ubiquitination reducing AMPK stability possibly targeting it for proteasomal degradation. In the same year Lee *et al.* showed that AKIN10 could also be degraded following ubiquitination. SUMOylation also involves the binding of ubiquitin-like modifiers to a protein receptor but the outcomes are different and include the control of protein-protein interactions and protein activity modulation (Wilkinson and Haenley, 2010). AMPKβ2 subunit but not AMPKβ1 was shown to suffer SUMOylation (Rubio *et al.*, 2013). The authors suggest that this differential sensitivity may allow the selective activation of organ-specific AMPK complexes. SUMOylation of AMPKβ2 increases the catalytic subunit phosphorylation status either by promoting phosphorylation or by preventing dephosphorylation. Interestingly, sumoylation seems to be antagonist and to compete with ubiquitination of the AMPKβ2 subunit adding yet another layer of complexity to these regulatory processes (Rubio *et al.*, 2013). In yeast SUMOylation was observed in the Snf1 catalytic subunit, an effect promoted by Gluc to inhibit its

activity (Simpson-Lavy and Johnston, 2013). In plants, the observation of high molecular weight SnRK1 complexes suggests SUMOylation events. Baene-Gonzalez and co-workers obtained SUMOylated SnRK1 using a reconstituted SUMOylation pathway in *E. coli* and are now studying the process *in planta* (unpublished). Myristoylation is another regulatory process and involves the irreversible addition of a myristoyl group usualy to a glycine residue during translation. In AMPK, myristoylation of the β subunit is necessary for AMP promoted phosphorylation of the catalytic subunit but not for its allosteric activation (Oakhill *et al.*, 2010). In yeast, preventing myristoylation of one of the β subunits reduces resistance to nutrient deprivation and shortens lifespan (Lin *et al.*, 2003). The myristoylation sequence of other β subunit is necessary for Snf1 trafficking from the plasma membrane to the nucleus (Lin *et al.*, 2003). This same effect is observed in plants, myristoylation of the β1 subunit negatively regulates nuclear SnRK1 activity by sequestering the complex at the plasma membrane (Pierre *et al.*, 2007). The authors suggest that this effect may be related to the developmental arrest observed in mutants with defects on the myristoylation machinery.

Moreover, fatty acids were also shown to allosterically activate AMPK (Clark *et al.*, 2004; Hebbachi and Saggerson, 2013). Interestingly, sugar phosphates like G6P (Toroser *et al.*, 2000) (1-10 mM) and T6P (Zhang *et al.*, 2009, Martínez-Barajas *et al.*, 2011) were found to inhibit SnRK1 *in vitro.* As previously detailed, trehalose is synthesized from G6P and UDPG (metabolites of Suc metabolism) placing this pathway right in the heart of primary carbon metabolism.

1.3.3. SnRK1 in the centre of plant metabolic and stress regulation

The importance of SnRK1 was first noticed when the activity of three key plant enzymes, 3-hydroxy-3-methylglutaryl-coenzime A (HMG-CoA) reductase, sucrose phosphate synthase (SPS) and nitrate reductase (NR), were shown to be regulated by phosphorylation through SnRK1 activity (Sugden *et al.*, 1999b). Another important enzyme that may be regulated by SnRK1 is the TOR kinase, as it is a

conserved enzyme complex phosphorylated and inhibited by AMPK (Gwinn *et al.*, 2008). TOR activation is opposite to that of the SNF1 family of PKs being triggered by feast nutrient-replete conditions. The conserved TOR signaling pathway is central in the responses to nutrients (sugars and amino-acids) and energy levels (Wullschleger *et al.*, 2006). Mutation of the Arabidopsis TOR gene is linked to chlorophyll breakdown and premature senescence (Depros *et al.*, 2007) but it is in fact embryo lethal (Menand *et al.*, 2002). The functional conservation of SnRKs and TOR pathways in all eukaryotes suggests a close interaction of these regulatory pathways which constitute an important regulatory module connecting nutrient sensing to the cell growth machinery (reviewed in Smeekens *et al.*, 2010; Robaglia *et al.*, 2012). The nature of this interaction needs to be further investigated.

Recently, the studies at the transcriptional level exposed the great number of genes whose expression is regulated by SnRK1 proteins (Baena-Gonzalez *et al.*, 2007; Polge and Thomas, 2007; Jossier *et al.*, 2009). Under low energy conditions, those related to biosynthetic processes like amino acids, cell wall, lipids, proteins, Suc and starch were shown to be repressed to conserve ATP and carbon. Those related to catabolism are, on the contrary, induced, to generate ATP through hydrolysis of Suc, starch, cell walls and polysaccharides and also lipid mobilization and β-hydrolysis. Moreover, SnRK1 was also shown to control the expression of genes related to regulatory processes. Several genes coding for TFs and histone deacetylases are activated or repressed by KIN10 (Contento *et al.*, 2004; Buchanan-Wollaston *et al.*, 2005; Baena-Gonzalez *et al.*, 2007). bZIP11 is one of such TF found to be significantly induced by SnRK1 activity (Baena-Gonzalez *et al.*, 2007). Metabolic analysis has shown that increased nuclear presence of bZIP11 completely rearranged carbohydrate metabolic profiles that to some extent mimic low-carbon conditions. In the same study trehalose metabolism genes were also shown to be regulated by bZIP11 (Ma *et al.*, 2011). Bearing in mind that T6P inhibits SnRK1 (Zhang *et al.*, 2009) a SnRK1–bZIP11–T6P regulatory circuit is expected to exist as previously discussed. Many genes related to signal transduction components like hormone-responsive genes, and calcium modulators are also affected by altered

SnRK1 activity (Baena-Gonzalez *et al.*, 2007). More recently miRNAs were also observed to act downstream of SnRK1 in the regulation stress response (Confraria *et al.*, 2013).

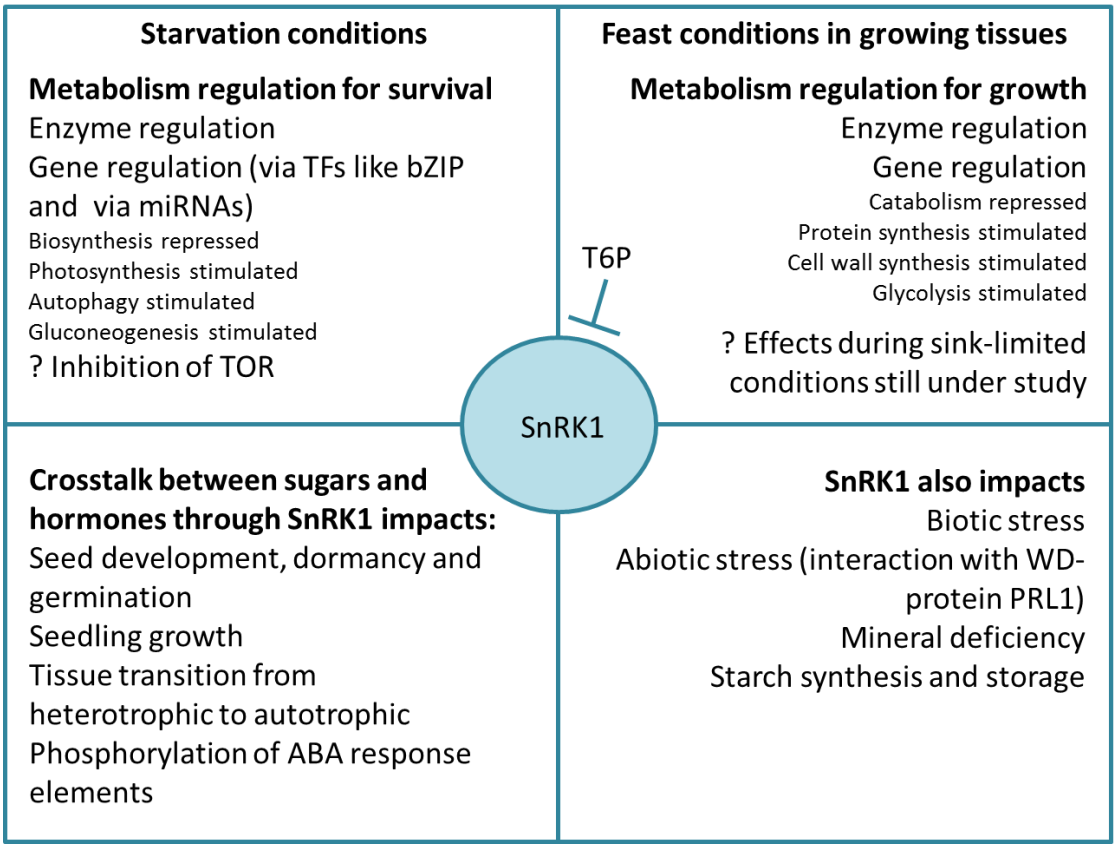

Figure 1.7. Overview of SnRK1 impacts on plant development and environmental responses. Most effects are still not fully described.

Several studies clearly show that SnRK1 impacts all aspects of plant metabolism (Fig. 1.7). Plants overexpressing SnRK1.1, for example, showed altered starch and sugar content, altered ADP-glucose pyrophosphorylase and nitrate reductase activity, altered sugar-regulated gene expression and ABA hypersensitive phenotype (Jossier *et al.*, 2009). The authors suggested that SnRK1.1 could be one of the elements linking ABA and sugar signals during transition from heterotrophic to

autotrophic stages in plants. Double snf1a and snf1b knockouts of the moss *Physcomitrella patens* showed that the total absence of Snf1-like protein kinase activity, although not lethal, led to severe phenotypic changes including shifts of the normal developmental programme, altered rhizoid and leaf balance formation, premature senescence, hypersensitivity to auxin and hyposensitivity to cytokinin. The effects found at the energy balance level led the authors concluded that the mutant had an inability to respond to reduced energy supply (Thelander *et al.*, 2004), now in agreement with transcriptional studies (Baena-Gonzalez *et al.*, 2007). Combining transient expression in leaf mesophyll protoplasts and stable expression in transgenic plants of both high and low SnRK1 activity constructs in tomato and Arabidopsis, Cho *et al.* (2012) have shown that SnRK1 activities critically influence gene expression related to stress responses as well as to plant growth and development throughout the life cycle (Fig 1.7).

Other studies link SnRK1 activity to seed germination and consequently to hormone signaling. Shoot and root measurements of “knockouts” of SnRK1A and SnRK1B showed that SnRK1A, but not SnRK1B, plays a major role in controlling rice seed germination and seedling growth (Lu *et al.*, 2007). Rice SnRK1A was shown to relieve Suc repression of α-Amy3 (major α-amylase expressed under sugar-depleted conditions). Antisense SnRK1 in pea revealed defects in seed maturation similar to an ABA insensitive phenotype (Radchuk *et al.*, 2006). In tomato seeds, the regulation of SNF4 by ABA and gibberellin is another indication of the link between hormonal and sugar-sensing controlling seed development, dormancy and germination (Bradford *et al.*, 2003) (Fig. 1.7).

Other more intricate networks also occur. SnRKs were indirectly connected to sugar, hormone and stress signaling through Pleiotropic Regulatory Locus 1 (PRL1) (Németh *et al.*, 1998). PRL1 encodes an α-importin-binding nuclear WD-protein that was shown to bind SnRK1 and inhibit its kinase activity (Bhalerao *et al.*, 1999). Lee *et al.* (2008) showed that the observed activity decrease was due to PRL1 –dependent recruitment of AKIN10 for proteasomal destruction through the ubiquitin machinery. SnRK1 association with the regulatory WD-protein PRL1 (Bhalerao *et al.*,

1999) connects it with water deficit responses. Other abiotic stresses were also related to these kinases. During phosphate starvation, AKIN11 protein levels decrease and an increase in AKIN10 activity (not due to altered phosphorylation state) is not enough to compensate for that loss and so overall SnRK1 activity significantly decreases (Fragoso *et al.*, 2009).

Responses to biotic stresses were also shown to recruit SnRK1 activity. SnRK1 allows tobacco plants to tolerate herbivory by allocating carbon to roots (Schwachtje *et al.*, 2006). It was also found that in the cytosol, the AKINβγ-subunit interacts with two leucine-rich repeats related to pathogen resistance proteins (Gissot *et al.*, 2006). This is further indication that the βγ-subunit could be related to plants specific functions like plant-pathogen interaction as previously pointed out.

Double snf1a and snf1b knockout mosses showed regular ability to degrade the accumulated starch but severely impaired capacity to accumulate it (Thelander *et al.*, 2004). SnRK1 was therefore also linked to starch biosynthesis which is a process associated to high carbon conditions. If such a link actually exists, it is still poorly understood. Transgenic potato overexpressing SnRK1 had higher starch content and lower Gluc levels than wild-type tubers and both SUS and ADP-glucose pyrophosphorylase, two key enzymes of the starch biosynthetic pathway, had increased activity (McKibbin *et al.*, 2006). The antisense expression of SnRK1 in transgenic barley led to the arrest of pollen development. The pollen grains were small, pear-shaped and contained little or no starch. At least SnRK1b expression was decreased in these pollen grains. This was the first work to associate SnRK1 with invertase activity in plants also found in yeasts. It was proposed that these pollen grains do not accumulate starch and starve just as snf1 mutants starve in Suc medium (Zhang *et al.*, 2001). Also, the SnRK1b gene expression pattern overlaps with that of starch accumulation in sorghum endosperm and microspores (Jain *et al.*, 2008). Tiessen *et al.* (2003) showed that SnRK1 is necessary for Suc-dependent redox activation of ADP-glucose pyrophosphorylase. It was suggested that SnRK1 directs carbon for storage as starch rather than for the glycolytic pathway. It is surprising how a mechanism mainly related to starvation responses also regulates

polysaccharide synthesis and storage. There is still no full explanation for this fact but Halford and Hey (2009) suggest a separation of the Suc-induced and starvation-induced pathway downstream of SnRK1, perhaps through the involvement of specific TFs. Specialized organs and storage tissues (like tubers, seeds and pollen grains) are unlikely to have a different regulatory mechanism than the one found in vegetative tissues. It could also be argued that the modification of SnRK1 activity, which has such a central function in integrating metabolism and development, produces such strong effects when its activity is reduced or increased that the primary and secondary effects are difficult to separate making cause and effect difficult to establish.

Once all these uncertainties are clarified, our improved knowledge of signaling networks and their effects will put us a step forward in the ability to develop new crop varieties with improved stress tolerance to cope with the changing climate and with better yield to satisfy the needs of a fast growing population.

1.4. Project aims and thesis outline

T6P was shown to inhibit SnRK1 (Zhang *et al.*, 2009), the central plant metabolic regulator that respond to fluctuations in energy supply and demand rearranging metabolism to restore plant homeostasis. The main purposes of this project are to understand more about the metabolic regulation of SnRK1 and to add to our understanding of how plants adjust growth to available carbon through the T6P/SnRK1 pathway.

In addition to this introductory **Chapter I**, the thesis comprises 4 more chapters where the obtained results are described and discussed:

Chapter II. *Inhibition of SnRK1 by metabolites: Tissue-dependent effects and cooperative inhibition by glucose 1-phosphate in combination with trehalose 6-phosphate*

To broaden our understanding of SnRK1 metabolic regulation we screened a number of compounds (other than T6P and G6P) for the ability to interact with SnRK1; evaluated the nature and better characterized the enzyme kinetic properties of those interactions; searched for effects on SnRK1 by combinations of compounds; established other SnRK1 regulation aspects related to developmental and tissue-specific characteristics. The experiments allowed us to:

- identify G1P as a novel SnRK1 inhibitor;
- show through kinetic models that T6P, G1P and G6P each provide distinct regulation of SnRK1;
- show that in combination with T6P, G6P produces cumulative inhibition of SnRK1 and G1P inhibited SnRK1 synergistically.

Chapter III. *Molecular characterization of SnRK1 inhibition by T6P – Factor I*

Simultaneously with SnRK1 metabolic regulation we tried to isolate and identify, or at least better characterize, the intermediary factor that mediates T6P inhibition of SnRK1, which was shown to be separable from the kinase complex. Different approaches like Arabidopsis mutants, co-immunoprecipitation of SnRK1 and factor and affinity chromatography were attempted:

- we were able to confirm the transient and weak nature of their interaction and found several proteins that interact with SnRK1. However, further work is needed, to clarify the involvement of these proteins in T6P inhibition of SnRK1.

Chapter IV. *In wheat grain, SnRK1 inhibition by T6P may be tissue-specific whereas inhibition by R5P is only apparent*

The work continued with the evaluation of SnRK1 regulation by T6P and ribose 5-phosphate (R5P) (previously referred as a novel SnRK1 regulator) during wheat seed development. SnRK1 activity and inhibition was tested in maternal and filial tissues dissected at different developmental stages:

- studies on the stability of R5P during the course of SnRK1 *in vitro* activity assays showed that the observed inhibition was in fact an experimental artefact;
- the observed T6P accumulation could however, underlie the shift in gene expression in maternal and filial tissues observed at about 10 days after anthesis that precede the grain filling period.

Chapter V. *The trehalose 6-phosphate/SnRK1 signaling pathway primes growth recovery following relief of sink limitation*

SnRK1 is active under sugar starvation conditions limiting growth to allow survival during periods of scarce resources. However, under certain stresses like low temperature or limited nutrient supply, sugars are readily available but growth is still limited (Paul and Stitt, 1993; Usadel *et al.*, 2008). This is termed sink-limited growth, when growth is limited by capacity of sinks, i.e. growing regions to use assimilate. These cases depart from the famine model of growth regulation by SnRK1. To understand how the model behaves under such conditions, Arabidopsis seedlings were grown under different conditions, of temperature, nutrient supply and sugar availability. The induced sink-limited growth allowed to:

- establish the interrelationship between T6P and Suc; T6P and SnRK1 activity; T6P and gene expression and between all these and growth;
- determine how plants with genetically decreased T6P content and SnRK1 overexpression respond to such conditions;
- conclude that under such sink-limited conditions, T6P is not directly related to growth rate but changes in gene expression caused by SnRK1 inhibition enables growth recovery following relief of limitations.

Finally, in **Chapter VI** it is discussed how the obtained results allowed the integration of data and added cues to the descriptive model of the regulation of growth by the T6P/SnRK1 signaling pathway; contributing with knowledge for future

crop improvement with added resilience under conditions of contrasting resources availability.

Each Chapter had different collaborators who are recognised in the corresponding acknowledgments sections and resulted in the indicated publications.

1.5. References

Alderson A, Sabelli PA, Dickinson JR, Cole D, Richardson M, Kreis M, Shewry PR, Halford NG (1991) Complementation of snf1, a mutation affecting global regulation of carbon metabolism in yeast, by a plant protein kinase cDNA. Proc Natl Acad Sci USA **88:** 8602-8605

Avila J, Gregory OG, Su D, Deeter TA, Chen S, Silva-Sanchez C, Xu S, Martin GB, Devarenne TP (2012) The β-subunit of the SnRK1 complex is phosphorylated by the plant cell death suppressor Adi3. Plant Physiol **159**: 1277-1290

Avonce N, Mendoza-vargas A, Morett E, Iturriaga G (2006) Insights on the evolution of trehalose biosynthesis. BMC Evol Biol **6**: 109

Baena-González E (2010) Energy signaling in the regulation of gene expression during stress. Mol Plant **3**: 300-313

Baena-Gonzalez E, Rolland F, Thevelein JM, Sheen J (2007) A central integrator of transcription networks in plant stress and energy signaling. Nature **448**: 938-942

Baena-González E, Sheen J (2008) Convergent energy and stress signaling. Trends Plant Sci **13**: 474-482

Barker L, Kühn C, Weise A, Schulz A, Gebhardt C, Hirner B, Hellmann H, Schulze W, Ward JM, Frommer WB (2000) SUT2, a putative sucrose sensor in sieve elements. Plant Cell **12**: 1153-1164

Bar-Peled M, O'Neill MA (2011) Plant nucleotide sugar for-mation, interconversion, and salvage by sugar recycling. Annu Rev Plant Biol **62**: 127–155

Barratt DHP, Derbyshire P, Findlay K, Pike M, Wellner N, Lunn J, Feil R, Simpson C, Maule AJ, Smith AM (2009) Normal growth of Arabidopsis requires cytosolic invertase but not sucrose synthase. Proc Natl Acad Sci USA **106**: 13124-13129

Barth I, Meyer S, Sauer N (2003) PmSUC3: Characterization of a SUT2/SUC3- type sucrose transporter from *Plantago major*. Plant Cell **15**: 1375-1385

Beddington J (2010) Food security: contributions from science to a new and greener revolution Phil Trans R Soc B **365**: 61–71

Bhalerao RP, Salchert K, Bako L, Okresz L, Szabados L, Muranaka T, Machida Y, Schell J, Koncz C (1999) Regulatory interaction of PRL1 WD protein with Arabidopsis SNF1-like protein kinases. Proc Natl Acad Sci USA **96**: 5322-5327

Bläsing OE, Gibon Y, Gunther M, Hohne M, Morcuende R, Osuna D, Thimm O, Usadel B, Scheible WR, Stitt M (2005) Sugars and circadian regulation make major contributions to the global regulation of diurnal gene expression in Arabidopsis. Plant Cell **17:** 3257-3281

Blázquez MA, Santos E, Flores CL, Martínez-Zapater JM, Salinas J, Gancedo C (1998) Isolation and molecular characterization of the Arabidopsis TPS1 gene, encoding trehalose-6-phosphate synthase. Plant J **13**: 685–689

Bockaert J, Pin JP (1998) Molecular tinkering of G protein-coupled receptors: an evolutionary success. EMBO J **18**: 1723–1729

Bolouri-Moghaddam MR, Le Roy K, Xiang L, Rolland F, Van den Ende W (2010) Sugar signaling and antioxidant network connections in plant cells. FEBS J **277**: 2022–2037

Borisjuk L, Rolletschek H, Wobus U, Weber H (2003) Differentiation of legume cotyledons as related to metabolic gradients and assimilate transport into seeds. J Exp Bot **54**: 503-512

Bradford KJ, Downie AB, Gee OH, Alvarado V, Yang H, Dahal P (2003) Abscisic Acid and Gibberellin Differentially Regulate Expression of Genes of the SNF1-Related Kinase Complex in Tomato Seeds. Plant Physiol **132**: 1560-1576

Brenner WG, Romanov GA, Kollmer I, Burkle L, Schmulling T (2005) Immediate-early and delayed cytokinin response genes of *Arabidopsis thaliana* identified by genome-wide expression profiling reveal novel cytokinin-sensitive processes and suggest cytokinin action through transcriptional cascades. Plant J **44:** 314-333

Buchanan-Wollaston V, Page P, Harrison E, Breeze E, Lim PO, Nam HG, Lin J-F, Wu S-H, Swidzinski J, Ishizaki K, Leaver CJ (2005) Comparative transcriptome analysis reveals significant differences in gene expression and signaling pathways between developmental and dark/starvation-induced senescence in Arabidopsis. Plant J **42**: 567-585

Cabib E, Leloir LF (1958) The biosynthesis of trehalose phosphate. J Biol Chem **231**: 259-275

Carling D, Aguan K, Woods A, Verhoeven AJ, Beri RK, Brennan CH, Sidebottom C, Davison MD, Scott J (1994) Mammalian AMP-activated protein kinase is homologous to yeast and plant protein kinases involved in the regulation of carbon metabolism. J Biol Chem **269**: 11442–11448

Carlson M (1999) Glucose repression in yeast. Curr Opin Microbiol **2**: 202–207

Carlson M, Botstein D (1982) Two differentially regulated mRNAs with different 5' ends encode secreted and intracellular forms of yeast invertase. Cell **28**: 145–154

Carlson M, Osmond BC, Botstein D (1981) Mutants of yeast defective in sucrose utilization. Genetics **98**: 25-40

Carvalho RF, Carvalho SD, Duque P (2010) The plant-specific SR45 protein negatively regulates glucose and ABA signaling during early seedling development in Arabidopsis. Plant Physiol **154**: 772-783

Chan MT, Yu SM (1998) The 3' untranslated region of a rice alpha-amylase gene functions as a sugar-dependent mRNA stability determinant. Proc Natl Acad Sci USA **95**: 6543-6547

Chary SN, Hicks GR, Choi YG, Carter D, Raikhel NV (2008) Trehalose-6-phosphate synthase/phosphatase regulates cell shape and plant architecture in Arabidopsis. Plant Physiol **146**: 97–107

Chen JG, Jones AM (2004) AtRGS1 function in *Arabidopsis thaliana*. Methods Enzymol. **389**: 338-350

Chen JG, Willard FS, Huang J, Liang J, Chasse SA, Jones AM, Siderovski DP (2003) A seven-transmembrane RGS protein that modulates plant cell proliferation. Science **301**: 1728-1731

Cheng WH, Endo A, Zhou L, Penney J, Chen HC, Arroyo A, Leon P, Nambara E, Asami T, Seo M, Koshiba T, Sheen J (2002) A unique short-chain dehydrogenase/reductase in Arabidopsis glucose signaling and abscisic acid biosynthesis and functions. Plant Cell **14**: 2723-2743

Cho JI, Ryoo N, Hahn TR, Jeon JS (2009). Evidence for a role of hexokinases as conserved glucose sensors in both monocot and dicot plant species. Plant Signal Behav **4**: 908-910

Cho JI, RyooN, Ko S, Lee S-K, Lee J, Jung K-H, Lee Y-H, Bhoo SH, Winderickx J, An G, Hahn T-R, Jeon J-S (2006). Structure, expression, and functional analysis of the hexokinase gene family in rice (*Oryzasativa* L.). Planta **224**: 598-611

Cho Y-H, Hong J-W, Kim E-C, Yoo S-D (2012) Regulatory functions of SnRK1 in stress-responsive gene expression and in plant growth and development. Plant Physiol **158**: 1955-1964

Cho Y-H, Yoo S-D (2011) Signaling Role of Fructose Mediated by FINS1/FBP in *Arabidopsis thaliana*. PLoS Genetics **7**(1): e1001263

Cho Y-H, Yoo S-D, Sheen J (2006) Regulatory functions of nuclear hexokinase 1 complex in glucose signaling. Cell **127**: 579-589

Clark H, Carling D, Saggerson D (2004) Covalent activation of heart AMP-activated protein kinase in response to physiological concentrations of long-chain fatty acids. Eur J Biochem **271**: 2215–2224

Coello P, Hey SJ, Halford NG (2011) The sucrose non-fermenting-1-related (SnRK) family of protein kinases: potential for manipulation to improve stress tolerance and increase yield. J Exp Bot **62**: 883-893

Coello P, Hirano E, Hey SJ, Muttucumaru N, Martínez-Barajas E, Parry MA, Halford NG (2012) Evidence that abscisic acid promotes degradation of SNF1-related protein kinase (SnRK) 1 in wheat and activation of a putative calcium-dependent SnRK2. J Exp Bot **63**: 913-924

Colaço C, Sen S, Thangavelu M, Pinder S, Roser B (1992) Extraordinary stability of enzymes dried in trehalose: Simplified molecular biology. Biotechnol **10**: 1007-1111

Conde C, Agasse A, Glissant D, Tavares RM, Gerós H and Delrot S (2006) Pathways of glucose regulation of monosaccharide transport in grape cells. Plant Physiol **141**: 1563-1577

Confraria A, Martinho C, Elias A, Rubio-Somoza I, Baena-González E (2013) miRNAsmediateSnRK1-dependentenergysignalinginArabidopsis. Front Plant Sci **4**: 197

Contento AL, Kim SJ, Bassham DC (2004) Transcriptome profiling of the response of Arabidopsis suspension culture cells to sucrose starvation. Plant Physiol **135**: 2330-2347

Corbesier L, Lejeune P, Bernier G (1998) The role of carbohydrates in the induction of flowering in *Arabidopsis thaliana*: comparison between the wild type and a starchless mutant. Planta **206**: 131-137

Coruzzi G, Bush DR (2001) Nitrogen and carbon nutrient and metabolite signaling in plants. Plant Physiol **125**: 61-64

Coruzzi GM, Zhou L (2001) Carbon and nitrogen sensing and signaling in plants: emerging 'matrix effects'. Curr Opin Plant Biol **4**: 247-253

Cotelle V, Meek SE, Provan F, Milne FC, Morrice N, MacKintosh C (2000) 14-3-3s regulate global cleavage of their diverse binding partners in sugar-starved Arabidopsis cells. EMBO J **19**: 2869-2876

da Silva Xavier G, Leclerc I, Varadi A, Tsuboi T, Moule SK, Rutter GA (2003) Role for AMP-activated protein kinase in glucose-stimulated insulin secretion and preproinsulin gene expression. Biochem J **371:** 761–774

Davies SP, Helps NR, Cohen PT, Hardie DG (1995) 5'-AMP inhibits dephosphorylation, as well as promoting phosphorylation, of the AMP-activated protein kinase. Studies using

bacterially expressed human protein phosphatase-2C alpha and native bovine protein phosphatase-2AC. FEBS Lett **377:** 421–425

Debast S, Nunes-Nesi A, Hajirezaei MR, Hofmann J, Sonnewald U, Fernie AR, Börnke F (2011) Altering trehalose-6-phosphate content in transgenic potato tubers affects tuber growth and alters responsiveness to hormones during sprouting. Plant Physiol **156**: 1754–1771

Dekkers BJ, Schuurmans JA, Smeekens SC (2004) Glucose delays seed germination in *Arabidopsis thaliana*. Planta **218:** 579-588

Dekkers BJ, Schuurmans JA, Smeekens SC (2008) Interaction between sugar and abscisic acid signaling during early seedling development in Arabidopsis. Plant Mol Biol **67**: 151-167

Delatte TL, Sedijani P, Kondou Y, Matsui M, Jong GJ, Somsen GW, Wiese Klinkenberg A, Primavesi LF, Paul MJ, Schluepmann H (2011) Growth arrest by trehalose-6-phosphate: an astonishing case of primary metabolite control over growth by way of the SnRK1 signaling pathway. Plant Physiol **157**: 160–174

Deprost D, Yao L, Sormani R, Moreau M, Leterreux G, Nicolaï M, Bedu M, Robaglia C, Meyer C (2007) The Arabidopsis TOR kinase links plant growth, yield, stress resistance and mRNA translation. EMBO Rep 8: 864-870

Duque P (2011) A role for SR proteins in plant stress responses. Plant Signal Behav **6**: 49-54

Eastmond PJ, van Dijken AJ, Spielman M, Kerr A, Tissier AF, Dickinson HG, Jones JD, Smeekens SC, Graham IA (2002) Trehalose-6-phosphate synthase 1, which catalyses the first step in trehalose synthesis, is essential for Arabidopsis embryo maturation. Plant J **29**: 225-235

Ellis C, Turner JG, Devoto A (2002) Protein complexes mediate signaling in plant responses to hormones, light, sucrose and pathogens. Plant Mol Biol **50**: 971-980

Emanuelsson O, Brunak S, von Heijne G, Nielsen H (2007) Locating proteins in the cell using TargetP, SignalP and related tools. Nat Protoc **2**: 953-971

Farrás R, Ferrando A, Jásik J, Kleinow T, Ökrész l, Tiburcio A, Salchert K, Pozo C, Schell J, Koncz C (2001) SKP1-SnRK protein kinase interactions mediate proteasomal binding of a plant SCF ubiquitin ligase. EMBO J **20**: 2742-2756

Fernandez O, Vandesteene L, Feil R, Baillieul F, Lunn JE, Clement C (2012) Trehalose metabolism is activated upon chilling in grapevine and might participate in Burkholderia phytofirmans induced chilling tolerance. Planta **236**: 355-369

Fernie AR, Carrari F, Sweetlove LJ (2004) Respiratory metabolism: glycolysis, the TCA cycle and mitochondrial electron transport. Curr Opin Plant Biol **7**: 254–261

Finkelstein RR, Gibson SI (2002) ABA and sugar interactions regulating development: cross-talk or voices in a crowd? Curr Opin Plant Biol **5**: 26-32

Finkemeier I, König A-C, Heard W, Nunes-Nesi A, Pham PA, Leister D, Fernie AR, Sweetlove LJ (2013) Transcriptomic Analysis of the Role of Carboxylic Acids in Metabolite Signaling in Arabidopsis Leaves. Plant Physiol **162**: 239–253

Finnie C, Borch J, Collinge DB (1999) 14-3-3 proteins: Eukaryotic regulatory proteins with many functions. Plant Mol Biol **40**: 545-554

Fragoso S, Espíndola L, Páez-Valencia J, Gamboa A, Camacho Y, Martínez-Barajas E, Coello P (2009) SnRK1 isoforms AKIN10 and AKIN11 are differentially regulated in Arabidopsis plants under phosphate starvation. Plant Physiol **149**: 1906-1916

Frison M, Parrou JL, Guillaumot D, Masquelier D, Francois J, Chaumont F, Batoko H (2007). The *Arabidopsis thaliana* trehalase is a plasma membrane-bound enzyme with extracellular activity. FEBS Lett **581**: 4010–4016

Gancedo JM (1998) Yeast carbon catabolite repression. Microbiol Mol Biol Rev **62**: 334–361

Gazzarrini S, McCourt P (2001) Genetic interactions between ABA, ethylene and sugar signaling pathways. Curr Opin Plant Biol **4**: 387–391

Geelen D, Royackers K, Vanstraelen M, De Bus M, Inzé D, van Dijck P, Thevelein JM, Leyman B (2007) Trehalose-6-P synthase AtTPS1 high molecular weight complexes in yeast and Arabidopsis. Plant Sci **173**: 426–437

Geigenberger P (2011) Regulation of Starch Biosynthesis in Response to a Fluctuating Environment. Plant Physiol **155**: 1566-1577

Ghillebert R, Swinnen E, Wen J, Vandesteene L, Ramon M, Norga K, Rolland F, Winderickx J (2011) The AMPK/SNF1/SnRK1 fuel gauge and energy regulator: structure, function and regulation. FEBS J **278**: 3978–3990

Gibson SI (2004) Sugar and phytohormone response pathways: navigating a signaling network. J Exp Bot **55**: 253-264

Gissot L, Polge C, Bouly JP, Lemaitre T, Kreis M, Thomas M (2004) AKINbeta3, a plant specific SnRK1 protein, is lacking domains present in yeast and mammals non-catalytic beta-subunits. Plant Mol Biol **56**: 747-759

Gissot L, Polge C, Jossier M, Girin T, Bouly J-P, Kreis M (2006) AKINβγ contributes to SnRK1 heterotrimeric complexes and interacts with two proteins implicated in plant pathogen resistance through its KIS/GBD sequence. Plant Physiol **142**: 931-944

Goddijn OJM, Verwoerd TC, Voogd E, Krutwagen RWHH, de Graaf PTHM, Poels J, van Dun K, Ponstein AS, Damm B, Pen J (1997) Inhibition of tehalase activity enhances trehalose accumulation in transgenic plants. Plant Physiol **113**: 181–190

Gómez LD, Baud S, Gilday A, Li Y, Graham IA (2006) Delayed embryo development in the ARABIDOPSIS TREHALOSE-6-PHOSPHATE SYNTHASE 1 mutant is associated with altered cell wall structure, decreased cell division and starch accumulation. Plant J **46**: 69-84

Gómez LD, Gilday A, Feil R, Lunn JE, Graham IA (2010) AtTPS1 mediated trehalose-6-phosphate synthesis is essential for embryogenic and vegetative growth and responsiveness to ABA in germinating seeds and stomatal guard cells. Plant J **64**: 1-13

Granot D, David-Schwartz R, Kelly G (2013) Hexose kinases and their role in sugar-sensing and plant development. Front Plant Sci **4**: 44

Guo Y, Xiong L, Song C-P, Gong D, Halfter U, Zhu J-K (2002) A calcium sensor and its interacting protein kinase are global regulators of abscisic acid signaling in Arabidopsis. Dev Cell **3**: 233–244

Gwinn DM, Shackelford DB, Egan DF, Mihaylova MM, Mery A, Vasquez DS, Turk BE, Shaw RJ (2008) AMPK phosphorylation of raptor mediates a metabolic checkpoint. Mol Cell **30**: 214-226

Halford NG, Bouly J-P, Thomas M (2000) SNF1-related protein kinases (SnRKs): regulators at the heart of the control of carbon metabolism and partitioning. Adv Bot Res 32: 405-434

Halford NG, Hardie DG (1998) SNF1-related protein kinases: global regulators of carbon metabolism in plants? Plant Mol Biol **37:** 735–748

Halford NG, Hey S, Jhurreea D, Laurie S, McKibbin RS, Zhang Y, Paul MJ (2003) Highly conserved protein kinases involved in the regulation of carbon and amino acid metabolism. J Exp Bot **55**: 35-42

Halford NG, Hey S, Jhurreea D, Laurie S, McKibbin RS, Zhang Y, Paul MJ (2004) Highly conserved protein kinases involved in the regulation of carbon and amino acid metabolism. J Exp Bot **55**: 35-42

Halford NG, Hey SJ (2009) SNF1-related protein kinases (SnRKs) act within an intricate network that links metabolic and stress signaling in plants. Biochem J **419**: 247-259

Hanson J, Hanssen M, Wiese A, Hendriks MM, Smeekens S (2008) The sucrose regulated transcription factor bZIP11 affects amino acid metabolism by regulating the expression of *ASPARAGINE SYNTHETASE1* and *PROLINE DEHYDROGENASE2.* Plant J **53**: 935-949

Hanson J, Smeekens S (2009) Sugar perception and signaling – an update. Curr Opin Plant Biol **12**: 562–567

Hardie DG (2007) AMP-activated ⁄ SNF1 protein kinases: conserved guardians of cellular energy. Nat Rev **8:** 774–785

Hardie DG, Carling D, Gamblin SJ (2011) AMP-activated protein kinase: also regulated by ADP? Trends Biochem Sci **36**: 470-477

Hare PD, Cress WA, Van Staden J (1998) Dissecting the roles of osmolyte accumulation during stress. Plant Cell Environ **21**: 535–553

Harthill JE, Meek SE, Morrice N, Peggie MW, Borch J, Wong BH, Mackintosh C (2006) Phosphorylation and 14-3-3 binding of Arabidopsis trehalose-phosphate synthase 5 in response to 2-deoxyglucose. Plant J **47**: 211–223

Hebbachi A, Saggerson D (2013) Acute regulation of 5′-AMP-activated protein kinase by long-chain fatty acid, glucose and insulin in rat primary adipocytes. Biosci Rep **33**: e00007

Hedbacker K, Carlson M (2006) Regulation of the nucleocytoplasmic distribution of Snf1-Gal83 protein kinase. Eukaryot Cell **5:** 1950–1956

Hey S, Mayerhofer H, Halford NG, Dickinson JR (2007) DNA sequences from Arabidopsis, which encode protein kinases and function as upstream regulators of Snf1 in yeast. J Biol Chem **282**: 10472-10479

Hey SJ, Byrne E, Halford NG (2010) The interface between metabolic and stress signaling. Ann Bot **105**: 197–203

Ho S, Chao Y, Tong W, Yu S (2001) Sugar coordinately and differentially regulates growth- and stress-related gene expression via a complex signal transduction network and multiple control mechanisms. Plant Physiol **125**: 877-890

Hong SP, Carlson M (2007) Regulation of snf1 protein kinase in response to environmental stress. J Biol Chem **282**: 16838–16845

Honigberg SM, Lee RH (1998) Snf1 kinase connects nutritional pathways controlling meiosis in *Saccharomyces cerevisiae*. Mol Cell Biol **18**: 4548–4555

Hsieh MH, Lam HM, van de Loo FJ, Coruzzi G (1998) A PII-like protein in *Arabidopsis*: putative role in nitrogen sensing. Proc Natl Acad Sci USA **95**: 13965-13970

Huber SC (1998) Starch-Sucrose metabolism and assimilate partitioning. *In* Raghavendra AS, eds, Photosynthesis: A comprehensive Treatise, Cambridge University Press, Cambridge, pp 163-175

Huber SC, Huber JL (1996) Role and regulation of sucrose-phosphate synthase in higher plants. Annu Rev Plant Phys **47**: 431-444

Inoki K, Zhu T, Guan KL (2003) TSC2 mediates cellular energy response to control cell growth and survival. Cell **115**: 577–590

Iturriaga G, Suárez R, Nova-Franco B (2009) Trehalose Metabolism: from osmoprotection to signaling. Int J Mol Sci **10**: 3793-3810

Jain M, Li Q-B, Chourey PS (2008) Cloning and expression analyses of sucrose non-fermenting-1-related kinase 1 (SnRK1b) gene during development of sorghum and maize endosperm and its implicated role in sugar-to-starch metabolic transition. Physiol Plant **134**: 161-173

Jang JC, León P, Zhou L, Sheen J (1997) Hexokinase as a sugar sensor in higher plants. Plant Cell **9**: 5-19

Jang JC, Sheen J (1994) Sugar sensing in higher plants. Plant Cell **6**: 1665–1679

Jiang R, Carlson M (1997) The Snf1 protein kinase and its activating subunit, Snf4, interact with distinct domains of the Sip1/Sip2/Gal83 component in the kinase complex. Mol Cell Biol **17:** 2099–2106

Jossier M, Bouly J-P, Meimoun P, Arjmand A, Lessard P, Hawley S, Hardie DG, Thomas M (2009) SnRK1 (SNF1-related kinase 1) has a central role in sugar and ABA signaling in *Arabidopsis thaliana*. Plant J **59**: 316-328

Kato-Noguchi H, Takaoka T, Izumori K (2005) Psicose inhibits lettuce root growth via a hexokinase-independent pathway. Physiologia Plantarum **125**: 293-298

Kazgan N, Williams T, Forsberg LJ & Brenman JE (2010) Identification of a Nuclear Export Signal in the Catalytic Subunit of AMP-activated Protein Kinase. Mol Biol Cell **21**: 3433–3442

Koch K (1996) Carbohydrate-modulated gene expression in plants. Ann Rev Plant Physiol Plant Mol Biol **47**: 509-540

Koch K (2004) Sucrose metabolism: regulatory mechanisms and pivotal roles in sugar sensing and plant development. Curr Opin Plant Biol **7**: 235–246

Kolbe A, Tiessen A, Schluepmann H, Paul M, Ulrich S, Geigenberger P (2005) Trehalose 6-phosphate regulates starch synthesis via posttranslational redox activation of ADP-glucose pyrophosphorylase. Proc Natl Acad Sci USA **102**: 11118-11123

Kötting O, Kossman J, Zeeman SC, Lloyd JR (2010) Regulation of starch metabolism: the age of enlightment. Curr Opin Plant Biol **13**: 320–328

Kuchin S, Vyas VK & Carlson M (2002) Snf1 protein kinase and the repressors Nrg1 and Nrg2 regulate FLO11, haploid invasive growth, and diploid pseudohyphal differentiation. Mol Cell Biol **22:** 3994–4000

Lee JH, Terzaghi W, Gusmaroli G, Charron JB, Yoon HJ, Chen H, He YJ, Xiong Y, Deng XW (2008) Characterization of Arabidopsis and rice DWD proteins and their roles as substrate receptors for CUL4-RING E3 ubiquitin ligases. Plant Cell **20**: 152-167

Lejay L, Gansel X, Cerezo M, Tillard P, Muller C, Krapp A, von Wiren N, Daniel-Vedele F, Gojon A (2003) Regulation of root ion transporters by photosynthesis: functional importance and relation with hexokinase. Plant Cell **15:** 2218-2232

Lejay L, Wirth J, Pervent M, Cross JM, Tillard P, Gojon A (2008) Oxidative pentose phosphate pathway dependent sugar sensing as a mechanism for regulation of root ion transporters by photosynthesis. Plant Physiol **146**: 2036-2053

Léon P, Sheen J (2003) Sugar and hormone connections. Trends Plant Sci **8**: 110-116

Leonhardt N, Kwak JM, Robert N, Waner D, Leonhardt G, Schroeder JI (2004) Microarray expression analyses of Arabidopsis guard cells and isolation of a recessive abscisic acid hypersensitive protein phosphatase 2C mutant. Plant Cell **16:** 596-615

Leyman B, van Dijck P, Thevelein JM (2001) An unexpected plethora of trehalose biosynthesis genes in *Arabidopsis thaliana*. Trends Plant Sci **6**: 510-13

Li Y, Li L-L, Fan R-C, Peng C-C, Sun H-L, Zhu S-Y, Wang X-F, Zhang L-Y, Zhang D-P (2012) Arabidopsis sucrose transporter SUT4 interacts with cytochrome b5-2 to regulate seed germination in response to sucrose and glucose. Mol Plant **5**: 1029-1041

Lin SS, Manchester JK, Gordon JI (2003) Sip2, an *N*-myristoylated beta subunit of Snf1 kinase, regulates aging in *Saccharomyces cerevisiae* by affecting cellular histone kinase activity, recombination at rDNA loci, and silencing. J Biol Chem **278**: 13390-13397

Liu F, Vantoai T, Moy LP, Bock G, Linford LD, Quackenbush J (2005) Global transcription profiling reveals comprehensive insights into hypoxic response in Arabidopsis. Plant Physiol **137:** 1115-1129

Lorenz DR, Cantor CR & Collins JJ (2009) A network biology approach to aging in yeast. Proc Natl Acad Sci USA **106:** 1145–1150

Lu C-A, Lin C-C, Lee K-W, Chen J-L, Huang L-F, Ho Shin-Lon, Liu H-J, Hsing Y-I, Yu S-M (2007) The SnRK1A protein kinase plays a key role in sugar signaling during germination and seedling growth of Rice. Plant Cell **19**: 2484-249

Lumbreras V, Alba MM, Kleinow T, Koncz C & Pages M (2001) Domain fusion between SNF1-related kinase subunits during plant evolution. EMBO Rep **2**: 55–60

Lunn JE, Feil R, Hendriks JHM, Gibon Y, Morcuende R, Osuna D, Scheible WR, Carillo P, Hajirezaei M-R, Stitt M (2006) Sugar-induced increases in trehalose 6-phosphate are correlated with redox activation of ADP-glucose pyrophosphorylase and higher rates of starch synthesis in *Arabidopsis thaliana*. Biochem J **397**: 139-148

Ma J, Hanssen M, Lundgren K, Hernández L, Delatte T, Ehlert A, Liu CM, Schluepmann H, Dröge-Laser W, Moritz T, Smeekens S, Hanson J (2011) The sucrose-regulated Arabidopsis transcription factor bZIP11 reprograms metabolism and regulates trehalose metabolism. New Phytol **191**: 733-745

Mair W, Morantte I, Rodrigues APC, Manning G, Montminy M, Shaw RJ, Dillin A (2011) Lifespan extension induced by AMPK and calcineurin is mediated by CRTC-1 and CREB. Nature **470:** 404–408

Martínez-Barajas E, Delatte T, Schluepmann H, de Jong GJ, Somsen GW, Nunes C, Primavesi LF, Coello P, Mitchell RAC, Paul MJ (2011) Wheat grain development is characterized by remarkable trehalose 6-phosphate accumulation pregrain filling: tissue distribution and relationship to SNF1-related protein kinase1 activity. Plant Physiol **156**: 373–381

Martínez-Noël G, Tognetti J, Nagaraj V, Wiemken A, Pontis H (2006) Calcium is essential for fructan synthesis induction mediated by sucrose in wheat. Planta **225**: 183-191

Martínez-Noël GM, Tognetti JA, Salerno GL, Wiemken A, Pontis HG (2009) Protein phosphatase activity and sucrose-mediated induction of fructan synthesis in wheat. Planta: **230**: 1071-1079

Martins MCM, Hejazi M, Fettke J, Steup M, Feil R, Krause U, Arrivault S, Vosloh D, Figueroa CM, Ivakov A, Yadav UP, Piques M, Metzner D, Stitt M, Lunn JE (2013) Feedback inhibition of starch degradation in Arabidopsis leaves mediated by trehalose 6-phosphate. Plant Physiol **163**: 1142-1163

McKibbin RS, Muttucumaru N, Paul MJ, Powers SJ, Burrell MM, Coates S, Purcell PC, Tiessen A, Geigenberger P, Halford NG (2006) Production of high-starch, low-glucose potatoes through overexpression of the metabolic regulator SnRK1. Plant Biotechnol J **4**: 409-418

Menand B, Desnos T, Nussaume L, Berger F, Bouchez D, Meyer C, Robaglia C (2002) Expression and disruption of the Arabidopsis TOR (target of rapamycin) gene. Proc Natl Acad Sci USA **99**: 6422-6427

Meyer RC, Steinfath M, Lisec J, Becher M, Witucka-Wall H, Torjek O, Fiehn O, Eckardt A, Willmitzer L, Selbig J, Altmann T (2007) The metabolic signature related to high plant growth rate in *Arabidopsis thaliana*. Proc Natl Acad Sci USA **104**: 4759-4764

Minokoshi Y, Shiuchi T, Lee S, Suzuki A & Okamoto S (2008) Role of hypothalamic AMP-kinase in food intake regulation. Nutrition **24:** 786–790

Miranda JA, Avonce N, Suárez R, Thevelein JM, van Dijck P, Iturriaga GA (2007) Bifunctional TPS-TPP enzyme from yeast confers tolerance to multiple and extreme abiotic-stress conditions in transgenic *Arabidopsis*. Planta **226**: 1411-1421

Miranda M, Sorkin A (2007) Regulation of receptors and transporters by ubiquitination: new insights into surprisingly similar mechanisms. Mol Interv **7**: 157-167

Mishra BS, Singh M, Aggrawal P, Laxmi A (2009) Glucose and auxin signaling interaction in controlling *Arabidopsis thaliana* seedlings root growth and development. PLoS One **4**: e4502

Mittler R, Vanderauwera S, Suzuki N, Miller G, Tognetti VB, Vandepoele K, Gollery M, Shulaev V, Van BF (2011) ROS signaling: the new wave? Trends Plant Sci **16**: 300-309

Momcilovic M, Iram SH, Liu Y & Carlson M (2008) Roles of the glycogen-binding domain and Snf4 in glucose inhibition of SNF1 protein kinase. J Biol Chem **283:** 19521–19529

Moore B, Zhou L, Rolland F, Hall Q, Cheng WH, Liu YX, Hwang I, Jones T, Sheen J (2003) Role of the Arabidopsis glucose sensor HXK1 in nutrient, light, and hormonal signaling. Science **300**: 332-336

Muller J, Aeschbacher RA, Wingler A, Boller T, Wiemken A (2001) Trehalose and trehalase in Arabidopsis. Plant Physiol **125**: 1086-1093

Müller R, Morant M, Jarmer H, Nilsson L, Nielsen TH (2007) Genome-wide analysis of the Arabidopsis leaf transcriptome reveals interaction of phosphate and sugar metabolism. Plant Physiol **143:** 156-171

Narbonne P, Roy R (2009) *Caenorhabditis elegans* dauers need LKB1/AMPK to ration lipid reserves and ensure long-term survival. Nature **457**: 210-214

Nemeth K, Salchert K, Putnoky P, Bhalerao R, Koncz-Kalman Z, Stankovic-Stangeland B, Bako L, Mathur J, Okresz L, Stabel S, Geigenberger P, Stitt M, Rédei GP,Schell J, Koncz C (1998) Pleiotropic control of glucose and hormone responses by PRL1, a nuclear WD protein, in Arabidopsis. Genes Dev **12**: 3059-3073

Nielsen TH, Rung JH, Villadsen D (2004) Fructose-2,6-bisphosphate: a traffic signal in plant metabolism. Trends Plant Sci **9**: 556-63

Niu X, Helentjaris T, Bate NJ (2002) Maize ABI4 binds coupling element1 in abscisic acid and sugar response genes. Plant Cell **14**: 2565-2575

Nwaka S, Holzer H (1998) Molecular biology of trehalose and trehalases in the yeast, *Saccharomyces cereviciae*. Prog Nucleic Acid Re **58**: 197-237

Oakhill JS, Chen ZP, Scott JW, Steel R, Castelli LA, Ling N, Macaulay SL, Kemp BE (2010) Beta-subunit myristoylation is the gatekeeper for initiating metabolic stress sensing by AMP-activated protein kinase (AMPK). Proc Natl Acad Sci USA **107**: 19237-19241

Ohto M, Nakamura K (1995) Sugar-Induced Increase of Calcium-Dependent Protein Kinases Associated with the Plasma Membrane in Leaf Tissues of Tobacco. Plant Physiol **109:** 973-981

Osuna D, Usadel B, Morcuende R, Gibon Y, Bläsing OE, Höhne M, Günter M, Kamlage B, Trethewey R, Scheible WR, Stitt M. (2007) Temporal responses of transcripts, enzyme activities and metabolites after adding sucrose to carbon-deprived seedlings. Plant J **49**: 463-491

Paiva CLA, Panek AD (1996) Biotechnological applications of the disaccharide trehalose. Biotechnol Annu Rev **2**: 293-314

Palenchar PM, Kouranov A, Lejay LV, Coruzzi GM (2004) Genome-wide patterns of carbon and nitrogen regulation of gene expression validate the combined carbon and nitrogen (CN)-signaling hypothesis in plants. Genome Biol **5**: R91

Pastore D, DiPede S, Passarella S (2003) Isolated Durum wheat and potato cell mitochondria oxidize externally added NADH mostly via the malate/oxaloacetate shuttle with a rate that depends on the carrier-mediated transport. Plant Physiol **133**: 2029-2039

Paul M (2007) Trehalose 6-phosphate. Curr Opin Plant Biol 10: 303-309

Paul MJ, Pellny TK (2003) Carbon metabolite feedback regulation of leaf photosynthesis and development. J Exp Bot **54**: 539-547

Paul MJ, Primavesi LF, Jhurrea D, Zhang Y (2008) Trehalose metabolism and signaling. Annu Rev Plant Biol **59**: 417-441

Paul MJ, Stitt M (1993) Effects of nitrogen and phosphorus deficiencies on levels of carbohydrates, respiratory enzymes and metabolites in seedlings of tobacco and their response to exogenous sucrose. Plant Cell Environ **16**: 1047–1057

Pellny TK, Ghannoum O, Conroy JP, Schluepmann H, Smeekens S, Andralojc J, Krause KP, Goddijn O, Paul MJ (2004) Genetic modification of photosynthesis with E. coli genes for trehalose synthesis. Plant Biotechnol J **2**: 71-82

Perfus-Barbeoch L, Jones AM, Assmann SM (2004) Plant heterotrimeric G protein function: insights from Arabidopsis and rice mutants. Curr Opin Plant Biol **7**: 719-731

Pierre M, Traverso JA, Boisson B, Domenichini S, Bouchez D, Giglione C, Meinnela T (2007) N-Myristoylation Regulates the SnRK1 Pathway in Arabidopsis. Plant Cell **19**: 2804-2821

Piippo M, Allahverdiyeva Y, Paakkarinen V, Suoranta UM, Battchikova N, Aro EM (2006) Chloroplast-mediated regulation of nuclear genes in *Arabidopsis thaliana* in the absence of light stress. Physiol Genomics **25:** 142-152

Polge C, Thomas M (2007) SNF1/AMPK/SnRK1 kinases, global regulators at the heart of energy control? Trends Plant Sci **12**: 20–28

Price J, Laxmi A, St Martin SK, Jang JC (2004) Global transcription profiling reveals multiple sugar signal transduction mechanisms in Arabidopsis. Plant Cell **16**: 2128-2150

Price J, Li TC, Kang SG, Na JK, Jang JC (2003) Mechanisms of glucose signaling during germination of Arabidopsis. Plant Physiol **132:** 1424-1438

Purcell P, Smith AM, Halford NG (1998). Antisense expression of sucrose non-fermenting-1-related protein kinase sequence in potato results in decreased expression of sucrose synthase in tubers and loss of sucrose-inducibility of sucrose ynthase transcripts in leaves. Plant J **14:** 195-203

Qi J, Gong J, Zhao T, Zhao J, Lam P, Ye J, Li JZ, Wu J, Zhou HM, Li P (2008) Downregulation of AMP-activated protein kinase by Cidea-mediated ubiquitination and degradation in brown adipose tissue. EMBO J **27**: 1537-1548

Radchuk R, Radchuk V, Weschke W, Borisjuk L, Weber H (2006) Repressing the expression of the sucrose nonfermenting-1-related protein kinase gene in pea embryo causes pleiotropic defects of maturation similar to an abscisic acid-insensitive phenotype. Plant Physiol **140**: 263–278

Raghavendra AS, Padmasree K (2003) Beneficial interactions of mitochondrial metabolism with photosynthetic carbon assimilation. Trends Plant Sci **8**: 546-553

Rahmani F, Hummel M, Schuurmans J, Wiese-Klinkenberg A, Smeekens S, Hanson J (2009) Sucrose control of translation mediated by an upstream open reading frame-encoded peptide. Plant Physiol **150**: 1356-1367

Raíces M, MacIntosh GC, Ulloa RM, Gargantini PR, Vozza NF, Téllez-Inón MT (2003) Sucrose increases calcium dependent protein kinase and phosphatase activities in potato plants. Cell Mol Biol **49**: 959-964

Ramon M, de Smet I, Vandensteene L, Naudts M, Leyman B, van Dijck P, Rolland P, Beeckman T, Thevelein JM (2009) Extensive expression regulation and lack of heterologous enzymatic activity of the class II trehalsoe metabolism proteins from *Arabidopsis thaliana*. Plant Cell Environ **32**: 1015-1032

Ramon M, Rolland F, Sheen J (2008) Sugar Sensing and Signaling. The Arabidopsis Book **6**: e0117, doi/10.1199/tab.0117

Ratnakumar S, Tunnacliffe A (2006) Intracellular trehalose is neither necessary nor sufficient for desiccation tolerance in yeast. FEMS Yeast Res **6**: 902-913

Robaglia C, Thomas M, Meyer C (2012) Sensing nutrient and energy status by SnRK1 and TOR kinases. Curr Opin Plant Biol **15**: 301-307

Rodrigues A, Adamo M, Crozet P, Margalha L, Confraria A, Martinho C, Elias A, Rabissi A, Lumbreras V, González-Guzmán M, Antoni R, Rodriguez PL, Baena-González E (2013) ABI1 and PP2CA Phosphatases Are Negative Regulators of Snf1-Related Protein Kinase1 Signaling in Arabidopsis. Plant Cell **25**: 3871-3884

Roessner-Tunali U, Urbanczyk-Wochniak E, Czechowski T, Kolbe A, Willmitzer L, Fernie AR (2003) *De novo* amino acid biosynthesis in potato tubers is regulated by sucrose levels. Plant Physiol **133**: 683-692

Roldán M, Gómez-Mena C, Ruiz-García L, Salinas J, Martínez-Zapater JM (1999) Sucrose availability on the aerial part of the plant promotes dark-morphogenesis and flowering in Arabidopsis. Plant J **20**: 581–590

Rolland F, Baena-Gonzalez E, Sheen J (2006) Sugar sensing and signaling in plants: conserved and novel mechanisms. Annu Rev Plant Biol **57**: 675-709

Rolland F, Moore B, Sheen J (2002) Sugar sensing and signaling in plants. Plant Cell **14** Suppl: S185-205

Romero C, Bellés JM, Vayá JL, Serrano R, Culiáñez-Macià FA (1997) Expression of the yeast trehalose-6-phosphate synthase gene in transgenic tobacco plants: pleiotropic phenotypes include drought tolerance. Planta **201**: 293-297

Rook F, Gerrits N, Kortstee A, van Kampen M, Borrias M, Weisbeek P, Smeekens S (1998) Sucrose-specific signaling represses translation of the Arabidopsis ATB2 bZIP transcription factor gene. Plant J **15:** 253-263

Rubio T, Vernia S, Sanz P (2013) Sumoylation of AMPKbeta2 subunit enhances AMP-activated protein kinase activity. Mol Biol Cell **24**: 1801-1811

Satoh-Nagasawa N, Nagasawa N, Malcomber S, Sakai H, Jackson D (2006) A trehalose metabolic enzyme controls inflorescence architecture in maize. Nature **441**: 227-230

Schluepmann H, Berke L, Sanchez-Perez GF (2012) Metabolism control over growth: a case for trehalose-6-phosphate in plants. J Exp Bot **63**: 3379-3390

Schluepmann H, Paul MJ (2009) Trehalose metabolites in Arabidopsis: elusive, active and central. The Arabidopsis Book **7**: e0122, doi/10.1199/tab.0122

Schluepmann H, Pellny T, van Dijken A, Smeekens S, Paul M (2003) Trehalose 6-phosphate is indispensable for carbohydrate utilization and growth in *Arabidopsis thaliana*. Proc Natl Acad Sci USA **100**: 6849-6854

Schwachtje J, Minchin PE, Jahnke S, van Dongen JT, Schittko U, Baldwin IT (2006) SNF1-related kinases allow plants to tolerate herbivory by allocating carbon to roots. Proc Natl Acad Sci USA **103**: 12935-12940

Scialdone A, Mugford ST, Feike D, Skeffington A, Borrill P, Graf A, Smith AM, Howard M (2013) Arabidopsis plants perform arithmetic division to prevent starvation at night eLife DOI: 10.7554/eLife.00669

Sheen J (1990) Metabolic repression of transcription in higher plants. Plant Cell **2:** 1027-1038

Shen W, Reyes MI, Hanley-Bowdoin L (2009) Arabidopsis protein kinases GRIK1 and GRIK2 specifically activate SnRK1 by phosphorylating its activation loop. Plant Physiol **150**: 996-1005

Simpson-Lavy KJ, Johnston M (2013) SUMOylation regulates the SNF1 protein kinase Proc Natl Acad Sci USA **doi: 10.1073/pnas.1304839110**

Smeekens S, Ma J, Hanson J, Rolland F (2010) Sugar signals and molecular networks controlling plant growth. Curr Opin Plant Biol **13**: 274-279

Smith AM, Stitt M (2007) Coordination of carbon supply and plant growth. Plant Cell Environ **30**: 1126-1149

Steinberg GR, Kemp BE (2009) AMPK in Health and Disease. Physiol Rev **89**: 1025–1078

Stitt M (1990) Fructose-2,6-bisphosphate as a regulatory molecule in plants. Annu Rev Plant Phys **41**: 153-185

Suárez R, Calderón C, Iturriaga G (2009) Enhanced Tolerance to Multiple Abiotic Stresses in Transgenic Alfalfa Accumulating Trehalose. Crop Sci **49**: 1791-1799

Sugden C, Crawford RM, Halford NG, Hardie DG (1999a) Regulation of spinach SNF1-related (SnRK1) kinases by protein kinases and phosphatases is associated with phosphorylation of the T loop and is regulated by 5'-AMP. Plant J **19**: 433-439

Sugden C, Donaghy PG, Halford NG, Hardie DG (1999b) Two SNF1- related protein kinases from spinach leaf phosphorylate and inactivate 3-hydroxy-3-methylglutaryl-coenzyme A reductase, nitrate reductase, and sucrose phosphate synthase *in vitro*. Plant Physiol **120**: 257–274

Sulpice R, Pyl ET, Ishihara H, Trenkamp S, Steinfath M, Witucka-Wall H, Gibon Y, Usadel B, Poree F, Piques MC, Von Korff M, Steinhauser MC, Keurentjes JJ, Guenther M, Hoehne M, Selbig J, Fernie AR, Altmann T, Stitt M (2009) Starch as a major integrator in the regulation of plant growth. Proc Natl Acad Sci USA **106**: 10348-10353

Takeda S, Mano S, Ohto MA, Nakamura K (1994) Inhibitors of protein phosphatases 1 and 2A block the sugar inducible gene expression in plants. Plant Physiol **106**: 567-574

Thelander M, Olsson T, Ronne H (2004) Snf1-related protein kinase 1 is needed for growth in a normal day–night light cycle. EMBO J **23**: 1900-1910

Tiessen A, Padilla-Chacon D (2013) Sub cellular compartmentation of sugar signaling: links among carbon cellular status, route of sucrolysis, sink-source allocation, and metabolic partitioning. Front Plant Sci **3**: 306

Tiessen A, Prescha K, Branscheid A, Palacios N, McKibbin R, Halford, NG, Geigenberger P (2003) Evidence that SNF1-related kinase and hexokinase are involved in separate sugar-signaling pathways modulating post-translational redox activation of ADP-glucose pyrophosphorylase in potato tubers. Plant J **35**: 490-500

Toroser D, Plaut Z, Huber SC (2000) Regulation of a plant SNF1-related protein kinase by glucose 6-phosphate. Plant Physiol **123**: 403-411

Townley R, Shapiro L (2007) Crystal structures of the adenylate sensor from fission yeast AMP-activated protein kinase. Science **315**: 1726-1729

Tsai A Y-L, Gazzarrini S (2012) Overlapping and distinct roles of AKIN10 and FUSCA3 in ABA and sugar signaling during seed germination. Plant Signal Behav **7**: 1238-1242

Tsai AY, Gazzarrini S (2012) AKIN10 and FUSCA3 interact to control lateral organ development and phase transitions in Arabidopsis. Plant J **69**: 809-821

Ullah H, Chen JG, Wang S, Jones AM (2002) Role of a heterotrimeric G protein in regulation of Arabidopsis seed germination. Plant Physiol **129**: 897-907

Usadel B, Bläsing OE, Gibon Y, Retzlaff K, Hohne M, Gunther M, Stitt M (2008) Global Transcript Levels respond to Small Changes of the Carbon Status during a Progressive Exhaustion of Carbohydrates in Arabidopsis Rosettes. Plant Physiol **146:** 1834-1861

van Dijck P, Mascorro-Gallardo JO, De Bus M, Royackers K, Iturriaga G, Thevelein JM (2002) Truncation of *Arabidopsis thaliana* and *Selaginella lepidophylla* trehalose-6-phosphate synthase unlocks high catalytic activity and supports high trehalose levels on expression in yeast. Biochem J **366**: 63-71

van Dijken AJ, Schluepmann H, Smeekens SC (2004) Arabidopsis trehalose-6-phosphate synthase 1 is essential for normal vegetative growth and transition to flowering. Plant Physiol. **135**: 969–977

Vandesteene L, López-Galvis L, Vanneste K, Feil R, Maere S, Lammens W, Rolland F, Lunn JE, Avonce N, Beeckman T, van Dijck P (2012) Expansive evolution of the trehalose-6-phosphate phosphatase gene family in Arabidopsis. Plant Physiol **160**: 884–896

Vandesteene L, Ramon M, Le Roy K, van Dijck P, Rolland F (2010) A single active Trehalose-6-P Synthase (TPS) and a family of putative regulatory TPS-like proteins in Arabidopsis. Mol Plant **3**: 406–419

Vargas WA, Salerno GL (2010) The Cinderella story of sucrose hydrolysis: alkaline/neutral invertases, from cyanobacteria to unforeseen roles in plant cytosol and organelles. Plant Sci **178**: 1-8

Vaughn MW, Harrington GN, Bush DR (2002) Sucrose-mediated transcriptional regulation of sucrose symporter activity in the phloem. Proc Natl Acad Sci USA **99:** 10876–10880

Vogel G, Aeschbacher RA, Muller J, Boller T, Wiemken A (1998) Trehalose 6-phosphate phosphatases from *Arabidopsis thaliana*: identification by functional complementation of the yeast tps2 mutant. Plant J **13**: 673-683

Wahl V, Ponnu J, Schlereth A, Arrivault S, Langenecker T, Franke A, FeiR, Lunn JE, Stitt M, Schmid M (2013) Regulation of flowering by trehalose-6-phosphate signaling in *Arabidopsis thaliana.* Science 339: 704-707

Wang R, Okamoto M, Xing X, Crawford NM (2003) Microarray analysis of the nitrate response in Arabidopsis roots and shoots reveals over 1,000 rapidly responding genes and new linkages to glucose, trehalose-6-phosphate, iron, and sulfate metabolism. Plant Physiol **132:** 556-567

Wang Z, Wilson WA, Fujino MA & Roach PJ (2001) Antagonistic controls of autophagy and glycogen accumulation by Snf1p, the yeast homolog of AMP-activated protein kinase, and the cyclin-dependent kinase Pho85p. Mol Cell Biol **21**: 5742–5752

Wiese A, Elzinga N, Wobbes B, Smeekens S (2004) A conserved upstream open reading frame mediates sucrose-induced repression of translation. Plant Cell **16**: 1717-1729

Wilkinson KA, Henley JM (2010) Mechanisms, regulation and consequences of protein SUMOylation. Biochem J **428**: 133-145

Wingenter K, Schulz A, Wormit A, Wic S, Trentmann O, Hoermiller II, Heyer AG, Marten I, Hedrich R, Neuhaus HE (2010) Increased Activity of the Vacuolar Monosaccharide Transporter TMT1 Alters Cellular Sugar Partitioning, Sugar Signaling, and Seed Yield in Arabidopsis. Plant Physiol **154**: 665–677

Wingler A, Delatte TL, O'Hara LE, Primavesi LF, Jhurreea D, Paul MJ, Schluepmann H (2012) Trehalose 6-phosphate is required for the onset of leaf senescence associated with high carbon availability. Plant Physiol 158: 1241–1251

Wingler A, Purdy S, MacLean JA, Pourtau N (2006) The role of sugars in integrating environmental signals during the regulation of leaf senescence. J Exp Bot **57**: 391–399

Woods A, Munday MR, Scott J, Yang X, Carlson M, Carling D (1994) Yeast SNF1 is functionally related to mammalian AMP-activated protein kinase and regulates acetyl-CoA carboxylase *in vivo*. J Biol Chem **269**: 19509-19515

Wu L, Birch RG (2010) Physiological basis for enhanced sucrose accumulation in an engineered sugarcane cell line. Funct Plant Biol **37**: 1161-1174

Wullschleger S, Loewith R, Hall MN (2006) TOR signaling in growth and metabolism. Cell **124**: 471-484

Xiao B, Sanders MJ, Underwood E, Heath R, Mayer FV, Carmena D, Jing C, Walker PA, Eccleston JF, Haire LF, Saiu P, Howell SA, Aasland R, Martin SR, Carling D, Gamblin SJ (2011) Structure of mammalian AMPK and its regulation by ADP. Nature **472**: 230-233

Xiao W, Sheen J, Jang JC (2000) The role of hexokinase in plant sugar signal transduction and growth and development. Plant Mol Biol **44:** 451-461

Yanagisawa S, Yoo SD, Sheen J (2003) Differential regulation of EIN3 stability by glucose and ethylene signaling in plants. Nature **425:** 521-525

Yu, SM (1999) Cellular and genetic responses of plants to sugar starvation. Plant Physiol **121**: 687–693

Yuan K, Wysocka-Diller J. (2006) Phytohormone signaling pathways interact with sugars during seed germination and seedling development. J Exp Bot **57:** 3359-3367

Zeeman SC, Kossmann J, Smith AM (2010) Starch: its metabolism, evolution, and biotechnological modification in plants. Annu Rev Plant Biol **61**: 209–234

Zhang H, Zhou C (2013) Signal transduction in leaf senescence. Plant Mol Biol **82**: 539-545

Zhang Y, Primavesi LF, Jhurreea D, Andralojc J, Mitchell RAC, PowersSJ, Schluepmann H, Delatte T, Wingler A, Paul MJ (2009) Inhibition of Snf1-related protein kinase (SnRK1) activity and regulation of metabolic pathways by trehalose 6-phosphate. Plant Physiol **149**: 1860–1871

Zhang Y, Shewry PR, Jones H, Barcelo P, Lazzeri PA, Halford NG (2001) Expression of anti-sense SnRK1 protein kinase sequence causes abnormal pollen development and male sterility in transgenic barley. Plant J **28**: 431-441

Zhou L, Jang JC, Jones TL, Sheen J (1998) Glucose and ethylene signal transduction crosstalk revealed by an Arabidopsis glucose insensitive mutant. Proc Natl Acad Sci USA **95:** 10294-10299

CHAPTER II

Inhibition of SnRK1 by metabolites: Tissue-dependent effects and cooperative inhibition by glucose 1-phosphate in combination with trehalose 6-phosphate

The work presented in this chapter was mostly performed by Cátia Nunes (see acknowledgments section) and partially included in the following publication:

Nunes C, Primavesi LF, Patel MK, Martínez-Barajas E, Powers SJ, Sagar R, Fevereiro PS, Davis BG, Paul MJ **(2013)** Inhibition of SnRK1 by metabolites: Tissue-dependent effects and cooperative inhibition by glucose 1-phosphate in combination with trehalose 6-phosphate. **Plant Physiology and Biochemistry** 63, 89-98.

2.1. Abstract

SnRK1 of the SNF1/ AMPK group of PKs is an important regulatory kinase in plants. SnRK1 was recently shown as a target of the sugar signal, T6P. T6P responds to sugar availability and through a separable factor inhibits SnRK1 which alters gene expression and promotes growth processes. This suggests the importance of *in vivo* metabolic regulation of SnRK1. G6P has also been shown to inhibit SnRK1 *in vitro* and more recently, R5P was reported to inhibit SnRK1 in wheat grain tissue. We have therefore sought to investigate if other metabolites could also inhibit this central regulator and establish if each could impart distinct inhibition of SnRK1. In Arabidopsis seedlings crude extract several nucleotides were shown to inhibit SnRK1 by direct competition with ATP. Analysis of protein extracts from different tissues revealed that some other candidates were in fact false positives. Apparent inhibition of SnRK1 from green tissue by R5P is suggested to be due to parallel consumption of ATP whereas UDPG inhibited SnRK1 only in extracts where it could be converted to G1P. G1P was the only other central metabolite shown to consistently inhibit SnRK1. The kinase activity profiles of partially purified extracts from Arabidopsis seedlings, mature leaves and cauliflower florets (*Brassica oleracea*) are quite similar and suggest a common intermediary factor for T6P, G6P and G1P inhibition. Kinetic models show that T6P, G1P and G6P each provide distinct regulation of SnRK1 (50% inhibition of SnRK1 at 5.4 µM, 480 µM, >1 mM, respectively). Strikingly, G6P in combination with T6P produces cumulative inhibition of SnRK1 and most interestingly G1P in combination with T6P inhibited SnRK1 synergistically. Data provide further insight into the sophisticated regulation of the important regulatory PK, SnRK1. We suggest that these interactions can be of critical importance for SnRK1 regulation *in vivo*.

2.2. Introduction

Active AMPK/ SnRK1/ SNF1, calcium-independent serine-threonine PKs, function to conserve energy and carbon supplies in response to energy or carbon

limitation (Baena-González *et al.*, 2007; Hardie, 2007; Polge and Thomas, 2007). They are typically heterotrimeric complexes, composed of an alpha catalytic subunit and two regulatory subunits, beta and gamma; plus a number of additional interacting and regulatory factors (Bhalerao *et al.*, 1999; Ananieva *et al.*, 2008). Sizes of SnRK1 complexes are thought to range from around 118 kDa to 165 kDa, but could be far more than this following multimerisation or complexing with other proteins. AMPK/ SNF1/ SnRK1 kinase activity regulation is far from being fully understood. They are active when a conserved threonine of the alpha subunit T-loop is phosphorylated (Shen *et al.*, 2009; Crozet *et al.*, 2010). Among other possibilities these PKs are subject to allosteric regulation. AMPK (but not SNF1 or SnRK1) is regulated directly by AMP/ ATP ratio (Hardie et al, 1999), ADP (Hardie *et al.*, 2011; Xiao *et al.*, 2011), glycogen (McBride *et al.*, 2009) and fatty acids (Clark *et al.*, 2004). Yeast SNF1 and plant SnRK1 are also, to some extent, affected by AMP (Momcilovic *et al.*, 2008; Sugden *et al.*, 1999 respectively). More interestingly, sugar phosphates like G6P (Toroser *et al.*, 2000) (1-10 mM) and T6P (Zhang *et al.*, 2009; Martínez-Barajas *et al.*, 2011) were found to inhibit SnRK1 *in vitro* constituting another form of regulating kinase activity. Significantly, T6P as a signal of sucrose availability inhibits SnRK1 through a separable interacting protein (Factor I), promoting the activation of SnRK1 target genes that promote biosynthetic and growth processes whilst at the same time repressing those involved in starvation responses (Zhang *et al.*, 2009; Paul *et al.*, 2010).

Given the available clues about AMPK/ SnRK1/ SNF1 regulation and evidence from Toroser *et al.* (2000) that other metabolites could interact with SnRK1, we screened a number of possible metabolic inhibitors. Analysis of protein extracts from different tissues exposed several false positives but also contributed with several other cues about SnRK1 regulation. ADP, as well as other nucleotides, were shown to compete with ATP for the catalytic site. T6P and its precursors (G6P and UDPG) together with G1P and F6P are interconvertible hexose-based central metabolic intermediates from which many plant products are synthesised, such as starch and cell walls (Granot *et al.*, 2013). Given the function of T6P in promoting

biosynthetic processes we compared these metabolites with T6P and G6P. A partial purification procedure was carried out in Arabidopsis seedlings, mature leaves and cauliflower florets (*Brassica oleracea*) in order to obtain cleaner extracts that still retained interacting proteins like Factor I. As G6P and T6P have similar structures we wished to establish if inhibition of SnRK1 by G6P could be explained through interaction at the same site on SnRK1, or whether each was capable of discrete inhibition of SnRK1. G1P was also found to inhibit SnRK1 in preparations inhibited by T6P and G6P. All three were found to interact at distinct sites on SnRK1. Inhibition by T6P and G6P together was cumulative, but, strikingly, inhibition of SnRK1 by T6P and G1P together was synergistic. Data provide further insight into the regulation of this important PK by metabolites and also expose an important caveat in the assessment of potential PK inhibitors.

2.3. Results

2.3.1. Screening for potential inhibitors of SnRK1

SnRK1 activity was shown to be inhibited *in vitro* by G6P (Toroser *et al.*, 2000) and by T6P (Zhang *et al.*, 2009). Given the strong effect of SnRK1 on biosynthetic pathways (Baena-Gonzalez *et al.*, 2007, Zhang *et al.*, 2009) we sought to examine a comprehensive range of compounds involved in these pathways that could potentially also regulate SnRK1 (Table 2.1). Because T6P inhibition of SnRK1 was shown to be mediated by a separable factor (Zhang *et al.*, 2009), the assays were performed in crude extracts to prevent false negatives due to loss of interacting proteins. SnRK1 activity from *A. thaliana* seedlings was assayed with 1 mM of each metabolite. The extracts were prepared with phosphatase inhibitors and therefore, regulation through dephosphorylation could not be detected, directing this survey to competitive or allosteric interactions only. From the 52 compounds tested, excluding T6P and G6P, 12 inhibited SnRK1 by more than 20%. From these, 8 were nucleotides: uridine triphosphate (UTP), uridine diphosphate (UDP), uridine diphosphate galactose (UDP galactose), guanosine triphosphate (GTP), adenosine

diphosphate (ADP) and adenosine monophosphate (AMP), adenosine diphosphate glucose (ADP glucose) and adenosine diphosphate ribose (ADP ribose); two were central metabolites: UDPG and G1P; and two were compounds from the pentose phosphate pathway: R5P and Ru5P. Two fatty acids abolished the assay giving readings below the control assay without peptide, whereas two others made the assay mixture cloudy and increased SnRK1 activity by more than 20%. These effects were not considered for further investigation because the compounds clearly interfered with the normal behavior of the assay.

Table 2.1. Impact of different metabolites on SnRK1 activity from *A. thaliana* seedlings crude extract.

Data expressed as % activity compared to control with no metabolite (100%). The assays were performed with 1 mM compound. Representative values of at least two independent assays are presented.

Compound	Activity %
T6P	30
Central Metabolites	
UDPG	45
G1P	55
G6P	75
F6P	90
Uridine Nucleotides	
UTP	35
UDP	24
UMP	85
UDP galactose	60
UDPG glucuronic acid	85
UDP-acetyl glucosamine	90
Guanosine Nucleotides	
GTP	61
GDP	80
GMP	100
GDPG	102
GDP mannose	98
GDP fucose	83
Cyclic GMP	92
Adenosine Nucleotides	
ADP	28
AMP	65
ADP glucose	73
ADP ribose	46
Cofactors	
NAD	81
NADH	81
NADP	96
NADPH	108

Table 2.1. (Continued)

Compound	Activity %
Pentose Phosphate Pathway	
Ribose 5-P	52
Ribulose 5-P	58
Ribulose 1,5-bisP	80
Xylulose 5-P	101
6-phosphogluconate	ns
Amino Acid Precursors	
Glutamate	102
Aspartate	98
Alpha-ketoglutarate	107
Fatty Acids Precursors	
Glycerol 3-P	104
Acetyl coenzyme A	103
Fatty Acids	
Tergitol	112
Myristic acid (14:0)	94
Palmitic acid (16:0)	124
Stearic acid (18:0)	126
Linoleic acid (18:1)	94
Oleic acid (18:1)	-
Palmitoleic acid (16:1)	-
Sugars	
Sucrose	95
Glucose	95
Maltose	95
Trehalose	95
Other	
Fructose 1,6-bisP	90
Fructose 2,6-bisP	95
Sucrose 6-P	103
Soluble Starch	102
D(+)Maltose monohydrate	95
Xylulose 5-P	101

ns: not soluble

-: readings below blank (control assay without peptide

2.3.2. Nucleotides inhibition of SnRK1 are pure competitive with respect to ATP

From the inhibiting nucleotides, ADP glucose and ADP ribose were tested in Arabidopsis mature leaves crude extract showing the same level of SnRK1 inhibition as in seedlings extracts, an effect not observed with T6P or G6P which only inhibit SnRK1 in growing tissues (Zhang *et al.*, 2009). This reinforced the hypothesis that nucleotides would inhibit SnRK1 through direct competition with ATP. This was shown to be the case for the tested nucleotides: ADP, UTP, ADP glucose and ADP ribose. The levels of SnRK1 activity for concentration series of both substrate (ATP) and the different inhibitors were determined and data analysed by linearization methods (Segel, 1993) (Fig. 2.1 and 2.2). Characterization of the linearized plots enables the identification of the type of inhibition involved. The direct representation of the effect of substrate (ATP) and inhibitor (ADP) variation on SnRK1 activity clearly shows that ATP concentration had an impact on inhibition, indicating competitive inhibition (Fig. 2.1A). After data linearization, lines crossing at y-axis in the reciprocal plots (Fig. 2.1C) confirm the competition model. The same properties were observed for UTP, ADP glucose and ADP ribose (Fig. 2.1B and D, Fig. 2.2A and C, Fig. 2.2B and D, respectively). The linear replot of slopes indicates that all tested nucleotides are in fact pure competitive with respect to ATP (Fig. 2.1E and F, Fig. 2.2E and F). The Dixon plots give Ki as 103, 133, 674 and 316 µM for ADP (Fig. 2.1G), UTP (Fig. 2.1H), ADP glucose (Fig. 2.2G), and ADP ribose (Fig. 2.2H) respectively. The linear replot of slopes of the Dixon plots passing through the origin confirm that the inhibitions are neither noncompetitive nor uncompetitive (Fig. 2.1I and J, Fig. 2.2I and J). The nucleotides UDP, GTP, GDP and AMP were not tested but due to structural similarity are suggested to inhibit SnRK1 in the same way, through direct competition with ATP.

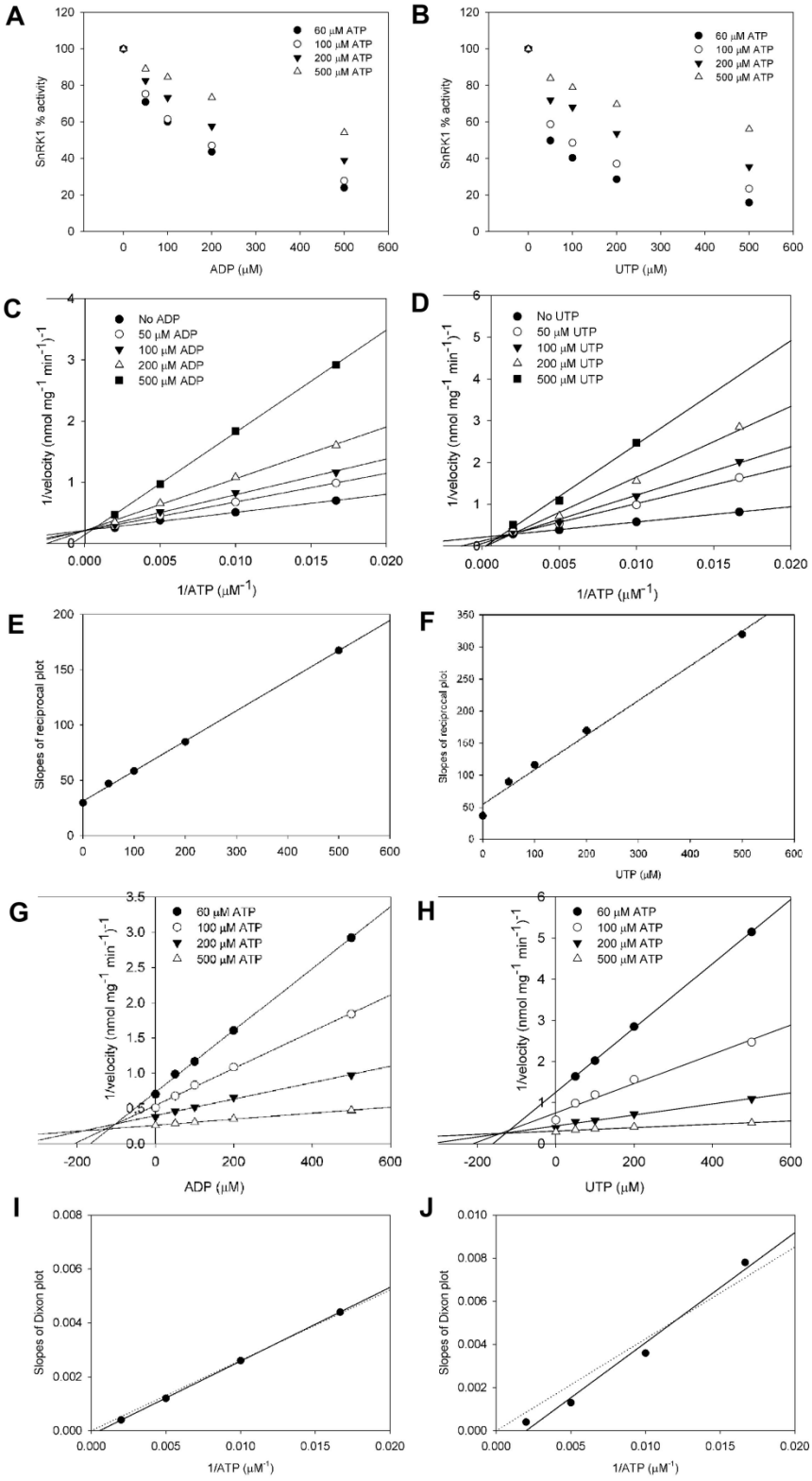
A
SnRK1 % activity
ADP (μM)
60 μM ATP
100 μM ATP
200 μM ATP
500 μM ATP
B
SnRK1 % activity
UTP (μM)
60 μM ATP
100 μM ATP
200 μM ATP
500 μM ATP
C
1/velocity (nmol mg-1 min-1)-1
1/ATP (μM-1)
No ADP
50 μM ADP
100 μM ADP
200 μM ADP
500 μM ADP
D
1/velocity (nmol mg-1 min-1)-1
1/ATP (μM-1)
No UTP
50 μM UTP
100 μM UTP
200 μM UTP
500 μM UTP
E
Slopes of reciprocal plot
F
Slopes of reciprocal plot
UTP (μM)
G
1/velocity (nmol mg-1 min-1)-1
ADP (μM)
60 μM ATP
100 μM ATP
200 μM ATP
500 μM ATP
H
1/velocity (nmol mg-1 min-1)-1
UTP (μM)
60 μM ATP
100 μM ATP
200 μM ATP
500 μM ATP
I
Slopes of Dixon plot
1/ATP (μM-1)
J
Slopes of Dixon plot
1/ATP (μM-1)

Figure 2.1. Inhibition kinetics of SnRK1 by ADP and UTP with respect to ATP in assays with AMARA peptide. Impact of different concentrations of **(A)** ADP, **(B)** UTP on SnRK1 activity with varying ATP concentrations; Lineweaver-Burk reciprocal plots (1/velocity versus 1/substrate concentration) of **(C)** ADP, **(D)** UTP; replot of slopes of the reciprocal plots of **(E)** ADP, **(F)** UTP; Dixon plots (1/velocity versus substrate concentration) of **(G)** ADP, **(H)** UTP; replot of the slopes of the Dixon plots of **(I)** ADP, **(J)** UTP. Regression solid lines in replots of the slopes of the Dixon plots are not significantly different from regression forced through origin (dotted line). Duplicate assays were performed in *Arabidopsis* seedling crude extracts.

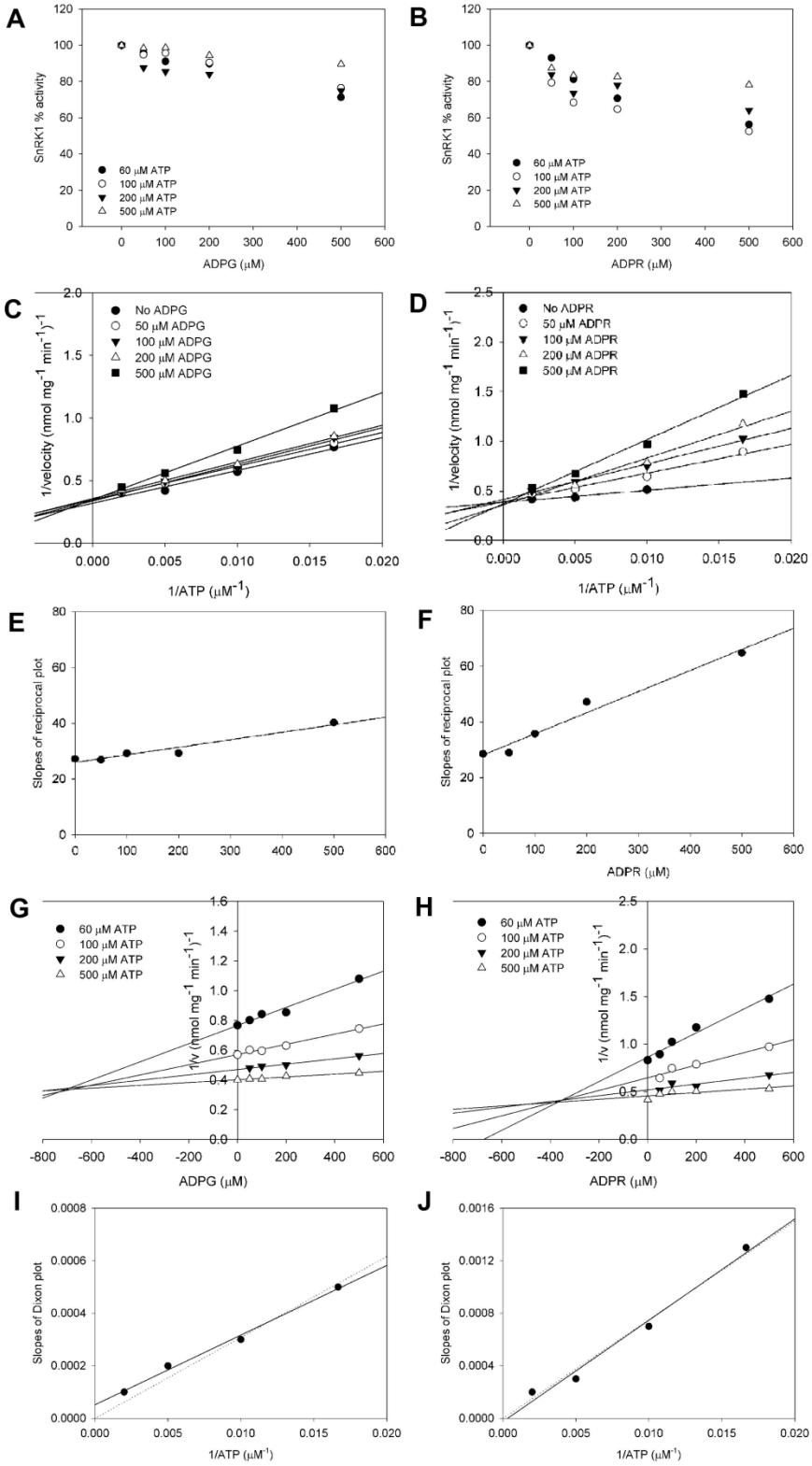
A
SnRK1 % activity
ADPG (μM)
60 μM ATP
100 μM ATP
200 μM ATP
500 μM ATP
B
SnRK1 % activity
ADPR (μM)
60 μM ATP
100 μM ATP
200 μM ATP
500 μM ATP
C
1/velocity (nmol mg-1 min-1)-1
1/ATP (μM-1)
No ADPG
50 μM ADPG
100 μM ADPG
200 μM ADPG
500 μM ADPG
D
1/velocity (nmol mg-1 min-1)-1
1/ATP (μM-1)
No ADPR
50 μM ADPR
100 μM ADPR
200 μM ADPR
500 μM ADPR
E
Slopes of reciprocal plot
F
Slopes of reciprocal plot
ADPR (μM)
G
1/v (nmol mg-1 min-1)-1
ADPG (μM)
60 μM ATP
100 μM ATP
200 μM ATP
500 μM ATP
H
1/v (nmol mg-1 min-1)-1
ADPR (μM)
60 μM ATP
100 μM ATP
200 μM ATP
500 μM ATP
I
Slopes of Dixon plot
1/ATP (μM-1)
J
Slopes of Dixon plot
1/ATP (μM-1)

Figure 2.2. Inhibition kinetics of SnRK1 by ADP glucose and ADP ribose with respect to ATP in assays with AMARA peptide. Impact of different concentrations of **(A)** ADP glucose, **(B)** ADP ribose on SnRK1 activity with varying ATP concentrations; Lineweaver-Burk reciprocal plots (1/velocity versus 1/substrate concentration) of **(C)** ADP glucose, **(D)** ADP ribose; replot of slopes of the reciprocal plots of **(E)** ADP glucose, **(F)** ADP ribose; Dixon plots (1/velocity versus substrate concentration) of **(G)** ADP glucose, **(H)** ADP ribose; replot of the slopes of the Dixon plots of **(I)** ADP glucose, **(J)** ADP ribose. Regression solid lines in replots of the slopes of the Dixon plots are not significantly different from regression forced through origin (dotted line). Duplicate assays were performed in *Arabidopsis* seedling crude extracts.

2.3.3. SnRK1 inhibition by metabolites is tissue specific

SnRK1 activity was assayed with 1 mM of metabolites that inhibited SnRK1 by more than 20% (other than the previously considered nucleotides), T6P, G1P, G6P, UDPG, UDP galactose, R5P and Ru5P in crude desalted extracts from different tissues (Table 2.2). The central metabolite F6P was also tested to exclude possible tissue-specific interactions. F6P did not inhibit SnRK1 in any of the tested extracts and therefore was not considered for further investigation. For the remaining metabolites there were strong tissue-specific differences in the degree to which each metabolite inhibited SnRK1. T6P inhibited SnRK1 in all tissues tested, with most inhibition in cauliflower curd (9% activity compared to control with no metabolite) and least inhibition in mature leaves (78% activity compared to control with no metabolite) as previously observed (Zhang *et al.*, 2009). G6P inhibited in all tissues, but to a far lesser extent than T6P. In comparison, G1P inhibited more strongly than G6P following a similar pattern to T6P with most inhibition in cauliflower curd and least inhibition in mature leaves. A different pattern was observed for the inhibition of SnRK1 by UDPG and UDP galactose, with activities reduced to the same level in all tissues. More interestingly, the extent of inhibition was very inconsistent between extracts from the same tissue, perceived by the large standard deviation values. Inhibition by R5P and Ru5P of SnRK1 activity from different tissues was the most variable of all tested metabolites. Very strong inhibition was observed in seedlings

and mature leaves, but no inhibition was found in seedling roots or cauliflower curd. Inhibition of SnRK1 by all these compounds was further investigated.

Table 2.2. Tissue comparison of inhibition of SnRK1 activity by 1 mM different metabolites.

Data expressed as % activity compared to control with no metabolite (100%) in 6-minute assays performed with AMARA peptide. Means of at least four biological replicates ± standard deviation. nd, not determined.

	Seedlings	Mature leaf	Seedling root	Cauliflower curd
T6P	20 ± 3	78 ± 2	34 ± 2	9 ± 1
G1P	59 ± 2	91 ± 1	73 ± 4	58 ± 3
G6P	70 ± 3	91 ± 3	91 ± 2	71 ± 3
F6P	95 ± 2	98 ± 2	96 ± 4	95 ± 2
UDPG	73 ± 32	77 ± 28	nd	62 ± 47
UDP galactose	66 ± 33	72 ± 25	nd	71 ± 27
R5P	23 ± 4	2 ± 0.3	100 ± 2	95 ± 3
Ru5P	5 ± 0.5	4 ± 0.2	95 ± 2	97 ± 2

2.3.3.1. Stability of T6P, G1P and G6P during SnRK1 assays

Even though SnRK1 inhibition by T6P is confirmed *in vivo* through gene expression analysis (Zhang *et al.*, 2009), we wanted to exclude the possibility of its degradation during the SnRK1 assays in Arabidopsis crude extracts. This analysis was also extended to G1P and G6P especially because of their ready interconversion.

^{31}P NMR spectra have shown only the presence of the starting phosphorylated carbohydrate, either T6P, G1P or G6P (Fig. 2.3A, Fig. 2.4A, Fig. 2.5A respectively) at the end of 10 min reaction assays confirming that no other phosphorylated end products are produced. In a different approach, all sugar phosphates were eluted by HPLC at around 15 mins (Fig. 2.3B, Fig. 2.4B, Fig. 2.5B respectively). Analysis of those peaks by ion exchange LC-MS in negative mode (inside pictures), shows, for all cases, only the mass of the original sugar phosphate, so again, no conversion was detected. Furthermore, the integral of the peaks is the

same as that of a control experiment with just the sugar phosphates (no extract) providing further evidence for stability of the sugars. To check for dephosphorylation we used C_{18} LC-MS in positive mode after per-*O*-acetylation of the crude reaction mixture. Dephosphorylated products, octaacetyl trehalose for T6P or pentaacetyl glucose for G1P and G6P, were not detected either through expected peak positions in the ion trace (Fig. 2.3C, Fig. 2.4C, Fig. 2.5C respectively), or through the underlying mass spectra. Hence, dephosphorylation of the starting carbohydrates is not occurring.

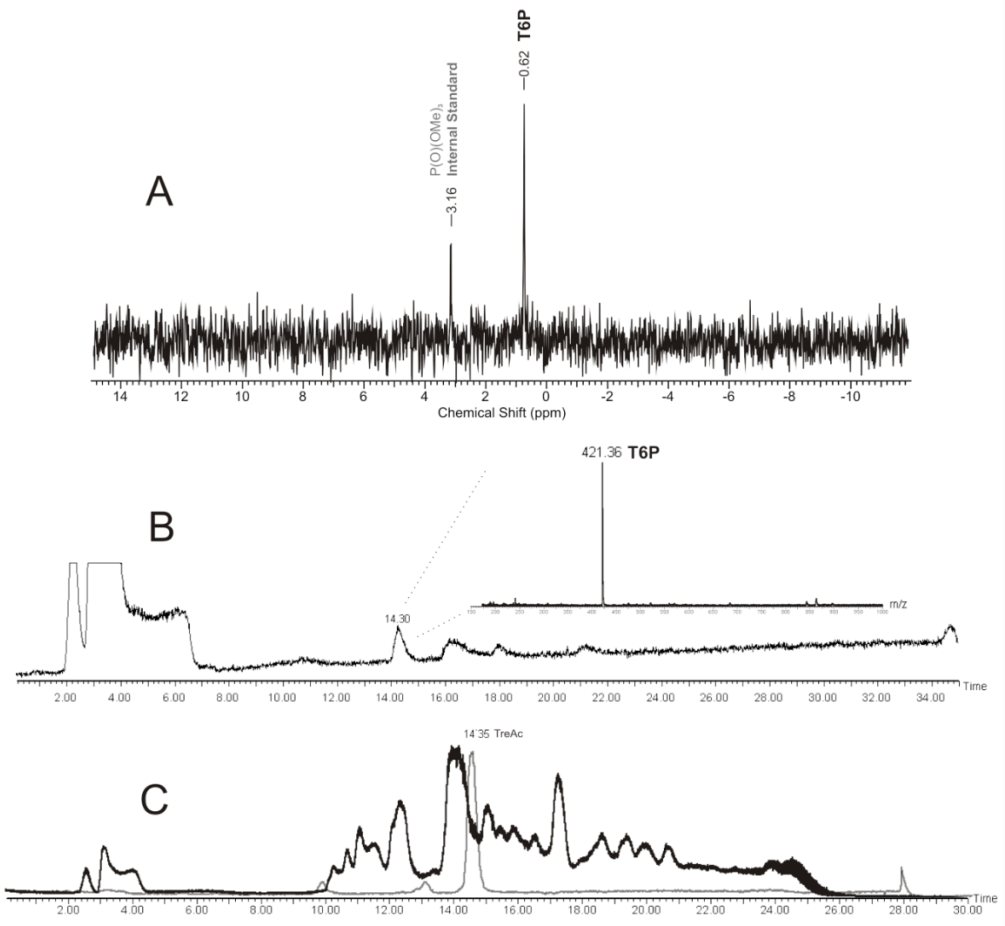

Figure 2.3. Analysis of T6P stability over the SnRK1 assay period. Reaction performed with 1 mM T6P at 30 °C for 10 mins. **(A)** ^{31}P NMR (referenced against $PO(OMe)_3$) shows only the presence of the starting phosphorylated carbohydrate **(B)** SAX LC-MS in negative mode isolates mono-phosphorylated carbohydrates at 14-15 mins. The integral of this peak is identical before and after the reaction. **(C)**

Black trace shows C_{18} LC-MS in positive mode after per-*O*-acetylation of the crude reaction mixture. Grey trace shows the expected position of the dephosphorylated sugars after per-*O*-acetylation (octaacetyl trehalose).

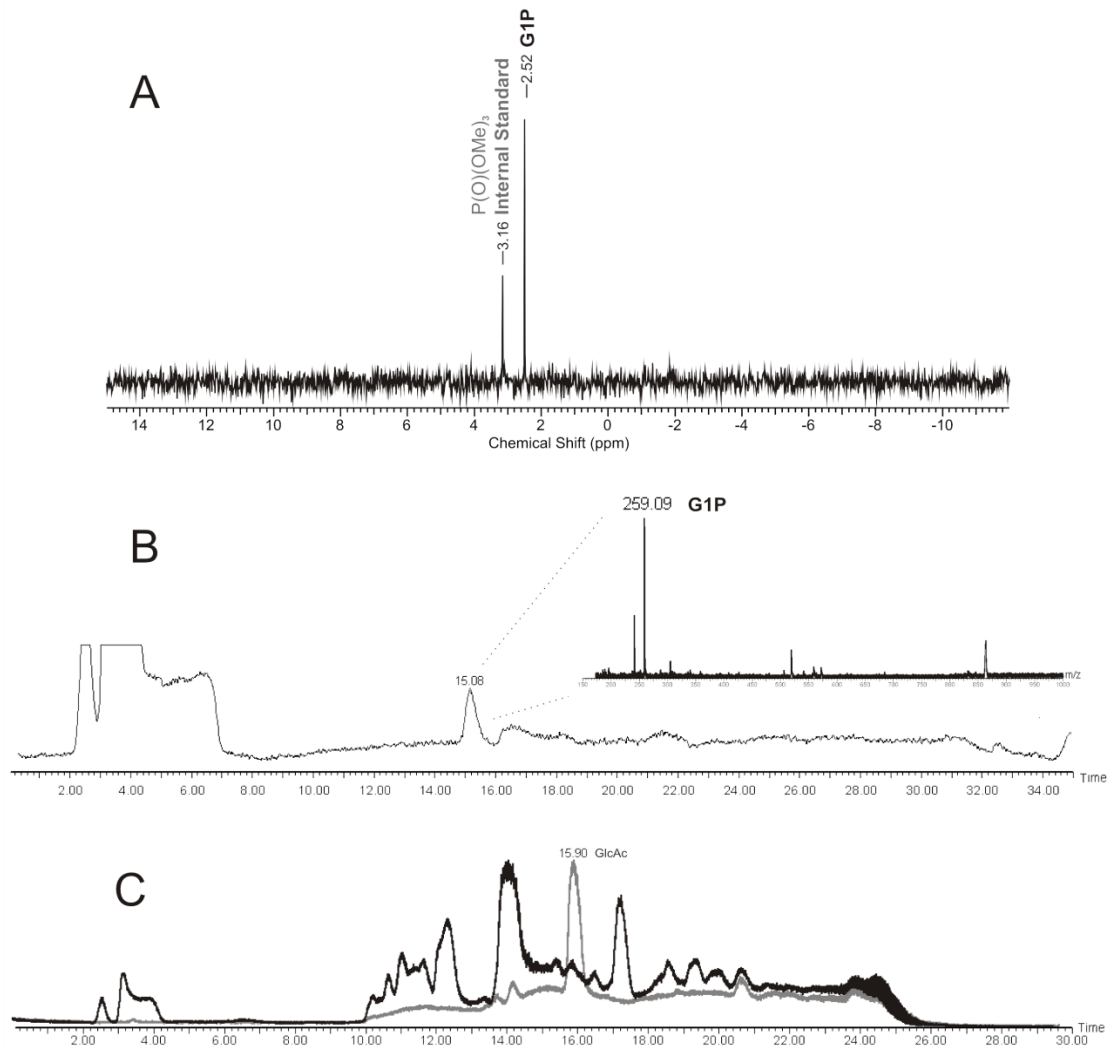

Figure 2.4. Analysis of G1P stability over the SnRK1 assay period. Reaction performed with 1 mM G1P at 30 °C for 10 mins. **(A)** ^{31}P NMR (referenced against $PO(OMe)_3$) shows only the presence of the starting phosphorylated carbohydrate **(B)** SAX LC-MS in negative mode isolates mono-phosphorylated carbohydrates at 14-15 mins. The integral of this peak is identical before and after the reaction. **(C)** Black trace shows C_{18} LC-MS in positive mode after per-*O*-acetylation of the crude reaction mixture. Grey trace shows the expected position of the dephosphorylated sugars after per-*O*-acetylation (pentaacetyl glucose).

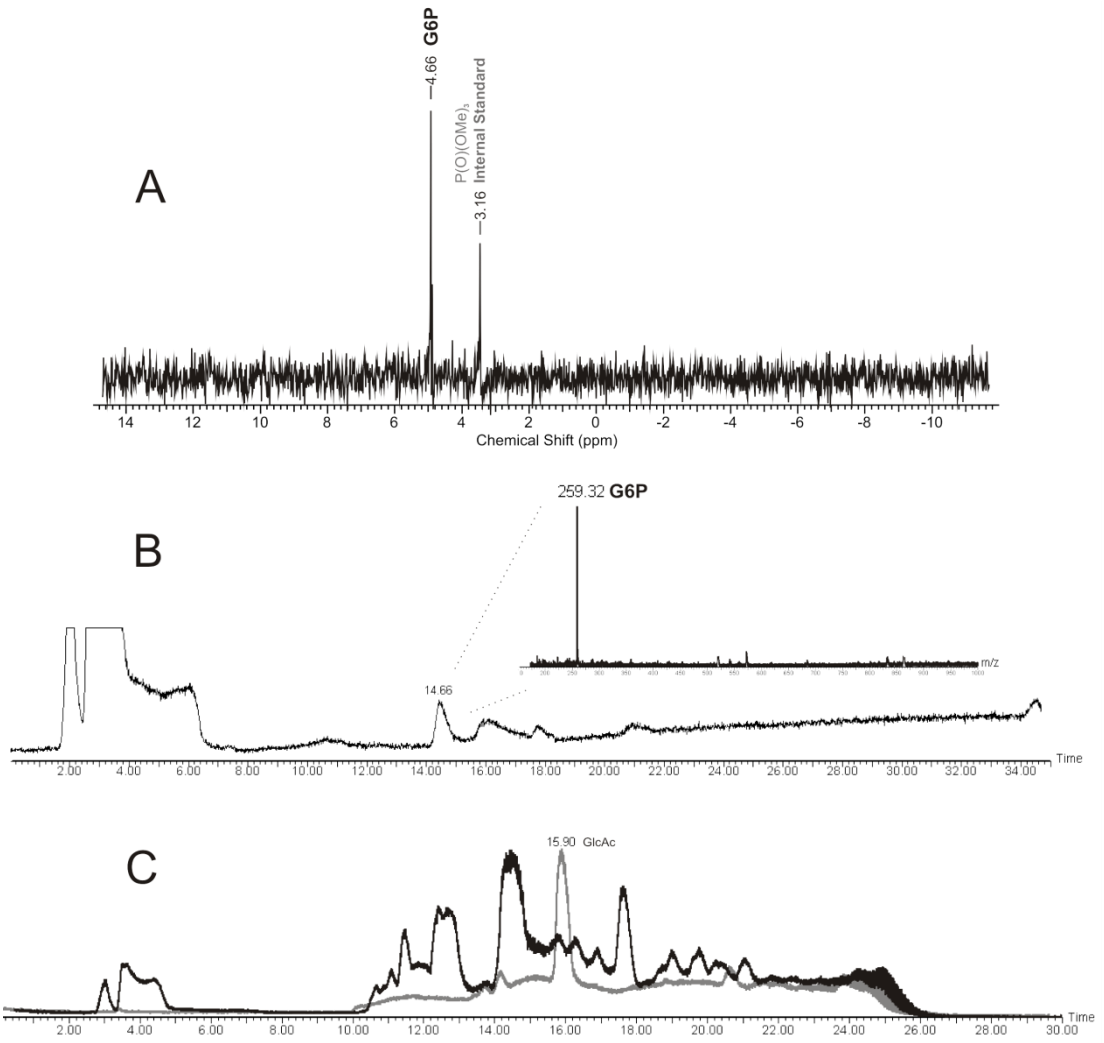

Figure 2.5. Analysis of G6P stability over the SnRK1 assay period. Reaction performed with 1 mM G6P at 30 °C for 10 mins. **(A)** ^{31}P NMR (referenced against $PO(OMe)_3$) shows only the presence of the starting phosphorylated carbohydrate **(B)** SAX LC-MS in negative mode isolates mono-phosphorylated carbohydrates at 14-15 mins. The integral of this peak is identical before and after the reaction. **(C)** Black trace shows C_{18} LC-MS in positive mode after per-*O*-acetylation of the crude reaction mixture. Grey trace shows the expected position of the dephosphorylated sugars after per-*O*-acetylation (pentaacetyl glucose).

These results show that there is no loss or interconversion of T6P, G1P and G6P in Arabidopsis protein crude extracts during the assay period further validating these metabolites as effective SnRK1 inhibitors.

2.3.3.2. Apparent inhibition of SnRK1 by UDPG and UDP galactose

The fact that inhibition of SnRK1 by UDPG and UDP galactose was extremely variable in assays performed in biological replicates of the same tissue raised the suspicion that inhibition could be artefactual. Careful analysis of time course experiments showed that the percentage inhibition of SnRK1 by 1mM UDPG and UDP galactose increased progressively with time over 6 min and with increasing sodium pyrophosphate (NaPPi) concentrations (Fig. 2.6A and B). In fact, inhibition by UDPG and UDP galactose was only observed in extracts prepared with NaPPi (Fig. 2.6C). These results indicate that the presence of NaPPi and UDPG or UDP galactose in crude extracts promotes a reaction that indirectly leads to inhibition of SnRK1 and therefore these compounds were no longer considered in this study.

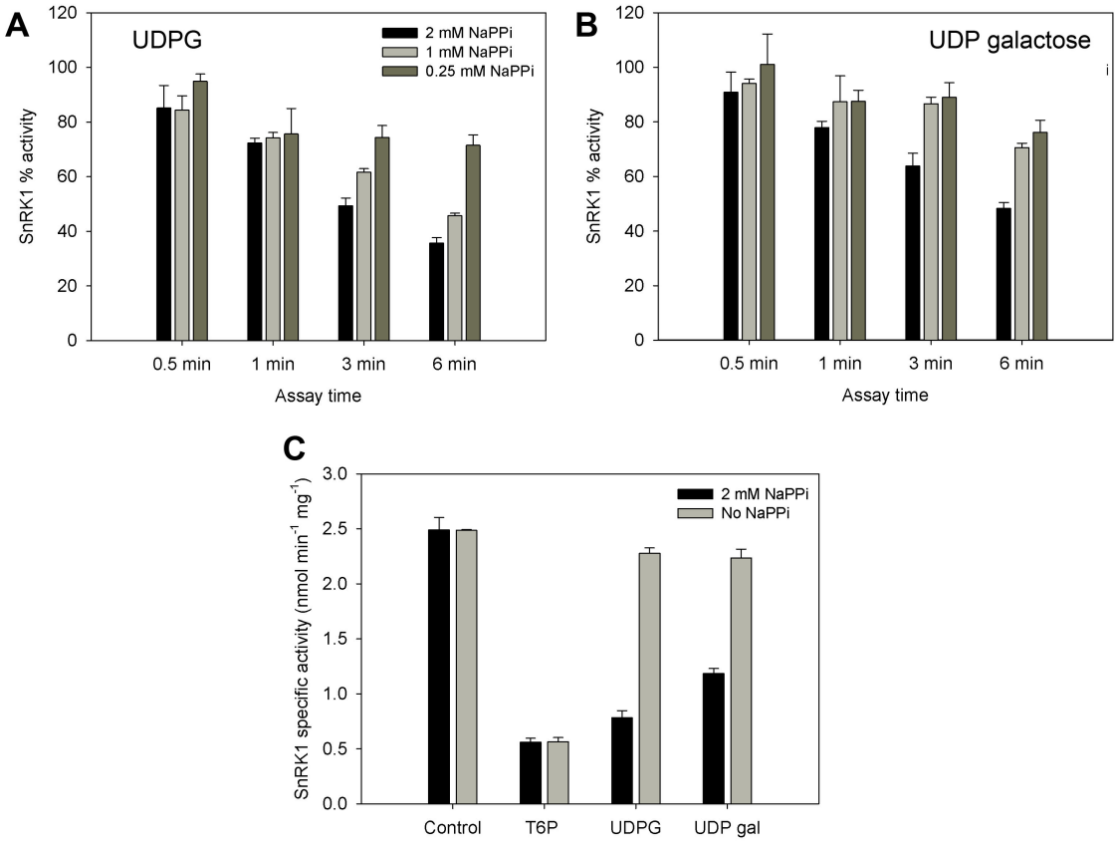

Figure 2.6. Effect of NaPPi on SnRK1 inhibition by, UDPG and UDP galactose. Seedlings crude extracts prepared as usual but with 2, 1 and 0.25 mM NaPPi were assayed over the course of 6 min with **(A)** 1 mM UDPG or **(B)** UDP galactose. **(C)** Seedlings crude extracts prepared as usual with or without 2 mM NaPPi assayed for 8 min with either 1 mM T6P, UDPG or UDP galactose. Means of 3 biological replicates with standard deviation.

2.3.3.3. Apparent inhibition of SnRK1 by R5P and Ru5P

The fact that R5P and Ru5P only inhibited SnRK1 in green tissues was intriguing and suspicious. To confirm the observed effect, Arabidopsis seedlings extract was assayed with 1 mM R5P and 1 mM Ru5P for different time lengths. It was observed that the percentage of SnRK1 inhibition by R5P and Ru5P increased progressively with time over 6 min, (Fig. 2.7A) an effect not observed for T6P inhibition of SnRK1 (Fig. 3.6B, Chapter III). This suggests that instead of R5P and

Ru5P inhibiting SnRK1 directly, a substrate could be limiting the assay. A possibility would be ATP depletion. We knew from previous optimisation of SnRK1 assays (Zhang *et al.*, 2009) that activities were linear at 200 µM ATP for at least 6 min (revisited in more detail in Chapter III). We then tested the effect of ATP concentration in the presence of R5P and Ru5P and found that inhibition of SnRK1 was much decreased in assays with 1000 µM ATP compared to 200 µM ATP (Fig. 2.7B) in contrast to the inhibition by T6P and G6P which are unaffected by ATP levels (Toroser *et al.*, 2000; Zhang *et al.*, 2009). The combined data strongly suggests that in the presence of R5P and Ru5P ATP level was limiting the SnRK1 assay. This could be mistakenly interpreted as a time-dependent inhibition of enzyme activity but it is in fact an experimental artefact. These compounds were also not considered further as SnRK1 inhibitors. However, a publication discussing R5P and Ru5P as SnRK1 inhibitors in wheat grain (Piattoni *et al.*, 2011) lead to a new series of experiments detailed in Chapter V.

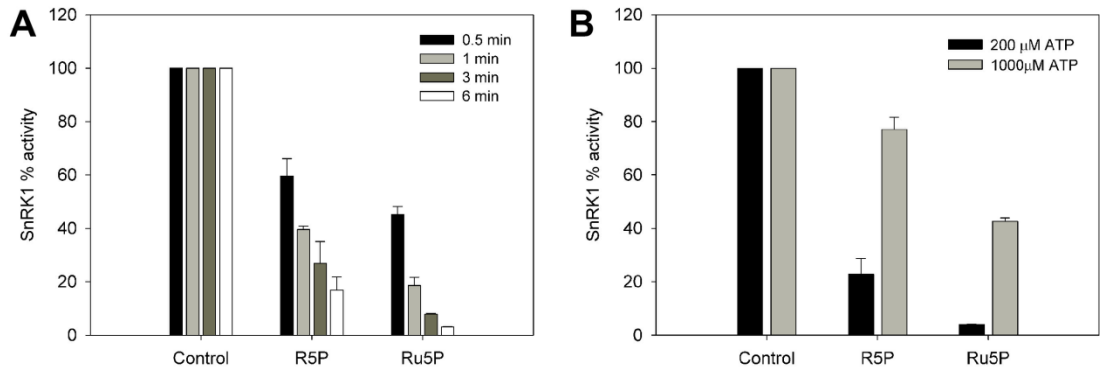

Figure 2.7. Effect of assay time and ATP concentration on SnRK1 inhibition by 1 mM R5P or 1 mM Ru5P. (A) Seedlings crude extracts prepared with 200 µM ATP assayed over the course of 6 min with R5P or Ru5P compared to control with no metabolite. **(B)** Effect of increasing ATP concentration on SnRK1 inhibition by R5P and Ru5P compared to control with no metabolite. Means of 3 biological replicates with standard deviation.

2.3.4. Inhibition profiles of partial purified SnRK1 extracts

Given the similar structure of the metabolites that did inhibit SnRK1 consistently - T6P, G6P and G1P - we went on to determine whether their inhibition of SnRK1 could be explained through interaction at the same inhibitory site, or whether each metabolite was capable of discrete inhibition of SnRK1. SnRK1 complexes from Arabidopsis seedlings, mature leaves and cauliflower florets were partially purified using a method to retain the intermediary factor necessary for inhibition of SnRK1 by T6P. SnRK1 activity following size fractionation is depicted in Fig. 2.8. SnRK1 activity and inhibition was sensitive to length and type of purification method. With the adopted protocol all extracts had their protein content reduced 10 to 15 times but specific activities did not increase more than 3 times producing low purification yields of 16% for seedlings, 5% for mature leaves and 39% for cauliflower. The activity profiles from the three tissues have similar characteristics. In accordance with previous work by Ball *et al.* (1994), two peaks of kinase activity were eluted. The main peak of SnRK1 activity at approximately 100 kDa (fractions 68-70) was inhibited by T6P whereas the second one of about 30 kDa was not. The higher molecular weight peak comprised mainly AKIN10 isoform (as shown in Chapter III) and as previously observed in SnRK1 preparations from Arabidopsis cell suspension cultures and leaves (Jossier *et al.*, 2009). Maximal inhibition by T6P expressed as a percentage compared to SnRK1 activity without T6P was seen in fraction 64 (174 kDa) where SnRK1 was inhibited to 14%, 60% and 6% in Arabidopsis seedlings, mature leaves and cauliflower curd respectively. AKIN10 is about 60 kDa, so the activity measured here is likely to be part of a complex that includes beta and gamma subunits, the predicted sizes of which range from 13-53 kDa (www.uniprot.org) and which theoretically can give SnRK1 complexes of 118-165 kDa depending on the particular subunits involved. All these fractions and those that preceded them up to a size of 315 kDa were inhibited by 1 mM T6P (Fig. 2.8).

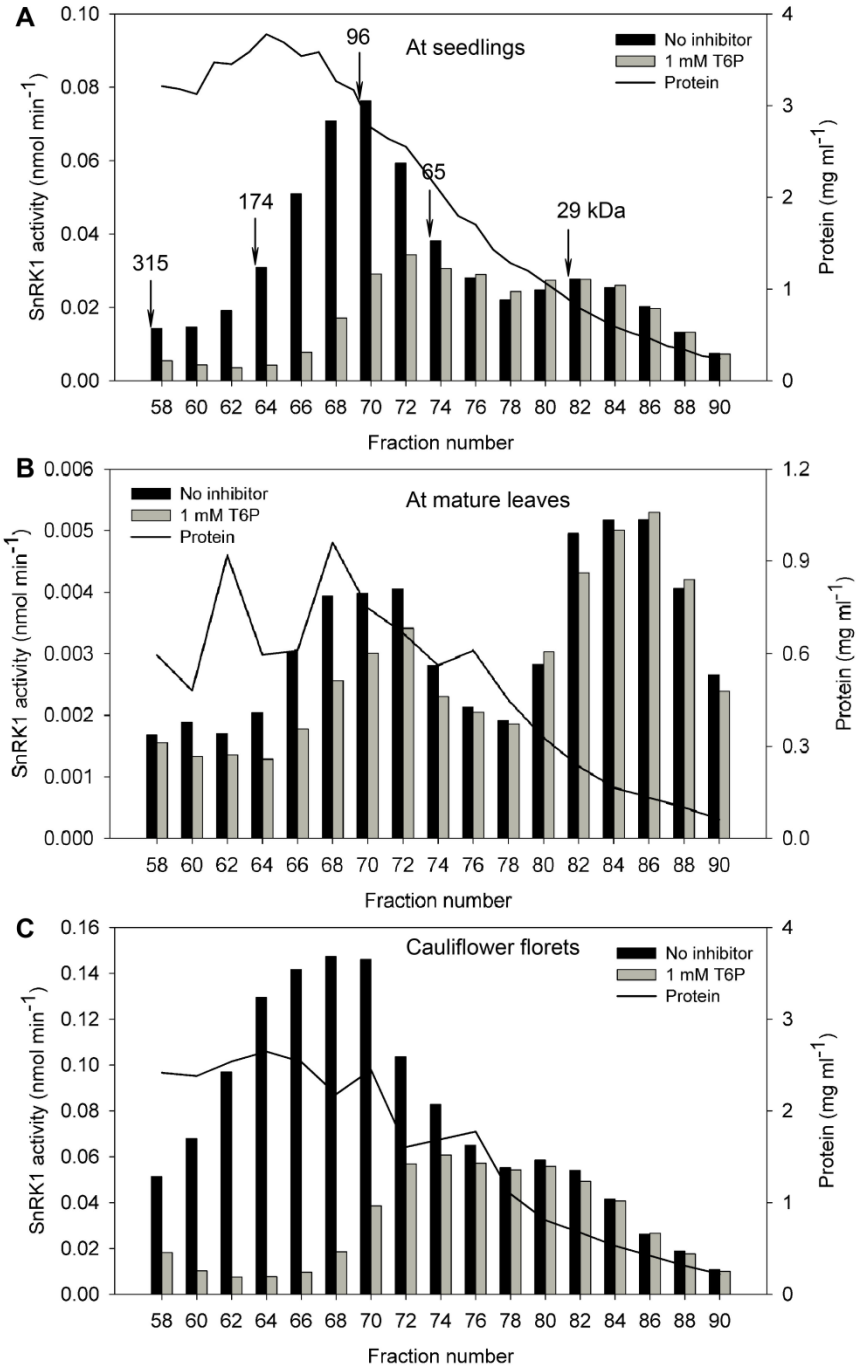

Figure 2.8. SnRK1 activity separated by size fractionation to retain intermediary factor I of SnRK1 complex. SnRK1 activity assayed with 1 mM T6P compared to no T6P (bars and left axis); line indicates protein concentration (right axis) (A) From Arabidopsis seedlings. (B) From Arabidopsis mature leaves (C) From cauliflower florets. Each point is the average of a technical duplicate.

G6P and G1P inhibited SnRK1 activities in the same extracts that were inhibited by T6P both with AMARA and SPS peptides (Fig. 2.9). The three inhibitors have coincident inhibition peaks around fraction 64. T6P is the strongest inhibitor regardless of the peptide used but inhibits less SnRK1 activity in assays with SPS peptide than with AMARA peptide. With SPS peptide maximal inhibition by T6P expressed as activity percentage compared to SnRK1 activity without T6P was 41%, 68% and 25% in Arabidopsis seedlings, mature leaves and cauliflower curd respectively. Similarly, G1P inhibition is much decreased in assays with SPS peptide (to the exception of mature leaves extracts where inhibition is virtually absent with both peptides). In fraction 64 of seedlings, inhibition by G1P dropped from 54% with AMARA peptide to 20% with SPS peptide and in cauliflower curd from 64% with AMARA peptide to 25% with SPS peptide. Interestingly, G6P inhibition of SnRK1 is, on the other hand, stronger in assays with SPS peptide, with about 30% inhibition in all tissues against minute inhibition with AMARA peptide.

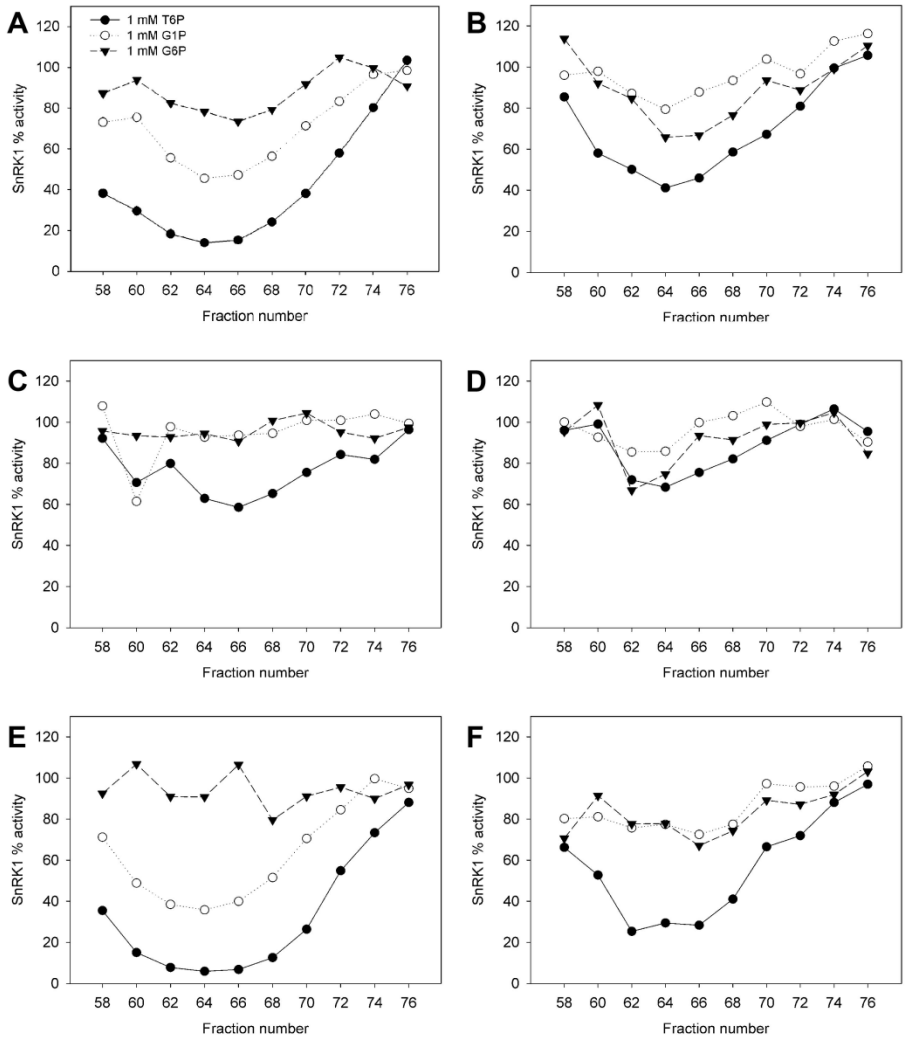

Figure 2.9. Inhibition of SnRK1 activity by 1 mM T6P in comparison with 1 mM G1P and 1 mM G6P expressed as a percentage compared to with no metabolite. **(A)** From Arabidopsis seedlings assayed with AMARA peptide and **(B)** SPS peptide, **(C)** From Arabidopsis mature leaves assayed with AMARA peptide and **(D)** SPS peptide, **(E)** From cauliflower florets assayed with AMARA peptide and **(F)** SPS peptide. Each point is the average of a technical duplicate.

As the inhibition profile of all three metabolites was coincident and it had been previously determined that inhibition of SnRK1 by T6P is dependent on an

intermediary factor that can be separated away by immunoprecipitation of SnRK1 (Zhang *et al.*, 2009), we went on to determine whether isolation of SnRK1 by this method also removed inhibition by G1P and G6P. The resuspended immunoprecipitated pellet of SnRK1 showed no inhibition by G1P and G6P leaving the expected SnRK1 inhibition percentages in the remaining SnRK1 activity left in the supernatant (Fig. 2.10). This demonstrates that inhibition of SnRK1 by G1P and G6P, as that by T6P, is dependent on an intermediary factor that can be separated from SnRK1.

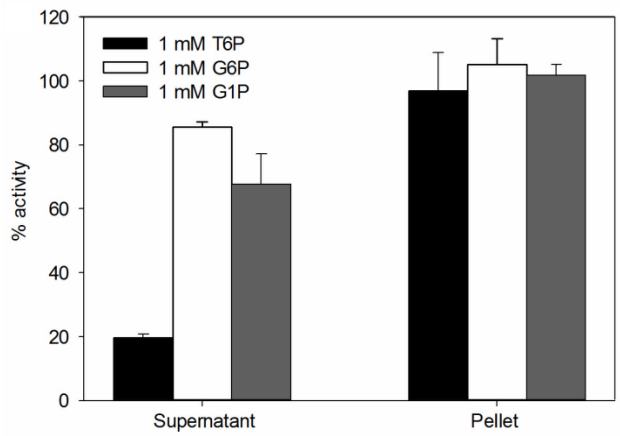

Figure 2.10. Inhibition of SnRK1 activity by 1 mM T6P, G1P and G6P after immunoprecipitation of SnRK1. Assays conducted on extract after immunoprecipation (supernatant) and after resuspension of immunoprecipitate (pellet). Inhibition expressed as a percentage compared to with no metabolite. Mean of duplicate assays with standard deviation.

2.3.5. Kinetics of the inhibition of SnRK1 by T6P, G1P and G6P

Inhibition kinetics of SnRK1 by T6P were analysed in fraction 64 from seedlings which approximated to the predicted size for a SnRK1 heterotrimeric complex. Kinetics showed that inhibition of SnRK1 by T6P fitted the partial non-competitive model (Fig. 9A) a simpler model than the mixed-type model previously characterised for crude extracts (Zhang *et al.*, 2009). In partial non-competitive

inhibition the inhibitor converts the enzyme to a modified enzyme inhibitor complex with a decreased rate of product formation but where inhibitor never decreases velocity to zero as happens in pure non-competitive inhibition. Substrate, ATP, and inhibitor, T6P, combine independently and reversibly with SnRK1 at different sites. T6P causes no change in the affinity of substrate ATP ($\alpha = 1$). Dissociation constant of the enzyme-inhibitor complex (Ki) was 4.0 µM. Fifty per cent inhibition was achieved at 5.1 µM T6P. Some studies of SnRK1 have used the SPS peptide as substrate (Baena-González *et al.*, 2007). When SPS peptide was used in kinetic studies instead of AMARA peptide, the same model of inhibition was found with similar kinetic parameters (Ki 5.4 µM). Kinetic analysis showed that inhibition by G6P fitted a hyperbolic mixed type model (Fig. 9B). Here G6P affects both the binding of ATP and the formation of product. Ki was 301 µM, reflecting the need for higher inhibitor concentration than for T6P. Inhibition of SnRK1 by G1P best fitted a partial non-competitive model (Fig. 9C), the same model found for T6P. This model predicts also that substrate, ATP, and inhibitor, G1P, combine independently and reversibly with SnRK1 at different sites. G1P causes no change in the affinity of substrate ATP. Ki was 55.2 µM; 50% inhibition was at 480 µM G1P.

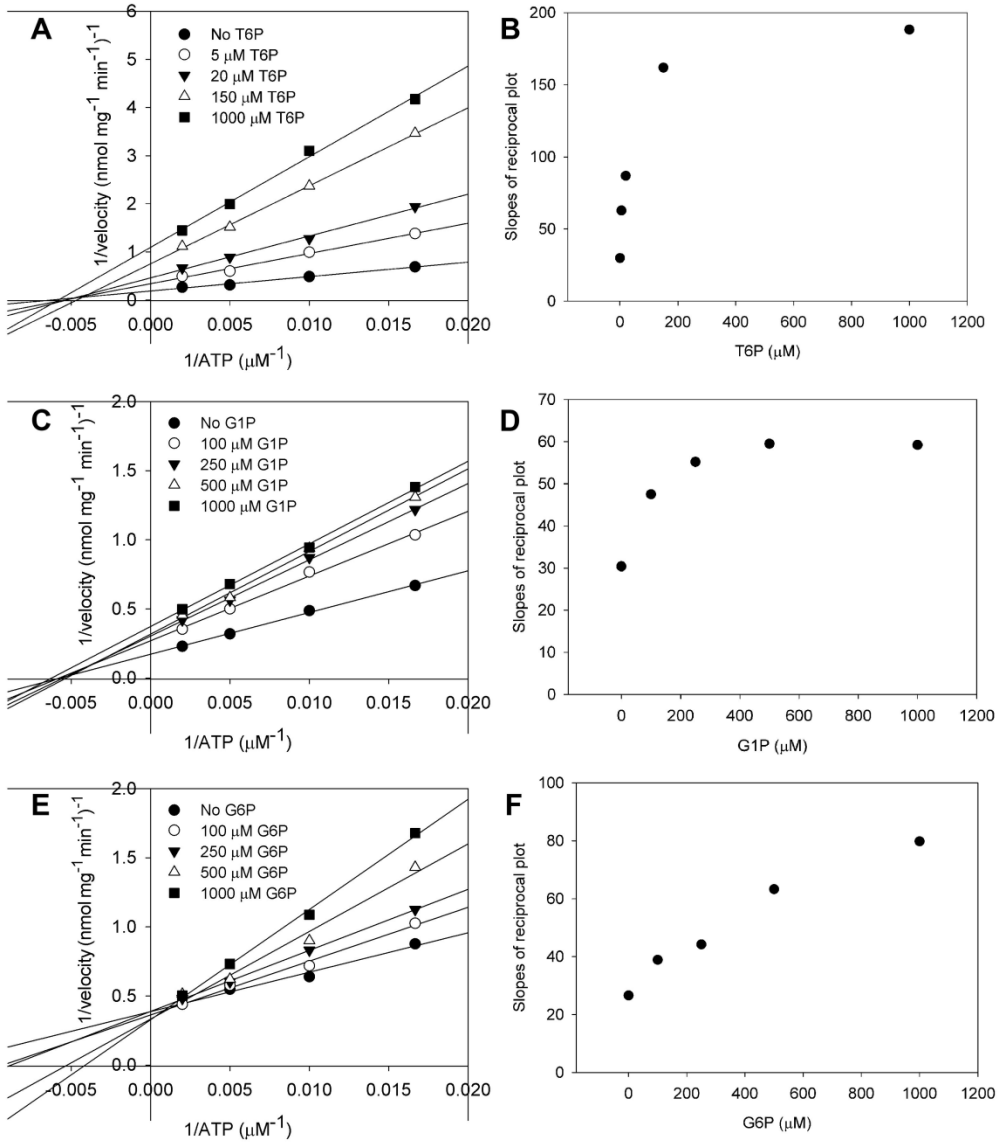

Figure 2.11. Kinetics of inhibition of SnRK1 by T6P, G6P and G1P with respect to ATP (A) Lineweaver-Burk reciprocal plot (1/velocity versus 1/substrate concentration) of the impact of T6P (0-1000 μM) on SnRK1 activity with varying ATP (60 - 500 μM) with AMARA peptide. **(B)** replot of slopes of the T6P reciprocal plot. **(C)** Lineweaver-Burk reciprocal plot of the impact of G1P (0-1000 μM) on SnRK1 activity with varying ATP (60 - 500 μM) with AMARA peptide. **(D)** replot of slopes of the G1P reciprocal plot. **(E)** Lineweaver-Burk reciprocal plot of the impact of G6P (0-1000 μM) on SnRK1 activity with varying ATP (60 - 500 μM) with SPS peptide. **(D)** replot of slopes of the G6P reciprocal plot. Each point is the average of technical duplicates.

Table 2.3. Best-fit models and obtained kinetics parameters for SnRK1 inhibiotn by T6P, G1P and G6P.

Kinetic assays were carried out in fraction 64 from partial purified seedling SnRK1 extracts. Models were fitted using non-linear least squares regression to estimate parameters along with standard errors presented in brackets.

Inhibitor	Peptide	Model	Estimated Parameters (SE)					
			Vmax (nmol min^{-1})	Ks (μM)	Ki (μM)	α	β	IC50 (μM)
T6P	AMARA	Partial non-competitive	0.056 (0.002)	138 (12.2)	4.0 (0.41)		0.198 (0.013)	5.1
T6P	SPS	Partial non-competitive	0.028 (0.0006)	69.9 (4.35)	5.4 (0.65)		0.483 (0.012)	
G1P	AMARA	Partial non-competitive	0.067 (0.002)	179 (12.7)	55.2 (10.6)		0.453 (0.012)	480
G6P	SPS	Hyperbolic mixed-type	0.027 (0.0007)	65.7 (6.6)	301 (112)	8.5 (6.8)	1.48 (0.54)	

α: value by which inhibitor affects substrate binding; β: factor by which inhibitor affects product formation.

2.3.6. Interactions between T6P, G1P and G6P and SnRK1

When T6P, G1P and G6P were combined in SnRK1 assays interactions were apparent (Fig. 9). Inhibition of SnRK1 with T6P and G1P together was particularly strong indicating cooperative inhibition (Fig. 10A). Inhibition by T6P and G6P together was cumulative (Fig.10B). More detailed kinetic analysis according to (Segel, 1993) of these interactions showed that T6P and G1P in combination impacted on maximum velocity altering the rate of product formation by parameter z=0.0167 when together compared to alterations of 0.198 (α) for T6P alone and 0.453 (β) for G1P alone. SnRK1 was inhibited to 6.5% of control activity when 1 mM of T6P and G1P were combined compared to 16.5% for 1 mM of T6P and 52.7% for 1 mM G1P separately. Inhibition of SnRK1 by G1P and G6P together and by T6P and G6P together was cumulative (Fig. 10C). Both cumulative and synergistic models indicate the binding of the metabolites at separate sites on the intermediary factor/ SnRK1 complex.

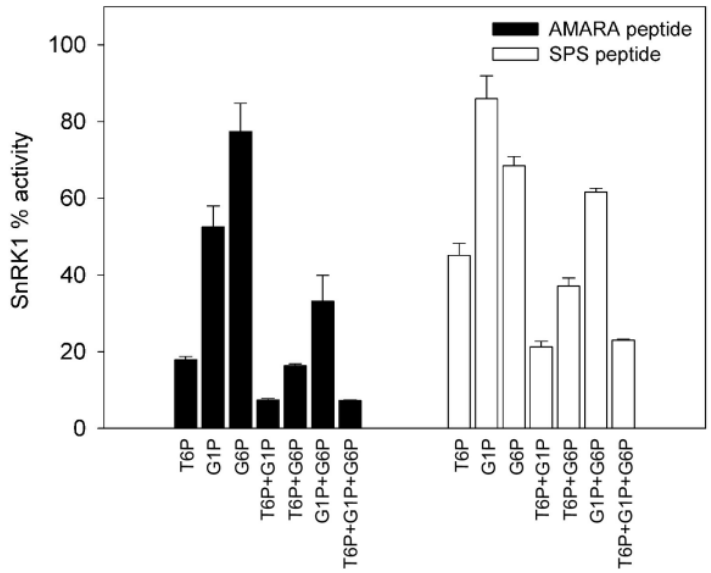

Figure 2.12. SnRK1 activity expressed as a percentage for combinations of 1 mM of T6P, G1P and G6P in fraction 64 of seedling extracts with assayed with AMARA or SPS peptide. Means of 3 biological replicates with standard deviation.

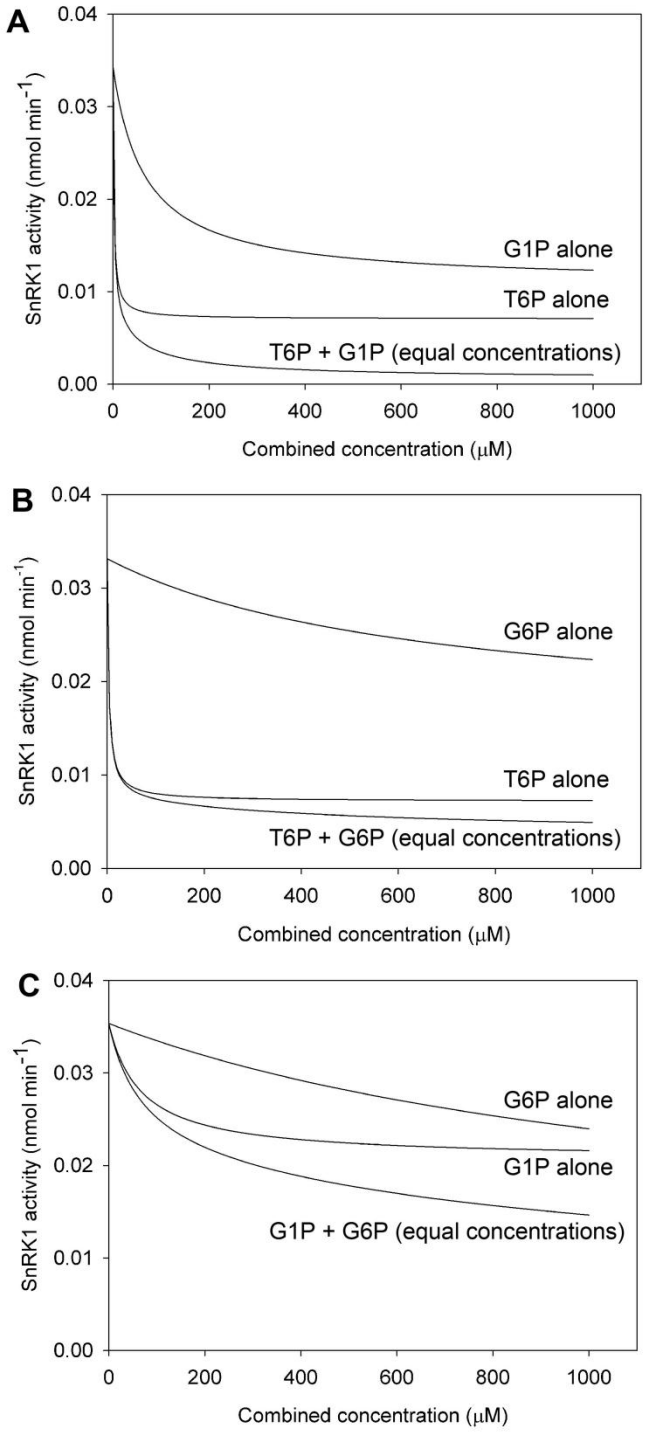

Figure 2.13. Synergistic and cumulative inhibition of SnRK1 by combinations of T6P, G1P and G6P. (A) Synergistic inhibition by T6P and G1P. **(B)** Cumulative inhibition by T6P and G6P **(C)** Cumulative inhibition by G1P and G6P.

Table 2.4. Best-fit models and obtained kinetics parameters for SnRK1 inhibition by combinations of T6P, G1P and G6P.

Kinetic assays were carried out in fraction 64 from partial purified seedling SnRK1 extracts. Models were fitted using non-linear least squares regression to estimate parameters along with standard errors presented in brackets.

Inhibitor	Model	Peptide	Estimated parameters (SE)					
			*Vmax	*Ks	Ki	x	y	z
T6P + G1P	Partial non-competitive Synergistic	AMARA	0.0615	158.3	T6P:1.88 (0.39) G1P:65.7 (17.8)	0.206 (0.024)	0.316 (0.038)	0.017 (0.016)
T6P + G6P	Partial non-competitive Cumulative	AMARA	0.056	137.8	T6P:3.22 (0.20) G6P:658 (170)	0.217 (0.007)	0.460 (0.069)	
G1P + G6P	Partial non-competitive Cumulative	AMARA	0.067	178.9	G1P:67.0 (19.4) G6P:1310 (827)	0.26 (0.19)	0.585 (0.023)	

x: value by which the first inhibitor affects product formation; y: factor by which the second inhibitor affects product formation; z:value by which binding of both inhibitors affects product formation.

2.4. Discussion

SnRK1 is a central regulatory PK of plant growth and development in relation to carbon supply (Baena-González *et al.*, 2007). Accordingly, modulation of its activity is an important aspect of plant survival and productivity. Inhibition of SnRK1 by T6P is a critical mechanism of regulation of SnRK1 in plants and crops regulating scores of genes (Baena-González *et al.*, 2007; Zhang *et al.*, 2009; Debast *et al.*, 2011; Martínez-Barajas *et al.*, 2011). G6P (Toroser *et al.*, 2000; Zhang *et al.*, 2009), and more recently R5P (Piattoni *et al.*, 2011) have also been reported to inhibit SnRK1 and could function in a similar capacity to T6P in inhibiting SnRK1 under conditions of abundant assimilate availability. They would, however, provide less sensitive regulation of SnRK1, because, as key substrates for biosynthetic pathways, R5P and G6P tend to fluctuate within a narrower concentration range compared to signals such as T6P (Lunn *et al.*, 2006; Martínez-Barajas *et al.*, 2011).

Nevertheless, inhibition by G6P and R5P could be a further means of metabolic regulation of SnRK1 activity. In this study, however, we found that inhibition of Arabidopsis SnRK1 by R5P is in fact an experimental error. More importantly, in addition to T6P and G6P, G1P was also shown to strongly inhibit SnRK1. These three inhibitors were shown to cooperatively inhibit SnRK1 which may constitute a strong means of inhibiting SnRK1 *in vivo*.

2.4.1. Caveats in interpreting inhibition of SnRK1 *in vitro*

Given the strong link between T6P and biosynthetic processes, SnRK1 inhibition by other core metabolites which are substrates for growth processes was also tested. From the 12 compounds that inhibited SnRK1 *in vitro*, eight were nucleotides (Table 1). Little is known about SnRK1 regulation especially compared to its mammalian homolog, however it is known, in contrast to AMPK, that it is not allosterically regulated by AMP (Mackintosh *et al.*, 1992). There is evidence, nevertheless, that AMP inhibits SnRK1 dephosphorylation, an effect not observed with the nucleotide GMP (Sugden *et al.*, 1999). Regulation through dephosphorylation is highly unlikely in our extracts prepared with phosphatase inhibitors. The observed inhibition by nucleotides was therefore hypothesised to be due to direct competition with ATP for the same binding site. Our hypothesis was confirmed and all tested nucleotides were competing directly with ATP for the catalytic site (Fig. 1 and 2). Measuring nucleotides in plant cells is especially challenging because of the three subcellular compartments (cytosol, mitochondria and chloroplasts) through which they can circulate. This type of inhibition would also be highly dependent on the relative amounts of each nucleotide as well as on the corresponding binding affinities for the binding site. We cannot, therefore, evaluate the importance of this interaction *in vivo*. However, if from one point of view this inhibition seems unlikely to occur in the cell because conditions that translate into increased nucleotide concentrations are also those where SnRK1 is expected to be more active, we cannot rule out a scenario of feedback regulation of SnRK1 by ADP. Also relevant would be the levels of nucleotides coordination with Mg^{2+}. *In vivo* most

ATP is complexed with a Mg^{2+} ion, whereas ADP and AMP are not (Xiao *et al.*, 2012) and in fact, enzyme regulation by nucleotides seems to be highly dependent on ratios of bound and unbound nucleotides to Mg^{2+} (Molnar and Vas, 1993; Jenkins *et al.*, 2011). In this perspective, the assay medium supplemented with 5 mM $MgCl_2$ may artificially induce this type of inhibition.

The apparent inhibition of SnRK1 by UDPG and UDP galactose was shown to happen only in extracts prepared with NaPPi (Fig. 2.6). The enzyme pyrophosphorylase, an important enzyme of carbohydrate metabolism, catalyzes the reversible cleavage of UDPG in the presence of pyrophosphate into G1P and UTP. These two products were shown to inhibit SnRK1 consistently (Table 2.1 and 2.2; Fig. 2.1B and 2.11C) and are likely the true SnRK1 inhibitors in these assays. The enzyme UDP-galactose 4-epimerase, which performs the final step in the Leloir pathway of galactose metabolism, catalyse the reversible conversion of UDP-galactose to UDP-glucose (Holden *et al.*, 2003), which could explain the observed inhibition of SnRK1 by UDP galactose.

We have also observed a strong apparent inhibition of SnRK1 activity by R5P (Table 2.1 and 2.2) that was in fact later described in wheat SnRK1 by Piattoni *et al.* (2011). The same type of inhibition was also observed in assays with Ru5P. Inhibition of SnRK1 by T6P and G6P has already been shown to be stable over time with linear catalytic rates of SnRK1 activity in the presence of inhibitor (Toroser *et al.*, 2000; Zhang *et al.*, 2009). However, in further characterisation of R5P- and Ru5P-dependent inhibition it was found that the potency of inhibition depended on the length of the assay (Fig. 2.7A) indicating that conditions in the assay were not optimised. We hypothesised that this was due to consumption of the substrate for the kinase, ATP, during the assay period. In accordance, supply of higher ATP concentration substantially reduced inhibition values (Fig. 2.7B). The fact that inhibition by R5P and Ru5P was found only in green tissue constituted an additional clue (Table 2.2). In tissue with active photosynthetic cells, activities of the enzymes phosphoribo-isomerase (PRI) and phosphoribulo-kinase (PRK) which synthesise ribulose 5-phosphate (RuBP) from R5P are several thousand fold higher than

activities of SnRK1 (Paul *et al.*, 2000). An apparent time-dependent inhibition of SnRK1 by R5P can be explained by conversion of R5P to RuBP with concomitant consumption of ATP which becomes limiting, giving an apparent strong inhibition of SnRK1. These observations highlight important caveats to be considered in the study of SnRK1 (as well as other enzymes) when not highly purified. Adding potential interacting compounds to the assay can cause apparent inhibition of the enzymes activities either by consumption of essential substrates or co-factors or by parallel transformation/cleavage into new compounds which can be the actual interacting players. Any observed interaction should be discussed cautiously and ultimately shown *in vivo*.

2.4.2. Purification profiles

We have previously found that an intermediary protein present in growing tissues is necessary for the inhibition of SnRK1 by T6P (Zhang *et al.*, 2009). SnRK1 was partially purified to retain this intermediary factor (Fig. 2.8). The majority of SnRK1 activity prepared from Arabidopsis seedling and cauliflower florets through size fractionation was inhibited by T6P (Fig. 2.8A and C). Despite the low level of SnRK1 inhibition by T6P in mature leaves, it was the fractions of the same size as seedling and cauliflower fractions which were slightly inhibited by T6P (Fig. 2.8B). Addition of intermediary factor from seedling extract to mature leaf SnRK1 increased the inhibition of mature leaf SnRK1 by T6P (Zhang *et al.*, 2009). The conclusion from these experiments is that there appear to be no large qualitative differences in the nature of T6P-inhibited SnRK1 from seedlings and mature leaves. Instead, quantitative changes in components such as of intermediary factor account for differences in susceptibility of inhibition of SnRK1 by T6P.

It has been shown in some preparations of SnRK1 that G6P also inhibits SnRK1 activity, although far higher concentrations of G6P are required than for T6P (Toroser *et al.*, 2000; Zhang *et al.*, 2009). SnRK1 fractions that were inhibited by T6P were also inhibited by G6P and G1P. This inhibition was exclusively detected in

fractions inhibited by T6P and the peaks of inhibition by all three metabolites coincided (Fig. 2.9). Using a different peptide substrate, the inhibition levels of T6P, G1P and G6P changed. T6P inhibits less with SPS petide than with AMARA peptide but remains the strongest inhibitor; G1P inhibits much less with SPS peptide than with AMARA peptide whereas G6P has an increased effect (Fig. 2.9 B, D and F). This suggests that the inhibitors may have different impact *in vivo* depending on the substrate being modified. Separation of intermediary factor necessary for T6P inhibition away from SnRK1 activity by immunoprecipitation of SnRK1 and subsequent re-assay of resuspended immunoprecipitate removed inhibition by G1P and G6P (Fig. 2.10) as it did for T6P (Zhang *et al.*, 2009). This shows that G1P, G6P and T6P inhibit SnRK1 via an intermediary factor that is separable from SnRK1. It is likely therefore that the SnRK1 complexes inhibited by these metabolites are very similar, requiring possibly the same intermediary factor. Efforts were made to identify this factor, results are presented in Chapter III.

2.4.3. Metabolic regulation of SnRK1 and *in vivo* relevance

Given the similar structures of T6P and G6P we wished to determine if each could impart distinct regulation of SnRK1. Having established that inhibition of SnRK1 by T6P, G1P and G6P is intermediary factor dependent we wished to understand if each was capable of discrete inhibition of SnRK1. G6P inhibited seedling SnRK1 through a hyperbolic mixed type model (Fig. 2.11E) whereas G1P inhibited SnRK1 by partial non-competitive inhibition (Fig. 2.11C). Kinetic modelling of inhibition of SnRK1 by T6P, G1P and G6P predicts that each provides distinct regulation of SnRK1 at discrete sites on the intermediary factor/ SnRK1 complex. Inhibition by T6P and G6P together was cumulative, and, strikingly, T6P and G1P inhibited SnRK1 synergistically such that 0.5 mM T6P and 0.5 mM G1P together inhibited SnRK1 to 6.5% of activity compared to 16.5% with 1 mM T6P and 52.7% with 1 mM G1P separately (Fig. 2.12 and 2.13). We have already concluded that T6P itself confers significant regulation of SnRK1 *in vivo* (Zhang *et al.*, 2009).

This shows that the regulation of SnRK1 by sugar phosphates in plants is more sophisticated than previously appreciated, perhaps not surprising given the importance of SnRK1 as a central metabolic regulator affecting plant productivity and survival. G6P and G1P are formed predominantly in the cytosol from the export of triose phosphate from chloroplasts in photosynthetic cells and from metabolism of sucrose and starch in heterotrophic tissues. High carbon supply leads to high abundance of G1P and G6P (Schluepmann *et al.*, 2003) and mostly T6P (Lunn *et al.*, 2006; Paul *et al.*, 2010). In combination, particularly T6P and G1P, would inhibit SnRK1 significantly. Metabolites rarely occur in isolation and hence this latter scenario more likely reflects conditions *in vivo*. G1P is the substrate for ADP-glucose pyrophosphorylase (AGPase), the key enzyme of starch synthesis. T6P has already been shown to activate starch synthesis through redox activation of chloroplastic AGPase (Wingler *et al.*, 2000; Kolbe *et al.*, 2005). Further, enzymes of starch metabolism have been shown to be transcriptionally regulated by SnRK1 (Baena-González *et al.*, 2007; Zhang *et al.*, 2009). In combination, T6P and G1P would inhibit SnRK1 significantly in response to high carbon supply, for example in tissues importing sucrose for starch synthesis. It is not known whether the combination of T6P and G1P inhibits SnRK1 to activate a subset of SnRK1 target genes involved in starch metabolism. This will require further investigation. But nevertheless it is possible that inhibition of SnRK1 by T6P and G1P is a part of a mechanism that promotes starch synthesis and turnover in a manner proportional to carbon availability. Inhibition by G6P is quite small but may provide further inhibition of SnRK1 additional to that of T6P and G1P under high carbon conditions.

In conclusion, we show that the similar glucose-based sugar phosphates, T6P, G1P and G6P all provide distinct regulation of SnRK1 at separate sites on the intermediary factor/ SnRK1 complex. Each metabolite provides distinct inhibition of SnRK1 and there is strong synergistic interaction between T6P and G1P. The data further support the view that SnRK1 is inhibited under conditions of high carbon availability.

2.5. Material and Methods

2.5.1. Biological material

Seeds of *Arabidopsis thaliana* (L.) ecotype Columbia-0 (Col 0) were weighed in batches of 2.5 mg and surface-sterilised for 10 min in a 10% sodium hypochlorite solution with triton x-100 and rinsed twice in sterile water. Each seed batch was grown in 50 ml half-strength Murashige and Skoog medium (ApolloScientific PMM524) plus Gamborg's vitamins (Sigma G1019) and 0.5% sucrose (0.25 g/ 50 ml medium) in culture flasks (300 ml polystyrene containers, Greiner). After cold treatment for 2 days in the dark at 4ºC they were transferred to the growth room for 7 days at 23ºC (16 h light/ 8 h dark) with 130 µmol quanta m^{-2} s^{-1} irradiance with gentle shaking (Fig. 2.14). At harvest, seedlings from each pot were weighed and snap-frozen in liquid nitrogen after gentle blotting to remove excess water. To grow adult plants on compost, seeds were stratified for 3 days at 4ºC in 0.1% (w/v) agar and pipetted onto Rothamsted Standard Compost Mix (Petersfield Products, Leicester, UK) and grown under the same conditions of temperature, light and day length in individual pots. Most recently fully expanded leaves were harvested from plants before bolting and snap-frozen in liquid nitrogen. Cauliflower was bought fresh from a local supermarket.

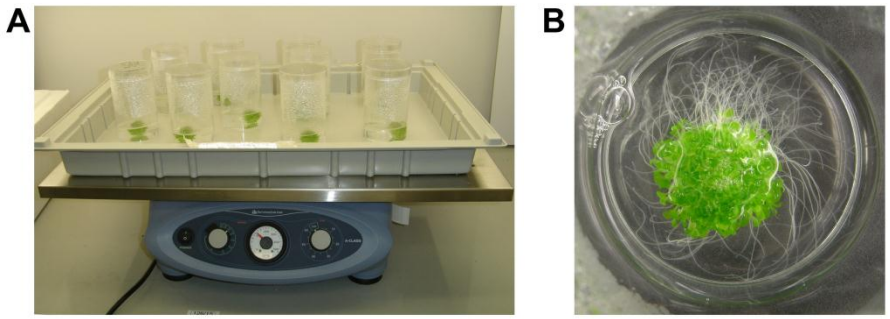

Figure 2.14. *Arabidopsis thaliana* (L.) (ecotype Col-0) growing in culture flasks in the growth room. (A) Shaker with culture flasks. **(B)** Seven-day-old seedlings germinated from 2.5 mg seeds in half-strength MS liquid culture and 0.5% sucrose weighing approximately 1 g. For scaling purposes, culture flasks have a diameter of 68 mm.

2.5.2. Preparation of SnRK1 extracts to analyse inhibition by metabolites

SnRK1 crude extracts from Arabidopsis seedlings, leaves and roots and cauliflower florets were prepared as described previously (Zhang *et al.*, 2009). Total soluble protein was extracted from 200 mg of tissue ground under liquid nitrogen in a pestle and mortar in 600 µL of ice-cold homogenization buffer of 100 mM Tricine-NaOH, pH 8, 25 mM sodium fluoride, 5 mM dithiothreitol, 2 mM tetrasodium pyrophosphate (or other concentrations - none, 0.25 mM, 1 mM - if indicated), 0.5 mM EDTA, 0.5 mM EGTA, 1 mM benzamidine, 1 mM phenylmethylsulfonyl fluoride, 1 mM protease inhibitor cocktail (Sigma P9599), phosphatase inhibitors (PhosStop; Roche) and insoluble polyvinylpyrrolidone to 2% (w/v). Homogenate was centrifuged at 13,000g at 4ºC. Supernatant (1 mL) was desalted in illustra NAP-10 columns (GE Healthcare) pre-equilibrated with homogenization buffer. Eluent was supplemented with protease inhibitor cocktail and okadaic acid to 2.5 µM before freezing in liquid nitrogen.

Previous work demonstrated that inhibition of SnRK1 by T6P was dependent on an intermediary factor that could be separated from SnRK1 activity (Zhang *et al.*, 2009). A short purification scheme was used to retain intermediary factor with SnRK1 activity minimizing losses of activity and inhibition levels due to excessive handling already described by Toroser *et al.* (2000) and empirically observed in this laboratory. Young tissues like Arabidopsis seedlings and cauliflower florets contain intermediary factor but intermediary factor is largely absent in Arabidopsis mature leaves (Zhang *et al.*, 2009). SnRK1 complexes from these three tissues were compared using S-300 sephacryl size fractionation as a final step. Seedling, leaf and cauliflower material (400-500 g) was homogenised at 4°C in a blender in 1.5 L buffer A (50 mM tricine, pH 8.0, 50 mM sodium fluoride, 1 mM EDTA, 1 mM EGTA, 1 mM dithiothreitol, 1 mM benzamidine, 0.1 mM phenylmethane sulphonyl fluoride, 0.02% Brij35, 10% glycerol) with 8 g polyvinylpolypyrrolidone (crude extract). The homogenate was filtered through three layers of Miracloth (Calbiochem) and then centrifuged at 18,000 x g for 30 min. Ammonium sulphate was added to the supernatant to give a 50% saturated solution. The suspension was stirred for 20 min and the precipitate was collected by

centrifugation at 18,000 x g for 30 min. The pellet was gently resuspended in 100 mL buffer A and dialysed overnight against 2 x 4 L buffer A. After dialysis the sample was clarified by centrifugation at 28,000 x g for 15 min. Because at 50% ammonium sulphate concentration most/all proteins precipitate (salting out) this step was used for concentrating the sample and not for purification purposes.

Ion exchange chromatography was used to achieve a certain level of purification. The sample was mixed gently for 1 h with DEAE-Sepharose (GE Healthcare) slurry pre-equilibrated in buffer A. Ion exchange chromatography relies on charge-charge interactions between the sample proteins and the charged groups immobilized on a resin. The binding capacity of the chosen matrix is 100 mg/ml of 14.3 kDa alpha-lactalbumin and ideally, no more than 30% of the total binding capacity should be loaded. After dialysis, the total protein content of the samples were 2275 mg for seedlings, 730 mg for mature leaves and 1437 mg for cauliflower and so the total volumes could be loaded onto 100 ml of matrix. After 1 h of gentle agitation in the cold the DEAE-sepharose was collected by centrifugation at 1000 rpm for 4 min and the supernatant removed. The pellet was resuspended in 150 mL buffer A and collected by gentle centrifugation at 1000 rpm for 4 min. This wash was repeated twice. The sample was eluted with 50 mL buffer A plus 0.5 M NaCl three times. The eluates were pooled and ammonium sulphate added to give a 50% saturated solution. After gentle stirring for 20 min, the precipitate was collected by centrifugation at 24,000 x g for 20 min and resuspended in 14 mL buffer B (buffer A adjusted to pH 7.0). At the end of this step the seedlings and cauliflower extracts had been purified about three times whereas the mature leaves extract had decreased specific activity. This behaviour of the mature extract was already expected based on previous observations of the much more fragile nature of this extract.

Sample fractionation was achieved by a subsequent gel filtration step. In gel filtration the components of a sample are separated according to differences in their molecular size. The best results for high-resolution fractionation are achieved with previously partially purified samples in order to eliminate proteins of similar size that are not of interest. However, the goal here was not to achieve high resolution

separation, not realistic in a yet too complex sample, but rather, determine the molecular weight of SnRK1 complexes together with interacting factors such as Factor I. Comparison between tissues was also desirable as well as some degree of separation. The fractionation range of the chosen HiPrep 16/60 Sephacryl S-300 HR column (GEHealthcare) goes from 10 kDa to 1500kDa, covering well SnRK1 complexes sizes (118–165 kDa) plus other potential interacting proteins. The column was calibrated using thyroglobulin (669 kDa), apoferritin (443 kDa), β-amylase (200 kDa), alcohol dehydrogenase (150 kDa), bovine serum albumin (66 kDa) and carbonic anhydrase (29 kDa) (Sigma). The actual samples were filtered through a 0.45-µm filter, and 3-mL aliquots were applied to the column equilibrated in buffer B plus 0.25 M NaCl. Flow rate was set at 0.5 ml min^{-1} as indicated by the manufacturer. The collected 1 mL fractions were desalted using Sephadex G-25 NAP10 columns (GE Healthcare) pre-equilibrated with buffer B. Eluent was supplemented with protease inhibitor cocktail and okadaic acid to 2.5 µM and assayed for SnRK1 activity and inhibition by 1 mM T6P, G1P and G6P.

2.5.3. Protein quantification

Protein concentrations were determined by measuring the fractions OD600 on a spectrophotometer and by comparing it to a standard curve produced from a range of bovine serum albumin (BSA) protein samples (5 µg ml^{-1} up to 25 µg ml^{-1}). 300 µl of Bradford's reagent (100 mg l^{-1} Coomassie Blue G250, 5% (v/v) ethanol, 10% (v/v) ortho-phosphoric acid) was added to up to 25 µl of each sample (usualy 3 µl plus 22 µl buffer) and the protein concentration determined.

2.5.4. SnRK1 activity assays

SnRK1 activity was determined as described by Zhang *et al.* (2009) following adaptation from Barker *et al.* (1996). Assays were conducted at 30ºC in a final volume of 25 µl in microtitre plate wells. Assay medium was 40 mM HEPES-NaOH, pH 7.5, 5 mM $MgCl_2$, 200 µM ATP (or other concentrations as indicated)

containing 12.5 kBq [γ-33P]ATP (PerkinElmer), 5 mM dithiothreitol, 1 µM okadaic acid, 1 mM protease inhibitor cocktail (Sigma P9599) and 200 µM AMARA peptide (A**M**A**R**AA**S**AAA**L**ARRR) (Enzo Life Sciences, UK, Ltd). AMARA peptide is a synthetic substrate for SnRK1 in which the minimal recognition motif for phosphorylation was retained (φ-x-basic-2x-S-3x-φ, where φ is a hydrophobic residue) (Weekes *et al.*, 1993; Halford *et al.*, 2003). Where indicated, AMARA peptide was substituted by sucrose-phosphate synthase peptide (SPS), RDH**M**P**R**IR**S**EMQ**I**WSED (Baena-González *et al.*, 2007). Assays were started with 5 µL extract and stopped after 6 min by transferring 15 µL to 4-cm^2 squares of Whatman P81 phosphocellulose paper immersed immediately in 1% phosphoric acid. The basic amino acid residues of the phosphorylated peptide substrates assure adhesion to the phosphocellulose paper through posterior steps. These were then washed with four 800-ml volumes of 1% phosphoric acid, immersed in acetone for 15 min, air-dried and transferred to vials with 3.5 ml of scintillation cocktail (Ultima Gold Cocktail, Perkin Elmer). Readings were taken over nigh in a liquid scintillation counter (Packard Tri-Carb 2100; Perkin Elmer, Waltham, MA, USA). Figure 2.15 illustrates this protocol.

Assays were performed with 1 mM of each metabolite unless otherwise stated and compared to assays performed without metabolite. For the nucleotides kinetic analysis it was used 0, 50, 100, 200 or 500 µM of either ADP, UTP, ADPG or ADPGal at each ATP concentrations of 60, 100, 200 and 500 µM. For the kinetic analysis of T6P, concentrations of 0, 5, 150 and 1000 µM of the metabolite at each referred ATP concentration were used. For the kinetic analysis of G1P the concentrations used were 0, 100, 500 and 1000 µM whereas for G6P 0, 250, 500 and 1000 µM were used at each ATP concentration. For the combined kinetic assays, each of these metabolites (T6P, G1P and G6P) were assayed combined at each indicated concentration at 200 µM ATP. Extracts containing SnRK1 were assayed for a normal assay period of 6 min unless otherwise stated as in the case of time-dependent studies where time intervals of up to 6 min following addition of R5P, Ru5P, UDPG and UDPGal were used

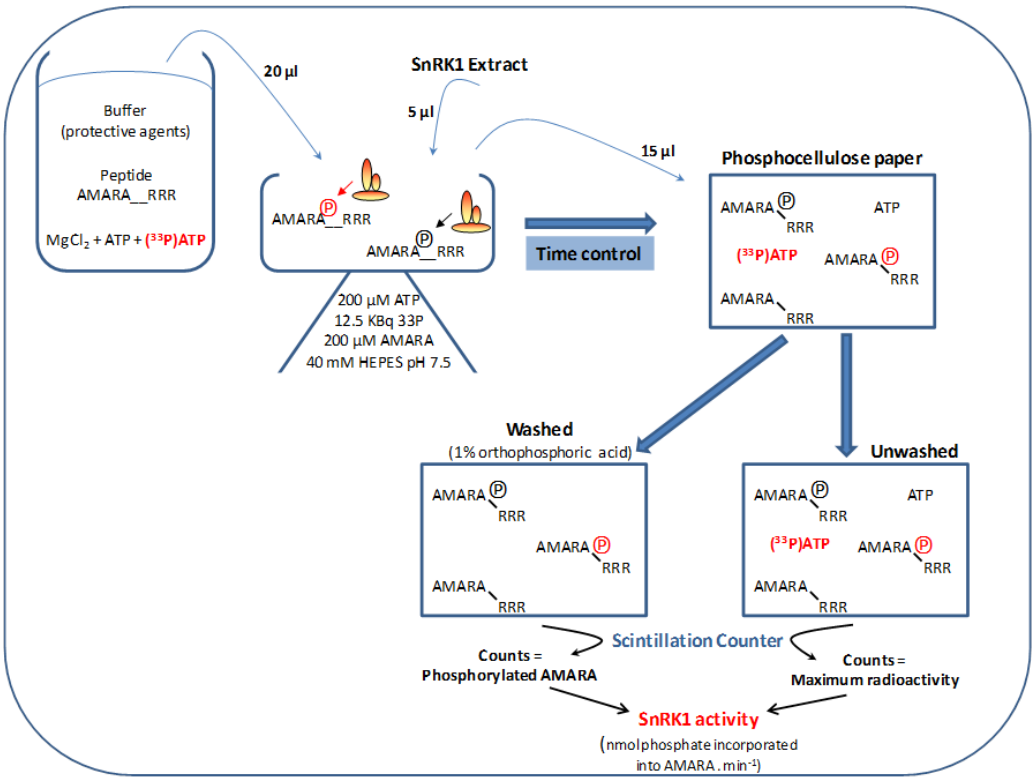

Figure 2.15. Schematic representation of the SnRK1 activity assays. The reaction takes place at 30°C in a final volume of 25 µl containing 20 µl of assay buffer with known amount of radio-labeled ATP and peptide AMARA. The reaction is initiated by adding 5 µl of extract and stopped, in a time-controlled manner, by transferring 15 µl of reaction mixture to 4-cm^2 squares of Whatman P81 phosphocellulose paper. The positively charged C-terminus of the AMARA peptide binds to the cation exchanger paper, which is immersed immediately in 1% phosphoric acid. These are then washed in 1% phosphoric acid, immersed in acetone and air-dried before radioactivity is measured. At least six squares with 15 µl of reaction mixture are not washed for estimation of maximum radioactivity. SnRK1 activity is then calculated as nmol phosphate incorporated into AMARA peptide per min.

2.5.5. Monitoring the stability of T6P, G1P and G6P during the SnRK1 assays

2.5.5.1. Reaction procedure for purified SnRK1 extracts

Plant extract was stored at -80 °C and allowed to thaw on ice and used immediately. Reactions were performed with 0.5 µl of carbohydrate solution (50 mM)

and 4.5 µl of plant extract. Reactions were further diluted with 20 µl of 0.04 M HEPES, 5.0 mM $MgCl_2$, 4.0 mM dithiothreitol (DTT) and 0.2 mM ATP at pH 7.5. The reaction mixtures were incubated at 30°C for 10 minutes (min) and then quenched by heating to 95°C for 2 min. Negative mode LC-MS analysis was conducted directly on this solution (10 µl injection). The remaining sample was dissolved in pyridine (100 µl) and acetic anhydride (100 µl). The reaction mixtures were gently shaken at room temperature for 15 h after which the reaction was quenched with methanol (100 µl). The solvents were removed under reduced pressure and the crude samples dissolved in methanol (10 µl) and analysed by C_{18} LC-MS (10 µl injection).

2.5.5.2. LC-MS negative mode

Samples were analysed through a Waters Spherisorb strong anion exchange column (250 x 4.6 mm, 5 µm). A gradient was applied from water (pH 7) to water + 10% formic acid (pH 2) over 30 min at a flow rate of 1.0 ml/min. Eluants were detected using a Waters Micromass ESI mass spectrometer in negative mode. The mass spectrometer was calibrated against the NaF cluster ion series.

2.5.5.3. LC-MS positive mode

Samples were analysed through a Phenomenex Synergi Hydro C_{18} column (150 x 4.6 mm, 4 µm). A gradient was applied from water + 0.1% formic acid to acetonitrile + 0.1% formic acid over 30 min at a flow rate of 1.0 ml/min. Eluants were detected using a Waters Micromass ESI mass spectrometer in positive mode. The mass spectrometer was calibrated against the Myoglobin ion series.

2.5.5.4. ^{31}P NMR analysis

For NMR experiments, the reactions were scaled up 100 fold. The reaction mixtures were incubated at 30°C for 10 min. The reaction mixtures were quenched by heating to 95°C for 2 min and centrifuged at 3000*g* for 10 seconds to remove

denatured protein debris. The supernatant was lyophilized and subsequently dissolved in 400 µl of water. Fifty microliters of D_2O was added as a deuterium lock. ^{31}P were referenced to $PO(OMe)_3$ (δ = 3.16 ppm), which was added as an internal standard.

2.5.6. Antibodies and immunoprecipitation

Antisera to the peptide sequence RASSGYLGAEFQETM of AKIN10 (Crawford *et al.*, 2001) and to the peptide sequence TDSGSNPMRTPEAGC of AKIN11 (Zhang *et al.*, 2009) were raised in rabbits and affinity purified by Eurogentec Ltd, Seraing, Belgium. To immunoprecipitate SnRK1 complexes, 50 mL Dynabeads Protein A (Invitrogen) pre-equilibrated with imunoprecipitation buffer (same as protein extraction buffer) was incubated with rotation at 4ºC for 30 min with 10 mg of AKIN10 and AKIN11 antibodies diluted in 200 mL 40 mM HEPES-NaOH, pH 7.5 to a final concentration of 0.06 mg/mL each. After washing the beads three times with immunoprecipitation buffer and completely removing the supernatant, 100 mL of SnRK1 extract was incubated with the beads under the same conditions. The supernatant was separated from the pellet through magnetic force. The Dynabeads-antibody-antigen complexes were washed three times with 200 mL immunoprecipitation buffer containing 4 mM DTT and 100 mM NaCl. The clean pellet was resuspended in 100 mL of the same buffer. Both supernatant and pellet were snap-frozen in liquid nitrogen and stored at -80 ºC.

2.5.7. Kinetic modelling

Modelling of inhibition kinetics of T6P, G1P and G6P was carried out using fraction 64 from partially-purified seedling SnRK1. Enzyme activity data were fitted to defined models of inhibitor action (Segel, 1993). Non-linear enzyme kinetics models appropriate for assays performed with either one or two inhibitors were investigated for their suitability to describe the observed systems. These models were fitted using non-linear least squares regression to estimate parameters along with standard

errors. The GenStat (2009, 12th edition, VSN International Ltd., Hemel Hempstead, UK) statistical system was used for this analysis. For each assay, nested models were compared based on residual variance, using the F-test, to find the best model for the data. The best-fit models for individual inhibitors are as presented in Table 2.5. and for combinations of inhibitors are as in Table 2.6.

Table 2.5. Best-fit models and statistical parameters for SnRK1 inhibition by T6P, G1P and G6P.

Inhibitor	Peptide	Model	Formula	RSS	df	R^2
T6P	AMARA	Partial non-competitive		0.0000868	36	97.9
T6P	SPS	Partial non-competitive	$v = V_{max}\left\{\frac{\left(\frac{S}{K_S}+\frac{\beta SI}{K_S K_I}\right)}{\left(1+\frac{S}{K_S}+\frac{I}{K_I}+\frac{SI}{K_S K_I}\right)}\right\}$	0.0000210	36	97.5
G1P	AMARA	Partial non-competitive		0.0000960	36	97.5
G6P	SPS	Hyperbolic mixed-type	$v = V_{max}\left\{\frac{\left(\frac{S}{K_S}+\frac{\beta SI}{\alpha K_S K_I}\right)}{\left(1+\frac{S}{K_S}+\frac{I}{K_I}+\frac{SI}{\alpha K_S K_I}\right)}\right\}$	0.0000292	34	97.2

Table 2.6. Best-fit models and statistical parameters for SnRK1 inhibition by combinations of T6P, G1P and G6P.

Inhibitor	Model	Peptide	RSS	df	R^2
T6P + G1P	Partial non-competitive Synergistic	AMARA	0.000168	45	93.6
T6P + G6P	Partial non-competitive Cumulative	AMARA	0.0000131	27	99.4
G1P + G6P	Partial non-competitive Cumulative	AMARA	0.0000834	28	92.9

The formula of the best-fit model for T6P + G6P and G1P + G6P (Partial Non-competitive inhibitors - cumulative) is:

$$v = V_{max}\left\{\frac{\left(\frac{S}{K_S}+\frac{xSI}{K_SK_I}+\frac{ySJ}{K_SK_J}+\frac{xySIJ}{K_SK_IK_J}\right)}{\left(1+\frac{S}{K_S}+\frac{I}{K_I}+\frac{J}{K_J}+\frac{SI}{K_SK_I}+\frac{SJ}{K_SK_J}+\frac{IJ}{K_IK_J}+\frac{SIJ}{K_SK_IK_J}\right)}\right\}$$

And the formula for the best-fit model of T6P + G1P (Partial Non-competitive inhibitors – synergy) is:

$$v = V_{max}\left\{\frac{\left(\frac{S}{K_S}+\frac{xSI}{K_SK_I}+\frac{ySJ}{K_SK_J}+\frac{zSIJ}{K_SK_IK_J}\right)}{\left(1+\frac{S}{K_S}+\frac{I}{K_I}+\frac{J}{K_J}+\frac{SI}{K_SK_I}+\frac{SJ}{K_SK_J}+\frac{IJ}{K_IK_J}+\frac{SIJ}{K_SK_IK_J}\right)}\right\}$$

Acknowledgements

I, Cátia Nunes, performed and analysed the presented experimental work with the following collaborations: Dr. Lucia Primavesi helped with the numerous SnRK1 assays, experimental layout and data interpretation; Dr. Stephen Powers performed the non-linear least squares regression analysis of kinetic assays; Dr. Mitul Patel did the NMR and LC-MS analysis on the stability of metabolites at Oxford University; and to whom I am deeply grateful. The planning of the research work and discussion of results was done by Cátia Nunes, Dr. Lucia Primavesi and Dr. Matthew Paul.

2.6. References

Ananieva EA, Gillaspy GE, Ely A, Burnette RN, Erickson FL (2008) Interaction of the WD40 domain of a myo-inositol polyphosphate 5-phosphatase with SnRK1 links inositol, sugar and stress signaling. Plant Physiol **148**: 1868-1882

Baena-González E, Rolland F, Thevelein JM, Sheen J (2007) A central integrator of transcription networks in plant stress and energy signaling. Nature **448**: 938-942

Ball KL, Dale S, Weekes J, Hardie DG (1994) Biochemical characterization of two forms of 3-hydroxy -3-methylglutaryl-CoA reductase kinase from cauliflower (*Brassica oleracia*). Eur J Biochem **219**: 743-750

Barker JHA, Slocombe SP, Ball KL, Hardie DG, Shewry PR, Halford NG (1996) Evidence that barley 3-hydroxy-3-methylglutaryl-Coenzyme A reductase kinase is a member of the sucrose nonfermenting-1-related protein kinase family. Plant Physiol **112**: 1141–1149

Bhalerao RP, Salchert K, Bako L, Okresz L, Szabados L, Muranaka T, Machida Y, Schell J, Koncz C (1999) Regulatory interaction of PRL1 WD protein with Arabidopsis SNF1-like protein kinases. Proc Natl Acad Sci USA **96**: 5322-5327

Clark H, Carling D, Saggerson D (2004) Covalent activation of heart AMP-activated protein kinase in response to physiological concentrations of long-chain fatty acids. Eur J Biochem **271**: 2215-2224

Crawford RM, Halford NG, Hardie DG (2001) Cloning of DNA encoding a catalytic subunit of SNF1-related protein kinase-1 (SnRK1-a1) and immunological analysis of multiple forms of the kinase in spinach leaf. Plant Mol Biol **45**: 731–741

Crozet P, Jammes F, Valot B, Ambard-Bretteville F, Nessler S, Hodges M, Vidal J, Thomas M (2010) Cross-phosphorylation between *Arabidopsis thaliana* Sucrose Nonfermenting 1-related Protein Kinase 1 (AtSnRK1) and its activating kinase (AtSnAK) determines their catalytic activities. J Biol Chem **285**: 12071–12077

Debast F, Nunes-Nesi A, Hajirezaei MR, Hofmann J, Sonnewald U, Fernie AR, Börnke F (2011) Altering trehalose 6-phosphate content in transgenic potato tubers affects tuber growth and alters responsiveness to hormones during sprouting. Plant Physiol **156**: 1754-1771

Granot D, David-Schwartz R, Kelly G (2013) Hexose kinases and their role in sugar-sensing and plant development. Front Plant Sci **4**: 44

Halford NG, Hey S, Jhurreea D, Laurie S, McKibbin RS, Paul M, Zhang Y (2003) Metabolic signaling and carbon partitioning: role of Snf1-related (SnRK1) protein kinase. J Exp Bot **54**: 467-475

Hardie DG (2007) AMP-activated/ SNF1 protein kinases: conserved guardians of cellular energy. Nature Rev Mol Cell Biol **8**: 774-785

Hardie DG, Carling D, Gamblin SJ (2011) AMP-activated protein kinase: also regulated by ADP? Cell Press **26**:470-477

Hardie DG, Salt IP, Hawley SA, Davies SP (1999) AMP activated protein kinase: an ultrasensitive system for monitoring cellular energy charge. Biochem J **338**: 717-722

Holden HM, Rayment I, Thoden JB (2003) Structure and function of enzymes of the Leloir pathway for galactose metabolism. J Biol Chem **278**: 43885–43888

Jenkins CM, Yang J, Sims HF, Gross RW (2011) Reversible high affinity inhibition of Phosphofructokinase-1 by Acyl-CoA: a mechanism integrating glycolytic flux with lipid metabolism. J Biol Chem **286**: 11937–11950

Jossier M, Bouly J-P, Meimoun P, Arjmand A, Lessard P, Hawkins S, Hardie DG, Thomas M (2009) SnRK1 (SNF1-related kinase 1) has a central role in sugar and ABA signaling in *Arabidopsis thaliana*. Plant J 58 316-328

Kolbe A, Tiessen A, Schluepmann H, Paul M, Ulrich S, Geigenberger P (2005) Trehalose 6-phosphate regulates starch synthesis via post-translational redox modification of ADP-glucose pyrophosphorylase. Proc Natl Acad Sci USA **102**: 11118-11123

Lunn JE, Feil R, Hendriks JHM, Gibon Y, Morcuende R, Osuna D, Scheible W-R, Carillo P, Hajirezaei M-R, Stitt M (2006) Sugar-induced increases in trehalose 6-phosphate are correlated with redox activation of ADP-glucose pyrophosphorylase and higher rates of starch synthesis in *Arabidopsis thaliana*. Biochem J **397**: 139-148

Mackintosh RW, Davies SP, Clarke PR, Weekes J, Gillespie JG, Gibb BJ, Hardie DG (1992) Evidence for a protein kinase cascade in higher plants. 3-Hydroxy-3-methylglutaryl-CoA reductase kinase. Eur J Biochem **209**: 923–931

Martínez-Barajas E, Delatte T, Schluepmann H, de Jong GJ, Somsen GW, Nunes C, Primavesi LF, Coello P, Mitchell RAC, Paul MJ (2011) Wheat grain development is characterized by remarkable trehalose 6-phosphate accumulation pregrain filling: tissue distribution and relationship to SNF1-related protein kinase1 activity. Plant Physiol **156**: 373–381

McBride A, Ghilagaber S, Nikolaev A, Hardie DG (2009) The glycogen-binding domain on the AMPK *β* subunit allows the kinase to act as a glycogen sensor. Cell Metab **9**: 23–34

Molnar M, Vas M (1993) Mg^{2+} affects the binding of ADP but not ATP to 3-phosphoglycerate kinase: correlation between equilibrium dialysis binding and enzyme kinetic data. Biochem J **293**: 595-599

Momcilovic M, Iram SH, Liu Y, Carlson M (2008) Roles of the glycogen-binding domain and Snf4 in glucose inhibition of SNF1 protein kinase. J Biol Chem **283**: 19521–19529

Paul MJ, Driscoll SP, Andralojc PJ, Knight JS, Gray JC, Lawlor DW (2000) Decrease of phosphoribulokinase activity by antisense RNA in transgenic tobacco: definition of the light environment under which phosphoribulokinase is not in large excess. Planta **211**: 122-119

Paul MJ, Jhurreea D, Zhang Y, Primavesi LF, Delatte T, Schluepmann H, Wingler A (2010) Up-regulation of biosynthetic processes associated with growth by trehalose 6-phosphate. Plant Signal Behav **5**: 386-392

Piattoni CV, Bustos DM, Guerrero SA, Iglesias A (2011) Nonphosphorylating glyceraldehydes 3-phosphate dehydrogenase is phosphorylated in wheat endosperm at

serine-404 by an SNF1-related protein kinase allosterically inhibited by ribose 5-phosphate. Plant Physiol **156**: 1337-1350

Polge C, Thomas M (2007) SNF1/ AMPK/ SnRK1 kinases, global regulators at the heart of energy control. Trends Plant Sci **12**: 1360-1385

Schluepmann H, Pellny T, van Dijken A, Smeekens S, Paul M (2003) Trehalose 6-phosphate is indispensable for carbohydrate utilisation and growth in *Arabidopsis thaliana*. Proc Natl Acad Sci USA **100**: 6849-6854

Segel IH (1993) Enzyme Kinetics, Wiley, New York.

Shen W, Reyes MI, Hanley-Bowdoin L (2009) Arabidopsis protein kinases GRIK1 and GRIK2 specifically activate SnRK1 by phosphorylating its activation loop. Plant Physiol **150**: 996-1005

Sugden C, Crawford RM, Halford NG, Hardie DG (1999) Regulation of spinach SNF1-related (SnRK1) kinases by protein kinases and phosphatases is associated with phosphorylation of the T loop and is limited by 5'-AMP. Plant J **19**: 433-439

Toroser D, Plaut Z, Huber SC (2000) Regulation of a plant SNF1-related protein kinase by glucose 6-phosphate. Plant Physiol **123**: 403-411

Weekes J, Ball KL, Caudwell FB, Hardie DG (1993) Specificity determinants for the AMP-activated protein kinase and its plant homologue analyzed using synthetic peptides. FEBS Lett **334**: 335-339

Wingler A, Fritzius T, Wiemken A, Boller T, Aescbacher A (2000) Trehalose induces the ADP-glucose pyrophosphorylase gene and starch synthesis in Arabidopsis. Plant Physiol **124**:105-114

Xiao B, Sanders MJ, Underwood E, Heath R, Mayer F, Carmena D, Jing C, Walker FA, Eccleston JF, Haire LF, Saiu P, Howell SA, Aasland R, Martin SR, Carling D, Gamblin SJ (2011) Structure of Mammalian AMPK and its regulation by ADP. Nature **472**: 230-233

Zhang Y, Primavesi LF, Jhurreea D, Andralojc PJ, Mitchell RAC, Powers SJ Schluepmann H, Delatte T, Wingler A,, Paul MJ (2009) Inhibition of SNF1-related kinase1 actvity and regulation of metabolic pathways by trehalose 6-phosphate. Plant Physiol **149**: 1860-1871

CHAPTER III

Molecular characterization of SnRK1 inhibition by T6P – Factor I

The work presented in this chapter was mostly performed by Cátia Nunes (see acknowledgments section) and refers to ongoing work.

3.1. Abstract

Sucrose non-fermenting-1-related protein kinase 1 (SnRK1) is an evolutionary conserved metabolic regulator. It is constituted by three different main subunits and additional interacting proteins seem to add to its complexity. The sugar signal trehalose 6-phosphate (T6P) inhibits SnRK1 *in vitro* through a separable interacting protein (Factor I). The importance of this inhibition was confirmed *in vivo*, with direct effects in gene expression, making the identity of this interacting protein a desired goal. Here, different approaches were explored to pave the way for that identification. SnRK1 activity assays were used to study binding strength and speed of interaction. Different chromatographic and immunological methods were followed in an attempt to isolate and identify the molecule. Arabidopsis mutants for several TPS genes, possible candidates as intermediate factors, were analysed. Results indicate that none of the tested T6P synthases (TPS) was the factor, however, redundancy between proteins cannot be ruled out. Mutants that grow on trehalose were also analysed, this phenotype could be due to absence of the intermediate factor yet, SnRK1 from all the mutants was inhibited by T6P. The (co)purification and separation by size of SnRK1 and T6P inhibition allowed the characterization of the inhibited SnRK1 complex by northern-blot. None of the main SnRK1 subunits appears to mediate SnRK1 inhibition by T6P. Western blots for the phosphorylated threonine 172 show no altered phosphorylation level upon inhibition. Attempts to co-immunoprecipitate SnRK1 complexes and factor further resolved by electrophoresis originated three protein identifications that potentially interact with SnRK1. Future work could clarify their involvement in T6P inhibition of SnRK1. This work gives further insights into SnRK1 complex composition and presents evidence for the transient and weak interaction between SnRK1 and interacting Factor I.

3.2. Introduction

In common with all organisms except vertebrates, plants synthesise the non-reducing disaccharide trehalose. Its precursor, T6P is synthesised by TPS1 (Cabib and Leloir, 1958), the only TPS shown to have T6P synthase activity in Arabidopsis (Blázquez *et al.*, 1998) and which deletion mutants are embryo-lethal (Eastmond *et*

al., 2002). The activity of the remaining 10 TPS Arabidopsis genes is still unknown (Leyman *et al.*, 2001; Avonce *et al.*, 2006; Ramon *et al.*, 2009; Vandesteene *et al.*, 2010) nonetheless the expression of most of them is highly regulated. The 10 Arabidopsis T6P phosphatases (TPP) seem to be active (Vogel *et al.*, 1998; Vandesteene, 2012). Due to this genetic profusion, to the fact that it is synthesised from G6P and UDPG both central molecules to primary metabolism and the involvement in biosynthetic and growth processes regulation, T6P is now recognised as a signal of the cellular energy status (Paul *et al.*, 2008). It has, in fact, been shown to directly correlate with sucrose levels both upon sugar feeding (Lunn *et al.*, 2006) or natural physiological variation (Martínez-Barajas *et al.*, 2011). Most importantly, it was shown that T6P inhibits SnRK1 from young tissues at physiological concentrations (1-100 µM) through a separable intermediate protein, Factor I (Zhang *et al.*, 2009). An association that provided a basis for understanding some of the effects of altered T6P levels. *In vivo* evidence of SnRK1 inhibition by T6P comes from the inverse correlation of SnRK1 marker genes and T6P levels (Zhang *et al.*, 2009).

The role of the AMPK/SNF1/SnRK1 PKs is to regulate transcription, metabolism and therefore development, in accordance to the available energy in the cell (Hardie, 2007). The complexes require an α catalytic subunit and two regulatory subunits, β and γ that contribute to protein stability, substrate specificity and subcellular localization. Due to the variable number of isoforms for each subunit possible combinations vary significantly between organisms. However, the exact number of possibilities is still uncertain due to differential expression, alternative splicing and alternative transcription initiation. Their better characterized activation system is through phosphorylation of a conserved threonine residue located in the activation loop of the kinase domain (Sugden *et al.*; 1999a). There are known upstream kinases two of them in plants (Shen and Hanley- Bowdoin, 2006; Hey *et al.*, 2007) and downstream phosphatases were recently identified (Rodrigues *et al.*, 2013). Other regulatory processes include allosteric regulation, and several post-translational processes.

Sizes of SnRK1 heterotrimeric complexes are thought to range from around 118 kDa to 165 kDa, but could be far more than this while interacting with other regulatory proteins. One such interacting protein is the one required for the inhibition of SnRK1 by T6P (Zhang *et al.*, 2009) whose identity was sought in this work. The experiments show that intermediate Factor I bind weakly and transiently to SnRK1. Three proteins that potentially interact with SnRK1 were isolated and identified. The involvement of these proteins in T6P inhibition of SnRK1 is not apparent however, further investigation may elucidate if there is a real association between these proteins and SnRK1.

3.3. Results

3.3.1. Screening TPS gene family mutants for the potential SnRK1 inhibition intermediate Factor I

SnRK1 inhibition by T6P changes during Arabidopsis development. Zhang *et al.* (2009) have shown how the inhibition drops progressively from a young seedling to a fully developed leaf. In the same publication they have shown that SnRK1 inhibition by T6P is mediated by a separable factor whose identity has been sought in the present study. One possibility was that one of the TPS proteins could be that factor. At present most of TPS-like proteins have no known function but potentially have affinity for T6P. Their gene expression patterns are highly regulated changing during development, under different environmental condition and across different tissues (Wang *et al.*, 2003; Contento *et al.*, 2004; Ùsadel *et al.*, 2008; Ramon *et al.*, 2009). To test this hypothesis we have looked at the expression levels of the TPS gene family during Arabidopsis development. Even though expression levels do not correlate with protein levels it could be possible to find a TPS gene with expression levels overlapping those observed previously for SnRK1 inhibition by T6P (Zhang *et al.*, 2009): high expression levels from seed germination to young rosette, then a decrease in fully developed rosettes and very low expression or none during senescence. This pattern was however not observed for any of the TPS genes (Fig.

3.1A). Available Arabidopsis TPS knock outs were still tested for T6P inhibition of SnRK1 (Fig. 3.1B and C) as other reasons such as post-transcriptional modifications or changes in SnRK1 affinities could account for the observed temporal pattern in T6P inhibition of SnRK1.

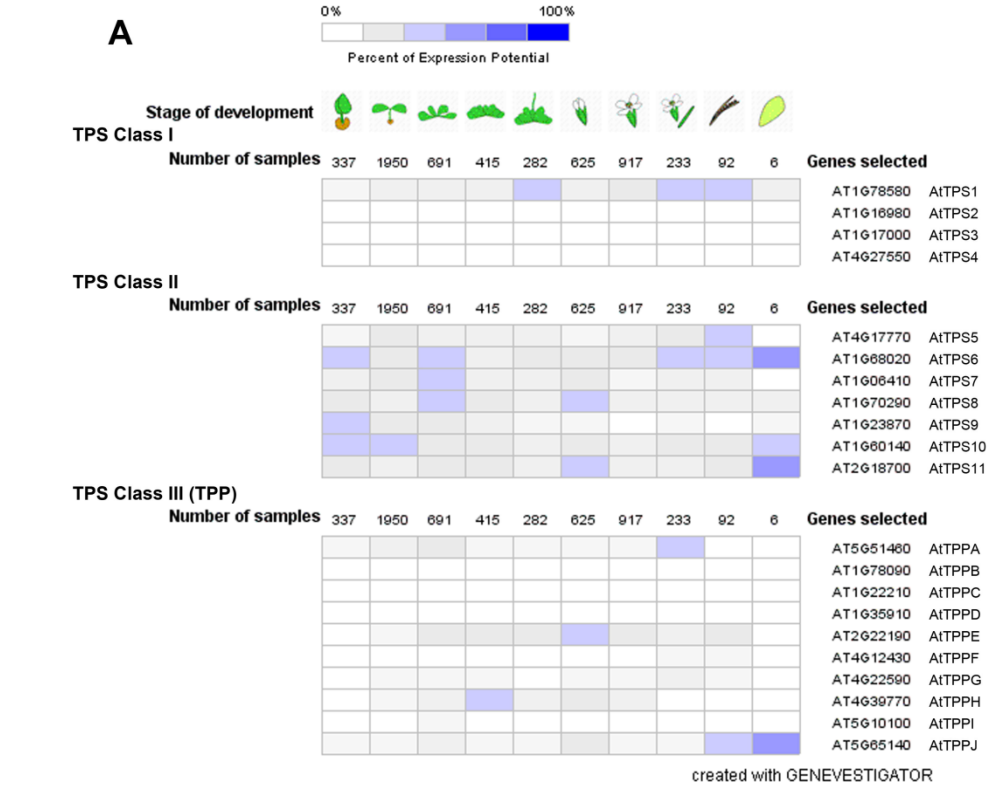
A
0%
100%
Percent of Expression Potential
Stage of development
TPS Class I
Number of samples 337 1950 691 415 282 625 917 233 92 6
Genes selected
AT1G78580 AtTPS1
AT1G16980 AtTPS2
AT1G17000 AtTPS3
AT4G27550 AtTPS4
TPS Class II
Number of samples 337 1950 691 415 282 625 917 233 92 6
Genes selected
AT4G17770 AtTPS5
AT1G68020 AtTPS6
AT1G06410 AtTPS7
AT1G70290 AtTPS8
AT1G23870 AtTPS9
AT1G60140 AtTPS10
AT2G18700 AtTPS11
TPS Class III (TPP)
Number of samples 337 1950 691 415 282 625 917 233 92 6
Genes selected
AT5G51460 AtTPPA
AT1G78090 AtTPPB
AT1G22210 AtTPPC
AT1G35910 AtTPPD
AT2G22190 AtTPPE
AT4G12430 AtTPPF
AT4G22590 AtTPPG
AT4G39770 AtTPPH
AT5G10100 AtTPPI
AT5G65140 AtTPPJ
created with GENEVESTIGATOR

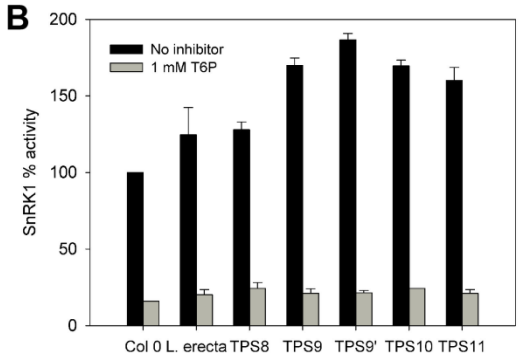
B
SnRK1 % activity
No inhibitor
1 mM T6P
Col 0 L. ercta TPS8 TPS9 TPS9' TPS10 TPS11

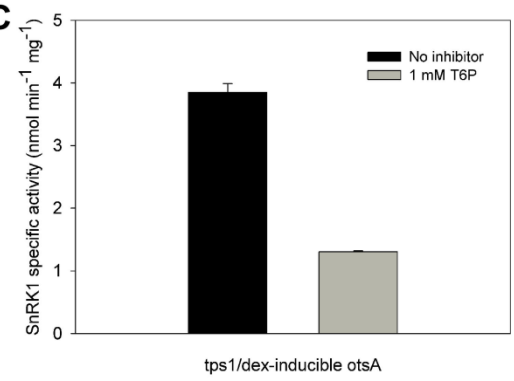
C
SnRK1 specific activity (nmol min-1 mg-1)
No inhibitor
1 mM T6P
tps1/dex-inducible otsA


D
WT 3 days
tps1 3 days
WT 16 days
tps1 16 days

Figure 3.1. Screening the TPS gene family for the potential SnRK1 inhibition intermediate Factor I. (A) Relative expression levels of TPS-like genes during Arabidopsis development as designed by Genevestigator software. Stages of development are: germinated seed, seedling, young rosette, developed rosette, bolting, young flower, developed flower, flowers and siliques, mature siliques and senescence. Data was obtained using the microarray database Meta-Analyzer provided by Genevestigator (Zimmermann *et al.*, 2004) and it is presented as percentage of expression potential from low in white to high in dark blue. **(B)** Inhibition of SnRK1 activity by 1 mM T6P in several Arabidopsis TPS mutants. Assays performed on crude extract of Arabidopsis knock outs for TPS8, two lines of TPS9, TPS10 and TPS11. Mutants and wt Landsberg *erecta* activity with no inhibitor compared to wt ecotype Col-0. Inhibition expressed as a percentage compared to each with no metabolite. Assays performed in duplicate, standard deviation shown. **(C)** Inhibition of SnRK1 activity by 1 mM T6P in crude extracts of 16-day-old Arabidopsis *tps1* dexamethasone (DEX)-inducible otsA transgenic line. **(D)** 3 and 16-day-old WT and Arabidopsis *tps1* DEX-inducible otsA transgenic line seedlings grown on 0.5x MS medium with 3% Suc (3 and 16-day old pictures at the same scale).

The available mutants for TPS8, TPS9, TPS10 and TPS11 were developed from the ecotype Landsberg *erecta* (L*er*) and did not show any differences in phenotype from the WT. SnRK1 assays showed that despite SnRK1 activity was not the same for every mutant, T6P inhibition was very consistent decreasing SnRK1 activity to about 20% in all tested lines (Fig. 3.1B). TPS1 was an especially strong candidate for the role of intermediary factor of SnRK1 inhibition by T6P, not only because the knockout is embryo-lethal but because it has been shown that its expression pattern is highest in sink tissues of high energy demand consistent with the need for higher SnRK1 inhibition by T6P, decreasing with leaf age (Vandesteen *et al.*, 2010). However, SnRK1 extracts from *tps1* mutants (DEX-rescued by otsA expression during embryo development) showed normal levels of SnRK1 activity (3.8 nmol min^{-1} mg^{-1}) and inhibition by T6P to around 30% (Fig. 3.1C), despite the impaired development (Fig. 3.1D)

3.3.2 Screening trehalose-insensitive mutants for the potential SnRK1 inhibition intermediate Factor I

Arabidopsis WT seedlings grown on 100 mM trehalose accumulate T6P (Schluepmann *et al.*, 2004) and that accumulation was recently associated to the observed growth arrest in trehalose medium (Delatte *et al.*, 2011). A possibility was that Arabidopsis mutants insensitive to this growth arrest in trehalose could lack the intermediate Factor I. Extracts were prepared from the available mutants and tested for T6P inhibition (Fig. 3.2). SnRK1 activities were quite variable; x-1 mutants exhibited significantly higher activity than WT whereas the activities of 19.3 II and 23.1 II were significantly lower. Considering the percentage of inhibition by T6P, only the 19.3 II mutants were significantly different from the WT seedlings with an inhibition level of only 25%.

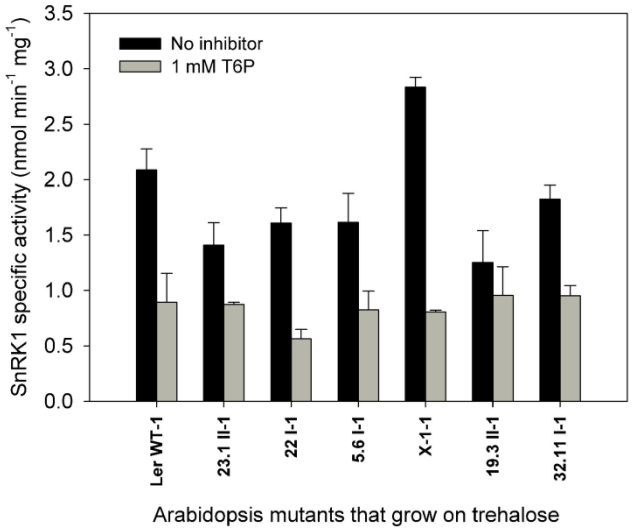

Figure 3.2. Screening of Arabidopsis mutants selected for their insensitive phenotype to trehalose growth-inhibition for the potential lack of Factor I. Inhibition of SnRK1 activity by 1 mM T6P in crude extracts of trehalose-insensitive Arabidopsis mutants. Assays performed in duplicate on 3 biological replicates, standard deviation shown.

3.3.3. Further purification of SnRK1 extracts by ATP-agarose

Size-separated fractions 62 and 71 from semi-purified seedlings SnRK1 extracts (see Chapter II for details) were applied to ATP-Sepharose columns. About 75 to 85% of all kinase activity bound to the columns. After gentle washing, elution was attempted several times with increasing ATP concentrations. Interestingly the unbound SnRK1 activity was no longer inhibited by T6P and no SnRK1 activity was ever released from the columns matrices (Fig. 3.3A and B). Davies *et al.* (1994) were able to purify AMPK proteins using this method with a yield of 50% and suggested that the 50% loss was a consequence of dephosphorylation during the procedure. Even though all care was taken to avoid dephosphorylation, western blots for AKIN10 were performed to rule out this possibility and to prove the actual absence of the catalytic subunits in washes and eluates (Fig. 3.3C and D). This experiment posed yet another possibility; the intermediate factor could have been released during the elution step. The easiest way to test this was to add directly the eluate to a non-inhibited fraction (to which inhibition can be induced, see Fig. 3.5) or to the actual supernatant not bound to the column. Adding eluate to both a non-inhibited fraction or to the ATP-unbound supernatant did not induce T6P inhibition of SnRK1 (Fig. 3.3E) indicating that the intermediary factor could have also been retained in the ATP-column.

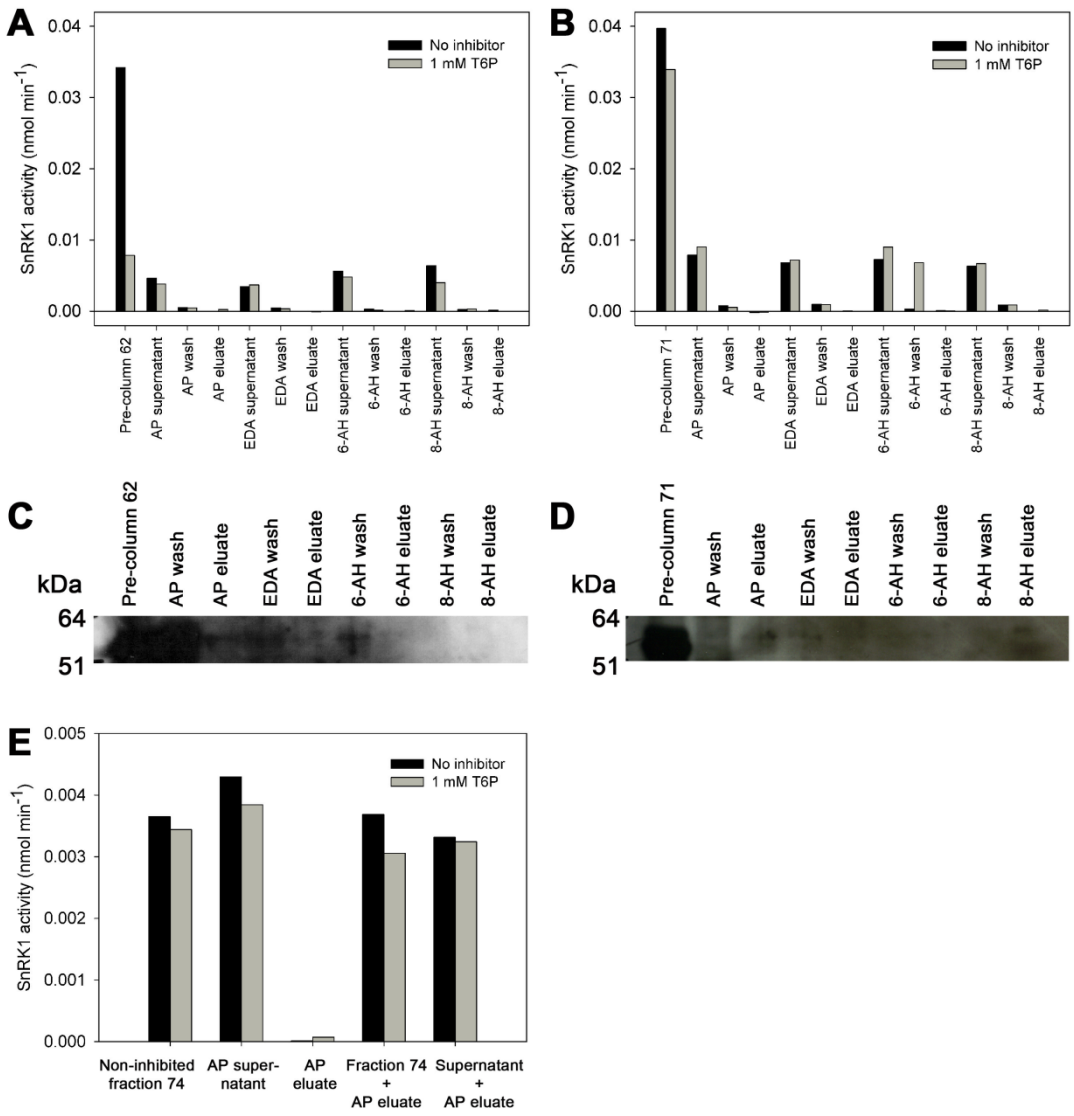

Figure 3.3. Effects of SnRK1 purification by ATP-Sepharose. SnRK1 activity and inhibition by 1 mM T6P in protein mixtures separated by different ATP-sepharose matrices (AP- EDA- 6AH – 8AH-; see Material and Methods for details) from seedlings fractions **(A)** 62 and **(B)** 71. Western blots for AKIN10 subunit on the obtained washes and eluates from fractions **(C)** 62 and **(D)** 71. **(E)** SnRK1 activity and inhibition by 1 mM T6P of AP-ATP-sepharose eluate added-back to non-inhibited protein fraction 74 and AP-ATP-sepharose supernatant. Results are representative of 3 independent experiments.

3.3.4. Assessing the composition of the SnRK1 complexes inhibited by T6P

The expression levels of the SnRK1 complex subunits genes seem to be highly regulated changing during development, under different environmental conditions and across different tissues (Bouly *et al.* 1999; Buitink *et al.*, 2003). To determine whether a particular subunit is associated with T6P inhibition, the expression pattern of the SnRK1 complex subunits during Arabidopsis development was assessed and depicted in Fig. 3.4A. None of the subunits presents an expression pattern that overlaps with that of SnRK1 inhibition by T6P (Zhang *et al.*, 2009). As previously stated, would be expected high expression levels from seed germination to young rosette, declining from there to fully developed rosettes and disappearing during senescence. However, the various post-transcriptional modifications of SnRK1 subunits, like phosphorylation (Sugden *et al.*, 1999a), myristoylation (Pierre *et al.*, 2007) and ubiquitination (Lee *et al.* 2008) could underlie the observed temporal pattern in T6P inhibition of SnRK1.

A different approach to characterize the SnRK1 complex inhibited by T6P was to define the distribution of the different subunits in the protein fractions obtained previously by size-separation (see Chapter II). This was achieved by western blot both in Arabidopsis seedlings and mature leaves (Fig. 3.4B and C). The western blots show that the distribution of some subunits shifted between seedlings and mature leaves protein profiles but overall there were no large qualitative differences in SnRK1 complexes in the two tissues. AKIN10 is present throughout the seedlings protein fractions and absent from mature leaf profile, a result that could be due to very low levels of AKIN10 in the mature leaves extract, predicted by the tenfold lower SnRK1 activities. Note also that SnRK1 activity assays have a much higher sensitivity than the western blot technique. AKIN11 and βγ subunits have the same distribution in seedlings and mature leaves profiles (first fractions). Both β1 and β3 are more abundant in the first fractions of the seedlings profile, and shift towards later fractions in the mature profile. β1 and especially β3 could be fractions necessary for SnRK1 inhibition by T6P, they span the range of inhibited fractions in the seedlings profile.

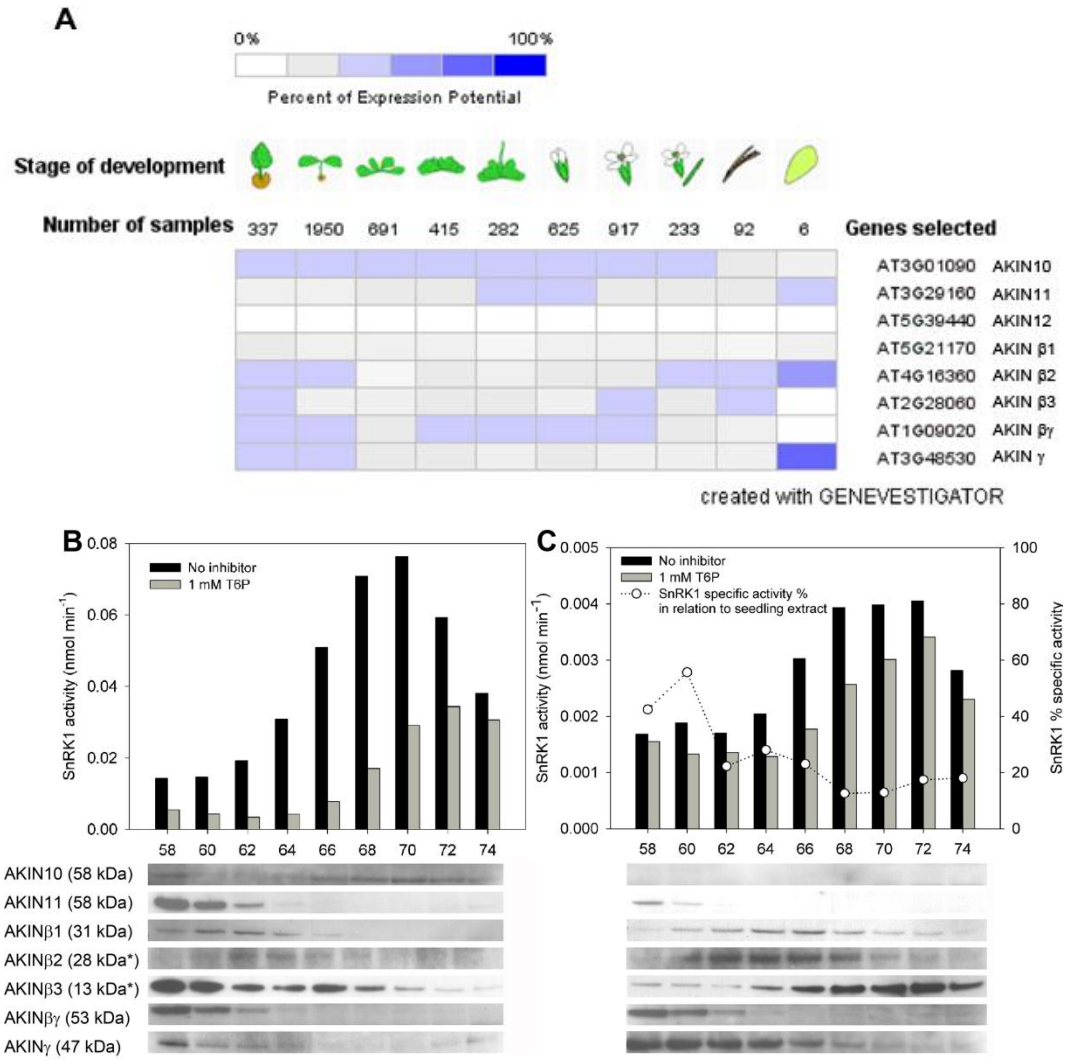

Figure 3.4. Screening the SnRK1 subunits for the potential SnRK1 inhibition intermediate Factor I. (A) Relative expression levels of SnRK1 subunits genes during Arabidopsis development as designed by Genevestigator software. Stages of development are: germinated seed, seedling, young rosette, developed rosette, bolting, young flower, developed flower, flowers and siliques, mature siliques and senescence. Data were obtained using the microarray database Meta-Analyzer provided by Genevestigator (Zimmermann *et al.*, 2004) and it is presented as percentage of expression potential from low in white to high in dark blue. **(B)** Arabidopsis seedlings and **(C)** Arabidopsis mature leaves SnRK1 activity assayed with 1 mM T6P compared to no T6P (bars and left axis) and western blots for subunits of the SnRK1 complex; the dotted line indicates mature SnRK1 specific activity percentage in relation to seedling SnRK1 specific activity (right axis). SnRK1 subunit predicted sizes are presented

between brackets and asterisks denote subunits with shifts in band size: AKINβ2 band was at 25 kDa and AKINβ3 band was of 17 kDa.

Another raised question was if the size predicted for the fraction of highest inhibition corresponded to the size of the SnRK1 complex and the size of the intermediate factor on their own, about 174 kDa each or if both ran the column attached as a complex, making the intermediate factor 174 minus the size of the SnRK1 complex. In this last case the intermediate factor would be a small protein of 10 to 55 kDa, depending of the SnRK1 complex size that theoretically can range from 118-165 kDa. To shed some light into this question seedlings fraction 62 with low activity and inhibited by 70% was added to seedlings fraction 72, with SnRK1 activity 3 times higher and only inhibited by 25% (Fig. 3.3). The resulting mixture was high in SnRK1 activity and was inhibited also by 70%.

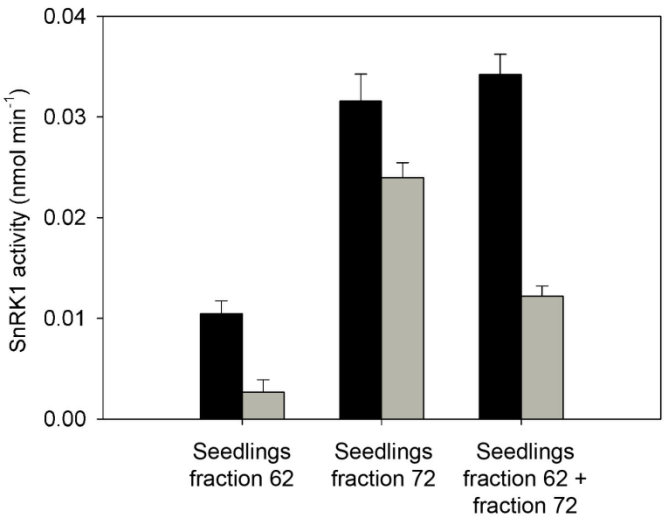

Figure 3.5. SnRK1 activity inhibition by T6P of fractions 62, 72 and a combination of both from the seedlings protein profile. Data are means of three technical replicates, standard deviation shown.

3.3.5. Characterization of SnRK1 inhibition by T6P

To tackle the problem from a different angle, the nature of the interaction of SnRK1 and interacting factor had to be first further characterized in order to facilitate future attempts of identification. To do so, the interaction effects and time progression of the inhibition were evaluated. Even though processes of (de)phosphorylation were unlikely to be responsible for T6P (and G1P and G6P) inhibition of SnRK1, the phosphorylation status of the SnRK1 catalytic subunit was assessed in the presence of each inhibitor (Fig. 3.6A). As expected, the inhibition process did not change the phosphorylation level of the threonine-175 from the activation loop of the catalytic subunit. A very important realization was that T6P inhibition of SnRK1 increased in the first seconds of reaction (Fig. 3.6B) showing that interaction between SnRK1 and intermediate Factor I happens (at least) during that short period of time. Also, as expected, the ionic strength of the reaction mixture affects inhibition, and by 0.5 M NaCl T6P inhibition of SnRK1 is completely abolished (Fig. 3.6C).

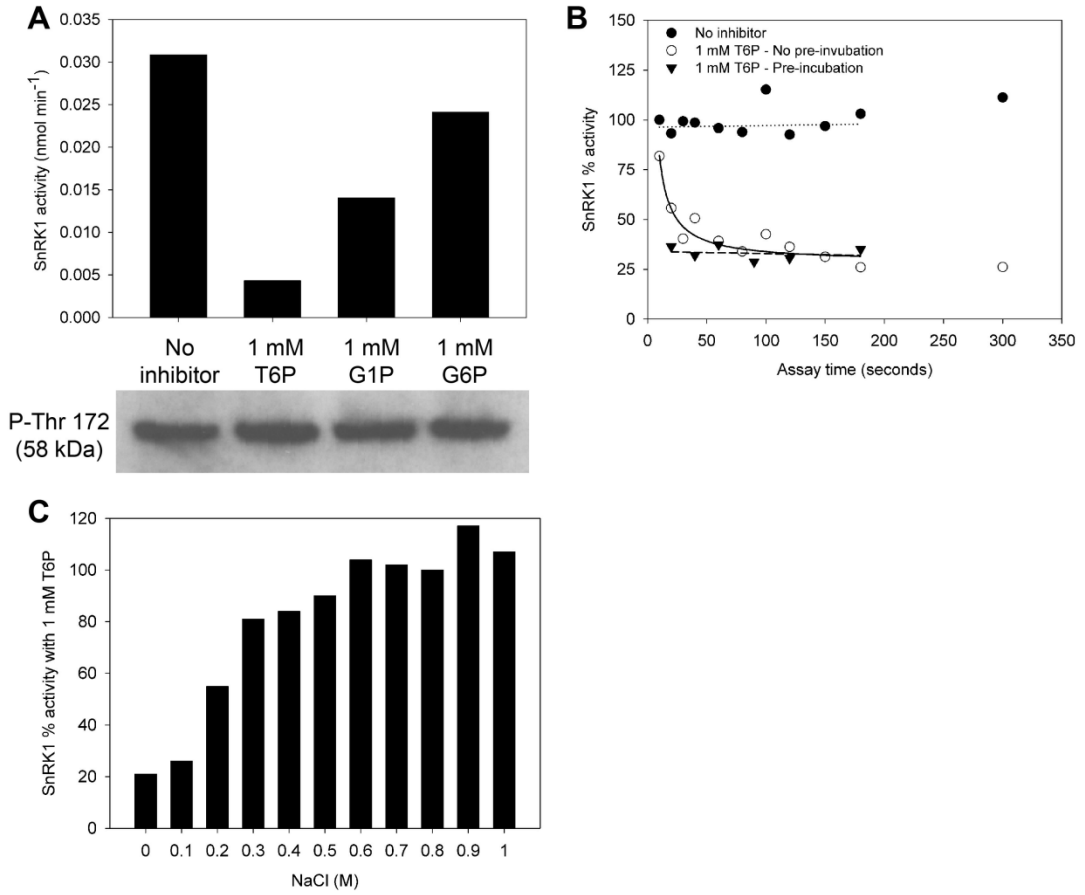

Figure 3.6. Characterization of SnRK1 inhibition by T6P. (A) SnRK1 activities without and with 1 mM T6P, G1P and G6P in fraction 64 from size fractionation of Arabidopsis seedlings protein extracts and corresponding western blot for the phosphorylated threonine of the catalytic subunits. **(B)** SnRK1 activities without and with 1 mM T6P in fraction 68 from size fractionation of cauliflower florets protein extracts at different assay times ranging from 10 seconds to 300 seconds. The dotted line reflects the SnRK1 activity linearity over time, the dashed line reflects the linear SnRK1 inhibited activity when incubated with T6P prior to the activity assay and the solid line shows how SnRK1 inhibition by T6P increases along the first 60 seconds of reaction when T6P is not pre-incubated with extract prior to the assay. **(C)** % of SnRK1 activity with 1 mM T6P assayed at different NaCl concentrations.

3.3.6 Co-immunoprecipitation of SnRK1 and intermediate Factor I

Co-immunoprecipitation of SnRK1 and intermediate factor was the chosen approach to attempt to isolate and identify the elusive protein. An antibody for the βγ

subunit proved to be very efficient for immunoprecipitation, bringing down more than 80% of total SnRK1 activity from Arabidopsis extracts. So far, immunoprecipitation experiments did not co-immunoprecipitate the intermediate Factor I (Zhang *et al.*, 2009). Co-immunoprecipitation did not occur even in the presence of T6P, which suggested a transient or loose/weak interaction between SnRK1 and intermediate factor. Bearing in mind this assumption, the immunoprecipitation procedure should be as quick and gentle as possible to avoid proteins separation. This was attempted and resulted in some degree of SnRK1 inhibition by T6P in the pellet (Fig. 3.7).

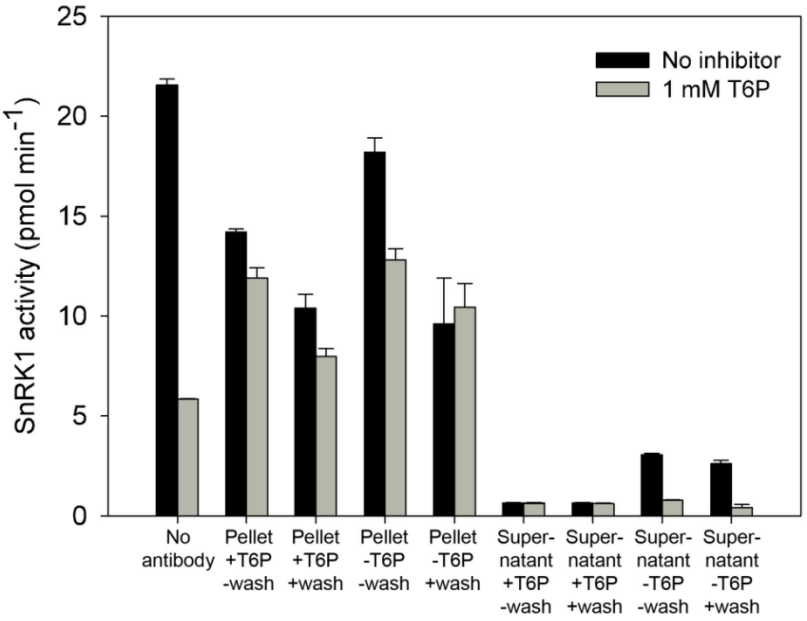

Figure 3.7. SnRK1 activities without inhibitor and with 1 mM T6P in Arabidopsis seedlings protein extracts after immunoprecipitation with and without T6P followed by no wash or vigorous wash. Experiment performed 3 times with identical results, data from one representative experiment. Means of 3 technical replicates ± standard deviation.

Without perturbing the pellet with washes and without T6P during immunoprecipitation the βγ antibody precipitates 84% of total SnRK1 activity, which was inhibited 30% by T6P. The amount of SnRK1 activity in the pellet decreases to 50% after 3 washes and T6P inhibition disappears. In the presence of T6P during

immunoprecipitation, the unwashed pellet has 66% of SnRK1 activity that correspond to already inhibited SnRK1. After 3 washes that pellet has 30% less SnRK1 activity. Supernatants obtained after immunoprecipitation without T6P had about 3 pmol.min^{-1} of SnRK1 activity which (without washes) sums up with pellet 18 pmol.min^{-1} activity to 100% (21 pmol min^{-1}) of control activity. After 3 washes supernatant and pellet add up to 12 pmol min^{-1}, only 55% of control activity. Vigorous washing led, therefore, to 45% loss of SnRK1 activity and complete loss of inhibition by T6P. The immunoprecipitation experiment performed in the presence of T6P has SnRK1 activity already inhibited in the assay without extra T6P, but its activity can be extrapolated to the value of the equivalent experiment performed without T6P during immunoprecipitation.

These results suggest that immunoprecipitated SnRK1 either in the presence or absence of T6P, not disturbed by washes, should have retained a certain level of intermediary factor. On the contrary, well washed pellets, should have lost the intermediary factor during the first washes. Given these assumptions, band differences in denaturing SDS gels could translate into potential candidates of intermediate Factor I. Electrophoresis of protein pellets obtained by immunoprecipitation with βγ-antibody presented an elevated number of bands (Fig. 3.8A). Protein separation of the antibody solution only showed two bands corresponding to the light and heavy chains of the antibody. This indicates a high level of unspecific binding either to the antibody or the used beads. Despite the elevated number of protein bands, three were consistently present in non-washed pellets and absent in washed pellets (Fig. 3.8A). From top to bottom, band 1, the one most difficult to isolate, was a distinctive very thin dark line, band 2 was clearly the bottom darker line of a doublet and band 3 was also very well isolated at a top of a doublet. These bands were also very clear in the pellet washes (Fig. 3.9). To further confirm these bands interest, the gel from the semi-purification profile (for details see Chapter II) was also analysed (Fig.3.8B). Band 1 was not identifiable in the profile gel but bands 2 and 3 were clearly present and seemed to fluctuate with the T6P inhibition pattern.

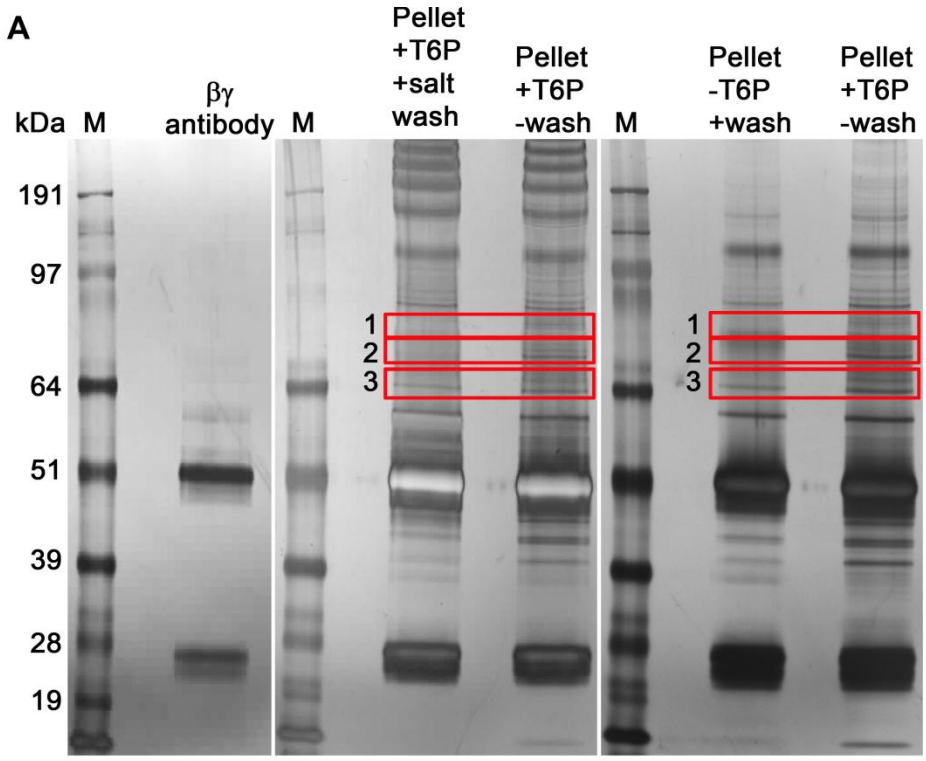
A
kDa
M
βγ antibody
M
Pellet +T6P +salt wash
Pellet +T6P -wash
M
Pellet -T6P +wash
Pellet +T6P -wash
191
97
64
51
39
28
19
1
2
3
1
2
3

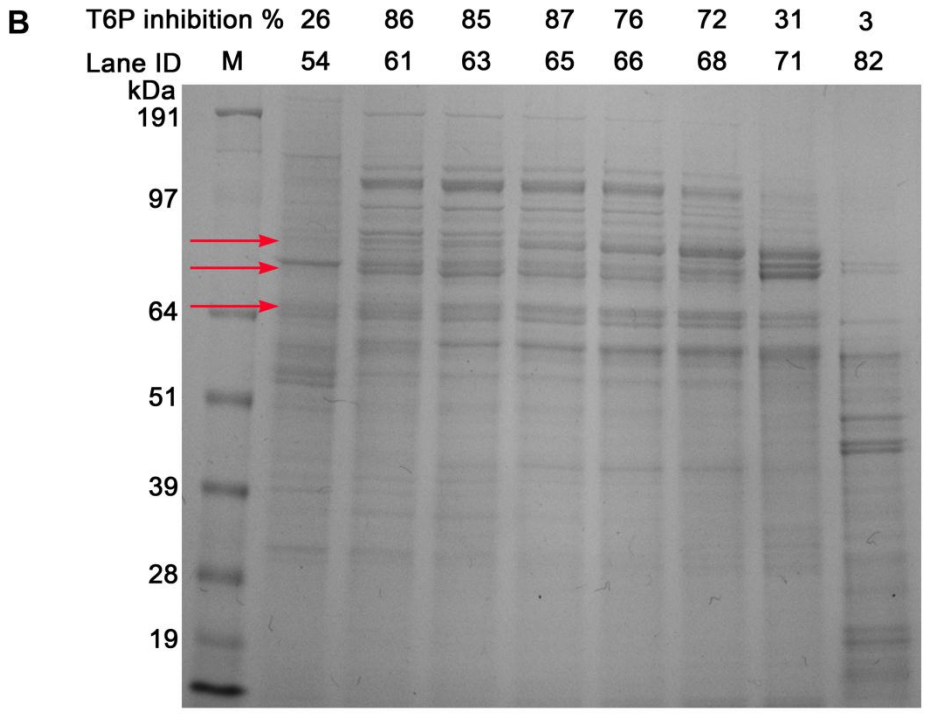
B
T6P inhibition %
26
86
85
87
76
72
31
3
Lane ID
M
54
61
63
65
66
68
71
82
kDa
191
97
64
51
39
28
19

Figure 3.8. Immunoprecipitated and size fractionated proteins separated by electrophoresis in 4-12 % polyacrylamide gels. (A) Silver stained proteins immunoprecipitated by βγ-subunit antibody; M, denotes protein marker and separates different gel runs, band sizes are presented in kDa on the left; βγ-antibody solution was run to indicate antibody subunits sizes, immunoprecipitation was performed either in the presence or absence of T6P (+T6P or –T6P respectively) and the pellets were either not washed, washed or washed with 1 M NaCl solution (-wash, +wash or +salt wash respectively). **(B)** Brilliant Blue G-Colloidal stained proteins fractionated by gel-filtration. M, denotes protein marker, band sizes are presented in kDa on the left; lanes are identified by fraction number and corresponding level of inhibition by T6P. Protein bands absent from washed pellets were considered proteins of interest.

Considering the assumptions above, the three bands of interest should be released during the pellets washes and possibly even enriched. The first and second washes of the pellets were also run in SDS-polyacrylamide gels (Fig. 3.9). The three bands were easily recognized: number 1 is a very thin and dark one positioned in a group of three similar bands, band number 2 has strong intensity and is the lowest of an easily identified doublet, band number 3 is also strong in intensity and it is the heaviest of another doublet.

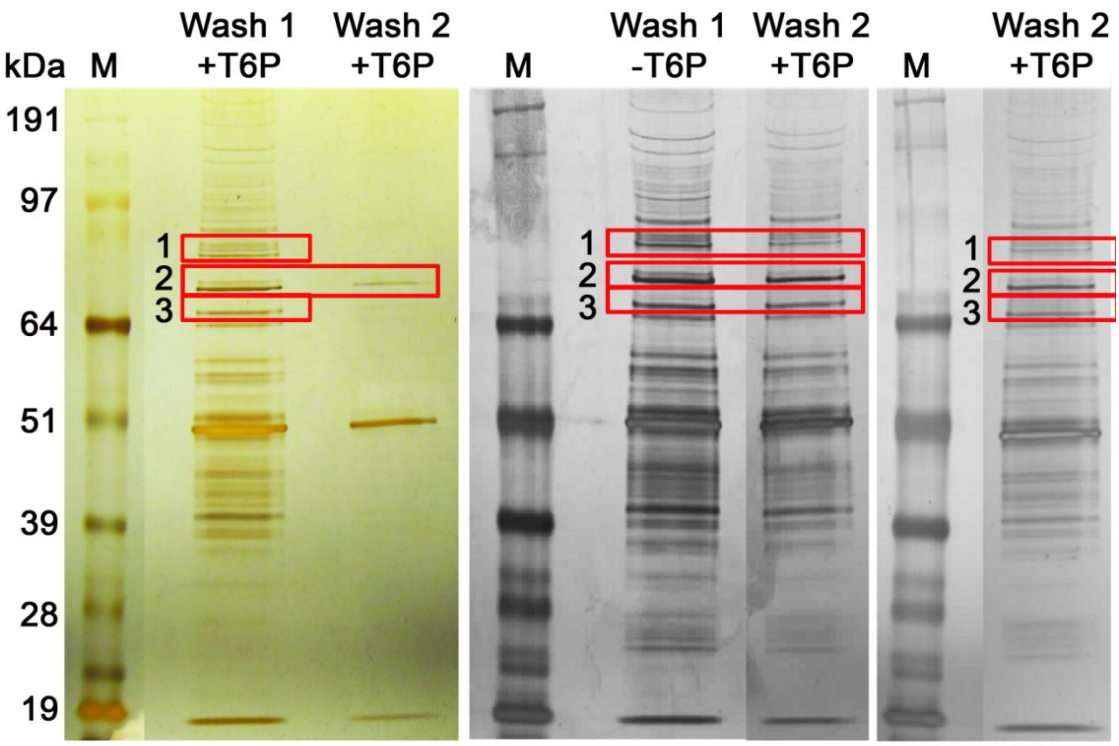

Figure 3.9. Silver stained proteins released during washes of βγ-subunit antibody immunoprecipitated pellets separated by electrophoresis in 4-12% polyacrylamide gels. M, denotes protein marker and separates different gel runs, band sizes are presented in kDa on the left; immunoprecipitation was performed either in the presence or absence of T6P (+T6P or -T6P respectively), pellet washes 1 and 2 are presented with proteins of interest highlighted and numbered 1, 2 and 3.

The three bands were excised from the SDS-PAGE and treated for mass spectrometry analysis. The 3 protein bands were identified (Table 3.1). Band 1 encodes a translation elongation factor 2-like protein of 665 amino acids and 74 kDa, involved in cold-induced translation. Mutants in this gene have their low temperature-induced transcription of cold-responsive genes blocked, fail to acclimate to cold and are freezing sensitive (Guo *et al.*, 2002). Band 2 is a Cobalamin-independent methionine synthase (MetE) of 765 amino acids and 84 kDa. These enzymes catalyze the transfer of a methyl group from methyltetrahydrofolate to L-

homocysteine without using an intermediate methyl carrier to form methionine (Taurog and Matthews, 2006). Band 3 is an unknown protein of 741 amino acids and estimated molecular weight of 80 kDa. It possesses 3 recognizable domains, a thiamine pyrophosphate-binding module, a pyrimidine (PYR) binding domain and a C-terminal domain of transketolase which has been proposed as a regulatory molecule binding site.

Table 3.1. Protein identification from gel bands 1, 2 and 3.

Gel band	Identification	Accession number/ Protein score	# peptides matched (MS/MS)
1	putative elongation factor [*Arabidopsis thaliana*]	gi|23397287/152	1
2	cobalamin-independent methionine synthase [*Arabidopsis thaliana*]	gi|47600741/653	5
3	Unknown protein [*Arabidopsis thaliana*]	gi|28058762/183	1

Identification scores obtained with the algorithm MOWSE in combined search mode (MS+MS/MS data). Protein identification was only accepted when significant protein homology scores were obtained ($p<0.05$). Data base: NCBI (minimum score >84). Search criteria: 2 missed-cleavages, peptide tolerance 50ppm, 0.3Da fragment mass tolerance, variable modifications Cys-carbamidomethylation; Met-oxidation; N-pyro-glu; and at least 1 peptide fragmented ($p<0.05$).

3.4. Discussion

SnRK1, a central metabolite sensor that maintains plant cellular homeostasis (Hardie, 2007; Polge and Thomas, 2007) was shown to be inhibited by the regulatory sugar T6P (Zhang *et al.*, 2009; Debast *et al.*, 2011; Delatte *et al.*, 2011; Martínez-Barajas *et al.*, 2011) through an intermediary protein (Factor I) (Zhang *et al.*, 2009) which identity is still elusive. In this study we used several available resources to identify that intermediary Factor I. Despite the fact that a definite identification was

not achieved, we managed to pave the way to ease future attempts and identified potential additional interacting players of the SnRK1/T6P signaling pathway.

3.4.1. Screening of available mutants

TPS1 synthesises T6P and associates functions as a regulatory protein (Vandesteene *et al.*, 2010). As previously stated *Arabidopsis thaliana* has 10 more TPS-like genes without recognised activity but whose expression patterns are highly regulated. These observations together with a potential affinity for T6P raised the possibility that one of these TPS proteins could be Factor I. In this experiment we looked at SnRK1 inhibition by T6P of several TPS mutants available at that time. Looking at TPS expression levels throughout Arabidopsis development (Fig. 3.1A) there was no indication of a particular gene with overlapping expression with that of SnRK1 inhibition by T6P, higher in young/sink tissues and lower in old/source tissues. But because protein levels can differ dramatically from those of gene expression, analysing each null mutant and combinations is still of interest. Mutants *tps8*, *tps 9*, *tps 10* and *tps11*, with higher SnRK1 activities did not show alterations of SnRK1 inhibition by T6P (Fig. 3.1B); neither did *tps1* dex-inducible otsA transgenic line (Fig. 3.1C). TPS1 was an especially interesting candidate as its knockout is lethal at the torpedo stage (Eastmond *et al.*, 2002) and additional regulatory roles are expected as for its yeast/fungus counterparts (Bonini *et al.*, 2003; Wilson *et al.*, 2007). This experiment does not rule out the possibility that one or more TPS-like proteins are the Factor I but encouraged to try a different approach. In fact, mutants *tps8*, *tps 9*, *tps 10* and *tps11* could be negative regulators of SnRK1 activity and only double or triple knockouts would allow us to see any effect on SnRK1 inhibition by T6P.

It was shown that Arabidopsis grown in trehalose-supplemented medium accumulate T6P and stop growing (Schluepmann *et al.*, 2004). In the presence of metabolizable sugars growth is restored. Screening for Arabidopsis mutants insensitive to trehalose feeding could be an elegant way to find Factor I. A possibility

is that one of these mutants lacked Factor I. The tested mutants had quite variable SnRK1 activity but in all of them SnRK1 was inhibited by T6P (Fig. 3.2). Again, this line of thought should not be rejected as it still may produce positive results, however, we moved on to more available resources.

3.4.2. ATP-agarose approach

In this experiment we used an affinity chromatography kit to identify which linker model of ATP to agarose would be useful for the isolation of SnRK1 and eventually Factor I. All four different matrices resulted in identical outcomes, about 75 to 85 % of SnRK1 activity was lost and the recovered activity was no longer inhibited by T6P (Fig. 3.3A and B). The absence of catalytic subunit in washes and eluates (Fig. 3.3C and D) confirmed that the lost activity was due to SnRK1 being trapped to the columns and not due to dephosphorylation as suggested by Davies *et al.*, 1994 who was also only able to recover 50% of AMPK activity using this technique. Using other methods, Sugden *et al.* (1999b) have purified two SnRK1 kinase activities from spinach leaves (named HRK-A and HRK-C) and were expecting to find metabolic regulation by G6P as previously described by McMichael *et al.* (1995). However, due to several purification procedures, storage and/or activity assays the inhibition was not observed and only later, testing different conditions, was the inhibition better characterized (Toroser *et al.*, 2000). These experiments describe well the sensitive nature of SnRK1 activity and its regulation.

Despite the loss in SnRK1 activity, Factor I could have been released during elution. However, adding eluates to both non-inhibited fraction and ATP-unbound supernatant did not restore inhibition by T6P (Fig. 3.3E) indicating that Factor I may have also been retained in the ATP-column. After several failed elution attempts this method was abandoned and a different approach was followed.

3.4.3. Immunoprecipitation approach

Even though mature leaf SnRK1 is far less inhibited by T6P than SnRK1 from seedlings (Zhang *et al.*, 2009), maximal inhibition by T6P in seedling and mature leaf SnRK1 was found in complexes of the same size (Fig. 3.4B and C). This seems to indicate that there were no large qualitative differences in SnRK1 complexes inhibited by T6P from seedlings and mature leaves. However, analysing the western blot for the different subunits there are clear differences. Subunits β1 and β3 shift from the first fractions in seedlings to later fractions in mature extract (Fig. 3.4B and C). One can argue that one of these subunits could be necessary for SnRK1 inhibition by T6P and that in mature tissues they suffer post-translational modifications and no longer permit T6P inhibition. One of our hypotheses was that differences might be observed for subunit βγ as it is plant specific (Gissot *et al.*, 2006). However this was not the case and in fact none of the subunits can be at this point unequivocally associated to T6P inhibition of SnRK1.

We also aimed to determine Factor I molecular size. The protein sizes of inhibited fractions separated by gel filtration did not clarify if size fractionation corresponded to the size of the SnRK1 complex and the size of the intermediate factor on their own or if both ran the column attached as a complex, making the intermediate factor a small protein of 10 to 55 kDa. The fact that the addition of a fraction of low SnRK1 activity and high T6P inhibition with a fraction with 3 times higher activity but with little inhibition resulted in a mixture high in SnRK1 activity and also inhibited by 70% (Fig.3.5) suggests that the intermediary factor is in excess to SnRK1 in fraction 62 or that if it is in complex to SnRK1 it is reversibly attached being able to interact with further available SnRK1 complexes. Both theories point towards a big protein of about 174 kDa.

Isolation of intermediary Factor I together with SnRK1 by co-immunoprecipitation would be another elegant way of identifying Factor I. Considering that so far, immunoprecipitation attempts never resulted in inhibited pellets, i.e. no Factor I was ever co-immunoprecipitated with SnRK1 (Zhang *et al.*, 2009), suggests that SnRK1 and Factor I have a transient interaction or that their

binding strength is so weak that they detach during the immunoprecipitation protocol. The progress of T6P inhibition (Fig. 3.6B) exposes a “lag” phase of about 1 min where inhibition increases to a steady state. The interaction of SnRK1 with Factor I happens (at least) during those first seconds of the reaction. The design of a co-immunoprecipitation protocol carried during that first min of reaction and with mild washing steps resulted in the identification of three protein bands (Table 3.1) that were absent when the immunoprecipitate was thoroughly washed.

Band 1 is a translation elongation factor 2-like protein. Mutants in this gene have low temperature-induced transcription of cold-responsive genes blocked, fail to acclimate to cold and are freezing sensitive (Guo *et al.*, 2002). No connection to SnRK1 or T6P signaling pathways had, to our knowledge, been described despite the known involvement of SnRK1 and T6P in abiotic stress responses (Almeida *et al.*, 2005; Fragoso *et al.*, 2009). It seems unlikely that this protein is Factor I but its ability to interact with SnRK1 may be actual and may be worth investigate further.

Band 2 is a MetE that catalyzes the synthesis of methionine from homocysteine. The reaction involves the direct transfer of a methyl group from methyltetrahydrofolate (transformed into tetrahydrofolate) to the sulfur atom of L-homocysteine to form methionine (Taurog and Matthews, 2006). Sulphur depletion leads to a systemic adjustment of metabolism and in fact, the sulfur-containing amino acids (homocysteine and methionine) directly link two major metabolic networks, the sulfur and one-carbon metabolisms (Ferrer *et al.*, 2004). To our knowledge neither SnRK1 or T6P were ever linked to either these networks, SnRK2s, however, are well known to be involved in sulphur stress responses (Kulik *et al.*, 2011) and trehalose was shown decrease in both systemic and induced sulphur stress (Nikiforova *et al.*, 2005). Again it seems unlikely that this protein could be Factor I, but a link to the SnRK1/T6P signaling pathway should not be ruled out and further investigation may unveil unexpected associations.

Band 3 is an unknown protein with a thiamine pyrophosphate-binding module, a PYR binding domain and a C-terminal domain of transketolase which has been proposed as a regulatory molecule binding site. In skeletal muscle and cardiac

myocites AMPK phosphorylation and activity is decreased with increasing glucose concentration (Itani *et al.*, 2003; Tabidi *et al.*, 2012). The glucose 6-phosphate dehydrogenase inhibitor (diehydroepiandeosterone, DHA) and thiamine, the precursor of the coenzyme for transketolase, increase AMPK activity. On the other hand, the NADPH oxidant phenazine methosulphate (PMS) decrease AMPK activity. The flux through the PPP is respectively decreased and increased by DHA and PMS. The authors suggest that the observed inactivation of AMPK by glucose may be mediated by the activity of the PPP which sets the level of Xu5P (Tabidi *et al.*, 2012). In fact AMPK activity was inversely related to Xu5P content which was increased with increasing glucose concentration. It had been previously suggested that Xu5P might be a signaling compound that reflected glucose levels (Kabashima *et al.*, 2003). Xu5P is formed in the nonoxidative arm of the pentose pathway via different ways one of which would be through a transketolase reaction acting on glyceraldehyde 3-phosphate (GAP) and F6P. Just as in animals transketolase links the PPP to glycolysis, in photosynthetic organisms transketolase is an enzyme of PPP and also the Calvin cycle. We can envisage a parallelism in plants linking transketolase activity, T6P (a signaling compound that reflected sucrose levels) and SnRK1 regulation. Again, a function as Factor I is highly unlikely for a transketolase-like protein, however intertwined effects are expected and of interest for future investigation. In fact, in pea embryo with anti-sense SnRK1, a putative transketolase was down-regulated (Radchuck *et al.*, 2006). The fact that bands 2 and 3 were also present in the semi-purification profile gel and seemed to fluctuate according with the T6P inhibition pattern (Fig. 3.8B) gives a new layer of interest to these proteins.

Conclusion

Identification of the Factor I that mediates SnRK1 inhibition by T6P was not achieved but the different tried approaches were useful in revealing experimental difficulties to be avoided in the future and indicating new possible upcoming methods for the identification of this elusive protein.

Any of the three identified proteins are unlikely to be Factor I but the notion that they could be modules of the SnRK1/T6P signaling pathway cannot be ruled out and deserve future attention.

3.5. Material and Methods

3.5.1. Biological material

Seeds of *Arabidopsis thaliana* (L.) wild type ecotypes Col-0 and Landsberg erecta (L*er*) and anti-sense TPS8, 9, 10, 11 were weighed, surface- sterilized and grown in liquid culture as described in Chapter II. Seeds of Arabidopsis *tps1* dexamethasone (DEX)-inducible otsA transgenic lines were surface- sterilized as described previously and germinated in plates with agar-solidified (0.8%, w/v) half-strength Murashige and Skoog medium (Sigma M0404) plus 3% sucrose. After stratification at 4ºC for 72 h in the dark seeds were transferred to the growth room at 23ºC in a long-day light cycle (16 h light/ 8 h dark) with 130 µmol quanta m^{-2} s^{-1} irradiance. The trehalose-insensitive mutants were also surface sterilized and grown under the same conditions as just described; except for the addition of filter-sterilized trehalose to the media to a final concentration of 3% (w/v). Semi-purified protein extracts from Arabidopsis seedlings and mature leaves were the same used and described in detail in Chapter II.

3.5.2. SnRK1 activity assays

Total soluble protein was extracted from 200 mg of ground tissue. For the detailed protocol please refer to Chapter II. SnRK1 activity was determined as in Zhang *et al.*, (2009), also described in detail in Chapter II.

3.5.3. ATP-agarose

In affinity chromatography the ability of a protein of interest to bind a specific small molecule (ligand) is used to purify it from a complex mixture of proteins. In our

case, the ligand (ATP) is immobilized on a matrix (agarose) and incubated with the complex protein mixture to be purified. The protein of interest (SnRK1) is expected to bind the ligand whereas most of the other proteins will be discarded in the flow through. The protein of interest can then be eluted by an excess of free ligand in the elution buffer. When using ATP as the ligand care must be taken as to how it is attached to the matrix. It needs to be modified with a linker that may interfere, reduce or prevent the protein-ATP biding interaction. To avoid this problem, different linkage strategies (Fig. 3.10) (attaching ATP by the adenine base, the sugar or the phosphate moiety) must be tested for each individual case.

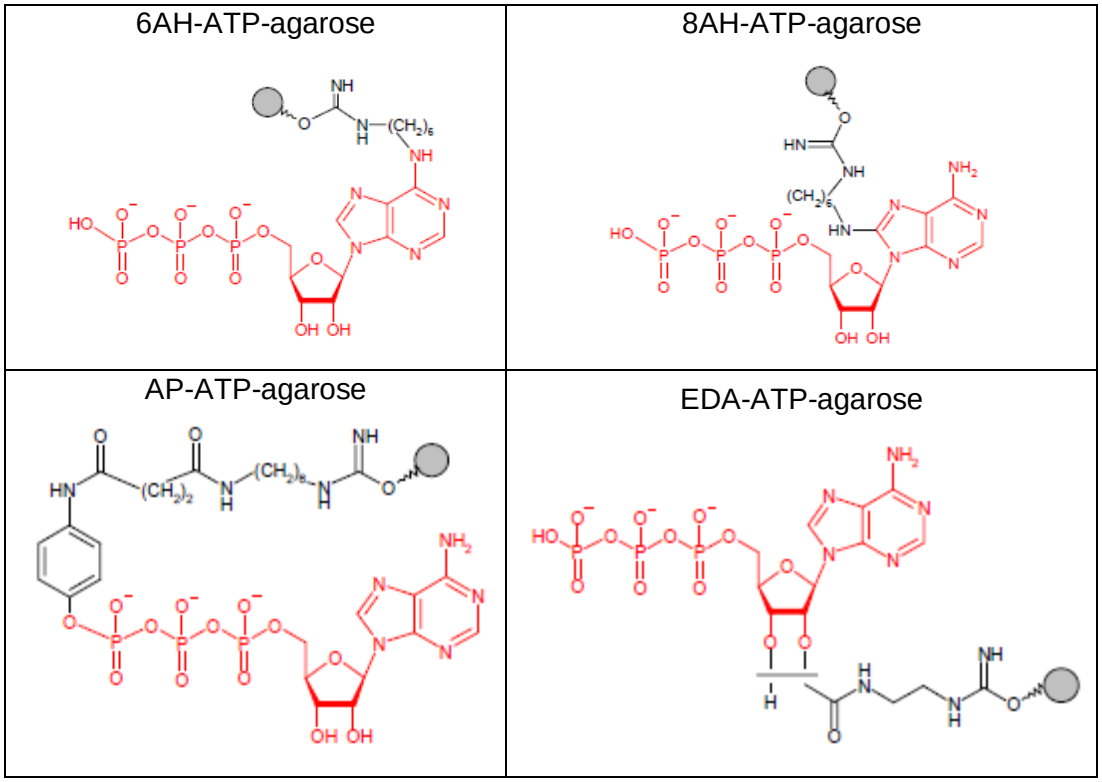

Figure 3.10. **Schematic representation of the different ATP-linker-agarose binding strategies**. In *6AH-ATP-Agarose* and *8AH-ATP-Agarose* the ATP is immobilized via the adenine base but varies by the actual position of the linker (C^6 and C^8, respectively). *AP-ATP-Agarose* and *EDA-ATP-Agarose* are phosphate and sugar modified derivatives, respectively.

Our semi-purified protein extracts contained active SnRK1 and did not contain free endogenous ATP. The manufacturer's protocol (Jena Biosciences, ATP Affinity Test Kit - AK-102) was closely followed except for the buffers which were the ones used in our semi-purification and known to retain SnRK1 activity. The exact protocol was as follows: a volume of 300 µl of fractions 64 and 74 from seedlings semi-purification was mixed with 75 µl of buffer A (see Chapter II) with added NaCl and MgCl to a final concentration of 0.05 M and 60 mM respectively (now named washing buffer) and kept on ice. A volume of 50 µl of each ATP-agarose was equilibrated by mixing and vortexing with 500 µl of washing buffer. After spinning at 1000 xg for 1 min the buffer was discarded. This step was repeated 2 more times. The protein solution was then added to the equilibrated ATP-agarose and incubated for 4 h at 4°C with gentle agitation. The supernatant was recovered by spinning at 1000x for 1 min. The pellet was ressuspended twice in 1 ml ice-cold washing buffer and span at 1000 xg for 1 min. Both washes were kept for future analysis. A volume of 100 µl of buffer A (see Chapter II) with added MgCl and ATP to final concentration of 60 mM and 100 mM respectively was mixed with the ATP-agarose and incubated at 4°C for 1 h with gentle agitation. The supernatant (eluate) was recovered after spinning at 1000 xg for 1 min. Elution was repeated 1 more time. A pool of both elutions was dialysed overnight in 5000 ml of buffer A and again for 3 more h. An overestimation of remaining ATP in the sample is of 0.004 µM, a concentration low enough to not disrupt the SnRK1 activity assay. This dialysis step was known to not significantly decrease SnRK1 activity or T6P inhibition but, nonetheless, it was confirmed again. The flow through, a pool of both washes and the dialysed eluate were assayed for SnRK1 activity.

3.5.4. Antibodies

Antisera raised against peptides from each SnRK1subunit (Table 3.2) were raised in rabbits and affinity purified by Eurogentec, Seraing, Belgium.

Table 3.2. Peptide sequence recognised by each SnRK1 subunit anti-body.

SnRK1 subunits	Peptide sequence
AKIN10	RASSGYLGAEFQETM
AKIN11	TDSGSNPMRTPEAGC
Beta1 (β1)	ANGKDEDAAAGSGGC
Beta2 (β2)	LMGQSPPHSPRATQC
Beta3 (β3)	YSSTEDETRDPPAVC
Betagamma (βγ)	CHISRQYDGSGRPYP
Gamma (γ)	SDSQDIEIRSDTSLC

Phosphorylation of the alpha subunit at the conserved activation T-loop threonine was detected with antibody against human AMPK phospho-threonine 172 (Anti-Phospho-AMPKα (Thr172) - Millipore).

3.5.5. Western blot

For western blot analysis, the proteins separated in gel by denaturing electrophoresis were transferred onto Hybond-P polyvinylidene fluoride (PVDF) membranes (GE Healthcare) using an XCell II Blot module (Invitrogen) according to the manufacturer's instructions. Proteins were detected using an ECL Western Blot Detection Kit (GE Healthcare). Membranes were blocked with TBST buffer (20 mM Tris base pH 7.6, 137 mM NaCl, 0.1% Tween 20) containing 2% ECL Blocking Reagent for 1 h at room temperature with gentle shaking and washed twice with TBST. The membranes were then incubated overnight with rabbit anti-serum for each SnRK1 subunit diluted to 1:12000 TBST buffer plus 2% ECL Blocking Reagent. After 5 washes with 100 mL TBST, the membranes were incubated for 1 h at room temperature with an anti-rabbit IgG secondary antibody conjugated to horseradish peroxidase diluted to 1:30000 and then washed 5 times with TBST. Immune complexes were detected by enhanced chemiluminiscence assay using ECL Advance Western Blotting detection kit (GE Healthcare) following the manufacturer's instructions. Washed membranes were covered with a thin layer of detection reagent for 5 min. Excess detection reagent was drained and the membrane protein-side was

placed on clean film, the membrane wrapped and placed inside an x-ray film cassette with the autoradiography film on top. The film was exposed for 30 sec and developed immediately after.

3.5.6. Immunoprecipitation

To immunoprecipitate SnRK1 complexes, 50 µL Dynabeads Protein A (Invitrogen) was incubated with rotation at 4°C for 30 min with βγ antibody diluted in 200 µL 40 mM HEPES-NaOH, pH 7.5 to a final concentration of 0.06 µg μL^{-1}. After washing the beads three times with buffer and completely removing the supernatant, 100 µL of SnRK1 extract was incubated with the beads under the same conditions. To promote co-immunoprecipitation of SnRK1 and Factor I, 10 µL of T6P to a final concentration of 1 mM (or water) was added to the Dynabeads-antibody-antigen complexes. After 30 seconds the supernatant was separated from the pellet through magnetic force and the pellet was either not washed, gently washed with 200 µL buffer containing 4 mM DTT or thoroughly washed with 200 µL buffer containing 4 mM DTT and 100 mM NaCl. The pellets were always resuspended in 100 µL buffer. Immunoprecipitate and supernatants were assayed for SnRK1 activity and inhibition by T6P as described in Chapter II.

3.5.7. Denaturing electrophoresis

Proteins were separated in precast 4-12% Bis-Tris polyacrylamide gels (NuPAGE® Novex® 4-12% Bis-Tris Gels, Life Technologies) under denaturing and reducing conditions. Protein solutions of known concentration (determined by Bradford method described in Chapter II) were prepared as indicated in the manufacturer's instructions: sample plus NuPAGE gel loading buffer plus reducing agent, in a proportion to obtain 15 µg of protein per 15 µl of prepared sample. The samples were then heated to 70°C for 10 min and 15 µl were loaded onto the gels. Electrophoresis was carried out at 200V for 50 min.

3.5.8. Gels staining

Brilliant Blue G-Colloidal Stain

The gels were kept at room temperature under gentle shaking. The proteins were fixed in gel for 30 min with a solution of 7% glacial acetic acid in 40% (v/v) methanol. The staining working solution was as indicated by the manufacturer: 800 ml of deionized water was added to the Brilliant Blue G-Colloidal Concentrate (Sigma) and mixed by inversion; the volume needed for the day was prepared as 4 parts of the working solution and 1 part methanol mixed well by vortexing. The gels were stained for 1-2 h and then destained for up to 60 sec with 10% acetic acid in 25% (v/v) methanol. The gels were rinsed with 25% methanol and kept destaining for more 24 h.

Rapid Silver Stain

The proteins were fixed in gel for 30 min with a solution containing 100 mL ethanol, 25 mL acetic acid and deionized water to a final volume of 250 mL. After several washes the gel was then sensitised for 30 min with a solution containing ethanol (75 mL), sodium thiosulphate (10 mL from a 5% w/v solution), sodium acetate (17 g) and deionized water to 250 mL. The silver reaction was initiated after 3 water washes of 5 min with a silver nitrate solution (0.25% w/v) for 20 min. Two quick washes of 1 min precede the developing step with a solution of 0.24 M sodium carbonate, 0.05 mL of formaldehyde (37% w/v) and deionized water to 250 mL that lasts until enough signal is obtained. The reaction is stopped with 0.04 M ethylenediaminetetraacetic acid disodium salt dihydrate.

3.5.9. Protein identification by MS/MS

The protein bands of interest were excised from the gels, cut into $1mm^3$ gel plugs, rinsed in deionized water for 20 min and then destained with 50 µl of 50% (v/v) acetonitrile at 37ºC for 30 min. Protein disulphide bonds were broken by reduction

with 10 mM DTT in 100 mM ammonium bicarbonate for 45 min at 56ºC with agitation. Excess liquid was removed and to prevent the reformation of disulphide bonds alkylation was performed with 55 mM of iodoacetamide in 100 mM ammonium bicarbonate for 30 min at room temperature in the dark. The gel pieces were washed with 100% acetonitrile first for 5 min and then for 30 min with agitation and finally dried until digestion. For in gel-digestion, gel pieces were rehydrated in buffer containing 50 mM ammonium bicarbonate and 6.7 ng μl^{-1} trypsin for 30 min at 4ºC. Trypsin cleaves at arginine R-X and lysine (K-X, except when X is proline) and typically generates peptides in the mass range of 800-2500 Da ideal for MALDI MS and LC-ESI-MS. After removing excess liquid that was not absorbed, 20 µl of the same buffer without trypsin was added and incubated overnight at 37ºC. The tryptic digest was acidified with an equal volume of formic acid 5%, desalted and concentrated with C18 microcolumns (POROS R2 from Applied Biosystems). Samples were eluted onto MALDI plates (Applied Biosystems).

Protein identification was done by MALDI-TOF/TOF analysis (4800 *plus* MALDI-TOF/TOF, Applied Biosystems) in both MS and MS/MS modes. MS experiments were performed in positive reflectron mode for monoisotopic peptide mass determination over the *m/z* range of 800–4000 Da. Each MS spectrum was obtained with a total of 1000 laser shots per spectra at a fixed intensity of 3500 V. The mass spectrometer was externally calibrated using the 4700 Calibration Mix (Applied Biosystems). The ten best precursors from each MS spectrum were selected for MS/MS analysis, the weakest precursors being fragmented first. MS/MS analyses were performed using Collision Induced Dissociation assisted with air, with energy of 1 kV and a gas pressure of 1×10^6 torr. Two thousand laser shots were collected for each MS/MS spectrum using a fixed laser intensity of 4500 V. Raw data were generated by the 4000 Series Explorer Software v3.0 RC1 (Applied Biosystems) and all contaminant *m/z* peaks originating from trypsin autodigestion were excluded from the analysis.

The generated mass spectra were used to search the NCBI protein database (minimum score >84). Proteins were identified by the GPS explorer

(Applied Biosystem) with the Mascot search engine (MOWSE algorithm, Version 2.3.2, Matrix-Science, Boston, MA, USA) in combined search mode using MS and MS/MS data and the following search parameters: 1) carboxyamidomethylation of cysteine, methionine oxidation and conversion of N-terminal glutamate to pyroglutamate were considered as variable modifications; 2) tolerance of two missed cleavages; 3) maximum error tolerance of 50 ppm for MS data and 0.3 Da for the MS/MS data. Protein identifications were only accepted when significant protein homology scores were obtained ($p<0.05$) and at least one peptide was fragmented with a significant individual ion score ($p<0.05$).

Acknowledgements

I, Cátia Nunes, performed and analysed the presented experimental work with the following collaborations: Dr. Ana Varela Coelho, head of the Mass Spectrometry Laboratory, ITQB, allowed for the protein identification by MS/MS performed by Dr. Renata Soares and to whom I am deeply grateful. The planning of the research work and discussion of results was done by Cátia Nunes, Dr. Lucia Primavesi and Dr. Matthew Paul.

3.6. References

Almeida AM, Villalobos E, Araújo SS, Leyman B, van Dijck P, Alfaro-Cardoso L, Fevereiro PS, Torné JM, Santos DM (2005) Transformation of tobacco with an *Arabidopsis thaliana* gene involved in trehalose biosynthesis increases tolerance to several abiotic stresses. Euphytica **146**:165–176

Avonce N, Mendoza-vargas A, Morett E, Iturriaga G (2006) Insights on the evolution of trehalose biosynthesis. BMC Evol Biol **6**: 109

Blázquez MA, Santos E, Flores CL, Martínez-Zapater JM, Salinas J, Gancedo C (1998) Isolation and molecular characterization of the Arabidopsis TPS1 gene, encoding trehalose-6-phosphate synthase. Plant J **13**: 685–689

Bonini BM, Van Dijck P, Thevelein JM (2003) Uncoupling of the glucose growth defect and the deregulation of glycolysis in *Saccharomyces cerevisiae Tps1* mutants expressing trehalose-6-phosphate-insensitive hexokinase from. *Schizosaccharomyces pombe*. Biochim Biophys Acta **1606**: 83–93

Bouly J-P, Gissot L, Lessard P, Kreis M, Thomas M (1999) *Arabidopsis thaliana* proteins related to the yeast SIP and SNF4 interact with AKINa1, an SNF1-like protein kinase. Plant J **18**: 541-550

Buitink J, Thomas M, Gissot L, Leprince O (2003) Starvation, osmotic stress and desiccation tolerance lead to expression of different genes of the regulatory β and γ subunits of the SnRK1 complex in germinating seeds of *Medicago truncatula.* Plant Cell Environ **27**: 55–67

Cabib E, Leloir LF (1958) The biosynthesis of trehalose phosphate. J Biol Chem **231**: 259-275

Contento AL, Kim SJ, Bassham DC (2004) Transcriptome profiling of the response of Arabidopsis suspension culture cells to sucrose starvation. Plant Physiol **135**: 2330-2347

Davies SP, Hawley SA, Woods A, Carling D, Haystead TAJ, Hard DG (1994) Purification of the AMP-activated protein kinase on ATP- y-Sepharose and analysis of its subunit structure. Eur J Biochem **223**: 351-357

Debast S, Nunes-Nesi A, Hajirezaei MR, Hofmann J, Sonnewald U, Fernie AR, Börnke F (2011) Altering trehalose-6-phosphate content in transgenic potato tubers affects tuber growth and alters responsiveness to hormones during sprouting. Plant Physiol **156**: 1754–1771

Delatte TL, Sedijani P, Kondou Y, Matsui M, Jong GJ, Somsen GW, Wiese Klinkenberg A, Primavesi LF, Paul MJ, Schluepmann H (2011) Growth arrest by trehalose-6-phosphate: an astonishing case of primary metabolite control over growth by way of the SnRK1 signaling pathway. Plant Physiol **157**: 160–174

Eastmond PJ, van Dijken AJ, Spielman M, Kerr A, Tissier AF, Dickinson HG, Jones JD, Smeekens SC, Graham IA (2002) Trehalose-6-phosphate synthase 1, which catalyses the first step in trehalose synthesis, is essential for Arabidopsis embryo maturation. Plant J **29**: 225-235

Ferrer J-L, Ravanel S, Robert M, Dumas R (2004) Crystal Structures of Cobalamin-independent Methionine Synthase Complexed with Zinc, Homocysteine, and Methyltetrahydrofolate. J Biol Chem 279: 44235-44238

Fragoso S, Espíndola L, Páez-Valencia J, Gamboa A, Camacho Y, Martínez-Barajas E, Coello P (2009) SnRK1 isoforms AKIN10 and AKIN11 are differentially regulated in Arabidopsis plants under phosphate starvation. Plant Physiol **149**: 1906-1916

Gissot L, Polge C, Jossier M, Girin T, Bouly J-P, Kreis M (2006) AKINβγ contributes to SnRK1 heterotrimeric complexes and interacts with two proteins implicated in plant pathogen resistance through its KIS/GBD sequence. Plant Physiol **142**: 931-944

Guo Y, Xiong L, Ishitani M, Zhu J-K (2002) An Arabidopsis mutation in translation elongation factor 2 causes superinduction of CBFDREB1 transcription factor genes but blocks the induction of their downstream targets under low temperatures. PNAS 99: 7786–7791

Hardie DG (2007) AMP-activated ⁄ SNF1 protein kinases: conserved guardians of cellular energy. Nat Rev **8:** 774–785

Hey S, Mayerhofer H, Halford NG, Dickinson JR (2007) DNA sequences from Arabidopsis, which encode protein kinases and function as upstream regulators of Snf1 in yeast. J Biol Chem **282**: 10472-10479

Itani SI, Saha AK, Kurowski TG, Coffin HR, Tornheim K, Ruderman NB (2003) Glucose autoregulates its uptake in skeletal muscle: involvement of AMP-activated protein kinase. Diabetes **52**: 1635-1640

Kabashima T, Kawaguchi T, Wadzinski BE, Uyeda K (2003) Xylulose 5-phosphate mediates glucose-induced lipogenesis by xylulose 5-phosphate-activated protein phosphatase in rat liver. PNAS **100**: 5107-5112

Kulik A, Wawer I, Krzywińska E, Bucholc M, Dobrowolska G (2011) SnRK2 Protein Kinases - Key Regulators of Plant Response to Abiotic Stresses. OMICS: J Integr Biol 15: 859-872

Lee JH, Terzaghi W, Gusmaroli G, Charron JB, Yoon HJ, Chen H, He YJ, Xiong Y, Deng XW (2008) Characterization of Arabidopsis and rice DWD proteins and their roles as substrate receptors for CUL4-RING E3 ubiquitin ligases. Plant Cell **20**: 152-167

Leyman B, van Dijck P, Thevelein JM (2001) An unexpected plethora of trehalose biosynthesis genes in *Arabidopsis thaliana*. Trends Plant Sci **6**: 510-13

Lunn JE, Feil R, Hendriks JHM, Gibon Y, Morcuende R, Osuna D, Scheible WR, Carillo P, Hajirezaei M-R, Stitt M (2006) Sugar-induced increases in trehalose 6-phosphate are correlated with redox activation of ADP-glucose pyrophosphorylase and higher rates of starch synthesis in *Arabidopsis thaliana*. Biochem J **397**: 139-148

Martínez-Barajas E, Delatte T, Schluepmann H, de Jong GJ, Somsen GW, Nunes C, Primavesi LF, Coello P, Mitchell RAC, Paul MJ (2011) Wheat grain development is characterized by remarkable trehalose 6-phosphate accumulation pregrain filling: tissue distribution and relationship to SNF1-related protein kinase1 activity. Plant Physiol **156**: 373–381

McMichael RW Jr, Kochansky J, Klein RR, Huber SC (1995) Characterization of the substrate specificity of sucrose-phosphate synthase protein kinase. Arch Biochem Biophys **321:** 71–75

Nikiforova VJ, Kopka J, Tolstikov V, Fiehn O, Hopkins L, Hawkesford MJ, Hesse H, Hoefgen R (2005) Systems Rebalancing of Metabolism in Response to Sulfur

Deprivation, as Revealed by Metabolome Analysis of Arabidopsis Plants. Plant Physiol 138: 304–318

Paul MJ, Primavesi LF, Jhurrea D, Zhang Y (2008) Trehalose metabolism and signaling. Annu Rev Plant Biol **59**: 417-441

Pierre M, Traverso JA, Boisson B, Domenichini S, Bouchez D, Giglione C, Meinnela T (2007) N-Myristoylation Regulates the SnRK1 Pathway in Arabidopsis. Plant Cell **19**: 2804-2821

Polge C, Thomas M (2007) SNF1/AMPK/SnRK1 kinases, global regulators at the heart of energy control? Trends Plant Sci **12**: 20–28

Radchuk R, Radchuk V, Weschke W, Borisjuk L, Weber H (2006) Repressing the expression of the sucrose nonfermenting-1-related protein kinase gene in pea embryo causes pleiotropic defects of maturation similar to an abscisic acid-insensitive phenotype. Plant Physiol **140**: 263–278

Ramon M, de Smet I, Vandensteene L, Naudts M, Leyman B, van Dijck P, Rolland P, Beeckman T, Thevelein JM (2009) Extensive expression regulation and lack of heterologous enzymatic activity of the class II trehalsoe metabolism proteins from *Arabidopsis thaliana*. Plant Cell Environ **32**: 1015-1032

Rodrigues A, Adamo M, Crozet P, Margalha L, Confraria A, Martinho C, Elias A, Rabissi A, Lumbreras V, González-Guzmán M, Antoni R, Rodriguez PL, Baena-González E (2013) ABI1 and PP2CA Phosphatases Are Negative Regulators of Snf1-Related Protein Kinase1 Signaling in Arabidopsis. Plant Cell **25**: 3871-3884

Schluepmann H, van Dijken A, Aghdasi M, Wobbes B, Paul M, Smeekens S (2004) Trehalose mediated growth inhibition of Arabidopsis seedlings is due to trehalose-6-phosphate accumulation. Plant Physiol **135**: 1-12

Shen W, Hanley-Bowdoin L (2006) Geminivirus infection up-regulates the expression of two Arabidopsis protein kinases related to yeast SNF1- and mammalian AMPK-activating kinases. Plant Physiol **142**: 1642–1655

Sugden C, Crawford RM, Halford NG, Hardie DG (1999) Regulation of spinach SNF1-related (SnRK1) kinases by protein kinases and phosphatases is associated with phosphorylation of the T loop and is regulated by 5'-AMP. Plant J **19**: 433-439

Sugden C, Donaghy PG, Halford NG, Hardie DG (1999) Two SNF1-related kinases from spinach leaf phosphorylate and inactivate 3-hydroxy-3-methylglutaryl-coenzyme A reductase, nitrate reductase, and sucrose phosphate synthase in vitro. Plant Physiol **120:** 257–274

Tabidi I, Saggerson D (2012) Inactivation of the AMP-activated protein kinase by glucose in cardiac myocytes: a role for the pentose phosphate pathway. Biosci Rep **32**: 229-239

Taurog RE, Matthews RG (2006) Activation of methyltetrahydrofolate by cobalamin-independent methionine synthase. Biochemistry 45: 5092-102

Toroser D, Plaut Z, Huber SC (2000) Regulation of a plant SNF1-related protein kinase by glucose 6-phosphate. Plant Physiol **123**: 403-411

Vandesteene L, López-Galvis L, Vanneste K, Feil R, Maere S, Lammens W, Rolland F, Lunn JE, Avonce N, Beeckman T, van Dijck P (2012) Expansive evolution of the trehalose-6-phosphate phosphatase gene family in Arabidopsis. Plant Physiol **160**: 884–896

Vandesteene L, Ramon M, Le Roy K, van Dijck P, Rolland F (2010) A single active Trehalose-6-P Synthase (TPS) and a family of putative regulatory TPS-like proteins in Arabidopsis. Mol Plant **3**: 406–419

Vogel G, Aeschbacher RA, Muller J, Boller T, Wiemken A (1998) Trehalose 6-phosphate phosphatases from *Arabidopsis thaliana*: identification by functional complementation of the yeast tps2 mutant. Plant J **13**: 673-683

Wang R, Okamoto M, Xing X, Crawford NM (2003) Microarray analysis of the nitrate response in Arabidopsis roots and shoots reveals over 1,000 rapidly responding genes and new linkages to glucose, trehalose-6-phosphate, iron, and sulfate metabolism. Plant Physiol **132:** 556-567

Wilson RA, Jenkinson JM, Gibson RP, Littlechild JA, Wang ZY, Talbot NJ (2007) Tps1 regulates the pentose phosphate pathway, nitrogen metabolism and fungal virulence. EMBO J **26**: 3673–3685

Zhang Y, Primavesi LF, Jhurreea D, Andralojc J, Mitchell RAC, PowersSJ, Schluepmann H, Delatte T, Wingler A, Paul MJ (2009) Inhibition of Snf1-related protein kinase (SnRK1) activity and regulation of metabolic pathways by trehalose 6-phosphate. Plant Physiol **149**: 1860–1871

Zimmermann P, Hirsch-Hoffmann M, Hennig L, Gruissem W (2004) GENEVESTIGATOR. Arabidopsis microarray database and analysis toolbox. Plant Physiol **136**: 2621-2632

CHAPTER IV

In wheat grain, SnRK1 inhibition by T6P may be tissue-specific whereas inhibition by R5P is only apparent

The work presented in this chapter was mostly performed by Cátia Nunes (see acknowledgments section) and partially included in the following publication:

Martínez-Barajas E, Delatte T, Schluepmann H, de Jong GJ, Somsen GW, **Nunes C**, Primavesi LF, Coello P, Mitchell RAC, Paul MJ **(2011)** Wheat grain development is characterized by remarkable trehalose 6-phosphate accumulation pregrain filling: tissue distribution and relationship to SNF1-related protein kinase1 activity. **Plant Physiology** 156: 373–381

4.1. Abstract

SnRK1 is also known to be important during seed development and germination. Trehalose 6-phosphate (T6P) is a sugar signal that inhibits SnRK1 which also affects seed growth and development. *In vivo* inhibition of SnRK1 by T6P was confirmed through profiling of SnRK1 target genes in Arabidopsis, potato and wheat grain. It was recently reported that ribose 5-phosphate (R5P) also inhibits wheat grain SnRK1 *in vitro* and suggested that this inhibition fits very well with the known involvement of SnRK1 in anabolism repression. To investigate the roles of T6P and R5P in wheat grain development, SnRK1 activity and inhibition was tested in maternal and filial tissues dissected at different developmental stages. *In vitro* SnRK1 activity varies little in all tissues both pre- and during grain filling (7 and 17 days after anthesis (DAA) respectively) in contrast to large changes in tissue distribution of T6P. At 7 DAA T6P was 49 to 119 nmol g^{-1} FW in filial and maternal tissues sufficient to inhibit SnRK1; at 17 DAA T6P accumulation was almost exclusively endospermal (43 nmol g-1 FW) with 0.6 to 0.8 nmol T6P g^{-1} FW in embryo and pericarp. The data show that T6P levels are detached from sucrose levels in the grain filling period (except for endosperm) and high T6P levels during pregrain filling suggest that T6P may be necessary for the early development of all grain tissues but not so in later stages. The apparent inhibition of SnRK1 activity by R5P can be explained through the depletion of ATP due to conversion to ribulose 5-phosphate (Ru5P) and then to ATP-dependent ribulose-1,5-bisphosphate (RuBP) formation. The enzymes that catalyze these reactions, phosphoribose-isomerase (PRI) and phosphoribulo-kinase (PRK) are very active in green plant extracts. In accordance, a 94% decrease of PRK activity in transgenic plants substantially reduced the apparent inhibition of SnRK1 by R5P and Ru5P. We concluded that inhibition of SnRK1 by R5P in wheat grain preparations is an experimental artefact that occurs only in the presence of green pericarp tissue and that, on the contrary, T6P could underlie the shift in gene expression in maternal and filial tissues observed at about 10 DAA.

4.2. Introduction

The trehalose pathway is ubiquitous in plants and it is known to be an indispensable component of seed development (Eastmond *et al.*, 2002) and vegetative development and transition to flowering (Van Dijken *et al.*, 2004) with the precursor T6P shown as the critical factor (Schluepmann *et al.*, 2003).

A signaling partner of T6P in growing tissues is SnRK1, of the SNF1/ AMPK group of PKs (Zhang *et al.*, 2009; Paul *et al.*, 2010). These kinases perform a fundamental role in the physiological response of cells to energy limitation and starvation of carbon source through regulation of processes (Hardie, 2007; Polge and Thomas, 2007; Halford and Hey, 2009) and gene expression (Baena-González *et al.*, 2007) involved in metabolism, growth and development. In growing tissues inhibition of SnRK1 by T6P is a mechanism of switching from catabolism to anabolism by activation of biosynthetic processes by T6P in response to Suc supply (Zhang *et al.*, 2009; Paul *et al.*, 2010). *In vitro* evidence suggests that other sugar-phosphates like G6P (Toroser *et al.*, 2000) and G1P (Chapter II) could also constitute a means of SnRK1 regulation. Moreover, it was recently reported that R5P inhibits SnRK1 from wheat grain (Piattoni *et al.*, 2011), an effect shown in partially purified SnRK1 (112x) from spinach leaves (Toroser *et al.*, 2000) and to be only apparent in crude Arabidopsis seedlings protein extract (Chapter II). However, unlike for T6P, there is still no *in vivo* evidence to support the physiological relevance of any of these interactions.

Wheat (*Triticum aestivum*) is the dominant crop in temperate countries and is the most widely grown of the major crops worldwide. There is evidence that wheat yields have reached a plateau http://energyfarms.wordpress.com/2009/09/03/crop-yield-projections-miss-biofuel-reporttarget/ and that to improve yields beyond this ceiling requires new insight and approaches. One means of doing this is to identify new regulatory processes as targets for manipulation, as that of SnRK1 metabolic regulation. The trehalose pathway is present in cereals as in all other plants. An interesting case is that of a maize TPP knockout mutant with affected inflorescence branching (ramosa3) (Satoh-Nagasawa *et al.*, 2006). Of the little that has been

documented on the trehalose pathway in wheat, active enzymes are present in roots and shoots (El-Bashiti *et al.*, 2005) and TPS and TPP transcripts were found in roots (Mohammadi *et al.*, 2007) and wheat grain (Weichert *et al.*, 2010). In cereals, studies from cDNA from rye endosperm resulted in the isolation of the first plant SnRK1 through complementation of a yeast snf1 mutant (Alderson *et al.*, 1991). SnRK1 of barley is thought to regulate storage product accumulation during grain filling (Sreenivasulu *et al.*, 2006). In rice and wheat SnRK1 enables seeds to respond to anoxic and starvation conditions (Laurie *et al.*, 2003; Lee *et al.*, 2009). Interestingly, it has been proposed that SnRK1 mediates responses to sugar signals required for early cotyledon establishment and patterning (Radchuk *et al.*, 2010). Radchuk *et al.* (2010) presented the first T6P measurements in a seed tissue in the embryos of pea. The significance of these data relative to the regulation of SnRK1 is not known, however. No combined analysis of T6P and SnRK1 has yet been performed in the seed of any major crop.

The recent report that R5P also inhibits wheat grain SnRK1 (Piattoni *et al.*, 2011) provides a potential means of regulating SnRK1 in response to availability of substrates of the oxidative pentose phosphate cycle (involved in the generation of NADPH) and the Calvin cycle (both related to biosynthetic processes) fitting well with the model that SnRK1 activity normally represses anabolism. However, as suggested in Chapter II, the presence of competing kinases in the *in vitro* assay could produce an underestimate of the activity of the enzyme under study. R5P is a substrate for PRI and PRK which activities are several thousand fold higher than activities of SnRK1 in tissues with active photosynthetic cells (Paul *et al.*, 2000; Zhang *et al.*, 2009). Even in developing wheat grain, rates of photosynthesis exceed rates of respiration (Caley *et al.*, 1990). These authors found peak photosynthetic activity at 20 days after anthesis (DAA) coinciding with maximum chlorophyll content in the inner green pericarp.

Here we measure T6P content and SnRK1 activities at two distinct phases of wheat grain development and assessed the effectiveness of R5P as an inhibitor of wheat grain SnRK1. Wheat grain consists largely of endosperm, embryo and

maternal pericarp tissue which go through phases of development defined by events in the endosperm. Three phases are typically defined as a pre-grain filling phase for the first 10 days or so after anthesis when cell division, expansion and differentiation give the characteristic structure of the endosperm before the storage or grain filling stage. The transition to the grain filling stage is marked by dramatic transcriptional and physiological changes (Wan *et al.*, 2008). It is thought that sugars and sugar signals play a role in this transition and in seed maturation, at least in legume seeds (Weber *et al.*, 2005). The desiccation phase then follows beyond 30 DAA.

Grain was dissected into filial and maternal tissues at 7 DAA and 17 DAA well into each of the two first periods to better understand the role of T6P. Unprecedented levels of T6P were found both in filial and maternal tissue pre-grain filling, sufficient to inhibit SnRK1, but during grain filling high T6P concentrations became limited to the endosperm. *In vitro* SnRK1 activity was strongly inhibited by T6P. As evidence that regulation of SnRK1 by T6P could operate *in vivo*, homologs of SnRK1 marker genes designated in Arabidopsis (Baena-Gonzalez *et al.*, 2007), identified in wheat using WhETS (Mitchell *et al.*, 2007) showed a shift in patterns of expression during the pre-grain filling period compared to the grain-filling period consistent with changes in T6P content. We have also found that in extracts of developing wheat grain (as that of Arabidopsis seedlings), where SnRK1 was assayed in the presence of R5P, a significant consumption of ATP, resulting from the conversion of R5P to ribulose-1,5-bisphosphate (RuBP). The apparent inhibition of SnRK1 by R5P (and Ru5P) can be explained by the competing action of PRK for ATP. Data provided the first clues about tissue-specific regulation of SnRK1 by T6P in wheat grain which can launch a new grain yield improvement approach and exposes an important caveat in the assessment of potential PKs inhibitors and concomitant conclusions.

4.3. Results

4.3.1. Analysis of T6P, SnRK1 activity and Suc in dissected wheat grain

Grain tissue was separated into filial and maternal tissue. At 7 DAA pre-grain filling T6P concentrations were high in both filial tissue (endosperm, 119 nmol g^{-1} FW) and maternal tissue (outer pericarp, 49 nmol g^{-1} FW and inner chlorophyll containing pericarp, 117 nmol g^{-1} FW) (Table 4.1). In contrast, at 17 DAA during grain filling T6P was largely restricted to the endosperm (43 nmol g^{-1} FW) with small amounts in the pericarp and embryo (0.6-0.8 nmol g^{-1} FW). In contrast to the marked changes in T6P SnRK1 activities *in vitro* were similar at both 7 DAA and 17 DAA (Table 4.2). Activities in maternal tissue decreased from 7 DAA to 17 DAA; whereas in endosperm SnRK1 activities were stable and embryo had the highest activities of all tissues at 17 DAA. SnRK1 activity in all tissues was inhibited *in vitro* by 1 mM T6P, although outer pericarp SnRK1 was only little affected by T6P at 17 DAA (Table 4.2). Suc was present in maternal and filial tissues pre-grain filling and during grain filling (Table 4.3), with 49 to 105 µmol g^{-1} FW at 7 DAA compared to 22 to 64 µmol g^{-1} FW at 17 DAA.

Table 4.1. T6P levels in dissected maternal and filial grain tissues at 7 DAA compared to 17 DAA.

Data are expressed as nmol g^{-1} FW with standard error of mean of four replicates. ND, not determined

	7 DAA	17 DAA
Maternal tissue		
Outer pericarp (white)	49 ± 9.0	0.8 ± 0.4
Inner pericarp (green)	117 ± 8.1	0.7 ± 0.5
Filial tissue		
Endosperm	119 ± 15	43 ± 4.2
Embryo	ND	0.6 ± 0.03

Table 4.2. SnRK1 activity in dissected maternal and filial grain tissues at 7 DAA compared to 17 DAA.

Data are expressed as nmol min^{-1} mg^{-1} protein with standard error of mean of three replicates. Percentage inhibition with inclusion of 1 mM T6P in the assay in parentheses. ND, not determined

	7 DAA	17 DAA
Maternal tissue		
Outer pericarp (white)	3.7 ± 0.3 (60%)	1.1 ± 0.1 (17 %)
Inner pericarp (green)	3.6 ± 0.4 (59%)	2.1 ± 0.2 (42%)
Filial tissue		
Endosperm	3.2 ± 0.5 (65%)	3.2 ± 0.5 (43%)
Embryo	ND	4.5 ± 0.6 (47%)

Table 4.3. Sucrose in dissected maternal and filial grain tissues at 7 DAA compared to 17 DAA.

Data are expressed as µmol g^{-1} FW with standard error of mean of four replicates. ND, not determined

	7 DAA	17 DAA
Maternal tissue		
Outer pericarp (white)	49 ± 3.2	22 ± 2.3
Inner pericarp (green)	105 ± 6.5	64 ± 3.4
Filial tissue		
Endosperm	74 ± 4.1	23 ± 1.9
Embryo	ND	41 ± 2.0

4.3.2. Apparent inhibition of SnRK1 extracts by R5P and Ru5P

Inhibition of SnRK1 activity by R5P and Ru5P was the most variable of all metabolites tested. Very strong inhibition was observed in seedlings, mature leaves and wheat grain, but no inhibition was found in seedling roots or cauliflower curd (see Chapter 2, Fig. 2.2). In further characterisation it was observed that the percentage inhibition by R5P and Ru5P increased progressively with time over 6 min (Fig. 4.1A). Hence there was the possibility that factors other than direct inhibition of SnRK1 by R5P and Ru5P were operating to limit the activity of SnRK1, such as substrate

limitation. To test this hypothesis we tested the effect of ATP concentration and found that inhibition of SnRK1 by R5P was much decreased in the presence of 2 mM and completely abolished at 10 mM ATP compared to 0.2 mM ATP (Fig. 4.1B), in contrast to the established inhibitors T6P and G6P which are unaffected by ATP content (Toroser *et al.*, 2000; Zhang *et al.*, 2009). In further confirmation we went on to monitor substrate ATP during the course of the assay period.

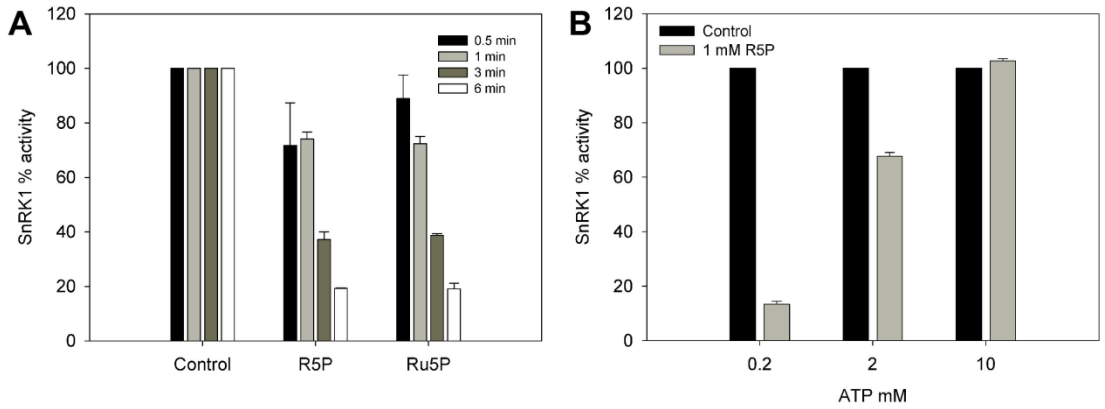

Figure 4.1. Effect of assay time and ATP concentration on whole wheat grain SnRK1 inhibition by 1 mM R5P or 1 mM Ru5P compared to control with no metabolite. (A) extracts prepared with 200 μM ATP assayed over the course of 6 min with R5P or Ru5P **(B)** Effect of increasing ATP concentration on SnRK1 inhibition by R5P. Data are means of three replicates with standard deviation.

4.3.3. Dramatic ATP depletion detected by UV absorbance HPLC during SnRK1 assay in the presence of R5P and Ru5P

ATP concentrations during the assay period were monitored by UV absorbance HPLC to check for large ATP depletion in the presence of R5P or Ru5P. In both Arabidopsis and wheat grain ATP was almost completely consumed over the assay period compared to the control without R5P or Ru5P (Fig. 4.2). Loss of ATP of this magnitude would severely compromise the activity of the PK and could therefore account for an apparent inhibition of SnRK1 activity. These combined data strongly

suggested that ATP was becoming limiting during the assay period when R5P and Ru5P were present. This could be mistakenly interpreted as a time-dependent inhibition of enzyme activity.

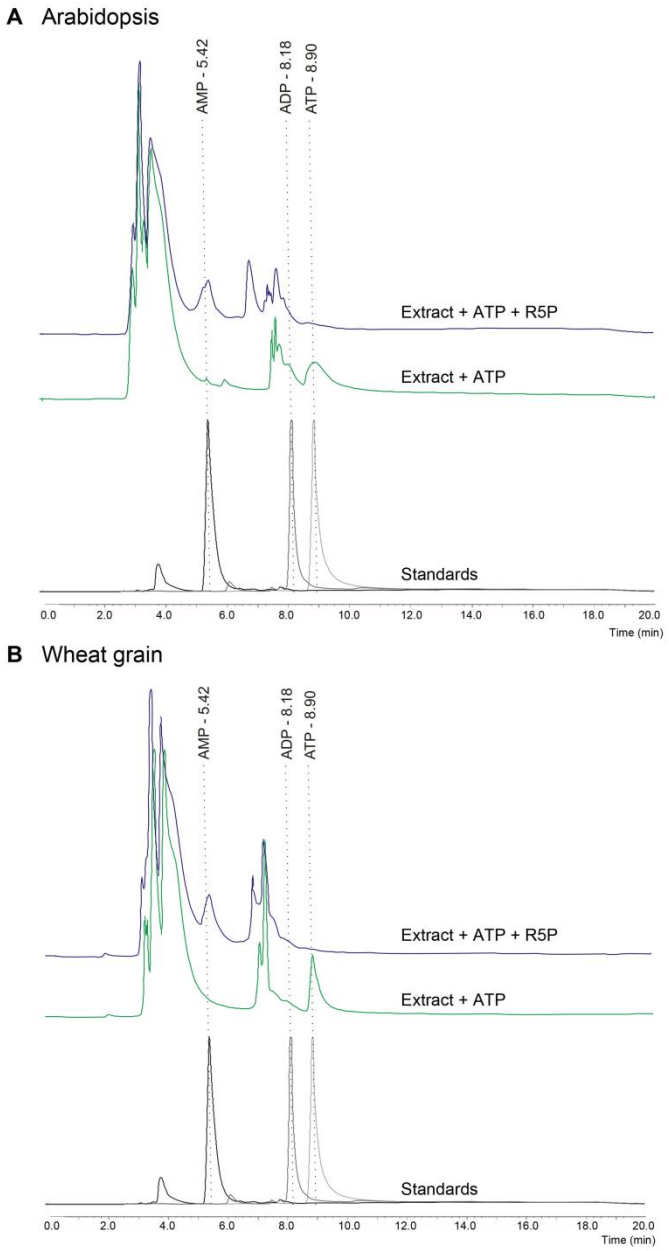

Figure 4.2. Disappearance of ATP and production of AMP during assay of Arabidopsis and wheat grain extracts with 1 mM R5P. (A) Arabidopsis and **(B)** whole wheat grain. HPLC chromatograms of plant extracts after 6 min at 30 °C with and without 1 mM R5P (upper and middle trace). HPLC chromatograms of pure standards of ATP, ADP and AMP showing the expected peak positions (bottom trace).

4.3.4. Formation of RuBP from R5P and Ru5P accompanies loss of ATP

In further analysis by LC-MS we noticed that RuBP formation accompanied the loss of ATP in the presence of R5P (Fig. 4.3A and B). In plants, PRK works together with PRI to catalyze ATP-dependent formation of RuBP from R5P and Ru5P (PRI reversibly converts R5P to Ru5P). To confirm the involvement of PRK in the ATP-dependent formation of RuBP, SnRK1 activity in the presence of R5P and Ru5P was assayed in plantlets of transgenic tobacco expressing antisense to PRK and with a 94% reduction in activity compared to wild type (Paul *et al.*, 2000). Compared to wild type, the inhibition by either metabolite was significantly reduced (Fig. 4.4), showing that inhibition by these metabolites is PRK dependent. PRK is a very active enzyme in green plant tissues (Paul *et al.*, 2000). Even 6% of maximum PRK activity would be in excess of SnRK1 activity and is still capable of sustaining RuBP synthesis sufficient for 50% of the wild type rate of photosynthesis (Paul *et al.*, 2000). In wild type SnRK1 activity was measured as 4.11 nmol/ min/ mg protein compared to 3.72 in the PRK antisense line. PRK activity in these plants has been previously measured as 3000 and 150 nmol/ min/ mg protein, respectively (Paul *et al.*, 2000). Hence, it would not be expected that ATP loss and RuBP formation would be completely abolished when PRK activity is still higher than SnRK1 activity. Accompanying the loss of ATP was the appearance of AMP (Fig. 4.2A and B) commonly observed as an end product in plant tissues (Santarius and Heber, 1965; Keys, 1968).

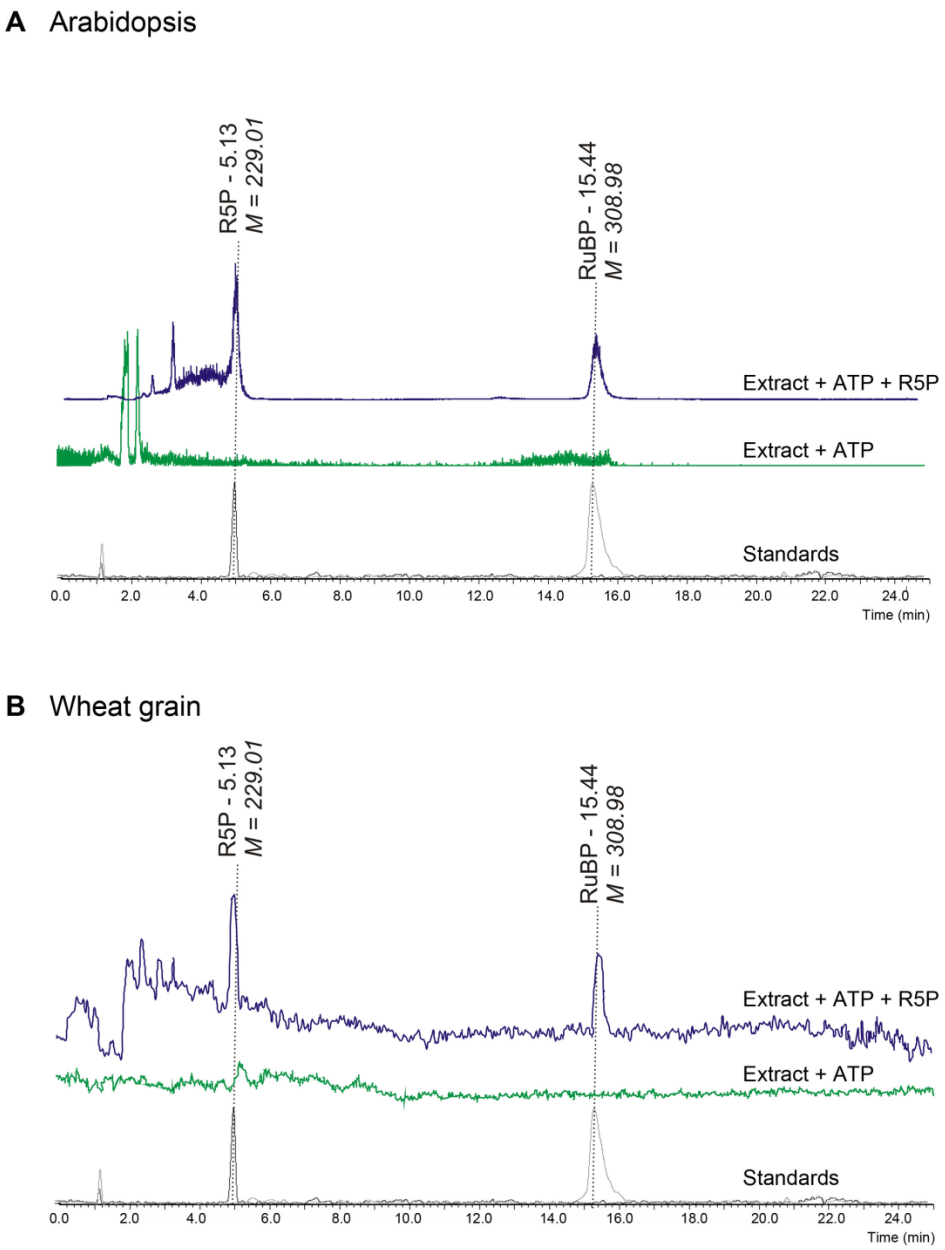

Figure 4.3. Production of RuBP during assay of Arabidopsis and wheat grain extracts with 1 mM R5P. (A) Arabidopsis. **(B)** Whole wheat grain. LC-MS traces of plant extracts after 6 min incubation at 30 °C with and without 1 mM R5P (upper and middle traces). LC-MS traces of pure standards of R5P and RuBP showing the expected peak positions (bottom trace). MS was performed in negative mode with single ion recording at 229.01 and 308.98 Da.

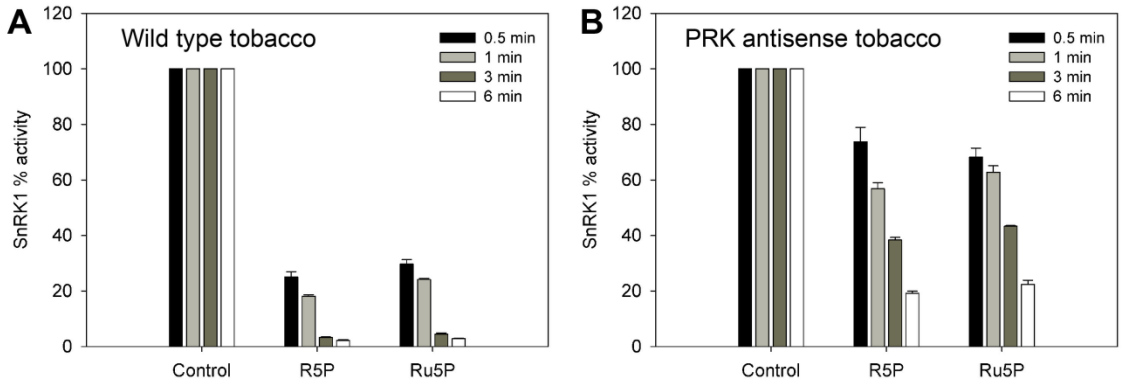

Figure 4.4. Inhibition of SnRK1 by R5P and Ru5P is PRK dependent. SnRK1 activity in the presence of 1 mM R5P or 1 mM Ru5P compared to control with no metabolite. (A) Wild type tobacco. **(B)** PRK antisense transgenic tobacco. Assays conducted over the course of 6 min. Data are means of three replicates with standard deviation.

4.3.5. Wheat grain tissue dissection

Piattoni *et al.* (2011) previously found that R5P inhibited SnRK1 in wheat grain. To examine this further and determine whether this is also associated with green tissue we dissected out endosperm, embryo, outer white pericarp and inner green pericarp from grain tissue. Inhibition of SnRK1 by R5P was found only when green tissue was present in the inner pericarp and where endosperm preparations contained inner pericarp and in whole grain (Fig. 4.5A). No inhibition was found in endosperm or embryo. The small amount of inhibition associated with outer pericarp is because this tissue also has a small amount of green tissue (Fig. 4.6B).

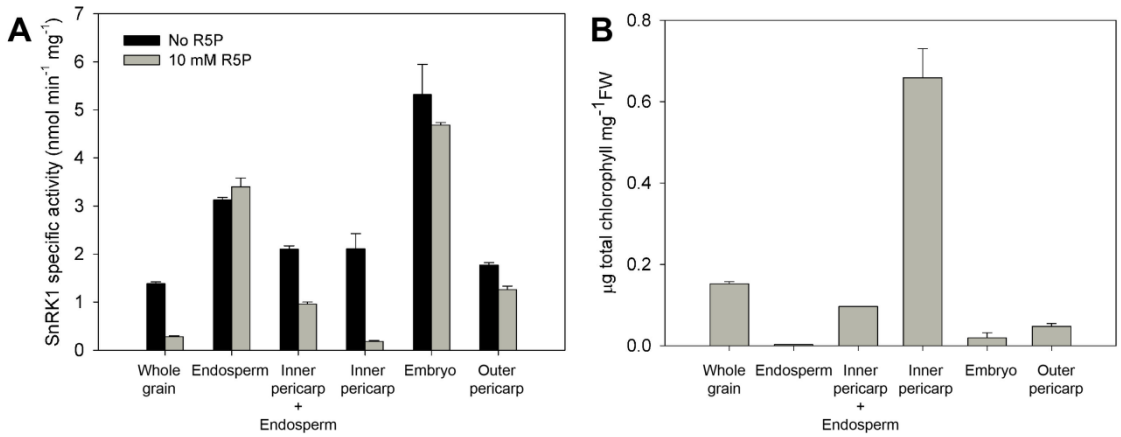

Figure 5.5. Dissected wheat grain assayed for (A) SnRK1 activity with no metabolite (black) and with 10 mM R5P (grey) and **(B)** chlorophyll content. Tissue sampled at 17 DAA. Error bars represent standard deviation of three biological replicates.

4.4. Discussion

During development, seeds undergo cell division, differentiation and maturation, changing from meristem-like tissues to storage organs following a developmental program that deeply alters/ depends on metabolic status (Weber *et al.*, 1997). SnRK1 as a central regulatory protein that manages metabolism according to nutritional, energy and stress conditions has an important role in these early steps of plant development (Radchuk *et al.*, 2006). T6P is an important regulatory molecule in plants which also has a large impact on metabolism, growth and development (Eastmond *et al.*, 2002; Schluepmann *et al.*, 2003; Paul *et al.*, 2008; Smeekens *et al.*, 2009). We recently established a mechanistic basis for the signaling function of T6P in growing tissues through inhibition of SnRK1 (Zhang *et al.*, 2009; Paul *et al.*, 2010). A working model for the function of T6P in Arabidopsis is that it signals Suc availability to regulate SnRK1. In this study we present the first data of T6P measurements in wheat grain showing large tissue specificity of T6P levels at contrasting developmental stages. Also, the impact of other potential inhibitors of

SnRK1 which could exert important physiological effects are understandably eagerly sought. R5P has been recently referred to inhibit wheat grain SnRK1 (Piattoni *et al.*, 2011) and suggested to potentially provide a means of regulating SnRK1 in response to availability of substrates of the oxidative pentose phosphate cycle involved in the generation of NADPH used in biosynthetic processes. However, as an alternative explanation to direct inhibition of SnRK1 by R5P we show that ATP is consumed by R5P-dependent reactions during the assay causing an apparent SnRK1 inhibition.

4.4.1. Tissue-specific regulation of SnRK1 by T6P during wheat grain development

All published data on amounts of T6P in plants are from Arabidopsis seedlings and leaf material with other data from pea embryos (Radchuk *et al.*, 2010). There has been no detailed and comprehensive analysis of T6P in the harvested parts of any major crop such as wheat. Given the important function of T6P in affecting growth processes and the high Suc content of sink tissues such as grain, knowledge of T6P content in such tissues is an important step for crop improvement through modification of the trehalose metabolism or the SnRK1/T6P signaling pathway.

The transition from pre-grain filling to grain filling is characterised by large developmental changes. To gain better insight into the interaction between T6P and SnRK1 over this time T6P levels and SnRK1 activities were measured in filial and maternal grain tissues in dissected grain at 7 DAA and 17 DAA coincident with pre-grain filling and grain filling phases. At 7 DAA T6P levels were high in filial and maternal tissue at concentrations sufficient to inhibit SnRK1 in all tissues (Table I). SnRK1 activity was similar in all these tissues. In marked contrast at 17 DAA high concentrations of T6P were confined to the endosperm with very low amounts in embryos and pericarp. T6P levels in wheat embryos (0.6 nmol g^{-1} FW) are of a similar order to those in pea embryos (2 nmol g^{-1} FW, Radchuk *et al.*, 2010) and more than 70-fold lower than amounts measured in endosperm. SnRK1 was again active in all

tissues, but it is likely that SnRK1 activity in pericarp and embryo is not inhibited by T6P at 17 DAA. To better understand SnRK1 activity *in vivo* in wheat grain we took an approach analogous to that in Zhang *et al.* (2009) for T6P and requested the expression analysis during grain development of genes known to be regulated by SnRK1 (Baena-Gonzalez *et al.*, 2007). Using the WhETS tool (Mitchell *et al.*, 2007) wheat transcripts which correspond most closely to genes induced and repressed by SnRK1 in Arabidopsis were identified and looked in the developing grain transcriptome from Wan *et al.* (2008). SnRK1-induced and SnRK1-repressed marker gene expression changed beyond the pre-grain filling period 10 DAA (Fig. 4.6) indicating inhibition of SnRK1 activity before 10 DAA, but greater SnRK1 activity after 10 DAA coincident with the observed shift in T6P levels from 7 DAA to 17 DAA (Table 4.1). Active SnRK1 is clearly important for embryo development (Radchuk *et al.*, 2010) as is T6P in Arabidopsis embryos (Eastmond *et al.*, 2002). However, T6P may not be sufficiently high to inhibit SnRK1 in embryos and regulation of SnRK1 by T6P may not be a primary function of T6P in this tissue. Interestingly, Suc is still present in all tissues at 17 DAA albeit two- to threefold lower than at 7 DAA (Table III). The exact nature of the interrelationship between T6P, Suc and trehalose pathway gene expression in the determination of the early grain development and yield of endosperm is the subject of further work.

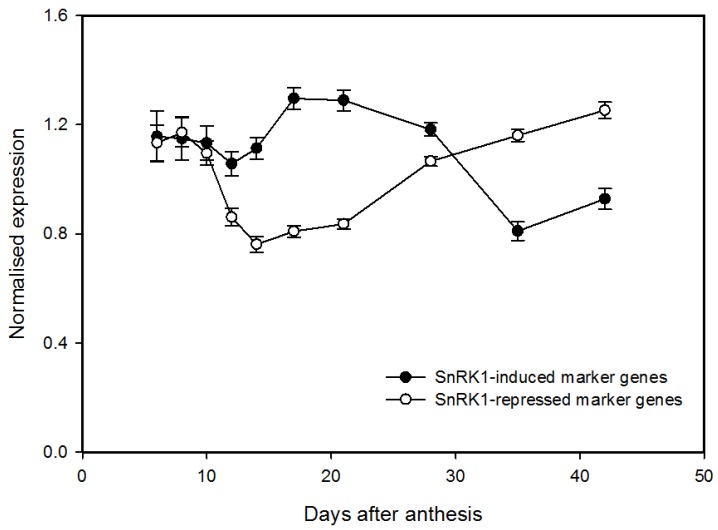

Figure 4.6. SnRK1 target gene transcript abundance. Transcript abundance of wheat Affymetrix probesets corresponding to sets of 600 SnRK1-induced and 600 SnRK1-repressed Arabidopsis genes according to Baena-Gonzalez *et al.* (2007) determined using WhETS tool (Mitchell *et al.*, 2007). Log of normalised expression (i.e. divided by the median expression for that probeset) was averaged and standard error calculated. The resulting averages with standard error are displayed, back-transformed to a linear scale. The 300 most abundantly expressed SnRK1-induced and 300 most abundantly SnRK1-repressed genes are presented.

4.4.2. Dissection of the apparent inhibition of SnRK1 by R5P in wheat grain

Robust methods for the assay of SnRK1 have been developed using γ^{33}P-ATP and peptides such as AMARA, the preferred substrate for this PK (Davies *et al.*, 1989; Weekes *et al.*, 1993; Dale *et al.*, 1995). With careful optimisation of assay conditions, the reaction proceeds linearly over time (Zhang *et al.*, 2009). Kinases are numerous and therefore it is important to ensure that when assessing the effect of compounds on the regulation of SnRK1 that this does not impact on the consumption of ATP by other kinases which will confound accurate estimates of SnRK1 activity and give rise to apparent enzyme inhibition. The inhibition afforded by R5P (Piattoni *et al.*, 2011) was distinct from that of other metabolites in that the activity of SnRK1 was almost completely inhibited at 10 mM R5P, something not observed with T6P or G6P (Toroser *et al.*, 2000; Zhang *et al.*, 2009) although 10 mM is higher than normal physiological concentrations in plants. In work described here we too found a strong apparent inhibition of SnRK1 activity by R5P and also by Ru5P (Fig. 4.1). Inhibition increased over the duration of the 6-min assay period (Fig. 4.1A) suggesting that conditions were not optimised. Inhibition was strongly decreased by supplying higher ATP concentrations (Fig. 4.1B)

Inclusion of R5P combined with ATP in SnRK1 extracts readily results in formation of RuBP with consumption of ATP, hence giving rise to an apparent inhibition of SnRK1 due to loss of ATP (Figs. 5.2 and 5.3). This can be explained through the presence of PRI and PRK required for the synthesis of RuBP, the receptor for CO_2 in photosynthesis. In tissue with active photosynthetic cells, activities

of PRI and PRK are several thousand fold higher than activities of SnRK1 (Paul *et al.*, 2000; Zhang *et al.*, 2009). Even in developing wheat grain rates of photosynthesis exceed rates of respiration (Caley *et al.*, 1990). These authors found peak photosynthetic activity at 20 DAA coinciding with maximum chlorophyll content in the inner green pericarp. Hence apparent inhibition of SnRK1 by R5P in wheat grain can be explained through this mechanism as well as in more obviously photosynthetic tissue such as Arabidopsis seedlings and leaves (as already mentioned in Chapter II). We carefully dissected out endosperm from wheat grain to remove all green tissue and found no inhibition of SnRK1 by R5P or Ru5P in these extracts (Fig. 4.5). Neither was inhibition found for other non-green tissues, such as cauliflower florets and Arabidopsis roots (Table 2.2, Chapter II). In complex tissues such as wheat grain where there is a mix of green and non-photosynthetic tissues the high activities of PRK and PRI from the green cells means that even a small carryover of green tissue into endosperm preparations can give rise to consumption of ATP due to PRI and PRK activities.

To further confirm the involvement of excess activity of PRK in the consumption of ATP in SnRK1 assays when R5P is present, we performed assays prepared from tobacco plantlets expressing antisense to PRK. These plants had a 94% decrease in enzyme activity (Paul *et al.*, 2000). In the presence of both R5P and Ru5P, consumption of ATP and apparent inhibition of SnRK1 were greatly reduced, although not completely abolished (Fig. 4.4). Even a 94% decrease in PRK activity would still leave enough residual PRK activity to consume ATP in the formation of RuBP.

In conclusion, we link T6P and SnRK1 in an important cereal crop and present data for T6P levels in different seed tissues at contrasting developmental stages. Unprecedented levels of T6P are reported for a plant species. The data suggests tissue-specific regulation of SnRK1 by T6P during wheat grain development. Moreover, we show that the promising inhibition of SnRK1 by R5P described by Piattoni *et al.* (2011) can be explained by its conversion to RuBP with concomitant consumption of ATP which subsequently limits the activity of SnRK1

giving an apparent strong inhibition of SnRK1. This highlights an important caveat to be considered in the assay of SnRK1 and other PKs in the presence of potential inhibitors, reinforcing the idea that these interactions should ideally be confirmed not only *in vitro* but also *in vivo*.

4.5. Material and Methods

4.5.1. Biological Material

Wheat var. Cadenza plants were grown in pots of soil containing Rothamsted standard compost mix and full nutrition in a glasshouse during summer with supplementary lighting to give a 16-h photoperiod and day/ night temperature of 18/ 15°C. Samples were taken during the middle of the photoperiod and material was snap frozen immediately in liquid nitrogen, ground in a pestle and mortar and stored at -80ºC until analysis. Ears were tagged at anthesis. Data are means of four biological replicates. Experiments were repeated at least twice and representative data from one experiment are presented. Grain from 7 and 17 DAA were dissected under the growing conditions. Each grain was cut in half through the central groove and separated under a light microscope into maternal and filial tissues (Fig. 4.7). At 7 DAA maternal tissue was separated into an outer white layer here called outer pericarp and the inner green chlorenchyma (chlorophyll-containing layers) of the pericarp. Embryo tissue was too small to dissect at this stage and filial tissue at 7 DAA is just endosperm. At 17 DAA embryo was dissected from the grain. Endosperm consisted mainly of the bulk of starchy endosperm and the aleurone layer. No clear observation was made concerning the fate of nucellar epidermis and integuments because they were too small. The two outermost grains of the eight middle spikelets from an ear were sampled. These were combined together with at least four other similar samples from different ears until enough material had been obtained for one biological replicate of at least 50 mg fresh weight in the case of embryos and at least 100 mg fresh weight in the case of endosperm, outer white pericarp and inner green

pericarp. Chlorophyll was extracted and measured from grain tissue (Porra *et al.*, 1989).

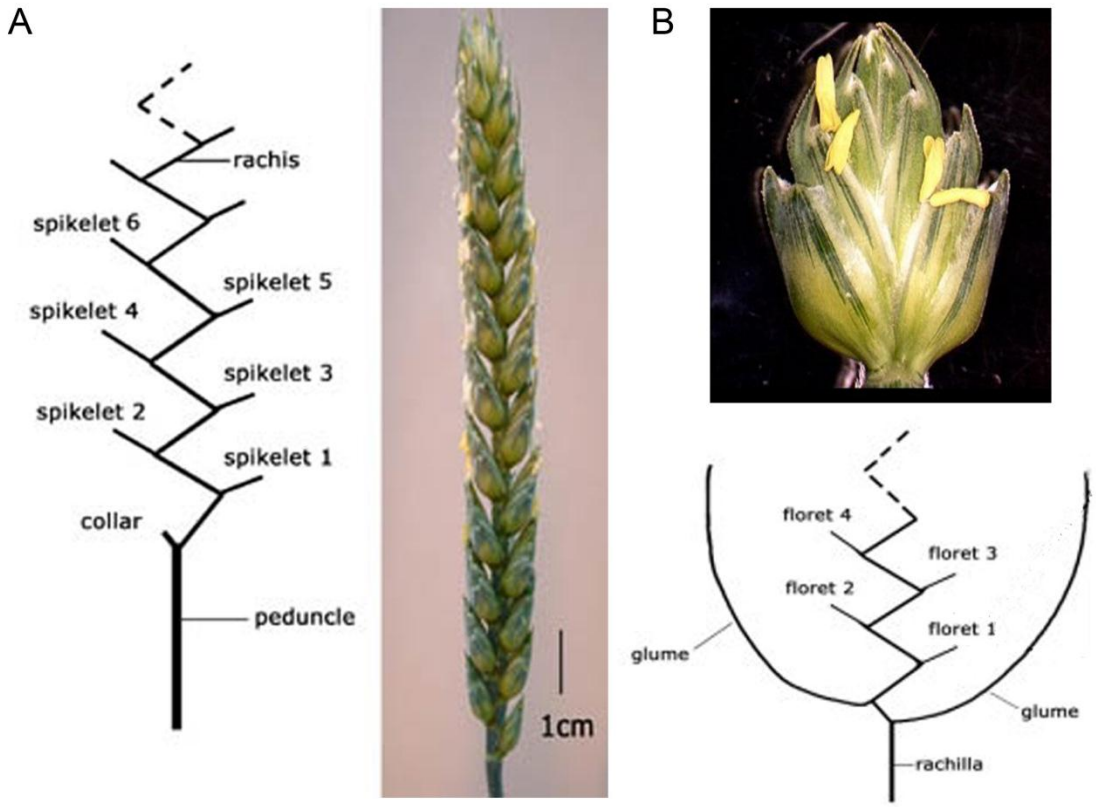

Figure 4.6. Wheat ear and spikelet exemplifications. (A) Wheat ear squeme and photograph showing spikelets arrangement on alternate sides of the rachis. After 7 and 17 DAA the eight middle spikelets from an ear were sampled. **(B)** Wheat spikelet squeme and photograph showing the florets protected by the glumes. Carpels are fertilized by pollen from the same floret after which grain development starts. Only four or five florets are fertile and for sapling only the two outermost grains were used. These were combined together with four other similar samples from different ears constituting one biological replicate. Figures adapted from Wheat, the big picture.

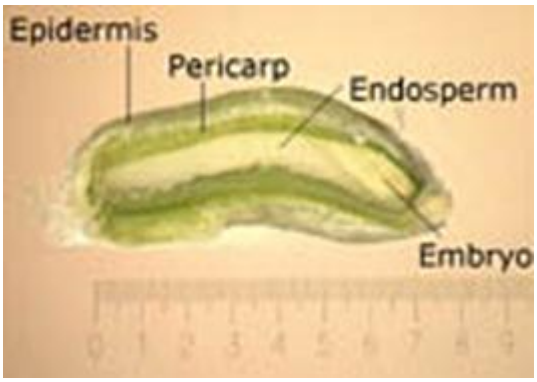

Figure 4.7. Wheat grain longitudinal cut at 17 DAA. During early grain development two maternal tissues are easily identifiable, the outer pericarp or epidermis (white) and the inner pericarp (green) enclosing the filial tissues, the endosperm and embryo (embryo differentiation starts only at 10 DAA and so its dissection at 7 DDA was not possible). Figure adapted from Wheat, the big picture.

Wild type and transgenic tobacco (*Nicotiana tabacum* cultivar Samsun) with 6% of wild type PRK activity (Line 1, Paul *et al.*, 2000) were grown in Rothamsted standard compost mix and full nutrition at 23^{o}C/ 16-h day, 150 µmol quanta m^{-2} s^{-1} and the shoots of two-week-old plantlets were harvested. Cauliflower was bought fresh from a local supermarket.

4.5.2. T6P determinations

T6P was quantified in wheat grain extracts using anion exchange HPLC coupled with electrospray ionisation mass spectrometry (Delatte *et al.*, 2009). For detailed description of the method please refer to Chapter V. The method achieved baseline resolution of all compounds from wheat grains with an m/z ranging from 418 to 423 that eluted in the vicinity of T6P (Fig. 4.8). Exogenous addition of the standards lactose-1-phosphate (Sigma-Aldrich), Suc-6-phosphate (Sigma-Aldrich) or maltose-6- phosphate (Prof. Jack Thompson, NIH, Bethesda, Maryland) showed that these compounds do not co-elute with T6P.

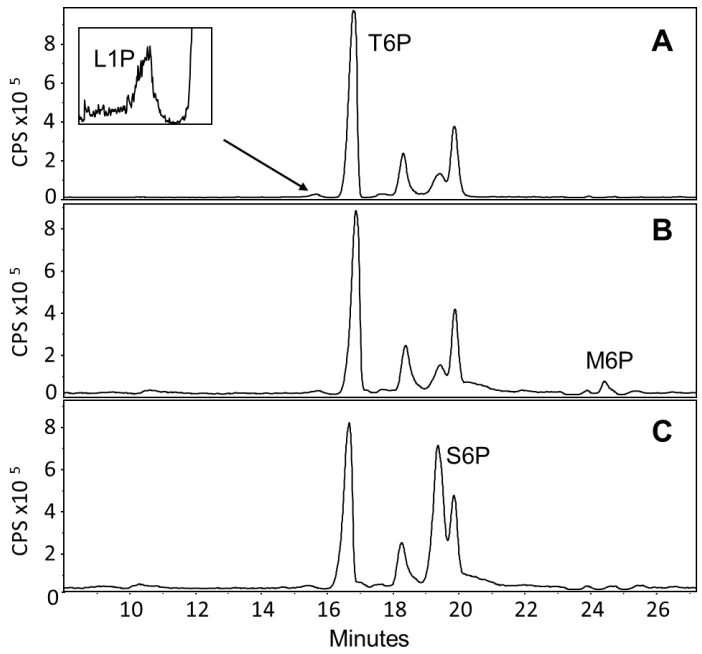

Figure 4.8. Separation of phospho-disaccharides with identical mass as T6P in wheat extracts using the LC/MS method described by Delatte *et al.* (2009). Counts per second (CPS) of ions of a specific mass. **(A)** Internal standard lactose-1-phosphate (L1P) added prior to extraction. **(B)** With maltose-6-phosphate (M6P) added before injection. **(C)** With sucrose-6-phosphate (S6P) added before injection.

4.5.3. Bioinformatics

Transcript profiles were derived from the dataset reported by Wan *et al.* (2008) with the normalisation protocols reported there. The full transcriptome set is available in the ArrayExpress database (Accession Number E-MEXP-1193). Transcripts were identified by blasting Affymetrix probeset target sequences to find the closest known nucleotide sequences present in EMBL/ GenBank/ DDBJ. For analysis of SnRK1 marker genes sets of 600 Arabidopsis genes for which expression is repressed or induced by SnRK1 were taken from Baena-Gonzalez *et al.* (2007). Wheat Affymetrix probesets which corresponded most closely to these were identified using the WhETS (Wheat Estimated Transcript Server) tool (Mitchell *et al.*, 2007). For each list, the top 300 most abundantly expressed in grain of these probesets were

selected. qRT-PCR profiling of the expression of genes including SnRK1 markers *myb3*, *Yab2* confirmed induction and repression respectively over the grain developmental period (Wan *et al.*, 2008).

4.5.4. SnRK1 activity assays

SnRK1 activity was extracted and assayed from developing grain as described in detail in Chapter II. Extracts were assayed for a normal assay period of 6 min or time intervals of up to 6 min following addition of R5P and Ru5P when checking for ATP consumption over the assay period. All extracts were tested for linearity and optimised as previously conducted (Zhang *et al.*, 2009).

4.5.5. Monitoring of conversion of R5P and Ru5P to RuBP with depletion of ATP

Stability of 1 mM R5P and Ru5P was performed using UV-HPLC and HPLC-MS analysis as below. Control reactions were run without R5P and with ADP instead of ATP. After 6 min the reaction mixtures were snap frozen in liquid nitrogen and lyophilized. The resulting solid was dissolved in water (10 µl) and the entire solution injected for UV-HPLC and HPLC-MS analysis as below.

4.5.6. Detection of R5P and RuBP

HPLC-MS was conducted on a Waters binary HPLC system. Samples were analysed through a Hichrom SiELC Primesep SM mixed mode anion exchange/ C18 reverse phase column (150 x 4.6 mm, 5 µm) with an applied gradient from 10 mM ammonium formate at pH 3 to 80 mM ammonium formate at pH 3 over 15 min at a flow rate of 1 ml min^{-1}. Eluants were fed directly into a Waters Quattro micro in negative mode either operating in Selected Ion Recording mode centred at the monoisotopic masses of R5P (229.01) and RuBP (308.98) with a detection width of 0.5 Da and a dwell time of 10 ms. The mass spectrometer was operated with a cone

voltage of 35 V, a source temperature of 100°C and desolvation temperature of 400°C. Chromatograms are presented after smoothing.

4.5.7. Detection of ATP, ADP and AMP

UV-HPLC was conducted on a Dionex UltiMate 4000. Samples were analysed through a Waters Spherisorb strong anion exchange column (250 x 4.6 mm, 5 µm). A gradient was applied from 40 mM sodium phosphate at pH 4.5 to 500 mM sodium phosphate buffer at pH 2.5 over 10 min and then eluted for a further 5 min at a flow rate of 1 ml min^{-1}. Eluants were detected using an in-line UV absorbance detector (λ = 260 nm).

Acknowledgements

I, Cátia Nunes, performed and analysed the presented experimental work with the following collaborations: Dr. Eleazar Martínez-Barajas performed the remaining spinal work that originated the publication indicated below; the analysis of transcripts during grain development was made possible through funding to Professor Peter Shewry and Dr. Yongfang Wan by the Biotechnology and Biological Sciences Research Council (grant nos. EGA17694 and D/10608); Dr. Thierry Delatte performed the T6P quantifications at Utrecht University; Dr. Mitul Patel did the UV-HPLC and HPLC-MS analysis at Oxford University; and to whom I am deeply grateful. The planning of the research work and discussion of results was done by Cátia Nunes, Dr. Eleazar Martínez-Barajas and Dr. Matthew Paul.

4.6 References

Alderson A, Sabelli PA, Dickinson JR, Cole D, Richardson M, Kreis M, Shewry PR, Halford NG (1991) Complementation of *snf1*, a mutation affecting global regulation of carbon metabolism in yeast, by a plant protein kinase cDNA. Proc Natl Acad Sci USA **88:** 8602-8605

Baena-González E, Rolland F, Thevelein JM, Sheen J (2007) A central integrator of transcription networks in plant stress and energy signaling. Nature **448:** 938-942

Caley CY, Duffus CM, Jeffcoat B (1990) Photosynthesis in the pericarp of developing wheat grains. J Exp Bot **41:** 303-307

Dale S, Wilson WA, Edelman AM, Hardie DG (1995) Similar substrate recognition motifs for mammalian AMP-activated protein kinase, higher plant HMG-CoA reductase kinase-A, yeast SNF1, and mammalian calmodulin-dependent protein kinase I. FEBS Lett **361**: 191-195

Davies SP, Carling D, Hardie DG (1989) Tissue distribution of the AMP-activated protein kinase, and lack of activation by cyclic AMP-dependent protein kinase, studied using a specific and sensitive peptide assay. Eur J Biochem **186**: 123-128

Delatte TL, Selman MHJ, Schluepmann H, Somsen GW, Smeekens JCM, de Jong GJ (2009) Determination of trehalose 6-phosphate content in Arabidopsis seedlings by successive extractions followed by anion exchange chromatographymass spectrometry. Anal Bioch **389:** 12-17

Eastmond PJ, van Dijken AJ, Spielman M, Kerr A, Tissier AF, Dickinson HG, Jones JD, Smeekens SC, Graham IA (2002) Trehalose-6-phosphate synthase 1, which catalyses the first step in trehalose synthesis, is essential for Arabidopsis embryo maturation. Plant J **29:** 225-235

El-Bashiti T-E, Hamamci H, Oktem HA, Yucel M (2005) Biochemical analysis of trehalose and its metabolising enzymes in wheat under abiotic stress conditions. Plant Sci **169:** 47-54

Halford NG, Hey SJ (2009) Snf1-related protein kinases act within an intricate network that links metabolic and stress signaling in plants. Biochem J **419:** 247-259

Hardie DG (2007) AMP-activated/SNF1 protein kinases: conserved guardians of cellular energy. Nature Rev Mol Cell Biol **8:** 774-785

Keys AJ (1968) The intracellular distribution of free nucleotides in the tobacco leaf. Biochem J **108:** 1-8

Laurie S, McKibbin RS, Halford NG (2003) Antisense SNF1-related (SnRK1) protein Kinase gene represses transient activity of an α-amylase (α-*Amy2*) gene promoter in cultured wheat embryos. J Ex Bot **54:** 739-747

Lee K-W, Chen P-W, Lu C-A, Chen S, Ho T-H D, Yu S-M (2009) Coordinated responses to oxygen and sugar deficiency allow rice seedlings to tolerate flooding. Sci Signal **2:** 61

Mitchell RAC, Castells-Brooke N, Taubert J, Verrier PJ, Leader DJ, Rawlings CJ (2007) Wheat estimated transcript server (WhETS): a tool to provide best estimate of hexaploid wheat transcript sequence. Nucleic Acids Res **35:** W148-151

Mohammadi M, Kav NNV, Deyholos MK (2007) Transcriptional profiling of hexaploid wheat (Triticum aestivum L.) roots identifies novel, dehydration-responsive genes. Plant, Cell Environ **30:** 630-645

Paul MJ, Driscoll SP, Andralojc PJ, Knight JS, Gray JC, Lawlor DW (2000) Decrease of phosphoribulokinase activity by antisense RNA in transgenic tobacco: definition of the light environment under which phosphoribulokinase is not in large excess. Planta **21:** 112-119

Paul MJ, Jhurreea D, Zhang Y, Primavesi LF, Delatte T, Schluepmann H, Wingler A (2010) Up-regulation of biosynthetic processes associated with growth by trehalose 6-phosphate. Plant Signal Behav **5:** 386-392

Paul MJ, Primavesi LF, Jhurreea D, Zhang Y (2008) Trehalose metabolism and signaling. Annu Rev Plant Biol **59:** 417-441

Piattoni CV, Bustos DM, Guerrero SA, Iglesias A (2011) Nonphosphorylating glyceraldehydes 3-phosphate dehydrogenase is phosphorylated in wheat endosperm at serine-404 by an SNF1-related protein kinase allosterically inhibited by ribose 5-phosphate. Plant Physiol **156**: 1337-1350

Polge C, Thomas M (2007) SNF1/AMPK/SnRK1 kinases, global regulators at the heart of energy control. Trends Plant Sci **12:** 1360-1385

Porra RJ, Thompson WA, Kriedmann PE (1989) Determination of accurate extinction coefficients and simultaneous equations for assaying chlorophylls a and b extracted with four different solvents: verification of the concentration of chlorophyll standards by atomic absorption spectroscopy. Biochim et Biophys Acta **975:** 384-394

Radchuk R, Emery NEJ, Weier D, Vigeolas H, Geigenberger P, Lunn JE, Feil R, Weschke W, Weber H (2010) Sucrose non-fermenting kinase1 (SnRK1) coordinates metabolic and hormonal signals during pea cotyledon growth and differentiation. Plant J **61:** 324-328

Radchuk R, Radchuk V, Weschke W, Borisjuk L, Weber H (2006) Repressing the expression of the sucrose nonfermenting-1-related protein kinase gene in pea embryo causes pleiotropic defects of maturation similar to an abscisic acid-insensitive phenotype. Plant Physiol **140:** 263–278

Santarius KA, Heber U (1965) Changes in the intracellular levels of ATP, ADP, AMP and Pi and regulatory function of the adenylate system in leaf cells during photosynthesis. Biochim. Biophys. Acta **102:** 39-54

Satoh-Nagasawa N, Nagasawa N, Malcomber S, Sakai H, Jackson D (2006) A Trehalose metabolic enzyme controls inflorescence architecture in maize. Nature **441:** 227-230

Schluepmann H, Pellny T, van Dijken A, Smeekens S, Paul M (2003) Trehalose 6-phosphate is indispensable for carbohydrate utilisation and growth in *Arabidopsis thaliana*. Proc Natl Acad Sci USA **100:** 6849-6854

Smeekens S, Ma J, Hanson J, Rolland F (2009) Sugar signals and molecular networks controlling plant growth. Curr Opin Plant Biol **13:** 1-6

Sreenivasulu N, Radchuk V, Strickert M, Miersch O, Weschke W, Wobus U (2006) Gene expression patterns reveal tissue-specific signaling networks controlling programmed cell death and ABA-regulated maturation in developing barley seeds. Plant J **47**: 310-327

Toroser D, Plaut Z, Huber SC (2000) Regulation of a plant SNF1-related protein kinase by glucose 6-phosphate. Plant Physiol **123**: 403-411

Van Dijken AJH, Schluepman H, Smeekens SC (2004) Arabidopsis trehalose-6- phosphate synthase 1 is essential for normal; vegetative growth and transition to flowering. Plant Physiol **135:** 969-977

Wan Y, Poole RL, Huttly AK, Toscano-Underwood C, Feeney K, Welham S, Gooding MJ, Mills ENC, Edwards KJ, Shewry PR, Mitchell RA (2008) Transcriptome analysis of grain development in hexaploid wheat. BMC Genomics **9:** 121

Weber H, Borisjuk L, Heim U, Sauer N, Wobus U (1997) A role for sugar transporters during seed development: molecular characterization of a hexose and a sucrose carrier in faba bean seeds. Plant Cell **9:** 895–908

Weber H, Borisjuk L, Wobus U (2005) Molecular physiology of legume seed development. Annu Rev Plant Biol **56**:253-279

Weekes J, Ball KL, Caudwell FB, Hardie DG (1993) Specificity determinants for the AMP-activated protein kinase and its plant homologue analysed using synthetic peptides. FEBS Lett **334**: 335-339

Weichert N, Saalbach I, Weichert H, Kohl S, Erban A, Kopka J, Hause B, Varshney A, Sreenivasulu N, Strickert M, Kumlehn J, Weschke W, Weber H (2010) Increasing sucrose uptake capacity of wheat grains stimulates storage protein synthesis. Plant Physiol **152:** 698-710

Zhang Y, Primavesi LF, Jhurreea D, Andralojc PJ, Mitchell RAC, Powers SJ, Schluepmann H, Delatte T, Wingler A, Paul MJ (2009) Inhibition of Snf1-related protein kinase (SnRK1) activity and regulation of metabolic pathways by trehalose 6-phosphate. Plant Physiol **149:** 1860-1871

Chapter V

The Trehalose 6-Phosphate/SnRK1 Signaling Pathway Primes Growth Recovery following Relief of Sink Limitation

The work presented in this chapter was mostly performed by Cátia Nunes (see acknowledgments section) and included in the following publications:

Nunes C, O'Hara LE, Primavesi LF, Delatte TL, Schluepmann H, Somsen GW, Silva AB, Fevereiro PS, Wingler A, Paul MJ **(2013)** The trehalose 6-phosphate/SnRK1 signaling pathway primes growth recovery following relief of sink limitation. **Plant Physiology** 162(3): 1720–1732

and,

Nunes C, Schluepmann H, Delatte TL, Wingler A, Silva AB, Fevereiro PS, Jansen M, Fiorani F, Wiese-Klinkenberg A, Paul M **(2013)** Regulation of growth by the trehalose pathway: Relationship to temperature and sucrose. **Plant Signaling & Behaviour** 8:e26626; PMID: 24084646; http://dx.doi.org/10.4161/psb.26626

5.1. Abstract

T6P is a sugar signal in plants that inhibits SNF1-related protein kinase, SnRK1, thereby altering gene expression and promoting growth processes. This provides a model for the regulation of growth by sugar. However, it is not known how this model operates under sink-limited conditions when tissue sugar content is uncoupled from growth. To test the physiological importance of this model, T6P, SnRK1 activities, sugars, gene expression, and growth were measured in Arabidopsis (*Arabidopsis thaliana*) seedlings after transfer to cold or zero N (N) compared with sugar feeding under optimal conditions. Maximum *in vitro* activities of SnRK1 changed little, but T6P accumulated up to 55-fold, correlating with tissue Suc content in all treatments. SnRK1-induced and -repressed marker gene expression strongly related to T6P above and below a threshold of 0.3 to 0.5 nmol T6P g^{-1} fresh weight close to the dissociation constant (4 mM) of the T6P/ SnRK1 complex. This occurred irrespective of the growth response to Suc. This implies that T6P is not a growth signal per se, but through SnRK1, T6P primes gene expression for growth in response to Suc accumulation under sink-limited conditions. To test this hypothesis, plants with genetically decreased T6P content and SnRK1 overexpression were transferred from cold to warm to analyse the role of T6P/SnRK1 in relief of growth restriction. Compared with the wild type, these plants were impaired in immediate growth recovery. It is concluded that the T6P/SnRK1 signaling pathway responds to Suc induced by sink restriction that enables growth recovery following relief of limitations such as low temperature.

5.2. Introduction

The trehalose pathway has developed into a specialized system that regulates and integrates metabolism with growth and development (Schluepmann *et al.*, 2003; Lunn *et al.*, 2006; Ramon and Rolland, 2007; Gómez *et al.*, 2010). The precursor T6P seems to be the critical signaling molecule. In plants trehalose phosphate synthase (TPS) synthesizes T6P from G6P and UDPG. T6P is then

converted to trehalose by trehalose phosphate phosphatase (TPP). The regulation of T6P content in plants by TPSs and TPPs is not well understood. TPS1 is thought to account for most TPS catalytic activity in plants (Vandesteene *et al.*, 2010), whereas all 10 TPPs are now known to be catalytically active (Vandesteene *et al.*, 2012). T6P responds strongly to Suc supply when Suc is fed to seedlings grown in culture and in response to an increase in Suc in illuminated leaves (Lunn *et al.*, 2006). Given the importance of T6P in the regulation of growth (Schluepmann *et al.*, 2003; Paul *et al.*, 2010) and end-product synthesis (Kolbe *et al.*, 2005; Gómez *et al.*, 2006), targets for its interaction have been eagerly sought.

Recently, it was found that T6P inhibits SnRK1 in growing tissues of plants (Zhang *et al.*, 2009; Debast *et al.*, 2011; Delatte *et al.*, 2011; Martínez-Barajas *et al.*, 2011) through an intermediary protein, Factor I. SnRK1 is a member of the central regulators SNF1-related AMPK group of PKs (Hardie, 2007). Baena-González *et al.* (2007) established that over 1000 genes are regulated by SnRK1 involved in biosynthetic, growth, and stress responses. A model is proposed where SnRK1 inhibits growth processes when sugar and energy supplies are scarce, thus enabling survival under starvation stress conditions. When sugar supply is plentiful, T6P accumulates and inhibits SnRK1 blocking expression of genes involved in the stress survival response and inducing genes involved in the feast response, including growth processes. It is therefore not surprising that plants with genetically decreased T6P content display similar phenotype to those with overexpressed SnRK1 and vice versa (Schluepmann *et al.*, 2003; Baena-González *et al.*, 2007; Wingler *et al.*, 2012).

Sugars fluctuate widely in plants in response to changes in photosynthesis and in response to environmental variables. Sugar starvation conditions, such as those induced by deep shade, limit growth through lack of sugar availability; SnRK1 would be active under such conditions. High sugar availability, however, does not necessarily indicate good conditions for growth and high growth rates. For example, under low-temperature and limiting nutrient supply, growth is limited in spite of abundant sugar availability (Paul and Stitt, 1993; Usadel *et al.*, 2008). This is termed sink-limited growth, when growth is limited by capacity of sinks, i.e. growing regions

to use assimilate. It departs from the famine model of growth regulation by SnRK1. The interrelationship between T6P, SnRK1, and growth is not known under such conditions. Here, we vary growth conditions by temperature and nutrient supply to induce sink-limited growth and feed Suc and Gluc at physiological levels (15 mM). We show a strong specific interrelationship between T6P and Suc and SnRK1-regulated gene expression under all conditions irrespective of growth rate. This implies that T6P is not a growth signal per se, but through SnRK1, T6P primes gene expression for growth. By priming, we mean being in a prepared state with an advanced capacity to activate growth following relief of a growth limitation, such as low temperature. To test that T6P/SnRK1 enable growth recovery following relief from sink limitation, plants with genetically decreased T6P content and SnRK1 overexpression were transferred from cold to warm. Compared with the wild type, these plants were impaired in immediate growth recovery. It is concluded that T6P responds to Suc induced by growth restriction. This enables growth recovery following relief of limitations downstream of T6P/SnRK1, such as low temperature. Our findings are included in a model for the regulation of growth by the T6P/SnRK1 signaling pathway.

5.3. Results

5.3.1. Effect of transfer to low temperature, low N and sugar feeding on growth, carbohydrate and T6P content

To test the physiological importance of the regulation of growth by the T6P/SnRK1 signaling pathway, T6P, SnRK1 activities, sugar contents, gene expression, and growth rate were measured in Arabidopsis (*Arabidopsis thaliana*) seedlings after transfer to low temperature or zero N compared with sugar feeding under optimal conditions. These conditions were used to uncouple sugars from growth, i.e. to test physiological importance of the T6P/SnRK1 pathway under sink-limited conditions.

The different treatments gave a wide range of rates of fresh weight accumulation over 72 h (Fig. 5.1A) calculated here as structural weight after subtraction of the large starch accumulation at low N (Fig. 5.1B). Biomass after 72 h was highest in seedlings grown on full medium with 0.5% Suc and lowest on full medium with no sugar source. Low temperature strongly inhibited growth, whereas feeding 0.5% Gluc gave an intermediate growth phenotype. Withdrawal of N did not reduce total growth over the course of the experiment, but there was a large change in shoot to root partitioning and accumulation of starch in these plants. Protein content was stable in all treatments except for N-deficient and sugar-starved seedlings where protein content decreased during the experiment, showing the importance of both carbon and N supply for protein synthesis (Fig. 5.1C). Suc contents displayed a range of responses (Fig. 5.1D), from 1.49 µmol g^{-1} FW at the start of the experiment rising maximally 9.9-fold higher to 14.8 µmol g^{-1} FW in the low N treatment, with a similar pattern at low temperature. Suc feeding on its own resulted in a large initial increase in Suc up to 6 h from feeding, but which then decreased during the rest of the experiment. Gluc feeding produced a small increase in Suc content from 1.49 to 2.82 µmol g^{-1} FW which remained stable during the rest of the experiment. Amounts of Gluc and Fru followed a similar pattern to Suc with the exception that Gluc levels were higher in Gluc-fed seedlings than Suc-fed seedlings (Fig. 5.1E and F). Large differences in T6P were found between the treatments (Fig. 5.1G). In seedlings grown with no sugar source and with 0.5% Gluc amounts of T6P were stable throughout the experiment between 0.18-0.4 nmol g^{-1} FW. Low temperature, low N and Suc feeding under optimal conditions led to large increases in T6P during the first 24 h, up to 9.9, 5.8 and 3.3 nmol g^{-1} FW, respectively. Amounts of T6P then decreased during the rest of the time course. There was a 55-fold difference between the beginning of the experiment (0.18 nmol g-1 FW) and the highest T6P content measured (9.89 nmol g^{-1} FW, 10^{o}C, 24 h). These data show the possible amplitude of T6P fluctuation that can be observed in seedlings through changes in conditions that restrict growth by sink limitation.

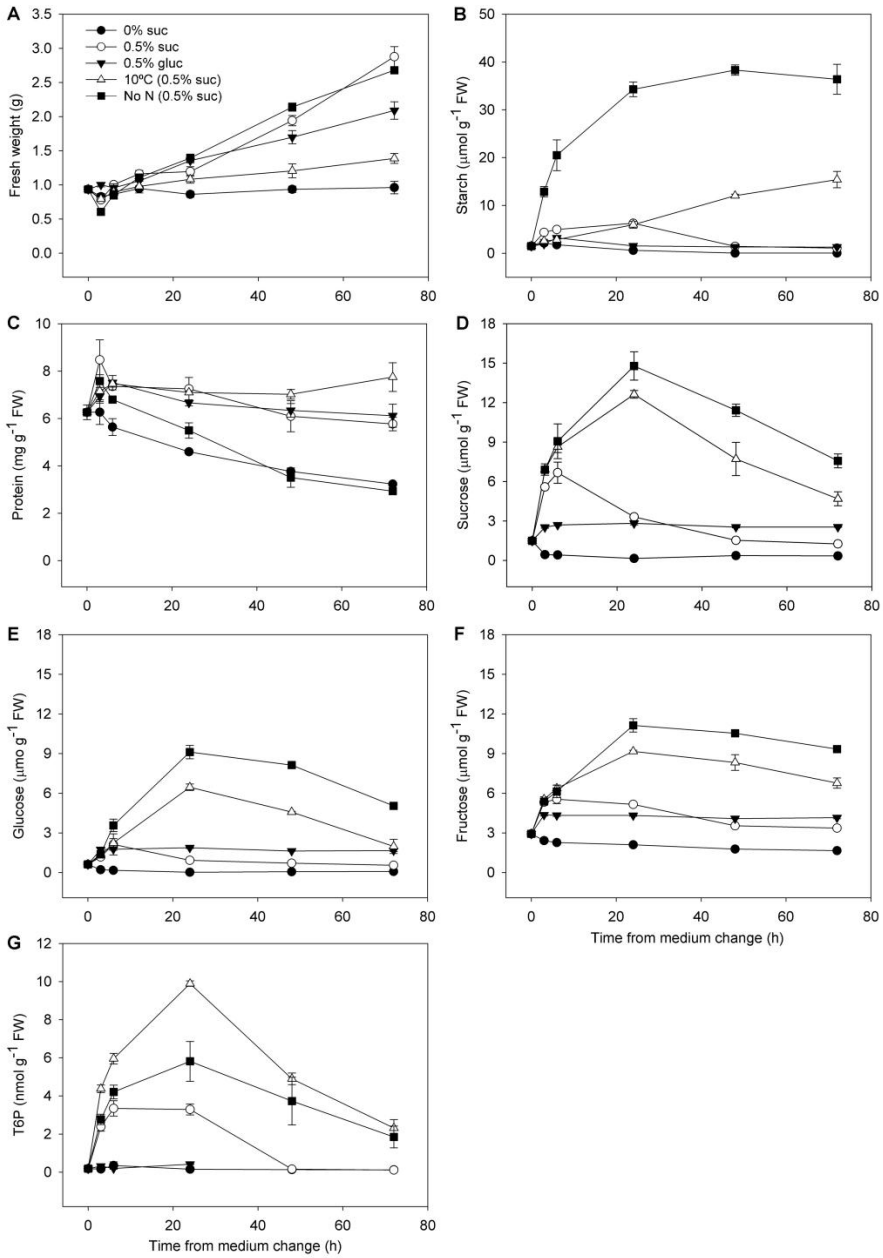

Figure 5.1. Impact on growth, starch, protein, sugars, and T6P contents in response to sucrose and glucose feeding with full nutrition at 22°C and after transfer to 10°C or zero nitrogen. Seedlings were grown with 0.5% (w/v) Suc for 7 d at 22°C and then transferred to fresh media without external sugar source (0% Suc), with 0.5% Suc (0.5% [w/v] suc), 0.5% Gluc (0.5% [w/v] gluc), 0.5% Suc at 10°C [10°C (0.5% suc; w/v)], and 0.5% Suc with zero nitrogen [No N (0.5% [w/v] suc)]. Measurements were performed over 72 h of treatment induction. FW (A), starch (B), protein (C), Suc (D), Gluc (E), Fru (F), and T6P (G). The data are means with SD of three independent samples.

5.3.2. T6P levels correlate with Suc content under sink-limited conditions

Out of all sugars analysed T6P levels correlated most closely with Suc content (Fig. 5.2A). The correlations of T6P with Gluc (Fig. 5.2B) and Fru (Fig. 5.2C) were weaker than between Suc and T6P particularly at low temperature and low N. In support of a specific relationship between Suc and T6P, Gluc feeding produced no increase in T6P levels (Fig. 5.1G).

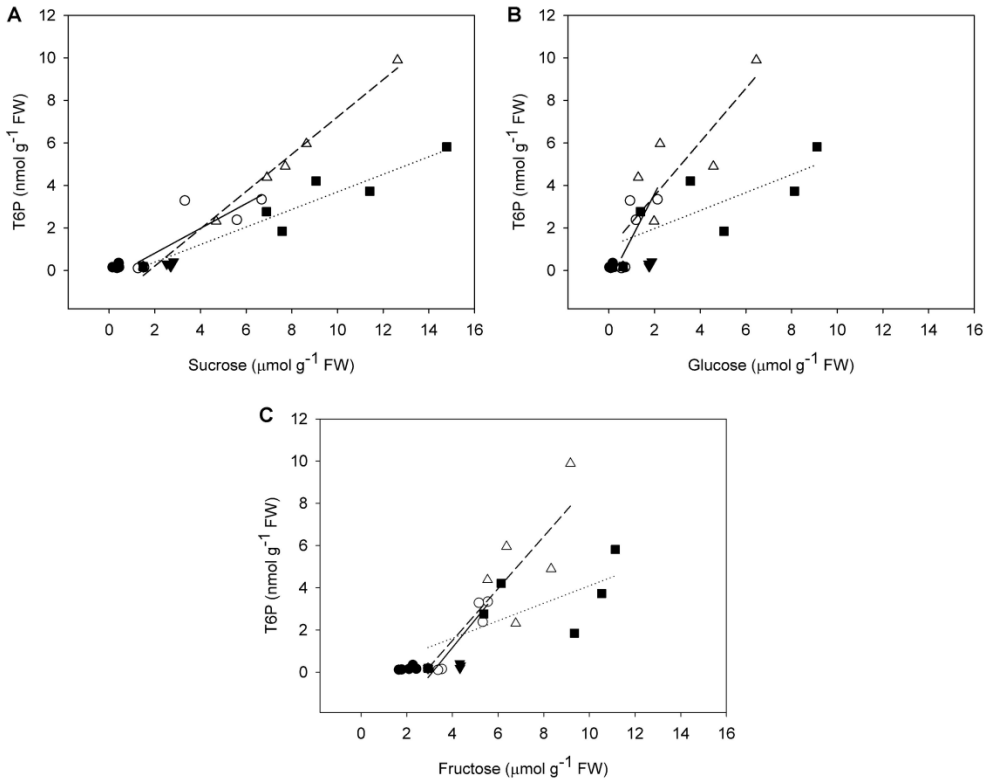

Figure 5.2. Interrelationship between T6P and sugars measured in the different treatments. (A), T6P and sucrose (0.5% suc, solid line r^2=0.84, SEE=0.56, P<0.011; 10 ºC, dashed line r^2=0.99, SEE=0.35, P<0.0001; No N, dotted line r^2=0.90, SEE=0.70, P<0.0041). (B), T6P and glucose (0.5% suc, solid line r^2=0.68, SEE=0.79, P<0.045; 10 ºC, dashed line r^2=0.80, SEE=1.04, P<0.016; No N, dotted line r^2=0.74, SEE=0.94, P<0.028). (C), T6P and fructose (0.5% suc, solid line r^2=0.73, SEE=0.72, P<0.029; 10 ºC, dashed line r^2=0.82, SEE=1.00, P<0.013; No N, dotted line r^2=0.72, SEE=0.96, P<0.032). The data are means of 3 independent samples.

5.3.3. Regulation of trehalose pathway gene expression by Suc

To examine how the trehalose pathway responded to the treatments, in comparison, transcript abundances of representative genes of the pathway were determined. The only TPS enzyme unequivocally known to synthesize T6P is TPS1, so we examined the interrelationship between *TPS1* expression and endogenous Suc levels. We also analyzed the interaction between Suc and *TPPA* and *TPPB* expression. These genes encode enzymes known to be catalytically active in the trehalose pathway. (Vandesteene *et al.*, 2012) Our data show a good interrelationship between Suc and *TPS1* expression when sugars were fed exogenously, but not when Suc content was altered by low temperature or by low N (Fig. 5.3A). The interrelationship between *TPS1* expression and T6P was very steep up to a level of 2.5 nmol T6P g^{-1} FW (Fig. 5.3B). Beyond this T6P was not related to *TPS1* expression. *TPPA* expression did not show any relationship to Suc or T6P content (Fig. 5.3C and D). However, *TPPB* expression correlated well with Suc both when fed exogenously and when altered by low temperature but not when altered by low N (Fig. 5.3E). There was a weak correlation between *TPPB* expression and T6P content for all treatments except low N (Fig. 5.3F).

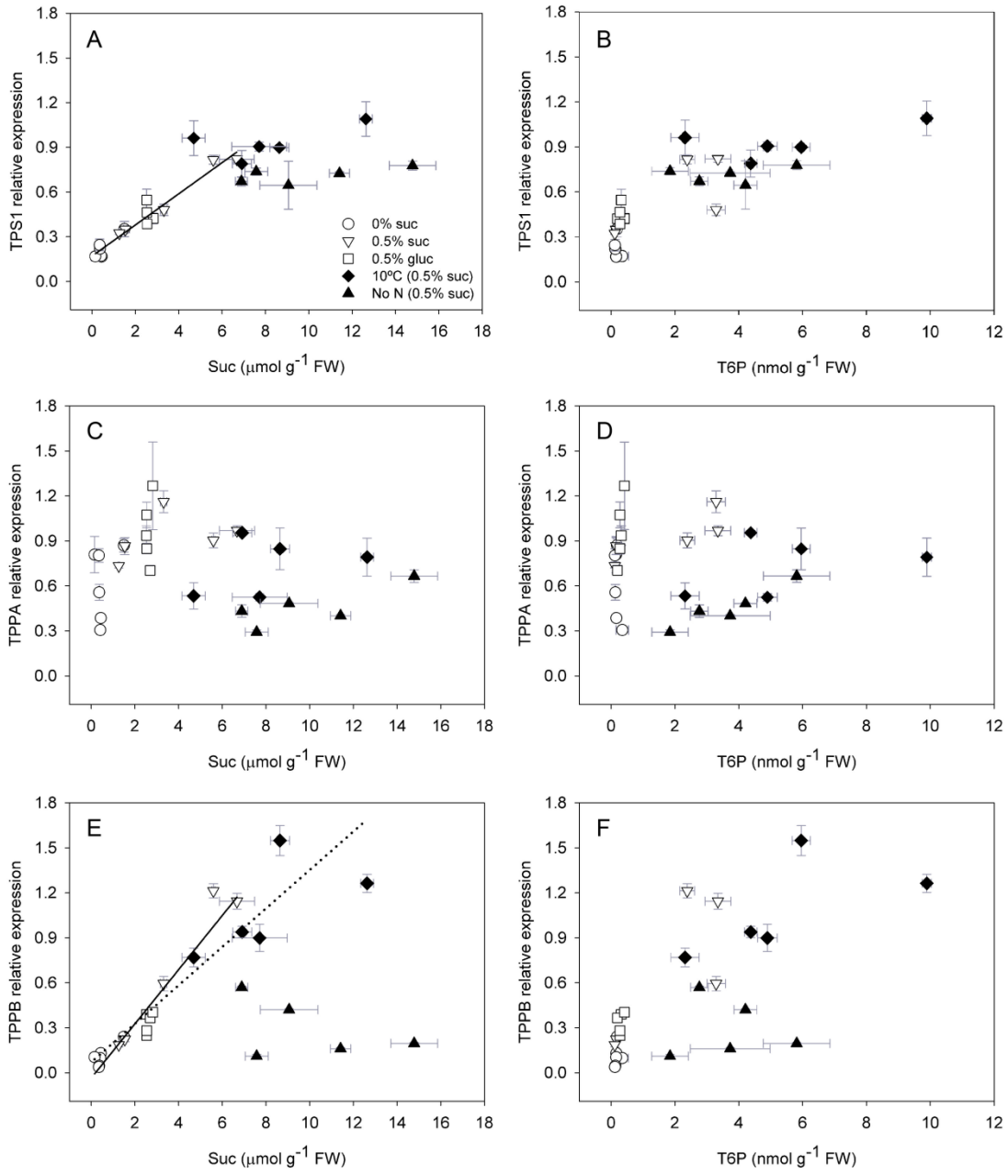

Figure 5.3. Interrelationship between trehalose pathway gene expression, sucrose, and T6P in response to Suc and Gluc feeding with full nutrition at 22°C and after transfer to 10°C or zero nitrogen compared with treatment with no supplementary sugar. (A) TPS1 (At1g78580) and sucrose (correlation for sugar feeding treatments, white symbols only, Pearson's r = 0.972; P < 0.001); (B) TPS1 and T6P; (C) TPPA (At5g51460) and sucrose (no correlation); (D) TPPA and T6P (no correlation); (E) TPPB (At1g78090) and sucrose (correlation for sugar feeding treatments, white symbols

only, solid line, Pearson's r = 0.960; P < 0.001 and correlation for sugar feeding together with 10 °C treatment, dotted line, Pearson's r = 0.921; P < 0.001); (F) TPPB and T6P. Horizontal error bars are the SD of 3 independent sucrose or T6P samples, and the vertical error bars are the SD of 3 independent qRT -PCR samples.

5.3.4. SnRK1 activities and expression

SnRK1 activities measured *in vitro* were relatively stable during the course of the experiment in the different treatments (Fig. 5.4A). However, N deficiency induced a 30% increase in *in vitro* SnRK1 activity during the experiment from 3.7 nmol min^{-1} mg^{-1} protein to 4.8 nmol min^{-1} mg^{-1} protein. SnRK1 activity in seedlings grown without sugar decreased from 3.7 nmol min^{-1} mg^{-1} protein to 2.9 nmol min^{-1} mg^{-1} protein. SnRK1 activities in the other three treatments changed little during the time course. SnRK1 was inhibited strongly by 1 mM T6P between 65 and 75% in all treatments (Fig. 5.4B), with the exception of deficient N where inhibition by T6P steadily decreased over the time course. Compared with the treatment where no supplementary sugar was supplied, transcripts of AKIN10 changed little during the experiment; amounts of AKIN11 transcript were decreased in all treatments compared to seedlings without sugar (Fig. 5.4C and D).

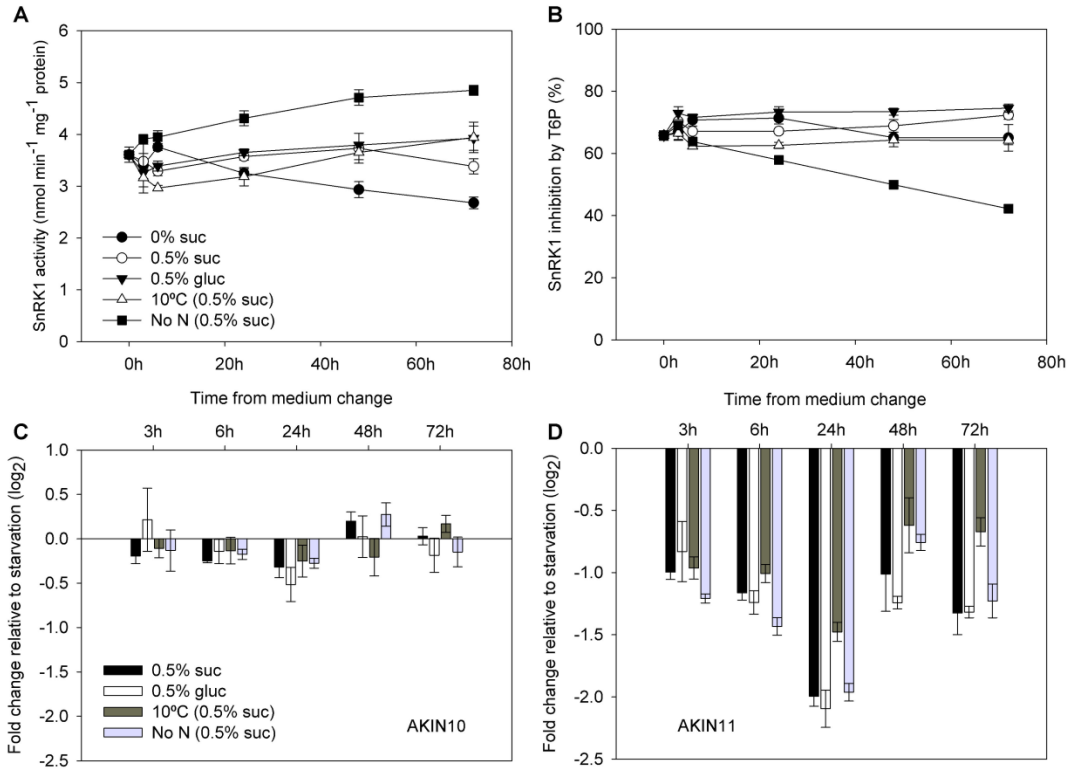

Figure 5.4. SnRK1 activity and inhibition by T6P and transcript abundance of the catalytic subunits AKIN10 and AKIN11 determined by qRT-PCR in response to sucrose and glucose feeding with full nutrition at 22ºC and after transfer to 10ºC or zero nitrogen. SnRK1 extracts were used to determine (a), SnRK1 activity and (b), inhibition of SnRK1 activity by 1 mM T6P. Transcript fold change of the catalytic subunits (c), AKIN10 (At3g01090) and (d), AKIN11 (At3g29160) relative to the starvation condition at 3, 6, 24, 48 and 72 h after start of treatment. The data are means with standard deviations of 3 independent samples.

5.3.5. SnRK1 marker genes impacted strongly by T6P content

Approximately 1,000 genes were established as SnRK1 marker genes (Baena-González *et al.,* 2007). These genes were shown to be regulated by T6P *in vivo* in transgenic seedlings with altered T6P content confirming *in vitro* inhibition of SnRK1 by T6P (Zhang *et al.,* 2009). Quantitative reverse transcription (qRT)-PCR analysis of the marker genes for the treatments determined relative to seedlings with no carbon source showed a relationship between T6P and transcript abundance.

SnRK1 marker genes - *ASN1, βGAL, AKINβ, TPS8* and *TPS10* - normally up-regulated by SnRK1 were down regulated by T6P (Fig. 5.5A-E). SnRK1 marker genes normally repressed by SnRK1 - *UDPGDH, MDH, bZIP11* and *TPS5* - were up regulated by T6P (Fig. 5.5F-I). There were differences in the magnitude of changes induced by T6P. Of the SnRK1-induced markers *ASN1* was repressed strongly compared with conditions with no supplementary sugar. Of the SnRK1-repressed markers, *TPS5* was the most strongly affected compared with treatments associated with low endogenous sugar. Changes in marker gene expression induced by these treatments relative to low sugar were larger than those induced by transgenic modification of T6P (2- to 3- fold; Zhang *et al.,* 2009) in agreement with the larger changes in T6P achieved by the environmental treatments (up to 55-fold). When transcript abundance was plotted against T6P clear biphasic relationships between T6P and transcript abundance were obtained for both SnRK1-induced (Fig. 5.6A-E) and SnRK1-repressed (Fig. 5.6F-I) marker genes. Most changes in gene expression occurred above and below a level of T6P of around 0.3 to 0.5 nmol g^{-1} FW. This would indicate a threshold level of T6P required before changes in transcript abundance occurred, which assuming cytosolic location, equates to about 3 to 5 µM, close to the K_i 4 µM of the SnRK1 complex (Chapter II). Gluc feeding induced changes in gene expression less than those induced by Suc feeding, low temperature and low N (Fig. 5.5 and 5.6). The changes in gene expression occurred in spite of no change in T6P content. It is known that G6P and G1P also inhibit SnRK1 (Toroser *et al.,* 2000; Chapter II). We measured these metabolites to determine if they could contribute to changes in SnRK1-induced gene expression in Gluc-fed seedlings. Amounts of both increased between 3- to 4- fold over 48 h of Gluc feeding (Fig. 5.7A and B). Gluc regulated marker genes were induced as predicted in this experiment (Fig. 5.8).

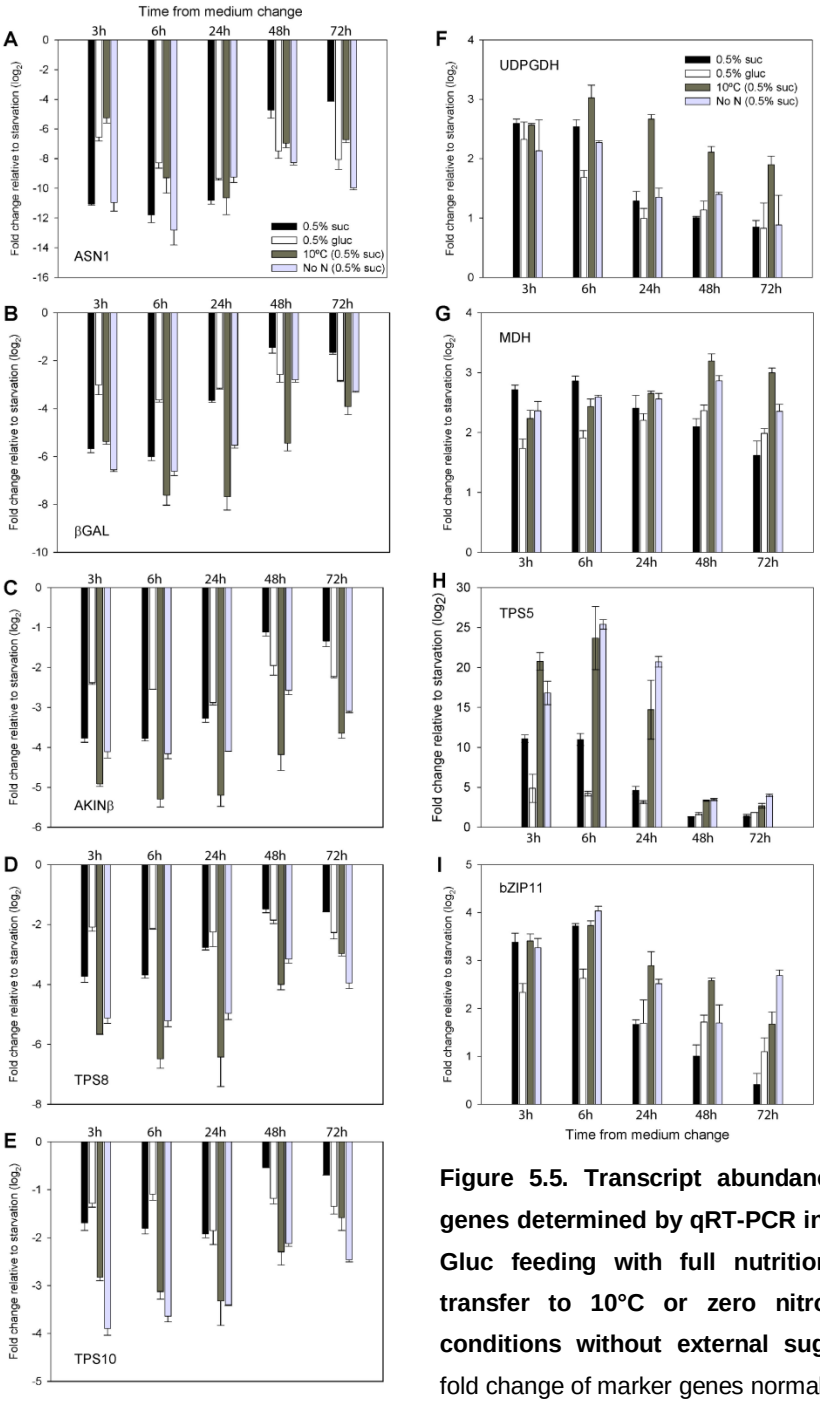

Figure 5.5. Transcript abundance of SnRK1 marker genes determined by qRT-PCR in response to Suc and Gluc feeding with full nutrition at 22°C and after transfer to 10°C or zero nitrogen relative to the conditions without external sugar source. Transcript fold change of marker genes normally up-regulated by SnRK1, ASN1 (At3g47340; A), bGAL (At5g56870; B),AKINb (At5g21170; C), TPS8 (At1g70290; D), and TPS10 (At1g60140; E), and marker genes normally down-regulated by SnRK1, UDPGDH (At3g29360; F), MDH (At3g15020; G), TPS5 (At4g17770; H), and bZIP11 (At4g34590; I). The data are means with SD of three independent samples.

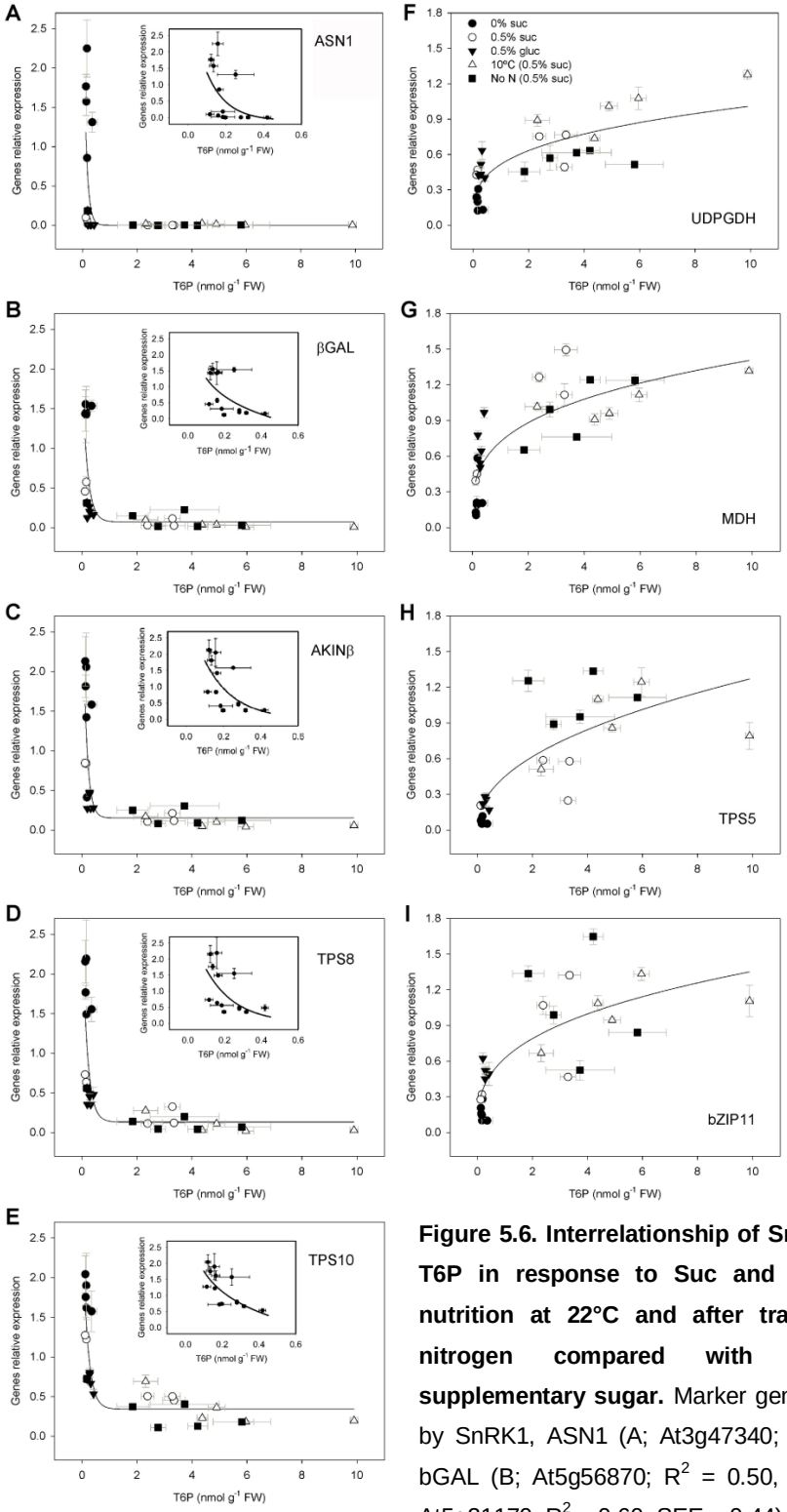

Figure 5.6. Interrelationship of SnRK1 marker genes and T6P in response to Suc and Gluc feeding with full nutrition at 22°C and after transfer to 10°C or zero nitrogen compared with treatment with no supplementary sugar. Marker genes normally up-regulated by SnRK1, ASN1 (A; At3g47340; R^2 = 0.36, SEE = 0.54), bGAL (B; At5g56870; R^2 = 0.50, SEE = 0.41), AKINb (C; At5g21170; R^2 = 0.60, SEE = 0.44), TPS8 (D; At1g70290;

R^2 = 0.59, SEE = 0.45), and TPS10 (E; At1g60140; R^2 = 0.72, SEE = 0.32) and marker genes normally down-regulated by SnRK1, UDPGDH (F; At3g29360; R2 = 0.64, SEE = 0.18), MDH (G; At3g15020; R2 = 0.70, SEE = 0.23), TPS5 (H; At4g17770; R2 = 0.68, SEE = 0.25), and bZIP11 (I; At4g34590; R2 = 0.62, SEE = 0.28). The inset graphs show the curves for values of T6P between 0 and 0.5 nmol g^{-1} FW. Horizontal error bars are the SD of three independent T6P samples, and the vertical error bars are the SD of three independent qRT-PCR samples. The fitted lines are significant for each data group (P , 0.001).

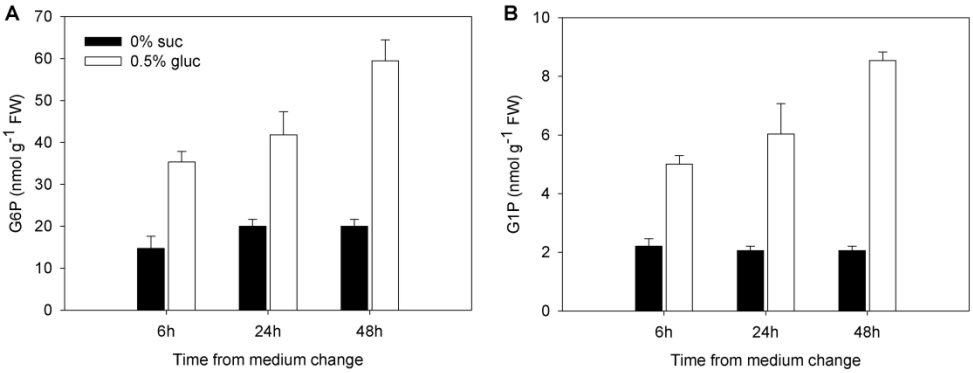

Figure 5.7. G6P and G1P accumulation in response to glucose feeding. (a), G6P and (b), G1P compared to the starvation control. Data are averages with standard deviations of 3 independent samples.

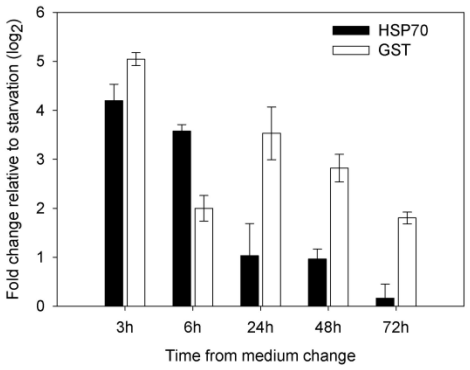

Figure 5.8. Transcript abundance of glucose marker genes determined by qRT-PCR in response to glucose feeding relative to starvation condition (HSP70, At3g12580 and GST, At1g17170). Data are averages with standard deviations of 3 independent samples.

5.3.6. Relationship between T6P, SnRK1 marker gene expression, and growth

There was no relationship between relative growth rate and T6P content (Fig. 5.9A) or between growth rate and SnRK1 marker gene expression (Fig. 5.9B and C). The close relationship between T6P and Suc and SnRK1 marker gene expression (Fig. 5.2 and 5.6) in contrast shows that T6P is primarily related to Suc and SnRK1 marker gene expression and not to growth rate. However, we hypothesised that large changes in gene expression induced by T6P, would prime growth to proceed once sink limitations to growth are removed.

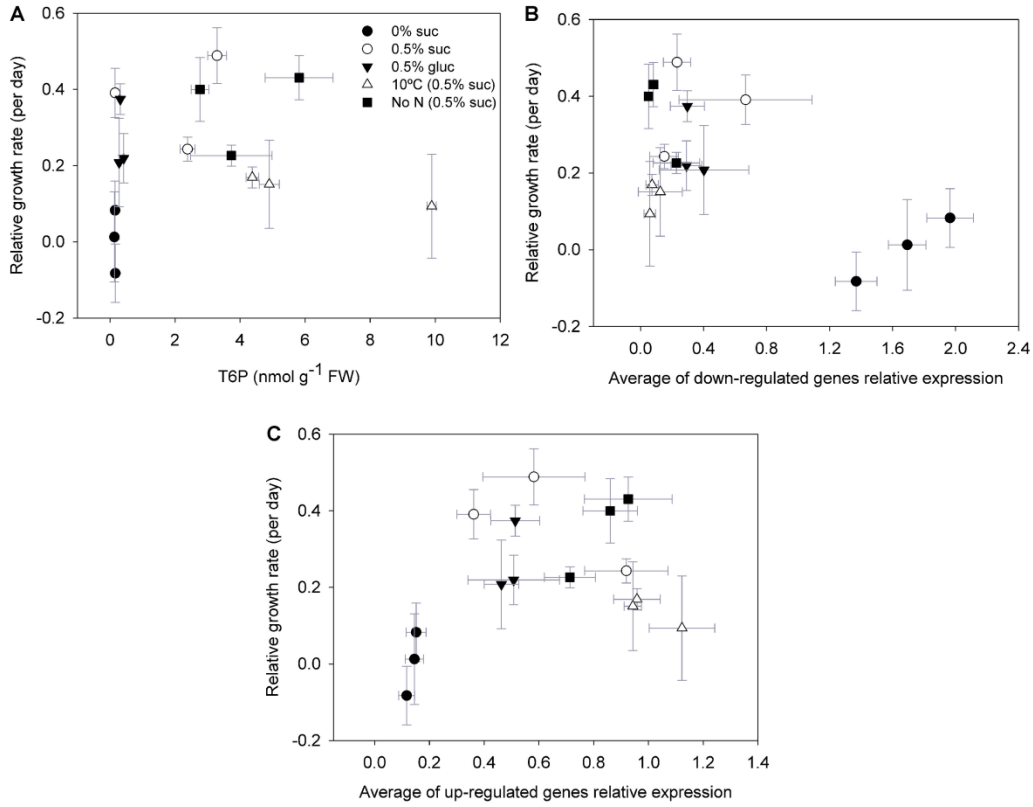

Figure 5.9. Interrelationship between growth and T6P levels and growth and SnRK1 marker gene expression. Growth was represented as the daily RGR during the 72 h of treatment. RGR versus T6P levels (A) and RGR versus averages of the relative expression of down-regulated (B) or up-regulated (C) SnRK1 marker genes. The data are means of three independent samples; error bars were omitted for

clarity. There was no statistically significant relationship between growth and T6P levels and growth and SnRK1 marker gene expression.

5.3.7. Growth recovery after 24 h cold

The hypothesis that T6P and SnRK1 are important in the growth recovery from low temperature was tested by transferring seedlings grown in the cold for 24 h and containing high T6P levels (Fig. 5.1G) to warm conditions. The experiment was also performed with plants expressing otsB to decrease T6P (Schluepmann *et al.*, 2003). In the warm condition at low exogenous sugar levels, otsB grows the same as the wild type (Fig. 5.10A; Schluepmann *et al.*, 2003). After 24 h in the cold and subsequent transfer to the warm (Fig. 5.10B), the relative growth rate of the wild type was strongly stimulated. In contrast, otsB was unable to increase growth rate upon warming ($P \leq 0.05$ at 4 h; Fig. 5.10B). T6P levels were very low in otsB seedlings (Fig. 5.10C) and growth in the cold was low in spite of high sugar levels in otsB seedlings (Fig. 5.10D). Between 11 and 24 h, growth rate of the wild type returned to former levels (Fig. 5.10B). In further confirmation of the role of the T6P/SnRK1 signaling pathway in growth recovery in warm conditions, seedlings overexpressing SnRK1 (KIN10; Baena-González *et al.*, 2007) were also subjected to the same temperature treatment (Fig. 5.10E and F). Despite some variation in the 4 h data point, growth of KIN10 was not stimulated in the short term upon transfer to the warm conditions after 24 h cold, compared with Ler, which was stimulated after 11 h ($P \leq 0.05$; Fig. 5.10F). Dry weights showed the same trend as FWs with statistical significance at 11 h ($P \leq 0.05$; Fig. 5.11). In conclusion, in these warm conditions, otsB and KIN10 grow the same as their respective wild-type controls, Col-0 and Ler, but upon transfer from cold to warm, growth recovery is impaired in the short term in otsB and KIN10, consistent with a role for T6P/SnRK1 in growth recovery from low temperature.

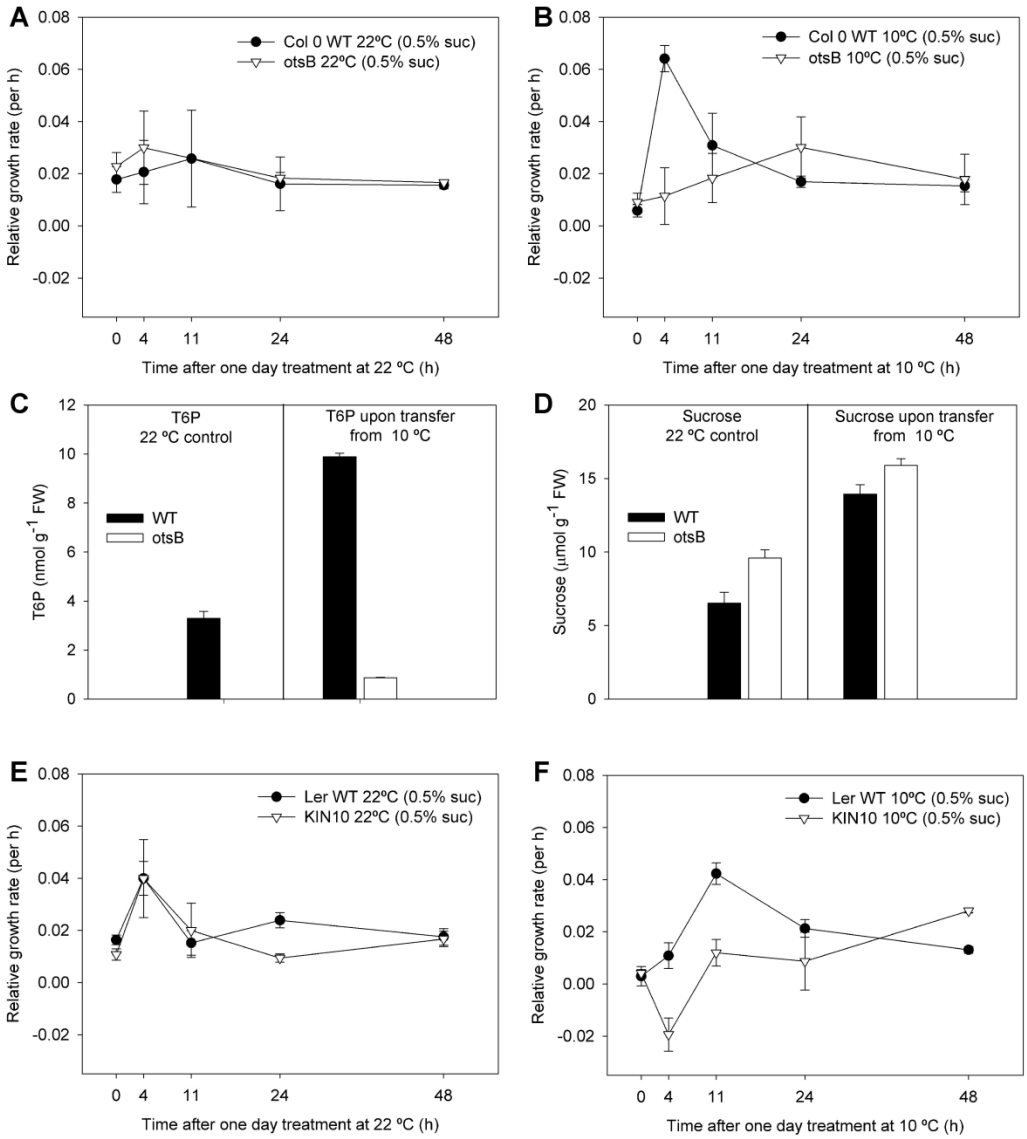

Figure 5.10. Effect on relative growth rate of altering the T6P/SnRK1 signaling pathway by transferring to 10°C for 24 h and through expression of otsB and KIN10. Seedlings were grown with 0.5% (w/v) Suc for 7 d at 22°C, either transferred to 10°C for 24 h (10°C) and then back to 22°C or held at 22°C throughout (22°C). All growth measurements were performed at 22°C. A, Relative growth rate of Col-0 WT compared with otsB maintained at 22°C. B, Relative growth rate of Col-0 WT compared with otsB transferred from 10°C. C, T6P contents of the wild type and otsB upon transfer from 10°C and control maintained at 22°C. D, Suc contents of the wild type and otsB upon transfer from 10°C and control maintained at 22°C. E, Relative growth rate of L*er* wild type compared with KIN10 maintained at 22°C. F, Relative growth rate of KIN10 compared with KIN10 control transferred from 10°C. The data are

means with SE of three independent samples. (Note: T6P levels of otsB control were below detection limit.)

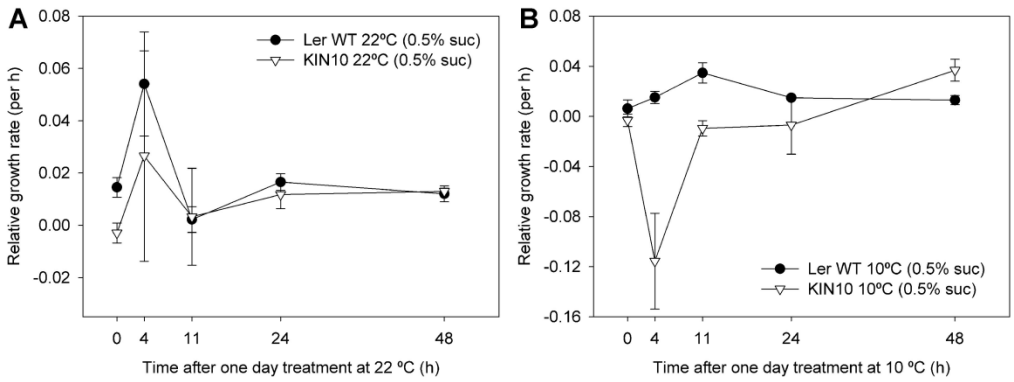

Figure 5.11. Relative growth rate calculated from dry weight of WT L*er* compared to KIN10 seedlings; (A) maintained at 22ºC or **(B)** transferred from 10ºC. Seedlings were grown with 0.5% sucrose for 7 days at 22ºC, either transferred to 10ºC for 24 h (10ºC) and then back to 22ºC or held at 22ºC throughout (22ºC). All growth measurements were performed at 22ºC. The data are means with standard errors of 3 independent samples.

5.4. Discussion

T6P is an established regulatory molecule which is indispensible for growth and has a strong impact on metabolism and development (Eastmond *et al.,* 2002; Schluepmann *et al.,* 2003; Gómez *et al.,* 2006). Strong effects of T6P can be attributed to inhibition of SnRK1 by T6P (Zhang *et al.,* 2009; Debast *et al.,* 2011; Delatte *et al.,* 2011). Inhibition of SnRK1 by T6P results in upregulation of genes involved in biosynthetic processes and growth (Zhang *et al.,* 2009; Paul *et al.,* 2010; Debast *et al.,* 2011; Martínez-Barajas *et al.,* 2011) whereas low T6P and active SnRK1 result in upregulation of plant stress responses and catabolism rather than anabolism (Baena-Gonzalez *et al.,* 2007; Zhang *et al.,* 2009; Debast *et al.,* 2011). T6P contents are related to those of Suc in plants (Lunn *et al.,* 2006; Martínez-Barajas *et al.,* 2011). Accordingly, a model has been developed where T6P elicits

changes in gene expression through regulation of SnRK1 promoting growth in relation to Suc supply. However, it is not known how the model functions under conditions where Suc is abundant but growth is limited by other factors i.e. when growth is sink-limited such as at low temperature. Is T6P simply a signal of Suc availability or is T6P also directly related to growth rate? This question was addressed through treatments that uncoupled Suc and growth through low temperature and removal of N from the growing medium.

5.4.1. T6P responds to Suc levels under all conditions

Large increases in T6P were induced in the experimental treatments (Fig. 5.1G). There was a 55-fold range of T6P levels observed overall from 0.18 nmol g^{-1} FW at the start of the experiment in seedlings with no sugar up to 9.9 nmol g^{-1} FW in cold-treated seedlings. Tissue Suc levels ranged from 1.5 µmol g^{-1} FW to 14.8 µmol g^{-1} FW, a 9.9-fold range. The relationship between tissue Suc and T6P was linear when tissue Suc was varied through feeding and through transfer of seedlings to 10^{o}C or to low N (Fig. 5.2A). This establishes that T6P responds to changes in Suc produced by environmental treatments which limit growth and not just to Suc fed externally or to Suc produced as a result of increased irradiance or changes in day length (Lunn *et al.,* 2006), i.e. T6P responds to Suc accumulation induced by sink limitation caused by low temperature and low N. The relationship between Suc and T6P was linear once a tissue level of 3 µmol Suc g^{-1} FW had been reached (Fig. 5.2A), which may represent a threshold necessary to induce T6P synthesis. It could also represent a possible famine threshold level of Suc above which growth is induced. While a strong relationship is seen between Suc and T6P, other studies (Martínez-Barajas *et al.*, 2011) in an analysis of wheat (*Triticum aestivum*) grain have shown a relationship with catabolites of Suc and T6P, including Gluc. To test the specificity of the interrelationship between Suc and T6P, feeding of 0.5% (w/v) Gluc was performed. Gluc feeding did not increase T6P (Fig. 5.1G and 5.2B) in comparison to feeding 0.5% (w/v) Suc. A recent work with a very close approach but concentrating the analysis to the first 3 h after sugar addition detected T6P correlation with Suc in Gluc-

fed seedlings. After 3 h of treatment induction we observed T6P levels of 0.16 nmol g^{-1} FW in the starved seedlings, 2.4 nmol g^{-1} FW in the Suc treatment, and 0.35 nmol g^{-1} FW in the Gluc treatment, values that, despite the first impression, are in fact of the same magnitude of those found by Yadav *et al.* (2014), who found close to 0.4 nmol g^{-1} FW T6P in the Gluc treatment. This holds true for the Suc accumulation levels. We cannot trace the correlations of this fast initial response due to not enough sampling points but argue that T6P values in the Gluc treatment must drop to starvation levels in the longer term as happened for the Suc treatment (about 0.15 nmol after 48 and 72 h) and that is the why we were not able to see any correlation between Suc and T6P in the Gluc treatment. Having said that, although the effects of these two sugars are difficult to separate in plants, because of their interconversion, this experiment provides evidence that T6P responds specifically to Suc. This was confirmed in analysis of regression between Suc, Gluc, Fru, and T6P from all the experiments (Fig. 5.2), which showed best relationships between Suc and T6P. This specific response was now confirmed by Yadav *et al.* (2014).

In terms of understanding T6P homeostasis the regulation of T6P synthesis may be explained by a general upregulation of trehalose pathway gene expression by Suc at the level of *TPS1* and *TPPB,* to catalyze flux of carbon through the pathway in relation to Suc availability. However, expression of these genes can be explained only in part by changes in Suc; other factors as indicators of sink activity or stress may also regulate *TPS1* expression and T6P content at other control points under low temperature and low N. Expression of these genes was not well related to endogenous Gluc but was still upregulated in this treatment, even though Gluc did not stimulate T6P synthesis to levels as elevated as the Suc treatment, possibly due to lower endogenous Suc levels, again indicating that a Suc specific activation component may be necessary for T6P synthesis.*TPPA* expression is likely regulated by factors other than Suc. Firmer conclusions were recently drawn by Yadav *et al.* (2014) who showed that *de novo* transcription is not required for T6P synthesis but *de novo* protein synthesis is, albeit not of TPS1, which activity together with that of TPP can be directly influenced by Suc but this is not the predominant reason for T6P

accumulation. Further research is still needed to elucidate all the factors that regulate the trehalose biosynthetic pathway when Suc accumulates under different conditions.

We then went on to determine the interrelationship between T6P and the transcript abundance of SnRK1 marker genes under the different conditions. T6P is known to promote growth and to promote transcription of genes associated with biosynthetic processes and growth (Baena-González *et al.*, 2007; Zhang *et al.*, 2009; Debast *et al.*, 2011). Given that T6P was related to Suc levels under all treatments with different growth rates, we wished to determine if transcript abundance of SnRK1 markers was related to T6P or to growth rate.

5.4.2. SnRK1 target gene expression changes in relation to T6P and not directly to growth rate

There was a strong correlation between T6P and SnRK1-regulated gene expression (Fig. 5.6), but not between T6P and relative growth rate (Fig. 5.9A). This establishes quite clearly that SnRK1 marker gene expression responds closely to T6P content irrespective of the growth outcome. Changes in gene expression were elicited above and below a threshold level of T6P of 0.3 to 0.5 nmol g^{-1} FW (Fig. 5.6). Assuming T6P is cytosolic and the cytosol accounts for 10% tissue water, cytosolic concentrations of T6P will be in the region of 10-fold higher than when expressed on a whole tissue basis. Strikingly, this would equate to 3 to 5 mM T6P close to the T6P/SnRK1 dissociation constant calculated as 4 mM (Chapter II). From what is known about the inhibition of SnRK1 by T6P, this would enable high SnRK1 activity at 1.8 mM T6P (at the start of the experiment) and strong inhibition possibly by 80% or more at 99 mM T6P (Zhang *et al.*, 2009) in the cold. In contrast, changes in *in vitro* SnRK1 activities measured without T6P in the assay were less than 2-fold throughout the experiment (Fig. 5.4A, C, and D). These measurements *in vitro* effectively show maximum catalytic potential or enzyme concentration and do not reflect regulation by T6P. *In vivo*, a large dynamic range of T6P in response to environmentally induced changes in Suc induced by sink limitation would provide a powerful means of

regulation of SnRK1 in response to Suc supply demonstrated in the readout of SnRK1 marker gene expression.

As the relationship between T6P and SnRK1 marker gene abundance held even when the growth rate was low, i.e. under sink-limited conditions, we went on to test the physiological significance of the increase in T6P and gene expression under sink-limited conditions. What could be the adaptive advantage of activating gene expression in this way if growth was inhibited? We posed the hypothesis that the T6P/SnRK1 signaling pathway primes growth to proceed once sink limitation is relieved. By priming, we mean being in a prepared state with an advanced capacity to activate growth following relief of a growth limitation, such as upon relief of low temperature.

5.4.3. T6P primes gene expression for growth when Suc availability is high

To test this idea, sink limitation was relieved while Suc and T6P contents were high, by transferring seedlings grown in the cold for 24 h to the warm. Growth rate of these seedlings with elevated T6P was 3-fold higher in the first few hours upon return to the warm conditions compared with controls that had been kept in the warm (Fig. 5.10A and B). The experiment was also performed with seedlings where T6P levels were decreased through expression of otsB encoding an E. coli TPP. T6P was strongly decreased in otsB compared with the wild type even though sugar contents of these seedlings were very high. When grown with low sugar content, otsB grows at a similar growth rate to the wild type (Schluepmann *et al.*, 2003). However, growth of these seedlings upon transfer to the warm was severely compromised (Fig. 5.10B). This would indicate that T6P is necessary for rapid growth after the cold-to-warm transfer. To further confirm the role of T6P/SnRK1, the experiment was also performed on seedlings overexpressing SnRK1 (KIN10; Baena-González *et al.*, 2007). These seedlings too were unable to rapidly increase growth in response to the warm conditions (Fig. 5.10E and F). Therefore, we conclude that the T6P/SnRK1

signaling pathway is necessary to potentiate rapid growth following relief from low temperature.

5.4.4. Gluc results in moderate regulation of SnRK1-regulated genes

In spite of no (or incredibly low) induction of T6P accumulation by Gluc feeding (Fig. 5.1G) there was a change in SnRK1 marker gene expression in response to Gluc feeding which was more moderate than that induced by Suc (Fig. 5.5 and 5.6). New results from Yadav *et al.* (2014) obtained in the first 3 h of Gluc treatment revealed that T6P accumulates in this treatment but to very low levels, an effect that we ca also observe in the inset graphs of Fig. 5.6. These low T6P levels may not be enough to induce the observed changes in gene regulation suggesting that other factors might regulate these genes either through SnRK1 or through other mechanisms. Both G6P and G1P increased during Gluc feeding (Fig. 5.7A and B). G6P and G1P inhibit SnRK1 (Toroser *et al.*, 2000; Chapter II), although far less potently than T6P. This milder effect on gene expression and smaller stimulation of growth compared with Suc control could be due to regulation of SnRK1 at least in part by a combination of these metabolites. The magnitude of gene expression and growth effects reflects less potent regulation of SnRK1 in response to Gluc.

In conclusion we show that restriction of growth by low temperature or low N leads to large increases in T6P. While the regulation of SnRK1 in response to endogenous Suc levels likely involves factors in addition to T6P, *in vitro* catalytic data, and now *in vivo* gene expression data in a physiological context, support the view that T6P regulation of SnRK1 provides an explanation at least in part for the control of growth in response to tissue Suc availability providing other factors are not limiting. Evidence presented suggests the mechanism operates above a level of Suc of 3 μmol g^{-1} FW and 0.3 to 0.5 nmol T6P g^{-1} FW likely to indicate a Suc starvation threshold. This starvation threshold (3–5 mM T6P) is close to the K_i of the T6P/SnRK1 complex (Zhang *et al.*, 2009; Chapter II). Increases in Suc above this

level through Suc feeding or through treatments that induce sink-limited growth resulted in a proportionate increase both in T6P content and changes in expression of SnRK1 marker genes. SnRK1 is likely inhibited *in vivo* by up to 80% or more by T6P under the physiological conditions caused by low temperature. Under such sink-limited conditions, T6P is not directly related to growth rate; the regulation of growth here is downstream of the T6P/SnRK1 mechanism. However, the changes in gene expression induced by T6P under such conditions would prime growth to proceed once the growth limitation is removed. The T6P/SnRK1 signaling pathway is necessary for the acceleration of growth following relief from sink-limited conditions, such as low temperature.

5.5. Materials and Methods

5.5.1. Plant material and growth conditions

Seeds of Arabidopsis (*Arabidopsis thaliana* (L.) ecotype Col-0) were weighed in batches of 2.5 mg and surface-sterilised for 10 min in a 10% sodium hypochlorite solution with triton x-100 and rinsed twice in sterile water. Each seed batch was grown in 50-ml half-strength Murashige and Skoog medium (ApolloScientific PMM524) plus Gamborg's vitamins (Sigma G1019) and 0.5% Suc (0.25 g/ 50 ml medium) in culture flasks (300 ml polystyrene containers, Greiner). After cold treatment for 2 days in the dark at 4ºC they were transferred to the growth room for 7 days at 23ºC (16 h light/ 8 h dark) with 130 µmol quanta m^{-2} s^{-1} irradiance with gentle shaking. At day 8 the medium was removed and the plantlets were washed thoroughly twice with sterile water. The same volume of fresh medium was added to five groups of plants. Group 1 had no added sugar; group 2, 0.5% Suc; group 3, 0.5% Suc and transferred to 10ºC; group 4, half-strength Murashige and Skoog medium without N (ApolloScientific PMM531) with everything else the same and 0.5% Suc; group 5, 0.5% Gluc (no Suc). Five plants were harvested before medium change (time 0) and 5 of each group were harvested 3, 6, 24, 48 and 72 h after medium change. Medium change was performed 4 h after the start of the light

period. Hence harvests at 3 h and 6 h were 7 and 10 h into the photoperiod and harvests at 24 h, 48 h and 72 h were 4 h into the photoperiod. Harvests were done within two minutes under the growth light conditions. Seedlings from each pot were rinsed in distilled water, gently blotted dry with tissue paper, weighed, and snap-frozen in liquid N. Transgenic Arabidopsis expressing the TPP gene otsB in Col-0 background and overexpressing KIN10 in L*er* background were as described previously (Schluepmann *et al.*, 2003; Baena-González *et al.*, 2007). For the relative growth rate (RGR) experiment, seedlings were grown with 0.5% (w/v) Suc for 7 d at 22°C, after which medium was changed as previously stated and either transferred to 10°C for 24 h and then back to 22°C or held at 22°C throughout. Harvests were all performed at 22°C as described above at time points -24, 0, 4, 11, 24, and 48 h. The RGR was calculated using the method indicated by Hoffmann and Poorter (2002):

$$RGR = \frac{\overline{ln\,(W2)} - \overline{ln\,(W1)}}{t2\ - t1}$$

Where $\overline{ln\,(W)_t}$ is the mean of the ln-transformed plant weights at time t.

5.5.2. Assay for SnRK1 activity

Total soluble protein was extracted from 200 mg of ground tissue. For the detailed protocol please refer to Chapter II. SnRK1 activity of three replicates for each time point was determined as in Zhang *et al.,* (2009), also described in detail in Chapter II.

5.5.3. Sugars, glucose 6-phosphate and glucose 1-phosphate quantification

Seedling material (100 mg) was ground to powder in liquid N and homogenised in 250 µl cold 5% (v/v) perchloric acid to denature any enzymes that might change sugars abundance. After 30 min on ice, homogenate was centrifuged for 2 min at 13,000g at 4ºC. The pellet was kept at -80 ºC for posterior starch

quantification and the supernatant was neutralized with 5 M KOH buffered with 1 M triethanolamine. Metabolites were measured using enzyme-linked assays as described by Jones *et al.* (1977). The assays are based on the change of absorbance at a wavelength of 340 nm when $NADP^+$ is converted to NADPH, coupled with the conversion of G6P to 6-phosphogluconate. Gluc, Fru and Suc were assayed together in 100 mM imidazole and 10 mM $MgCl_2$ adjusted to pH 6.9 with HCl. Just before quantification 1.1 mM ATP, 0.5 mM $NADP^+$ and 0.14 U G6PDH were added to the necessary buffer volume. After centrifugation at 13,000g at 4 ºC for 2 min, 5 to 20 µl of seedling extract was added to 200 µl of buffer plus additions in a 96-well microplate. The change in absorbance relative to the background value was measured in a SpectraMax 96-well plate reader. The sequential addition of 0.12 U hexokinase, 0.035 U phosphoglucoisomerase and 4 U invertase to the reaction buffer, enables the quantification of Gluc, Fru and Suc in sequence (Fig. 5.12).

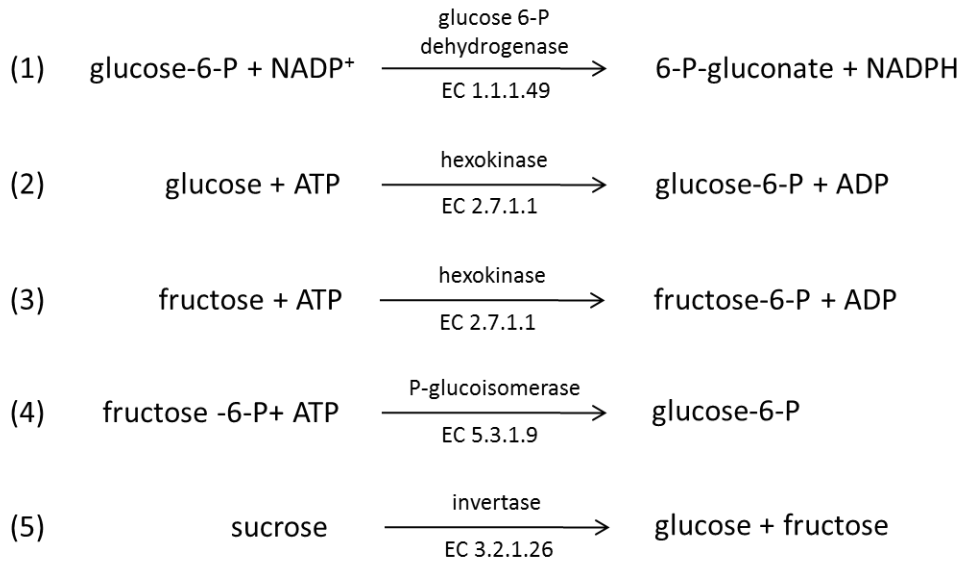

Figure 5.12 Enzyme reactions for the determination of carbohydrates. The assay measures the change of absorbance at a wavelength of 340 nm when $NADP^+$ is converted to NADPH, coupled with the conversion of G6P to 6-phosphogluconate. When hexokinase is added to the assay glucose and fructose are phosphorylated to G6P and F6P respectively (2 and 3). G6P is therefore subsequently converted to 6-P-gluconate by the G6P dehydrogenase already in the reaction mixture (1) quantifying

glucose. Phosphoglucoisomerase then converts F6P to G6P (4) which react again quantifying fructose. Finally, invertase cleaves sucrose to glucose and fructose (5), both taken through the reactions and sucrose is quantified.

For the quantification of starch, the stored pellet from the carbohydrates extraction is washed twice with 1 ml of water to remove any present soluble carbohydrates. After centrifugation at 13,000g for 2 min at 4ºC the pellet was ressuspended in 250 µl sodium acetate buffer (100 mM, pH 4.8) containing 2 U α-amylase and 0.05 U amyloglucosidase. Full conversion of starch to Gluc was achieved after 36 h at 37ºC. The pellet can be discarded after centrifugation. The Gluc in the supernatant can then be quantified as described above (2 and 1).

For the quantification of sugar-phosphates, G6P was determined according to reaction (1) and for G1P a further enzyme was necessary, 0.05 U phosphoglucomutase.

(6) glucose 1-P $\xrightarrow[\text{EC 5.4.2.2}]{\text{P-glucomutase}}$ glucose-6-P

Figure 5.13. Enzyme reaction for the determination of G1P.

Sugar-phosphates were assayed on a dual-wavelength spectrophotometer DW2000 at 340 and 410 nm. A 1 ml cuvette was used with 100 µl of sample, and 900 µl 50 mM HEPES buffer pH 7, with 5 mM $MgCl_2$, 0.25 mM NADP and 0.12 mM Na pyrophosphate. After reaching a stable background reading, 0.1 U G6PDH was added in a volume of 2 µl HEPES buffer using a plastic cuvette stirrer to quantify G6P (1). After reaching a stable reading 0.05 U PGM was added in the same way to measure G1P (6) (Fig. 5.13).

5.5.4. T6P determinations

T6P was quantified in Arabidopsis seedling extracts using anion exchange HPLC coupled with electrospray ionisation mass spectrometry following liquid-liquid and solid-phase extraction as described by Delatte *et al.* (2009) and detailed below.

5.5.4.1. Extraction of T6P from Arabidopsis seedlings

Seedling material (50mg) was ground to fine powder at liquid N temperature. To each sample was added 3 µl of 1 nmol/10ul 10x concentrated solution of lactose 1-phosphate as an internal standard. The plant material was homogenized in 500 µl of fresh 70% acetonitrile and 30% chloroform (v/v) solution and immediately vigorously mixed in the vortex for 30 sec. Samples were incubated for 2 h at -20 ºC with occasional mixing (every 10 to 15 min). In the cold room water soluble compounds (including T6P) were extracted with 400 µl ice-cold water with vigorous shaking in the vortex for 30 sec. Phases were separated by centrifugation at 13000g for 5 min at 4 ^{o}C. The top aqueous layer containing T6P is transparent to red and it is separated from the bottom organic green phase by a thin white starch layer. The top layer is carefully transferred to a new tube and water extraction is repeated one more time giving approximately 800 µl of water and acetonitrile. Each sample was evaporated to dryness in the vacuum dry evaporator. The sample is stable at this point and was reconstituted with 2 ml of water only on the day of solid phase extraction. Only half of the volume was loaded onto the column (therefore only the equivalent to 25 mg of tissue). Oasis-Max columns (Oasis MAX flangeless cart.1cc/30mg Waters Ref.186001883) were used to remove lipophilic substances like pigments. In the vacuum manifold draw through by gravity flow 1 mL methanol, followed by 1 mL of water and 1 ml of sample. The columns were then washed with 1 ml of water followed by 1 ml of methanol, the pump must be used at this point to dry the column beads. Elution was performed thrice with 500 µl of freshly made 2% formic acid in methanol. The 3 elutes were collected to the same tube and the pump was used only if necessary to remove bubbles and to finish dry the last elute step. If the samples are

red in colour due to antocianines (not this case), an additional cleaning column should be used, the Mix Mode cation exchange (Oasis MCX cart.1cc/30mg Waters Ref.186000252). Samples were dried again, this time under N flow and stored at -20 °C. On the quantification day samples are reconstituted in 200 µl of water.

5.5.4.2. Liquid chromatography

To achieve enough selectivity, anion exchange chromatography (AEC) was coupled with negative mode electrospray ionization (ESI)–MS using an ion trap mass spectrometer. To make these compatible an ion suppressor was added between the liquid chromatography (LC) column and the MS sprayer. A DX 500 high-performance liquid chromatography (HPLC) system (Dionex, Sunnyvale, CA, USA) was used for AEC. The LC system consisted of a Dionex IonPac AS11-HC column (250 x 2.0 mm, particle size 9 µm) and a GP-40 gradient pump coupled with an AS-3500 autosampler. The AEC gradient program was as summarized in Table 5.1. The injection volume was 20 µl and the flow rate was 0.2 ml min^{-1}. Detection was achieved using MS system.

Table 5.1. Gradient program used for T6P analysis by anion exchange chromatography.

Time (min)	100 mM NaOH (%)	Water (%)
0	5	95
5	5	95
25	29	71
26	100	0
46	100	0
50	5	95
60	5	95

5.5.4.3. Mass spectrometry

An ion trap series 6330 XCT model mass spectrometer (Agilent Technologies, Palo Alto, CA, USA) prepared with an ESI source using an LC sprayer (Agilent Technologies) was coupled with the AEC system. The on-line coupling of AEC and

ESI–MS detection was only possible with an ASRS–MS ion suppressor (Dionex) installed between the AEC column and the ESI sprayer; which exchanges sodium ions for hydrogen ions in the mobile phase forming water with the hydroxide ions present in the mobile phase. The suppressor was adjusted to an electrical current of 50 mA, with an external water flow of 3 ml min^{-1}. The ion trap mass spectrometer was operated in negative ion mode. The electrospray voltage was 5 kV, and the MS capillary voltage was 137.7 V. The nebulizing gas pressure was fixed at 40 psi, the dry gas flow rate was 8 L min^{-1}, and the dry gas temperature was set at 325 ºC. Target ion charge control (ICC) was set at 30,000 with a maximum filling time at 50 ms. Data were collected using a scan range of 418 to 423 m/z and analyzed with DataAnalysis 3.4 software from Agilent Technologies.

5.5.4.4. Quantitative analysis

The data acquired from the AEC–MS was used to produce ion chromatograms corresponding to T6P (421 ± 0.5 m/z). T6P peaks were integrated using DataAnalysis 3.4 software. Aqueous T6P standards were used to create five-point calibration curves in the range of 19.5 nM to 2.5 µM, one calibration curve per day was found enough for accurate T6P quantification. The T6P peak areas in the Arabidopsis samples were determined and T6P concentration inferred from the calibration curve.

5.5.5. RNA extraction and qRT-PCR

Total RNA was extracted from 100 mg of snap-frozen ground Arabidopsis seedlings using RNeasy Plant Mini Kit (Qiagen, Hilden, Germany) following the protocol provided. RNA was quantified by Nanodrop Spectrophotometer (ND-1000) and its integrity evaluated by agarose gel electrophoresis. Potential present DNA was removed with RQ1 RNase-free DNase (Promega, Madison, USA; M610A). cDNA was synthesized by reverse transcribing 1 µg of RNA using SuperScript III First-Strand Synthesis System for RT-PCR (Invitrogen) according to the manfacturer's protocol. Gene expression was quantified using SYBR Green chemistry on a iQ™

Real-Time PCR system (Bio-Rad) in 20 µL for each reaction, containing 10 µL of iQ^{TM} SYBR Green Supermix (Bio-Rad), 3 µL of cDNA, and 0.5 µM of gene-specific primers shown in Table 5.2 PCR used an initial denaturing stage of 95ºC for 3 min followed by 45 cycles of 95ºC for 10 s, followed by an annealing step at 60ºC for 10 s and an extension step at 72ºC for 10 s. The specificity of products was confirmed by performing a melting temperature analysis at temperatures ranging from 55°C to 95°C in intervals of 0.5°C. PCR was performed with two technical replicates repeated on three biological replicates. Data were normalized using a combination of 3 reference genes: yellow-leaf-specific protein 8 (At5g082290), ubiquitin-transferase family protein (At3g53090) and protein phosphatase 2A subunit (At1g13320) (Czechowski *et al.,* 2005), and setting the expression of each gene in relation to the gene expression level of the control samples (0% Suc). Intron-spanning primers (Table 5.2) were designed using the Primer Express software version 2.0 (Applied Biosystems).

Table 5.2. Sequences of the gene-specific primers used for qRT-PCR analysis. Specific primers for 4 up-regulated and 5 down-regulated SnRK1 marker genes and 4 reference genes.

Annotation	AGI	Sense (5' to 3')
UBQ1	At3g53090	Fwd: 5'-TTCAAATACTTGCAGCCAACCTT-3' Rev: 5'-CCCAAAGAGAGGTATCACAAGAGAC^T-3'
YLS8	At5g08290	Fwd: 5'-TCTGCACTCCGGTTGGGCTG-3' Rev: 5'-GCAACAGACGCAAGCACCTCA-3'
UBC9	At4g27960	Fwd: 5'-TGGATCGTGGGATTTTGGAAATGGC-3' Rev: 5'-GCAACGGGTCCTGCGCTACAT-3'
PP2A	At1g13320	Fwd: 5'-GCTGCTGCAAACAATCTGAAGCG-3' Rev: 5'-GCGAGAAGCGATACTGCACGAAG-3'
TPS1	At1g78580	Fwd: 5'-ACCATAGTTGTTCTGAGCGGAAGCA-3' Rev: 5'-TCATCCACTCTCCATTCGTAAGCCT-3'
TPPA	At5g51460	Fwd: 5'-TGCCAAGTATTTCCCTACCGCGA-3' Rev: 5'-CCATTCCATGGCTTCCGGCGT-3'
TPPB	At1g78090	Fwd: 5'-GGGACAAGGGCCAGGCACTC-3' Rev: 5'-ACACCGGCACAACATCATCCGA-3'
AKIN10	At3g01090	Fwd: 5'-CCGCTCCAGAGGTAATTTCG-3' Rev: 5'-CACACCACAGCTCCAGACATCT-3'

AKIN11	At3g29160	Fwd: 5'-CACCATTCCTGAGATCCGTCA-3' Rev: 5'-GAGACAGCAAGATAACGAGGGAG-3'
ASN1	At3g47340	Fwd: 5'-TGATGTCGAACGCGGGGCAT-3' Rev: 5'-CCACGGTGGCACCTCCAGGA-3'
βGAL4	At5g56870	Fwd: 5'-ACTCAGGAACATGGGACATGTCGA-3' Rev: 5'-TCCTTGAGTCCATCTCACACCGGA-3'
AKINβ1	At5g21170	Fwd: 5'-CCCTTTGTAGCAGACGAAGTTGGCA-3' Rev: 5'-CAGGTGATGGTGGCGCCTCA-3'
TPS8	At1g70290	Fwd: 5'-GCACAGTGACAAATCCGGAAC-3' Rev: 5'-GCTTGGTTTTCTTCCAACCG-3'
TPS10	At1g60140	Fwd: 5'-AAACCGAGCAAAGCCAAATAC-3'T Rev: 5'-CTTGAAGCAACTTCACCACGTC-3'
UDPGDH	At3g29360	Fwd: 5'-GGAGGGCGGGAAACCCCAGA-3' Rev: 5'-GGCCTTCAGGAACCCAGTGTGC-3'
MDH	At3g15020	Fwd: 5'-AGGGCCACTCTCAGACTTTGAA-3' Rev: 5'-GGATTTGAGTTCTGCCTTGAGG-3'
TPS5	At4g17770	Fwd: 5'-TCTCGGTTTGGGTGCAGAGCA-3' Rev: 5'-ACCAAACTCGACGTTTCCCAGTC-3'T
bZIP11	At4g34590	Fwd: 5'-TGGGCATGTGTTCGAACCCTCT-3' Rev: 5'-AGACGCCATGAGAGGCTGGT-3'

5.5.6. Statistical analysis

The relationship between T6P and sugars and T6P and SnRK1 marker genes relative expression was tested using Pearson Product Moment Correlation analysis. The analysis was performed using SigmaPlot 11.0 (Systat Software, San Jose, CA). Each regression is associated to the r^2 value, the standard error of estimates (SEE) and the P value that characterizes the model.

Acknowledgements

I, Cátia Nunes, performed and analysed the presented experimental work with the following collaborations: Liam O'Hara performed the WT L*er* and AKIN10 mutants growth experiments; Dr. Thierry Delatte performed the T6P quantifications at Utrecht University; and to whom I am deeply grateful. The planning of the research work and discussion of results was done by Cátia Nunes and Dr. Matthew Paul.

5.6. References

Baena-González E, Rolland F, Thevelein JM, Sheen J (2007) A central integrator of transcription networks in plant stress and energy signaling. Nature **448**: 938-942

Czechowski T, Stitt M, Altmann T, Udvardi MK, Scheible WR (2005) Genome-wide identification and testing of superior reference genes for transcript normalization in Arabidopsis. Plant Physiol **139**: 5–17

Debast S, Nunes-Nesi A, Hajirezaei MR, Hofmann J, Sonnewald U, Fernie AR, Börnke F (2011) Altering trehalose-6-phosphate content in transgenic potato tubers affects tuber growth and alters responsiveness to hormones during sprouting. Plant Physiol **156**: 1754-1771

Delatte TL, Selman MHJ, Schluepmann H, Somsen GW, Smeekens JCM, de Jong GJ (2009) Determination of trehalose 6-phosphate content in Arabidopsis seedlings by successive extractions followed by anion exchange chromatography-mass spectrometry. Anal Biochem **389**: 12-17

Delatte TL, Sedijani P, Kondou Y, Matsui M, de Jong GJ, Somsen GW, Wiese-Klingenberg A, Primavesi LF, Paul MJ, Schluepmann H (2011) Growth arrest by trehalose-6-phosphate: an astonishing case of primary metabolite control over growth by way of the SnRK1 signaling pathway. Plant Physiol **157**: 160-174

Eastmond PJ, van Dijken AJ, Spielman M, Kerr A, Tissier AF, Dickinson HG, Jones JD, Smeekens SC, Graham IA (2002) Trehalose-6-phosphate synthase 1, which catalyses the first step in trehalose synthesis, is essential for Arabidopsis embryo maturation. Plant J **29**: 225-235

Gómez LD, Baud S, Gilday A, Li Y, Graham IA (2006) Delayed embryo development in the Arabidopsis trehalose 6-phosphate synthase 1 mutant is associated with altered cell wall structure, decreased cell division and starch accumulation. Plant J **46**: 69-84

Gómez LD, Baud S, Gilday A, Feil R, Lunn JE, Graham IA (2010) AtTPS1 mediated trehalose 6-phosphate synthesis is essential for embryonic and vegetative growth and responsiveness to ABA in germinating seeds and stomatal guard cells. *Plant J.* doi: 10.1111/j.1365-313X.2010.04312.x

Hardie DG (2007) AMP-activated/SNF1 protein kinases: conserved guardians of cellular energy. Nat Rev Mol Cell Bio **8**: 774-785

Hoffmann WA, Poorter H (2002). Avoiding bias in calculations of relative growth rate. Ann Bot 80: 37-42

Jones MGK, Outlaw WH, Lowry OH (1977) Enzymic assay of 10−7 to 10−4 mol of sucrose in plant tissues. Plant Physiol **60**: 379–383

Kolbe A, Tiessen A, Schluepmann H, Paul M, Ulrich S, Geigenberger P (2005) Trehalose 6-phosphate regulates starch synthesis via post-translational redox activation of ADP-glucose pyrophosphorylase. Proc Natl Acad Sci USA **102**: 11118-11123

Lunn JE, Feil R, Hendriks JHM, Gibon Y, Morcuende R, Osuna D, Scheible W-R, Carillo P, Hajirezaei M-R, Stitt M (2006) Sugar-induced increases in trehalose 6-phosphate are correlated with redox activation of ADP-glucose pyrophosphorylase and higher rates of starch synthesis in *Arabidopsis thaliana*. Biochem J **397**: 139-148

Martínez-Barajas E, Delatte T, Schluepmann H, de Jong GJ, Somsen GW, Nunes C, Primavesi LF, Coello P, Mitchell RAC, Paul MJ (2011) Wheat grain development is characterized by remarkable trehalose 6-phosphate accumulation pregrain filling: tissue distribution and relationship to SNF1-related protein kinase1 activity. Plant Physiol **156**: 373-381

Paul MJ, Stitt M (1993) Effects of nitrogen and phosphorus deficiencies on levels of carbohydrates, respiratory enzymes and metabolites in seedlings of tobacco and their response to exogenous sucrose. Plant Cell Environ **16**: 1047-1057

Paul MJ, Jhurreea D, Zhang Y, Primavesi LF, Delatte T, Schluepmann H, Wingler A (2010) Up-regulation of biosynthetic processes associated with growth by trehalose 6-phosphate. Plant Signal Behav **5**: 386-392

Ramon M, Rolland F (2007) Plant development: introducing trehalose metabolism. *Trends* Plant Sci **12**: 185-188

Schluepmann H, Pellny T, van Dijken A, Smeekens S, Paul M (2003) Trehalose 6-phosphate is indispensable for carbohydrate utilisation and growth in *Arabidopsis thaliana*. Proc Natl Acad Sci USA **100**: 6849-6854

Toroser D, Plaut Z, Huber SC (2000) Regulation of a plant SNF1-related protein kinase by glucose 6-phosphate. Plant Physiol **123**: 403-411

Usadel B, Bläsing O, Gibon Y, Poree F, Hähne M, Günter M, Trethewey R, Kamlage B, Poorter H, Stitt M (2008) Multilevel genomic analysis of the response of transcripts, enzyme activities and metabolites in Arabidopsis rosettes to a progressive decrease of temperature in the non-freezing range. Plant Cel Environ **31**: 518-547

Vandesteene L, López-Galvis L, Vanneste K, Feil R, Maere S, Lammens W, Rolland F, Lunn JE, Avonce N, Beeckman T, Van Dijck P (2012) Expansive evolution of the *TREHALOSE-6-PHOSPHATE PHOSPHATASE* gene family in *Arabidopsis thaliana*. Plant Physiol **160**: 884-896

Vandesteene L, Ramon M, Le Roy K, Van Dijck P, Rolland F (2010) A single active trehalose-6-P synthase and a family of putative regulatory TPS-like proteins in Arabdiopsis. Mol Plant **3**: 406-413

Wingler A, Delatte TL, O'Hara LE, Primavesi LF, Jhurreea D, Paul MJ, Schluepmann H (2012) Trehalose 6-phosphate is required for the onset of leaf senescence associated with high carbon availability. Plant Physiol 158: 1241–1251

Yadav UP, Ivakov A, Feil R, Duan GY, Walther D, Giavalisco P, Piques M, Carillo P, Hubberten HM, Stitt M, Lunn JE (2014) The sucrose-trehalose 6-phosphate (Tre6P) nexus: specificity and mechanisms of sucrose signaling by Tre6P. J Exp Bot **65**: 1051-1068

Zhang Y, Primavesi LF, Jhurreea D, Andralojc PJ, Mitchell RAC, Powers SJ, Schluepmann H, Delatte T, Wingler A, Paul MJ (2009) Inhibition of Snf1-related protein kinase (SnRK1) activity and regulati*Arabidopsis thaliana*on of metabolic pathways by trehalose 6-phosphate. Plant Physiol **149**: 1860-1871

CHAPTER VI

Concluding Remarks and Future Perspectives

6.1. Project Summary

In our exceedingly populated world, science is unequivocally needed to fulfil food and energy increasing demand. Because plant growth, development and yield are the basis of those requirements, natural fluctuations due to environmental conditions constitute an important vulnerability issue. It is a scientific (challenging) goal to understand the regulatory mechanisms that underlie those fluctuations. The multitude of intertwined pathways that regulate plant environmental responses must be identified, studied in detail and cross points identified so that manipulation strategies can become a concrete alternative for improved plant production. The overall goal of this study was to increase our knowledge about one of those pathways, the SnRK1/T6P signaling pathway, both at the biochemical, molecular and physiological levels. SnRK1 of the SNF1/ AMPK group of PKs is an evolutionary conserved plant metabolic regulator that integrates energy availability with growth responses. SnRK1 was recently shown as a target of the sugar signal, T6P. T6P responds to sugar availability and through a separable factor inhibits SnRK1 which reprograms the transcriptome to promote growth processes. This suggests the importance of *in vivo* metabolic regulation of SnRK1. Concisely we started this work by analyzing the enzyme kinetics of SnRK1 inhibition by T6P as well as that of other inhibitors that we found to be cumulative and synergistic with T6P in SnRK1 inhibition. The identification of the intermediate Factor I that mediates the inhibitory effect of T6P over SnRK1 could have contributed with further insight on where and how T6P exerts its effects *in vivo*. We were able however to pave the way to ease future attempts of identification. Highly relevant was the inclusion of wheat in this study, providing the first clues about the tissue-specific regulation of SnRK1 by T6P during wheat grain development. Our findings can become a new means of improving yield of this important global food source. Finally, establishing the role of the pathway under sink limited conditions confirmed the hypothesis that the T6P/SnRK1 signaling pathway enables growth recovery following relief of stress imposed limitations.

6.2. SnRK1 metabolic regulation

When we started our work, besides T6P (Zhang *et al.*, 2009), G6P (Toroser *et al.*, 2000) had also been identified as a SnRK1 metabolic inhibitor. Therefore we started out by analysing a list of compounds to potentially identify additional SnRK1 regulators. Among others, several nucleotides inhibited SnRK1 by directly competing with ATP. In fact, this inhibition seems unlikely to occur in the cell because conditions that translate into increased nucleotide concentrations are also those where SnRK1 is expected to be more active, we cannot rule out however, a scenario of feedback regulation of SnRK1 by ADP or AMP. SnRK1 protection from dephosphorylation by AMP observed by Sugden *et al.* (1999) fits much better with what is known about its counterparts. Both mammalian AMPK and yeast SNF1 are activated in different ways by AMP and ADP. The *in vivo* relevance of the observed competition would be highly dependent on relative amounts of each nucleotide, the corresponding binding affinities as well as on binding levels with Mg^{2+}. In fact, enzyme regulation by nucleotides seems to be highly dependent on ratios of bound and unbound nucleotides to Mg^{2+} (Molnar and Vas, 1993; Jenkins *et al.*, 2011). On the one hand the lack of sequence conservation in critical regulatory points between SNF1 and AMPK (Xiao *et al.*, 2011) and certainly SnRK1 suggest differences in the regulatory mechanisms of these homologous enzymes but on the other hand parallelisms are also very expected. In order to fully understand these regulatory mechanisms full-length structures of the SnRK1 catalytic subunits containing the phosphorylated kinase domain must be obtained in the presence of Mg^{2+}, ATP and the other nucleotides.

At that point we have also observed a strong inhibition of SnRK1 by R5P and Ru5P, absent from non-chlorophyllous tissues like Arabidopsis roots and cauliflower florets (Chapter II). Together with the observation that gene expression related to photosynthesis is particularly strongly correlated with SnRK1 activity (Zhang *et al.*, 2009) the argument that these Calvin cycle metabolites could constitute a SnRK1 regulation pathway directly connecting growth to photosynthesis was quite tempting. Also, Piattoni *et al.* (2011) later on concluded that SnRK1 from wheat

endosperm was too inhibited by R5P, an effect that the authors associated with the oxidative pentose-P pathway (to which R5P is an end product) and considered to fit very well with SnRK1 involvement in anabolism repression. However, experimental inconsistencies led us to investigate further and find that this inhibition was in fact an experimental artefact caused by ATP depletion during the conversion of R5P to RuBP by PRI and PRK. This was shown to be the case for both Arabidopsis (Chapter II) and wheat grain (Chapter IV). It is imperative that any observed interaction between a metabolite and SnRK1 (or any enzyme in fact) be discussed cautiously and always aim for *in vivo* confirmation of the observed effects before drawing conclusions.

The analysis of partially purified SnRK1 activity profiles from different tissues (At seedlings and mature leaves and cauliflower florets) revealed that despite the differences in inhibition intensities, levels fluctuated equally along the profiles for the 3 consistent inhibitors, T6P, G1P and G6P. Inhibition levels also varied with different SnRK1 substrates. These results suggest that metabolic regulation of SnRK1 varies not only during development as previously observed by Zhang *et al.* (2009) but also depending on the specific subunit compositions of the complexes and more importantly depending on the substrate being regulated by SnRK1. Kinetic modelling of T6P, G1P and G6P inhibition of SnRK1 predicts that each regulate SnRK1 activity by acting at different sites on the SnRK1/Factor I complex. The observed interactions/synergisms between T6P and G6P and T6P and G1P add to the complexity described above suggesting that SnRK1 regulation could also depend on ratios of metabolites.

Identification of Factor I, the protein that mediates SnRK1 inhibition by T6P was a desired goal of our work. However, the sensitive and difficult nature of *in vitro* SnRK1 handling, already witnessed previously in our group and elsewhere (Sugden *et al.*, 1999b) made us tackle the problem cautiously, testing different approaches and available resources instead of concentrating all attempts in one technique. While searching for mutants with suggestive phenotypes of anomalies in the SnRK1/T6P pathway (either TPSs mutants, trehalose insensitive mutants or others) may indeed

produce positive results, it could also be an endless task. Yet, testing already available mutants is easy and fast enough and therefore always worthy. Unfortunately, those we had available were not mutants for Factor I. The purification procedure carried out to isolate SnRK1 and interacting proteins was especially relevant for the prediction of the molecular size of Factor I. Mixing a low activity highly inhibited fraction with a high activity with little inhibition fraction originates a mixture of high activity highly inhibited by T6P, suggesting that Factor I runs in excess or in loose equilibrium with SnRK1 around fraction 62, making it a protein of about 174 KDa. The purification profiles were also used to characterize the inhibited SnRK1 complex composition. While interesting to see that subunits composition change in equivalent sized fractions in Arabidopsis seedlings and mature extracts, no conclusion can be drawn for the T6P inhibited complex composition except to say that the AKINβγ subunit, a plant-specific protein, hoped to be involved in plant-specific SnRK1 inhibition by T6P, seems not to be essential for the process. This subunit was, however, very recently recognized to be the true canonical γ subunit required for the heterotrimeric complex formation in plants and suggested to retain a starch, starch breakdown products or analogous carbohydrates binding ability necessary for retrograde signaling (plastid to nucleus) of carbon homeostasis regulation (Ramon *et al.*, 2013). The ATP-agarose purification approach was, while promising, suspected to be difficult to use as already described by Davies *et al.* (1994) who tried to purify AMPK in this way. Indeed, we were not able to recover most SnRK1 activity and inhibition was lost during the procedure. New takes on the protocol might however be worth trying.

Our next strategy was to look at immunoprecipitation techniques with fresh eyes (Zhang *et al.*, 2009). Given that T6P inhibition of SnRK1 increases in the first minute of reaction reaching a steady state after that, we assumed that SnRK1-Factor I-T6P interaction had to happen at least in that time frame. Together with the knowledge that the interaction is most likely weak (due to failed co-immunoprecipitation in Zhang *et al.* (2009)), we designed a protocol for that first minute of reaction with gentle washing steps in an attempt to keep SnRK1-Factor I

attached in the immunoprecipitated pellet and/or obtain wash fractions enriched with Factor I. After electrophoresis, this approach revealed 3 protein bands of interest: bands that were simultaneously absent from thoroughly washed pellets, present in gently washed pellets with some degree of conserved T6P inhibition and present in washes. Band 1, a factor 2-like protein, linked to cold responses (Guo *et al.*, 2002) has no known connection to SnRK1 or T6P and was absent from highly inhibited fractions in the purification profile. Band 2, a cobalamin-independent methionine synthase (Met E) that catalyze the synthesis of methionine, links sulphur and one-carbon metabolism (Ferrer *et al.*, 2004). Besides trehalose fluctuation with sulphur stress (Zhang *et al.*, 2011) no other links to T6P or SnRK1 are described. While unlikely to be Factor I, Band 2 is present in inhibited fractions in the purification profile and might be worth to investigate further. Band 3 is an unknown protein with no known function with 3 recognized domains, a thiamine pyrophosphate-binding module, a Pyr binding domain and a C-terminal domain of transketolase. In mammals, AMPK regulation by glucose levels seem to be dependent on the levels of Xu5P set by the PPP activity and in part related to a transketolase reaction. In Arabidopsis seedlings Xu5P does not alter SnRK1 activity (see Table 2.1, Chapter II) but a putative transketolase was down-regulated in pea embryos with anti-sense SnRK1 (Radchuk *et al.*, 2006). In plants, transketolase links the PPP and the Calvin Cycle and while a direct link to T6P and SnRK1 is difficult to assume one should remember that before T6P inhibition of SnRK1 was described in plants, both elements were known to be involved in sucrose/energy coordination with growth, however, a direct link between them might have sounded has unrealistic as a link with the identified proteins since the only parallelism came from yeasts where T6P was known to inhibit HXK (Blázquez *et al.*, 1993) and not SnRK1 (Zhang *et al.*, 2009).

6.3. SnRK1/T6P signaling pathway

In addition to the biochemical studies of SnRK1 regulation we aimed to clarify the physiological role of the SnRK1/T6P pathway. We looked both to the

responses of the pathway under sink-limited conditions, in other words, when the plant does not grow despite carbon being readily available and initiated the analysis of its physiological role during the development of a highly relevant crop, the wheat grain.

Concerning our studies in wheat grain we present the first data of T6P measurements in an important feeding grain. We observed interesting tissue specificity of T6P levels shifting during development. The transition from pre-grain filling to grain filling stages is marked by dramatic transcriptional and physiological changes where sugars are expected to play a key role (Aoki *et al.*, 2006). At 7 DAA (pre-grain filling period) T6P levels were high enough in both filial and maternal tissues to inhibit SnRK1. However, at 17 DAA (during grain-filling) high T6P concentrations were confined to the endosperm, making it unlikely the inhibition of SnRK1 activity in the pericarp and embryo. The observation that Suc levels are still high (albeit two to three times lower) in all tissues at 17 DAA is a further indication that an additional Suc signal must control T6P synthesis as suggested by our analysis of the trehalose pathway genes in Arabidopsis (Chapter V) and also recently reaffirmed by Yadav *et al.* (2014) by showing that a direct biochemical effect of Suc on trehalose biosynthetic enzymes transcripts and activity is not sufficient to explain T6P levels variation. The observation of a shift in SnRK1-marker genes expression at 10 DAA is in agreement with SnRK1 inhibition by T6P in the pre-grain filling period. These results constitute a very preliminary approach to the subject but are a promise that the T6P/SnRK1 signaling pathway constitutes an important means of directed genetic crop improvement for enhanced food production.

Regarding the effects of the T6P/SnRK1 signaling pathway on the physiological responses observed under sink-limited conditions (impaired growth despite carbon availability) we wondered whether T6P simply signal Suc levels or if it is directly related to growth. To answer this question an experiment was designed to obtain Arabidopsis seedlings with contrasting sugar levels and biomass outcome. Plants grown in sugar-fed media under optimal conditions were compared with plants grown in the cold and under N deficiency. Similarly to the previously observed

linearity between T6P and Suc levels altered either by external Suc feeding, increased irradiance or changes in day length (Lunn *et al.*, 2006), we showed that T6P also responds to Suc accumulation due to sink limitation caused by low temperature and N deficiency. T6P responded to Suc levels above the value of 3 μmol g^{-1} FW which we suggest could constitute a famine threshold value above which T6P synthesis is induced and growth promoted. Since a direct relationship had also been previously established for T6P and Suc metabolites like Gluc (Martínez-Barajas *et al.*, 2011), an effect also observed here but to a far lesser extent, we went on to compare Gluc fed plants to Suc fed plants and established that T6P responds specifically to Suc accumulation and not Gluc. More recently, Yadav *et al.* (2014) looking at the same relationship but in a shorter time frame (3 h) showed that T6P does accumulate in Gluc treated seedlings but in response to endogenous Suc levels as we proposed for all our other treatments. In an attempt to start to understand T6P synthesis regulation under these conditions we analysed trehalose pathway gene expression. There was a general upregulation of the pathway, the level of correlation between expression levels of TPS1 and TPPB genes and endogenous Suc suggested that a Suc signal must be involved in transcription stimulation but the lack of correlation under sink-limited conditions advocates the existence of additional regulatory players. Yadav *et al.* (2014) also found a Suc induced general upregulation of the pathway but ruled out the need for *de novo* transcription for T6P accumulation. They have however, also suggested the existence of additional regulatory points and show that an unknown protein must be synthesized for T6P to accumulate in response to Suc.

T6P was determined as a regulator of SnRK1 marker genes expression rather than a regulator of growth. Changes in gene expression were observed above a threshold value of 0.3 to 0.5 nmol g^{-1} FW which can be extrapolated to 3 to 5 mM T6P in the cytosol (considering that the cytosol accounts for 10% of the tissue water content). This concentration fits very well with our biochemical studies where we found a T6P/SnRK1 dissociation constant of 4 mM (Chapter II). Considering what is known about SnRK1 inhibition by T6P, at the beginning of the experiment SnRK1 is

expected to be highly active (1.8 mM T6P) whereas at the end, activity must be decreased by 80% or more since high T6P concentrations were reached (99 mM T6P in the cold treatment). The expected increase of other metabolites like G1P and G6P with Suc accumulation would increase even more the extent of SnRK1 inhibition due to the observed cumulative and synergistic effects of these metabolites in SnRK1 inhibition by T6P (Chapter II). In fact, a recent mathematical modelling study shows that allosteric effects on SnRK1 activity by metabolites are indeed sufficient to induce dramatic metabolic reajustments (Nägele and Weckwerth, 2014).

Interestingly, the relationship between T6P levels and growth promoting gene expression was kept even under conditions where growth rates were low due to sink-limitation. This observation led us to hypothesise that the T6P/SnRK1 signaling pathway would prime growth to proceed once constraints were relieved, i.e. prepare the plant to resume growth as soon as constraints disappear. In further experiments we observed an elevated growth rate (3-fold higher) when seedlings under sink-limited conditions imposed by low temperature were transferred back to favourable conditions. Plants with decreased T6P content due to over-expression of a T6P phosphatase, that under low carbon conditions present similar growth rates as those of WT (Schluepmann *et al.*, 2003) failed to follow the WT in this increased (primed) growth rate observed upon stress relief. Our suggested priming effect was confirmed to happen through SnRK1 regulation because seedling overexpressing SnRK1 (Baena-González *et al.*, 2007) also failed to grow at an increased rate upon stress relief.

6.4. Future perspectives

The regulatory loop involving T6P-Factor I-SnRK1 is a critical node in the carbon sensing and signal transduction network in plants. Despite the latest interest around it, our understanding of its functionality is still insipient. Plenty of work is needed in all fronts. Related to the presented work, a few lines for future ventures are presented below.

SnRK1 activity regulation is far from being fully understood. The broad range of already observed regulatory processes and the probable parallelisms with AMPK and SNF1 suggests a myriad of other mechanisms. The study of these mechanisms is essential to fully understand SnRK1 activity control and would permit the identification of novel metabolic links. From direct regulation by phosphorylation/ dephosphorylation where additional upstream kinases (Hey *et al.*, 2007; Shen *et al.*, 2009) and phosphatases (Rodrigues *et al.*, 2013) are expected to exist in plants to the additional processes that may or may not influence that main regulatory mechanism are important lines for future work. The significant regulation of AMPK by nucleotides (Davies *et al.*, 1995; Xiao *et al.*, 2011) and the observation by Sugden *et al.* (1999) that SnRK1 dephosphorylation is decreased by AMP together with our results showing possible direct competition of nucleotides with ATP in the active site suggest that SnRK1 regulation by nucleotides may be far more complex then up to know realized. Evidence of post-translational modifications has also been observed, myristoylation (Pierre *et al.*, 2007), ubiquitination (Farrás *et al.*, 2001; Lee *et al.*, 2008) and SUMOylation (Baene-Gonzalez and co-workers, unpublished results) may affect different subunits for different outcomes. Regulation by metabolites was first described for SnRK1 (Toroser *et al.*, 2000) and later shown for AMPK (Clark *et al.*, 2004). In addition to differential regulation depending on plant developmental stage (Zhang *et al.*, 2009) our work adds additional layers of complexity to this type of regulation with interactive effects among metabolites and differential regulation depending on substrate. All these regulatory mechanisms need further in-depth studies and would greatly benefit from full length or regional high-resolution structure analysis of all the complex subunits. Starting from secondary structure predictions, as recently done for the starch-binding domain of Arabidopsis AKINβγ and AKINβ2 (Ávila-Castañeda *et al.*, 2014), regions of interest could then be crystalized for theory direct confirmation as different groups have been doing for AMPK (Xiao *et al.*, 2011). The gathering of structural information would allow comparison of subunits isoforms possibly revealing relevant differences as observed for AKINβ1 and AKINβ2 (Sanz *et al.*, 2013). As well as comparison of homology between SnRK1 and its counterparts as done for MARK and AMPK where structural similarities beyond those predicted by

sequence homology were found (Marx *et al.*, 2010). The recognition of SnRK1 structural specificities would greatly benefit the integration of the kinase in the global picture of plant metabolism.

The identification of Factor I remains a critical line of work that would bring clarity to the T6P/SnRK1 signaling pathway. The identification of unknown proteins, whatever the chosen method, always starts by relying in a good purification/isolation technique. After trying different approaches to purify Factor I the co-immunoprecipitation experiment was the only one to produce effective results and also the one that seemed to be most easily perfected to reach the desired goal. As a future effort cross-linking reagents could be attempted to capture the SnRK1-Factor I complex. The rapid reactivity of crosslinkers with protein functional groups would allow the stabilization of the weak and transient interaction in hands and the co-immunoprecipitate would hopefully be stable enough for thorough washing. Not only Factor I could be identified but also the exact SnRK1 trimeric complex involved in T6P signaling. More elaborate techniques would probably constitute elegant ways of solving this problem. Yeast two-hybrid technique has already been used to confirm interactions between the three main SnRK1 subunits (Bouly *et al.*, 1999; Ferrando *et al.*, 2001; Lumbreras *et al.*, 2001; Bradford *et al.*, 2003) and could also be used to catch proteins that interact in the presence of T6P. A possible drawback could be the unawareness of with which main subunit does Factor I interact with. Possibly, the inclusion of a second subunit in a yeast three-hybrid experiment could solve this problem as it was already used successfully to show interaction between an ATPase, a ubiquitin ligase and SnRK1 kinase subunit (Chiang *et al.*, 2013).

Another very important question concerns T6P differential synthesis regulation under diverse stresses (Lee *et al.*, 2011) and under different sugars availability as observed in Chapter V. As the first primary metabolite shown to control metabolism and the incredibly low levels in which it operates, in fact of the same magnitude of those of hormones, suggests an elaborate and fine synthesis control. Only a biochemical revision on the properties of the different TPSs and TPPs enzymes together with genetic and post-translational studies on their expression and

activity and that of other regulatory proteins (Yadav *et al.*, 2014) may unravel the complexity of this synthetic pathway.

Once all these questions were answered new challenges would include the identification of the type of cells and intracellular localization where T6P interact with SnRK1 via Factor I. This would also disclose T6P effects independent from SnRK1 and vice-versa. At this point we would be in a good position to transfer our knowledge to crops and effectively improve yield through this growth regulatory pathway.

6.5. References

Aoki N, Scofield GN, WangX-D, Offler CE, Patrick JW, Furbank RT (2006) Pathway of Sugar Transport in Germinating Wheat Seeds. Plant Physiol **141**: 1255–1263

Ávila-Castañeda A, Gutiérrez-Granados N, Ruiz-Gayosso A, Sosa-Peinado A, Martínez-Barajas E, Coello P (2014) Structural and functional basis for starch binding in the SnRK1 subunits AKINβ2 and AKINβγ. Front Plant Sci **5**: 199

Baena-Gonzalez E, Rolland F, Thevelein JM, Sheen J (2007) A central integrator of transcription networks in plant stress and energy signaling. Nature **448**: 938-942

Blázquez MA, Lagunas R, Gancedo C, Gancedo JM (1993) Trehalose-6-phosphate, a new regulator of yeast glycolysis that inhibits hexokinases. FEBS Lett **329**: 51-54

Bouly J-P, Gissot L, Lessard P, Kreis M, Thomas M (1999) *Arabidopsis thaliana* proteins related to the yeast SIP and SNF4 interact with AKINa1, an SNF1-like protein kinase. Plant J **18**: 541-550

Bradford KJ, Downie AB, Gee OH, Alvarado V, Yang H, Dahal P (2003) Abscisic Acid and Gibberellin Differentially Regulate Expression of Genes of the SNF1-Related Kinase Complex in Tomato Seeds. Plant Physiol **132**: 1560-1576

Chiang C-P, Li C-H, Jou Y, Chen Y-C, Lin Y-C, Yang F-Y, Huang N-C, Yen HE (2013) Suppressor of K^+ transport growth defect 1 (SKD1) interacts with RING-type ubiquitin ligase and sucrose non-fermenting1-related protein kinase (SnRK1) in the halophyte ice plant. J Exp Bot **64**: 2385–2400

Clark H, Carling D, Saggerson D (2004) Covalent activation of heart AMP-activated protein kinase in response to physiological concentrations of long-chain fatty acids. Eur J Biochem **271**: 2215-2224

Davies SP, Hawley SA, Woods A, Carling D, Haystead TAJ, Hard DG (1994) Purification of the AMP-activated protein kinase on ATP- y-Sepharose and analysis of its subunit structure. Eur J Biochem **223**: 351-357

Davies SP, Helps NR, Cohen PT, Hardie DG (1995) 5'-AMP inhibits dephosphorylation, as well as promoting phosphorylation, of the AMP-activated protein kinase. Studies using bacterially expressed human protein phosphatase-2C alpha and native bovine protein phosphatase-2AC. FEBS Lett **377:** 421–425

Farrás R, Ferrando A, Jásik J, Kleinow T, Ökrész I, Tiburcio A, Salchert K, Pozo C, Schell J, Koncz C (2001) SKP1-SnRK protein kinase interactions mediate proteasomal binding of a plant SCF ubiquitin ligase. EMBO J **20**: 2742-2756

Ferrando A, Koncz-Kálmán Z, Farràs R, Tiburcio A, Schell J, Koncza C (2001) Detection of *in vivo* protein interactions between Snf1-related kinase subunits with intron-tagged epitope-labelling in plants cells. Nucleic Acids Res **29**: 3685–3693

Ferrer J-L, Ravanel S, Robert M, Dumas R (2004) Crystal Structures of Cobalamin-independent Methionine Synthase Complexed with Zinc, Homocysteine, and Methyltetrahydrofolate. J Biol Chem 279: 44235-44238

Guo Y, Xiong L, Ishitani M, Zhu J-K (2002) An Arabidopsis mutation in translation elongation factor 2 causes superinduction of CBFDREB1 transcription factor genes but blocks the induction of their downstream targets under low temperatures. PNAS 99: 7786–7791

Hey S, Mayerhofer H, Halford NG, Dickinson JR (2007) DNA sequences from Arabidopsis, which encode protein kinases and function as upstream regulators of Snf1 in yeast. J Biol Chem **282**: 10472-10479

Jenkins CM, Yang J, Sims HF, Gross RW (2011) Reversible high affinity inhibition of Phosphofructokinase-1 by Acyl-CoA: a mechanism integrating glycolytic flux with lipid metabolism. J Biol Chem **286**: 11937–11950

Lee JH, Terzaghi W, Gusmaroli G, Charron JB, Yoon HJ, Chen H, He YJ, Xiong Y, Deng XW (2008) Characterization of Arabidopsis and rice DWD proteins and their roles as substrate receptors for CUL4-RING E3 ubiquitin ligases. Plant Cell **20**: 152-167

Lee SC, Mustroph A, Sasidharan R, Vashisht D, Pedersen O, Oosumi T, Voesenek LA, Bailey-Serres J (2011) Molecular characterization of the submergence response of the *Arabidopsis thaliana* ecotype Columbia. New Phytol **190**: 457-471

Lumbreras V, Alba MM, Kleinow T, Koncz C & Pages M (2001) Domain fusion between SNF1-related kinase subunits during plant evolution. EMBO Rep **2**: 55–60

Martínez-Barajas E, Delatte T, Schluepmann H, de Jong GJ, Somsen GW, Nunes C, Primavesi LF, Coello P, Mitchell RAC, Paul MJ (2011) Wheat grain development is characterized by remarkable trehalose 6-phosphate accumulation pregrain filling: tissue

distribution and relationship to SNF1-related protein kinase1 activity. Plant Physiol **156**: 373–381

Marx A, Nugoor C, Panneerselvam S, Mandelkow E (2010) Structure and function of polarity-inducing kinase family MARK/Par-1 within the branch of AMPK/ Snf1-related kinases. FEBS J **24:** 1637-1648

Molnar M, Vas M (1993) Mg^{2+} affects the binding of ADP but not ATP to 3-phosphoglycerate kinase: correlation between equilibrium dialysis binding and enzyme kinetic data. Biochem J **293**: 595-599

Nägele T, Weckwerth W (2014) Mathematical modelling reveals that metabolic feedback regulation of SnRK1 and hexokinase is sufficient to control sugar homeostasis from energy depletion to full recovery. Front Plant Sci **5**: 365

Piattoni CV, Bustos DM, Guerrero SA, Iglesias A (2011) Nonphosphorylating glyceraldehydes 3-phosphate dehydrogenase is phosphorylated in wheat endosperm at serine-404 by an SNF1-related protein kinase allosterically inhibited by ribose 5-phosphate. Plant Physiol **156**: 1337-1350

Pierre M, Traverso JA, Boisson B, Domenichini S, Bouchez D, Giglione C, Meinnela T (2007) N-Myristoylation Regulates the SnRK1 Pathway in Arabidopsis. Plant Cell **19**: 2804-2821

Radchuk R, Radchuk V, Weschke W, Borisjuk L, Weber H (2006) Repressing the expression of the sucrose nonfermenting-1-related protein kinase gene in pea embryo causes pleiotropic defects of maturation similar to an abscisic acid-insensitive phenotype. Plant Physiol **140**: 263–278

Ramon M, Ruelens P, Li Y, Sheen J, Geuten K, Rolland F (2013) The hybrid Four-CBS-Domain KINbc subunit functions as the canonical c subunit of the plant energy sensor SnRK1. Plant J **75**: 11–25

Rodrigues A, Adamo M, Crozet P, Margalha L, Confraria A, Martinho C, Elias A, Rabissi A, Lumbreras V, González-Guzmán M, Antoni R, Rodriguez PL, Baena-González E (2013) ABI1 and PP2CA Phosphatases Are Negative Regulators of Snf1-Related Protein Kinase1 Signaling in Arabidopsis. Plant Cell **25**: 3871-3884

Sanz P, Rubio T, Garcia-Gimeno MA (2013) AMPKβ subunits: more than just a scaffold in the formation of AMPK complex. FEBS J **280**: 3723–3733

Schluepmann H, Pellny T, van Dijken A, Smeekens S, Paul M (2003) Trehalose 6-phosphate is indispensable for carbohydrate utilization and growth in *Arabidopsis thaliana*. Proc Natl Acad Sci USA **100**: 6849-6854

Shen W, Reyes MI, Hanley-Bowdoin L (2009) Arabidopsis protein kinases GRIK1 and GRIK2 specifically activate SnRK1 by phosphorylating its activation loop. Plant Physiol **150**: 996-1005

Sugden C, Crawford RM, Halford NG, Hardie DG (1999) Regulation of spinach SNF1-related (SnRK1) kinases by protein kinases and phosphatases is associated with phosphorylation of the T loop and is regulated by 5'-AMP. Plant J **19**: 433-439

Toroser D, Plaut Z, Huber SC (2000) Regulation of a plant SNF1-related protein kinase by glucose 6-phosphate. Plant Physiol **123**: 403-411

Xiao B, Sanders MJ, Underwood E, Heath R, Mayer F, Carmena D, Jing C, Walker FA, Eccleston JF, Haire LF, Saiu P, Howell SA, Aasland R, Martin SR, Carling D, Gamblin SJ (2011) Structure of Mammalian AMPK and its regulation by ADP. Nature **472**: 230-233

Yadav UP, Ivakov A, Feil R, Duan GY, Walther D, Giavalisco P, Piques M, Carillo P, Hubberten HM, Stitt M, Lunn JE (2014) The sucrose-trehalose 6-phosphate (Tre6P) nexus: specificity and mechanisms of sucrose signaling by Tre6P. J Exp Bot **65**: 1051-1068

Zhang J, Sun X, Zhang Z, Ni Y, Zhang Q, Liang X, Xiao H, Chen J, Tokuhisa JG (2011) Metabolite profiling of Arabidopsis seedlings in response to exogenous sinalbin and sulfur deficiency. Phytochemistry **72**: 1767-1778

Zhang Y, Primavesi LF, Jhurreea D, Andralojc J, Mitchell RAC, PowersSJ, Schluepmann H, Delatte T, Wingler A, Paul MJ (2009) Inhibition of Snf1-related protein kinase (SnRK1) activity and regulation of metabolic pathways by trehalose 6-phosphate. Plant Physiol **149**: 1860–1871